Optimal Sizing of Distributed Renewable and Battery Storage Systems for Australian Residential Consumers

by

Rahmat Khezri

Thesis

Submitted to Flinders University

for the degree of

Doctor of Philosophy

College of Science and Engineering

October 2021

List of Contents

List of Figures

List of Tables

Abstract

Recently, renewable energy resources and battery energy storages are broadly used in Australian residential sector to decrease the electricity cost. The installed renewable energy resources, such as solar photovoltaic and wind turbine, supply the loads of the residential consumer and export the extra power to the main grid, with a certain feed-in-tariff rate. The recent feed-in-tariff rates are, however, not significant so that make a high profitability by the renewable energy resources. On the other hand, the electricity generation of renewable energy resources is accounted as an uncertainty which may not match with the electricity profile of consumers. Adding battery energy storage to the renewable energy resources in residential sector is, therefore, becoming a key component to reach higher profitability with higher usage of renewable power in the residential. Since the costs of renewable energy resources and battery energy storages are still heavy for the consumers and there is no specific guideline to show that what capacity of components should be purchased, a practical optimal sizing and subsequently an accurate guideline are crucial.

This thesis develops optimal sizing frameworks for renewable energy resources and battery energy storages in grid-connected and standalone Australian residential sector. The main aim of optimal sizing is to minimise the cost of electricity of electricity consumers. Actual data set of electricity profiles, weather data such as wind speed and solar insolation, market prices of renewable energy resources and battery energy storage, as well as electricity prices in Australian context are used as input data for optimal sizing. Rule-based home energy management systems are conducted for the operation of the systems.

A practical guideline is rendered for the consumers to purchase the right capacity of solar photovoltaic and battery energy storage to minimise their electricity cost. This guideline is generated based on the household's average daily electricity consumption and available rooftop area for solar photovoltaic installation. An

appropriate annual cash flow analysis is conducted for grid-connected households with solar photovoltaic and battery energy storage. A home energy management system is developed for grid-connected households with wind turbine, battery energy storage, and electric vehicle. A novel demand side management strategy is developed to decrease the optimal capacity of battery energy storage for standalone residential households in South Australian remote areas. The demand side management strategy is based on the state-of-charge level of battery energy storage and day-ahead forecasts of solar insolation and wind speed. The core of the demand side management is a fuzzy logic method which decides for efficient load shifting and/or load curtailment. A multi-objective optimal sizing of wind turbine, solar photovoltaic and battery energy storage is conducted based on triple objectives: (1) cost of electricity, (2) grid dependency, and (3) total curtailed energy. The developed optimal sizing framework depends on a long-period operation of the system by considering battery degradation, stochastic behaviour of renewable generation and electricity profile, as well as updated electricity price.

Acronyms

BD	Battery Degradation
BES	Battery Energy Storage
BESS	Battery Energy Storage System
BS	Battery Storage
CD	Capacity Degradation
COE	Cost of Electricity
CRF	Capital Recovery Factor
DC	Direct Current
DG	Diesel Generator
DOD	Depth of Discharge
DR	Demand Response
DSM	Demand Side Management
EMS	Energy Management System
ESS	Energy Storage System
EV	Electric Vehicle
FIT	Feed-in-Tariff
GA	Genetic Algorithm
GCH	Grid-Connected Household
GD	Grid Dependency
HES	Hybrid Energy System
HEMS	Home Energy Management System
NPC	Net Present Cost
NSGA-II	Non-dominated Sorting Genetic Algorithm II
PSO	Particle Swarm Optimization
PV	Photovoltaic
RAES	Remote Area Electricity Supply
RCAA	Rainflow Cycle Counting Algorithm

RES	Renewable Energy Source
RP	Retail Price
RTP	Real-Time Pricing
SA	South Australia
SOC	State of Charge
SWT	Small Wind Turbine
WT	Wind Turbine
TOU	Time of Use
TCE	Total Curtailed Energy

Declaration

Hereby, I certify that,

1- the work in this thesis has been carried out by me in the College of Science and Engineering.
2- the material of this thesis was not previously submitted for a degree or diploma in any institution.
3- the thesis does not contain any material previously published by another person except where due acknowledgement has been made in the text.

Rahmat Khezri
October 2021

Acknowledgements

Firstly, I would like to express my sincere thanks to my principal supervisor Dr Amin Mahmoudi for his generous support, remarkable encouragement, and valuable guidance during my PhD. His support, guidance and patience motivated me to overcome the challenges that I encountered throughout the endeavours of my whole PhD study.

I would like to acknowledge the contribution of “Australian Government Research Training Program Scholarship” that supported my PhD career.

Besides my principal supervisor, I was fortunate to have Dr Mohammed H. Haque as an adjunct supervisor for my PhD study. I am grateful for his unconditional support, insightful comments, and assistance at different stages of my path, and I will remain indebted to him. I would also like to thank A/Prof. Fangpo He and A/Prof. Nesimi Ertugrul. My appreciation also goes to A/Prof. Hirohisa Aki and Dr Mohammad Hassan Khooban for their worthy comments and supports.

My greatest thanks go to my friends and colleagues for their inspiration, support, encouragement, and attention throughout my PhD.

I would like to gratefully thank my wonderful wife, Kouyestan, for her tremendous support, encouragement, and sacrifice. She has always been beside me all these years and made my life more enjoyable with her love and support. Finally, I wish to thank my parents, Masoumeh and Mohammad Shafiee, who have raised me with love, and I would not have been here without their support. Their unconditional love and encouragement have motivated me to pursue my goals.

To my parents, Shafiee and Masoumeh.
And to my brothers, Mohsen, and Amin.
And my beloved wife, Kouyestan.
without whom I would not be here today.

Chapter 1

Introduction

This chapter presents the research background and motivation for this thesis, as well as the research objectives, contributions and publications, and the thesis outline.

1.1 Research Background and Motivation

Electricity demand is increasing in the global market. Figure 1-1 shows the global electricity demand by region from 2000 to 2018 [1]. The electricity demand is increased by about 72% from 2000 to 2018 in which the annual growth is around 4%. The global electricity demand at the end of 2018 was more than 23,000 TWh. Most of the electricity demand increment is observed in China and the other developing countries. This is the result of industrialization development, boosting of the human comfort level, and population increment [1]. As the electricity demand grows, the fossil fuels are decreasing in a way that they may not last for more than a few decades. Furthermore, the cost of petroleum products is rising. The request for renewable energy as a prominent alternative for fossil fuels is, therefore, increasing rapidly in the world.

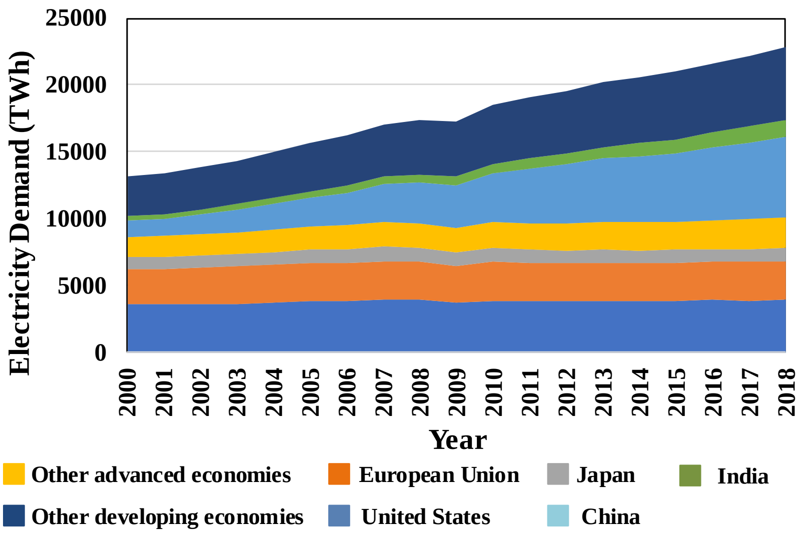

Figure 1-1. Global electricity demand by region [1].

Renewable energies are valuable sources in terms of sustainability since they can reduce the green-house gases worldwide. Recently, distributed renewable energy sources (RESs) are installed in residential sector for electricity generation. Taking advantages of compact design, simple structure, portability, low noise and reasonable capital cost, small wind turbine (SWT) is an appropriate candidate for distributed renewable generators in GCHs [2]. The installed SWT can supply the household load and export the excess power, if any, to the grid at a feed-in-tariff (FIT) rate to reduce the annual electricity cost of the household. An excellent and popular distributed RES for residential sector is rooftop solar PV. Solar PV systems take advantages of absence of rotating parts, convenient accommodation in rooftops, and less maintenance cost. Like SWTs, solar PV systems in a grid-connected house would supply the load and export the extra power to the main grid with FIT.

Integration of solar PV and SWT in a grid-connected residential sector would decrease the electricity bill, grid dependency, emission, and so forth. In recent years there has been an increased deployment of PV in residential sector. Rooftop solar PV systems are increasingly integrated in Australian households. According to an Australian clean energy report [3], five rooftop solar PV systems were installed in each hour of 2018. At the end of June 2019, more than one-third of Australian dwellings had rooftop solar PV systems [4]. Such a high penetration of PV systems in Australia is the result of high retail price (RP), falling PV system costs, and incentives from the government in forms of FIT and rebates [5].

There are several challenges for further deployment of PV and SWT systems in GCHs. First, the FIT rates are considerably decreasing in the countries with high penetration of renewable energy systems [6]. Second, the intermittency of solar PV and SWT generations would be a challenge in the recent electricity markets when the time-of-use (TOU) and real time pricing (RTP) are used. To overcome these challenges, the manifest destiny in GCHs is the integration of battery energy storage (BES) into the system [7]. The BES is a qualified technology to absorb the extra power of distributed RESs after feeding the load, and then release the saved power to supply the load when there is no renewable generation.

Renewable-battery systems are also used to supply the loads for off-grid rural areas especially for remote area residential sector. In those standalone systems, the capacity of BES

On the other hand, Australia is planning to ban the sale of internal combustion engine (ICE) vehicles by 2035 and that will increase the growth of electric vehicle (EV) significantly in near future [8]. Hence, if the homeowner owns an EV, the installed distributed RESs can also charge the EV and reduce the electricity cost further by reducing the imported electricity from the grid. In the standalone households, the battery of EV can be used as an alternative to supply the loads by the vehicle-to-home (V2H) technology. These topics need further investigations to attain proper energy managements while doing the optimal sizing.

Currently, battery energy storage (BES) is an expensive technology and its viability for economic integration in households needs investigation [9]. Rooftop PV system, if not selected optimally, may not offer economic benefits [10]. There are not adequate studies to investigate the optimal sizing of SWT for GCHs to achieve the minimum cost of electricity. Thus, the selection of optimal capacity of PV, SWT, and BES is a crucial task for grid-connected and standalone households to achieve the maximum technical and economic benefits.

1.2 Research Questions

Based on the provided literature review, the following research questions can be extracted:

- How to achieve more practical and accurate capacity of renewable and battery components for residential households?
- How to generate practical guidelines for residential customers to invest the right money for the components?

- How the capacity of PV, WT and BES change if the homeowner owns an electric vehicle?
- How to develop new demand response strategies for standalone households with renewable-battery system? And what is the effect of demand response on the optimal capacity of components?
- How to generate new multi-objective optimal sizing for residential customers by considering a long period operation and battery degradation?

1.3 Research Objectives

The main research objectives of this thesis

- To achieve practical optimal renewable-battery systems for residential sector with the lowest electricity cost.
- To generate guidelines for residential customers to select the optimal capacity of PV and BES.
- To investigate the impact of EV on optimal sizing problem.
- To decrease the capacity of battery in standalone residential systems by development of new demand response strategies.
- To develop a comprehensive design framework for optimal sizing of renewable-battery system under long period operation

1.4 Contributions

This thesis addresses the problem of optimal sizing of renewable energies (solar PV and WT) and BES for residential sector in urban and rural areas. It is notable that this PhD thesis considers the optimal renewable and battery system for Australian residential sector. Hence, the load of electrified heating is considered in the total load of the system, and it is not separated. The main contributions of this thesis can be classified as follows:

- A practical optimal sizing of rooftop solar PV and BES for grid-connected households is conducted. Actual data of solar insolation, ambient temperature, electricity consumption, components data, as well as electricity prices and grid constraint for residential consumers in South Australia are conducted. The results of the optimal sizing model are evaluated by conducting an uncertainty analysis of solar insolation and ambient temperature using 10 years real data. A practical guideline is presented for the consumers to select the right capacities of PV and BES based on the average daily electricity demand and the available rooftop space for PV installation.

- A practical capacity optimisation model is developed for WT and BES in a GCH with/without an EV by analysing all uncertainties associated with wind, load, and EV. Novel rule-based HEMSs, with grid constraints, are developed for all possible cases (with/without BES as well as with/without EV) of the GCH. All uncertainties of EV's arrival/departure time and initial SOC are incorporated in the optimal sizing model. The optimal results are evaluated by analysing stochastic SWT power generation and load consumption using 10-year of real wind speed data and load uncertainty.
- A new DSM strategy is adopted for a comprehensive and practical optimal sizing of standalone renewable-battery systems. A fuzzy-based DSM strategy developed based on day-ahead forecasted renewable generation and battery state-of-charge (SOC) level. All essential parameters like operating reserve, salvation cost and battery capacity degradation are considered. A certain level of operating reserve based on the day-ahead forecasted errors of renewable generation and load consumption is maintained in the standalone system. Three system configurations: PV-BS, WT-BS and PV-WT-BS are optimally sized and compared.
- An optimisation framework is developed based on a long-period operation for a GCH with PV, WT and BES by incorporating real data. The solar PV and battery capacity degradations are incorporated in the long-period operation of the residential GCH. The capacities of PV, WT and BES are optimised based on electricity cost, grid dependency and curtailed energy. The long-period optimal sizing framework is compared with short-period optimisation.

1.5 Thesis Outline

The remaining chapters of this thesis are organized as follows:

Chapter 2 presents a literature review on the topic of optimal sizing of distributed RES and BES for residential sector. The review is conducted on four aspects of optimal sizing. First, existing studies on practical optimal sizing of PV and battery in grid-connected households are investigated. Second, a literature review is presented on optimal sizing of WT and battery for EV-owner grid-connected households. Third, the studies on capacity optimisation of renewable-storage systems for standalone households, when demand response incorporated, are reviewed. Four, a review on multi-objective optimisation for sizing of hybrid energy systems is conducted.

Chapter 3 determines the optimal capacity of rooftop solar PV and BES for grid-connected households in South Australia and other Australian states and territories. This chapter, at first, presents rule-based HEMS for two system configurations, (1) only PV, and (2) PV-BES. Then, the optimisation formulation for sizing of PV and BES is presented. The initial optimal sizing results are first presented, and then various sensitivity analyses are indicated to study the effects of PV and battery costs, as well as the electricity consumption and grid constraint on the COE of the household. The effects of solar insolation and load consumption uncertainties on COE are also investigated. Chapter 3 provides a practical guideline for the consumers to purchase the right capacity of PV and BES to minimise their electricity cost.

Chapter 4 investigates optimal sizing of WT and BES for grid-connected households with and without an EV. In this chapter, a novel rule-based HEMS is developed to manage the power flow between WT, grid, BES, EV, and load. The effects of uncertainties of wind speed, load, availability time of EV in the household, and the initial SOC of EV’s battery when arriving home are considered in the capacity optimisation problem. Chapter 4 compares the operating cost of EV in the optimal sizing problem with an internal combustion vehicle.

Chapter 5 presents a demand side management strategy to contribute to optimal sizing of solar PV, WT, and BES for a standalone household in remote area. This chapter, at first, describes the system model including the controllable loads in the household. Then, the DSM strategy by forecasting day-ahead renewable generation and electricity demand is presented. The NPC of electricity is selected as the objective function by considering capital, maintenance, replacement, and salvation costs of components. Chapter 5 applies the developed optimal sizing for three system configurations, (1) PV-BES, (2) WT-BES, and (3) PV-WT-BES. The optimal results of these systems are compared with each other, an actual system in South Australia, and two recently published articles.

Chapter 6 develops a new optimal sizing framework for multi-objective sizing of a PV-WT-BES system based on a long-period operation. The capacities of WT, solar PV, and BES are optimised by considering triple objectives: (1) cost of electricity, (2) grid dependency, and (3) total curtailed (dumped) energy. The battery's capacity, as well as purchase and sell back electricity prices are updated for each year of long-period operation during the project lifetime. In this chapter, the proposed optimisation technique is applied to a grid-connected household in South Australia by incorporating long-period (10 years) real data of wind speed, solar insolation, ambient temperature, and load consumption. Chapter 6 compares the renewable-battery electricity system optimised by the long-period data to the same system optimised by short-period data (one year).

Chapter 7 presents the overall conclusion and summary of the main findings from this research. This chapter also exhibits the recommendations and future perspectives.

References

[1] International Energy Agency, World Energy Outlook, 2018.

[2] N.A. Orlando, M. Liserre, R.A. Mastromauro, and A. Dell'Aquila, "A survey of control issues in PMSG-based small wind-turbine systems" *IEEE Transactions on Industial Informatics*, vol. 9, no. 3, pp. 1211-1221, Aug. 2013.

[3] Clean Energy Council. "Clean Energy Australia Report," [Online]. Available: https://assets.cleanenergycouncil.org.au/documents/resources/reports/cleanenergy-australia/clean-energy-australia-report-2019.pdf Accessed on: Apr. 2019.

[4] Australian Renewable Energy Agency, "Australian PV Institute Solar Map," [Online]. Available: pv-map.apvi.org.au. Accessed on: Jun. 2019.

[5] Australian Energy Market Operator. "South Australian Electricity Report," [Online]. Available: https://www.aemo.com.au/media/Files/Electricity/NEM/Planning_and_Forecasting/SAAdvisory/2018/2018-South-Australian-Electricity-Report.pdf. Accessed on: Nov. 2018.

[6] M.A. Hayat, F. Shahnia, and GM Shafiullah, "Replacing flat rate feed-in tariffs for rooftop photovoltaic systems with a dynamic one to consider technical, environmental, social, and geographical factors," *IEEE Transactions on Industial Informatics*, vol. 15, no. 7, pp. 3831-3844, Jul. 2019.

[7] A. S. Hassan, L. Cipcigan, and N. Jenkins, "Optimal battery storage operation for PV systems with tariff incentives," *Applied Energy*, vol. 203, pp. 422-441, 2017.

[8] https://thedriven.io/2020/02/06/australia-urged-to-copy-uk-ban-on-new-fossil-fuel-cars-by-2035/

[9] M. Stecca, L. R. Elizondo, T. B. Soeiro, P. Bauer and P. Palensky, "A Comprehensive Review of the Integration of Battery Energy Storage Systems Into Distribution Networks," in *IEEE Open Journal of the Industrial Electronics Society*, vol. 1, pp. 46-65, 2020.

[10] A. Sangwongwanich, Y. Yang, D. Sera, F. Blaabjerg, and D. Zhou, "On the impacts of PV array sizing on the inverter reliability and lifetime," *IEEE Trans. Ind. Appl.*, vol. 54, no. 4, pp. 3656–3667, Jul./Aug. 2018.

Chapter 2

Literature Review

The main focus of this thesis is on optimal sizing of renewable-battery systems for grid-connected and standalone households in residential sector. A comprehensive literature review is, therefore, conducted on this topic. The literature review is presented in three aspects:

- Optimal sizing of PV and BES for grid-connected households
- Capacity optimisation of remote area electricity supply systems
- Multi-objective optimal sizing of hybrid standalone/grid-connected electricity systems

The contributions of this chapter are presented in three published review papers.

2.1 Review on Optimal Sizing of PV and BES in Grid-Connected Households

Integration of solar PV and battery storage systems is an upward trend in residential sector to achieve various targets like minimising the electricity bill, grid dependency, emission and so forth. In recent years there has been an increased deployment on PV and battery installation in residential sector. In this regard, optimal planning of PV-battery systems is a critical topic for the designers, consumers, and network operators due to the high number of parameters which affect the optimisation problem. This review chiefly aims to presents a comprehensive and critical survey on the effective parameters in the optimal planning process of solar PV and battery storage systems for grid-connected residential sector. The most important parameters in process of optimal planning for PV-battery system are recognized and explained. These parameters involve economic and technical data, objective functions, energy management systems, design constraints, optimisation algorithms and electricity pricing programs. A timely review on the state-of-the-art studies in PV-battery optimal planning is presented. The challenges, trends and latest developments in the field are investigated. At the end, scopes for future studies are developed. It is found that new guidelines should be provided to the customers based on various electricity rates and demand response program. Also, several design considerations like grid dependency and resiliency need further investigation in the optimal planning of PV-battery systems.

The contribution of this review is presented in one published review paper.
R. Khezri, A. Mahmoudi, and H. Aki, "Optimal Sizing of Solar Photovoltaic and Battery Storage Systems for Grid-connected Residential Sector: Review, Challenges and New Perspectives," *Renewable and Sustainable Energy Review*, 2021.

The student has developed the conceptualization and necessity of this review study. Analysis and review of research data has been done by him and the co-author. The student prepared a draft of the review paper. Revisions and comments were provided by the co-author so as to contribute to the interpretation.

2.1.1 Background and Motivation of the Review

Electricity demand is increasing in the global market. The electricity demand is increased by about 72% from 2000 to 2018 in which the annual growth is around 4%. The global electricity demand at the end of 2018 was more than 23,000 TWh. Most of the electricity demand increase is observed in China and the other developing countries. This is the result of industrialization development, boosting of the human comfort level, and population increment [1]. As the electricity demand grows, the fossil fuels are decreasing in a way that they may not last for more than a few decades. Furthermore, the cost of petroleum products is rising. Therefore, the request for renewable energies as prominent alternatives for fossil fuels is increasing rapidly in the world [2].

Renewable energies are valuable sources in terms of sustainability since they can reduce the green-house gases worldwide. In addition, the falling cost of renewable energies such as solar photovoltaic (PV) has made them an attractive source of electricity generation [3]. Solar PVs take advantages of absence of rotating parts, convenient accommodation in rooftops and less maintenance cost. Fig. 2-1 illustrates the global solar PV capacity and its annual addition [4]. The total worldwide installed solar PV electricity generation capacity exceeded 625 GW at the end of 2019 compared to only 23 GW at 10 years earlier [5]. The annual addition of solar PV capacity was more than 115 GW in 2019 compared to only 8 GW in 2009. According to the estimations, solar PV electricity generation would supply 3,518 TWh and 7,208 TWh by 2030 and 2040, respectively [6].

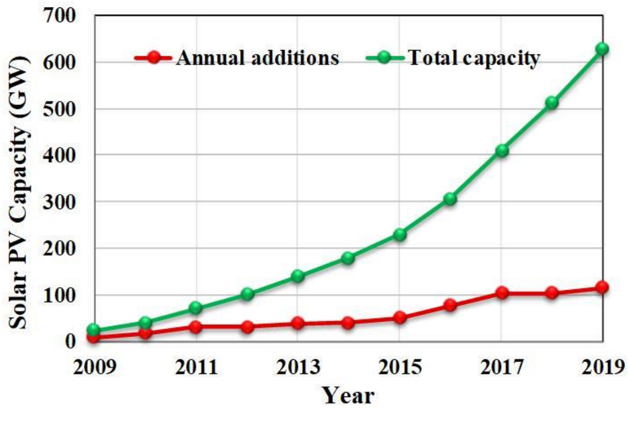

Figure 2-1. Global solar PV capacity and annual addition.

Solar PV is the most popular renewable energy resource in residential sector. A solar PV system in a grid-connected system would supply the load and export the extra power to the main grid with feed-in-tariff (FIT). Integration of solar PV in a grid-connected residential sector (GCRS) would decrease the electricity bill (because of the FIT), grid dependency, emission and so forth. In recent years there has been an increased deployment of PV in residential sector.

There are several challenges for further deployment of PV systems in GCRS. First, the FIT rates are decreasing in the countries with high penetration of rooftop solar PV systems [7-8]. Second, the intermittency of solar PV generation would be a challenge in the recent electricity markets when the time-of-use (TOU) and real time pricing (RTP) are used. To overcome the challenges, the manifest destiny in GCRS is the battery energy storage (BES) integration into the system. The BES is a qualified technology to absorb the extra power of PV (after feeding the load), and then supply the load when there is no renewable generation. Several applications of the PV-battery system have been reported such as energy arbitrage, resiliency improvement and time-shifting [9-10]. However, the high price of BES technology is an impediment for efficient integration. Thus, further investigations are required for PV and BES integration in grid-connected systems in terms of planning, operation, and control. In this regard, optimal sizing of PV and BES is the utmost critical challenge for the consumers and network analyzers due to the high number of the parameters which can affect the optimisation problem.

Literature survey indicates plenty of review studies on solar PV and battery storage systems in power systems. In [11], the standards for grid-connected solar PV systems were investigated. Grid integration of small-scale solar PV systems was introduced in [12]. Technical specifications of solar PV systems were discussed in [13]. In [14], a review was conducted on the solar PV technologies. The potential problems and technical issues in grid-connected solar PV systems were described in [15] and [16], respectively. The inverter technology development in solar PV systems was reviewed in [17-18]. Self-consumption of solar PV system was investigated in [19]. The technical and economic aspects of solar PV for grid-connected homes was investigated for Palestine, Brazil, and South Africa in [20-22], respectively. However, the above-mentioned review studies did not investigate integration of the battery storage for the PV systems.

An overview on current developments of PV-battery systems for grid-connected buildings was conducted in [23]. The PV-battery architectures for residential sectors were investigated in [24]. The economic viability of PV-battery systems for residential buildings was surveyed in [25]. The economic aspects of solar PV and battery integration in residential sector was reviewed in [26]. In [27], an economic analysis was conducted for residential solar PV systems with battery in the United States. A review on the application of distributed solar PV system with battery was presented in [28]. Energy management of small-scale PV-battery systems in residential households was reviewed in [29]. The Australian consumers motivations for installing PV-battery system in their households was overviewed in [30]. Various battery discharge strategies for PV-battery in grid-connected households were compared in [31]. However, none of these studies investigated optimal planning of PV systems with or without battery.

Application of artificial intelligence methodologies for optimal sizing of solar PV system was investigated on [32]. In [33], a review was conducted on optimal sizing of energy storage and solar PV in standalone power systems. A review on optimal planning of solar PV for water pumping systems was conducted in [34]. In [35-37], optimal sizing of hybrid systems with PV and BES was surveyed. Optimal allocation of BES in renewable energy systems and distribution networks was investigated in [38] and [39], respectively. Although, numerous review papers were conducted on optimal planning, but to the best of authors' knowledge, the PV-battery optimal planning in GCRS was not investigated by the existing studies. This is a very critical area that should be broadly reviewed. In other word, a review study on optimal planning of PV and BES in GCRS is much important because of the large deployment of rooftop solar PV and BES systems in residential sector worldwide. An efficient optimal planning of PV and battery for grid-connected residential customers may result in decreasing electricity bills. The recent high penetration of residential solar PV in distribution network has created serious challenges for the network operators by increasing the voltage level at noon time and hardening the voltage and frequency control. A strategical optimal planning of PV and battery can resolve the network problems.

2.1.2 PV-Battery Optimal Sizing Overview

A general schematic diagram of a GCRS with solar PV and BES is demonstrated in Fig. 2-2. The energy management system monitors and controls the energy flow between the PV, BES, grid and GCRS based on the data from forecasting, smart meter, and available loads for demand response. The effective parameters on optimal sizing of PV-battery for grid-connected residential sectors are discussed in this section.

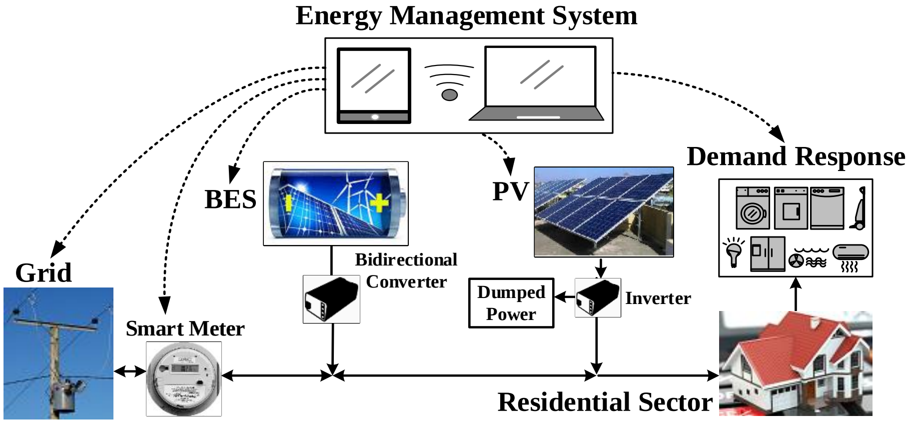

Figure 2-2. A general schematic of a GCRS with solar PV and BES.

A) Input Data

The input data used in optimal sizing of PV-battery system for grid-connected residential sector are illustrated in Fig. 2-3. Three groups of input data are needed: (1) financial data, (2) periodic data and (3) technical data.

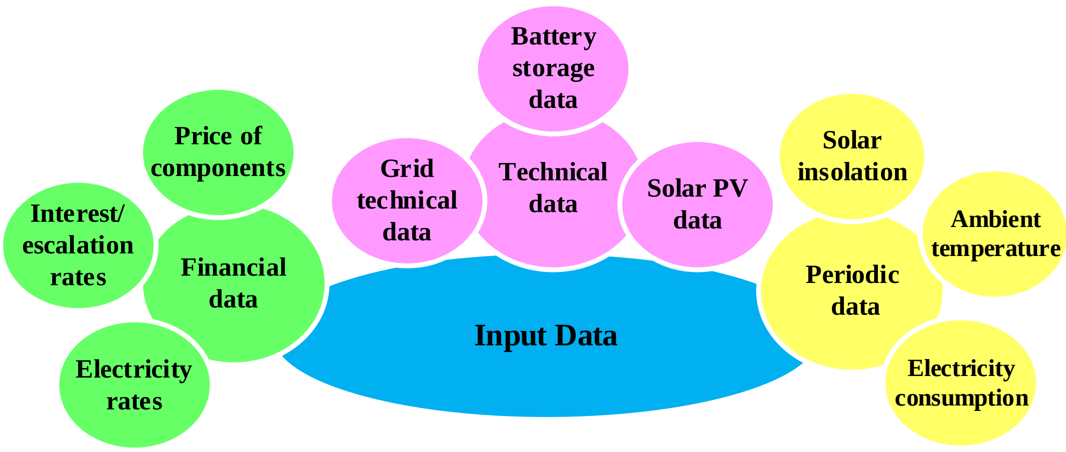

Figure 2-3. Important input data for optimal sizing of PV-battery systems in grid-connected residential sectors.

Financial data contains the installation costs of PV and BES, interest/discount and escalation/inflation rates, as well as the electricity rates. Mostly, all these data depend on the country of the case study. Since the optimal planning is a long-term problem, periodic data is used for electricity consumption, solar radiation, and ambient temperature. The periodic data can be realistic data or probabilistic data. The periodic data can be collected for very-short-period (e.g., one day of each season), short-period (e.g., one year) and long-period (e.g., ten years). The data can be arranged in hourly basis or high temporal resolution (e.g., 5 min). Technical data involves PV, BES, and grid data. The grid technical data is mostly associated with the limitations on export/import power to/from the main grid. The components' technical data are related to the lifetime, efficiency and other data of PV and BES. The array tilt angle, temperature coefficient and insolation at standard test conditions are among the important factors of technical data for solar PV system [40].

Table 2-1 lists the specifications of different solar PV technologies [41]. The first generation of solar PV technology is produced by semiconducting p–n junctions from silicon. In most of the cases, the payback period of the first generation takes 5-6 years. The main idea for the development of the second generation is to decrease the price of the first generation in the market. The used thin-film solar cell (TFSC) in second generation takes benefits from compatibility with low cost substrates, variety of deposition process, and low material usage. The TSFC technology has different types like copper–zinc-–in–sulfide (CZTS), amorphous silicon (a-Si) solar cells, and copper–indium–gallium–diselenide (CIGSe) [41]. The main aim of development of the third generation of solar PV cells is to improve the average electrical performance while maintaining a low cost of the technology.

Table 2-1. Specifications of different solar PV technologies [41].

Generation	First generation		Second generation			Third generation
Feature	Cristal silicon solar cells		Thin film solar cells			Perovskite, organic, multi-junction solar cells
Type	Mono-crystalline cells	Multi-crystalline cells	CdTe cells	Amorphous silicon cells	CIGS cells	Multi-junction solar cells
Efficiency	18%~25%	17%~21%	18%~22%	13.4%	20%~23%	45%
Price	High		Low			Medium
Discussion	accounted for 89.6% of commercial production in 2007		already entered into the commercialization stage nearly 10 years ago			still in progress

Table 2-2 lists the technical characteristics of battery energy storage technologies that are suitable for solar PV systems in grid-connected residential sector. These battery energy storages technologies are lead-acid (LA) battery, lithium-ion battery (LIB), sodium sulphur (NaS) battery, and vanadium redox battery (VRB) [42-44]. As illustrated in Table 2, the LIBs have higher efficiency and lifetime compared to other technologies. However, the LA batteries are traditionally used in electrical systems and their cost is low. It is notable that the LA and LIB are generally used in residential systems.

Table 2-2. Characteristics of four types of battery energy storage technologies available in the market [42-44].

Energy storage technology	Capital cost ($/kWh)	Power rating (MW)	Discharge time	Power density (W/l)	Energy density (Wh/l)	Efficiency (%)	Lifetime (years)	Lifetime (cycles)
LA	300-600	0-20	s-h	90-700	50-80	50-90	3-15	250-1500
LIB	700-3000	0-100	s-h	1300-10,000	200-400	85-95	5-20	600-1200
NaS	1000-3000	0.05-40	s-h	120-160	15-300	80-90	10-15	2500-4500
VRB	600-1500	0.03-3	1-10h	0.5-2	20-70	80-90	5-10	12,000+

1.1. Objective Functions

Objective function is the most important parameter in an optimal sizing problem. Fig. 2-4 shows the two groups of applicable objective functions for optimal sizing of PV and BES in GCRS. Objective functions should be maximised or minimised using the optimisation algorithms. The problems can be defined with one or more objective functions. If more than one objective function is assumed, then the problem is a multi-objective optimisation challenge in which the results will be shown in terms of set of non-dominated solutions in Pareto-fronts.

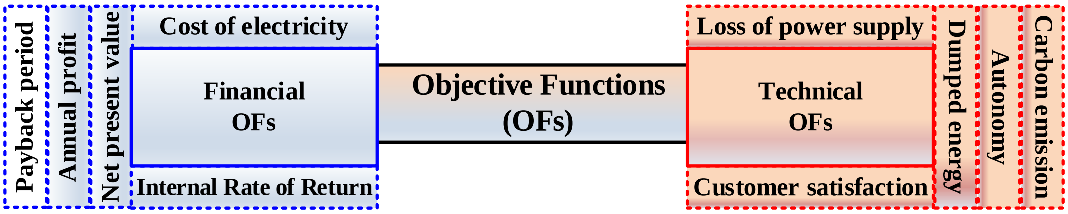

Figure 2-4. Applicable objective functions for optimal sizing of PV-battery system in grid-connected residential sectors.

a) Financial

The financial objective functions are the important group of targets for residential customers. There are five commonly used financial objective functions: (1) net present value (NPV), (2) cost of electricity (COE), (3) annual profit (AP), (4) payback period (PP), and (5) internal rate of return (IRR). Each objective function is sufficiently discussed in this sub-section.

b) Technical

The technical objective functions mostly depend on the targets of the designer. The commonly used technical objective functions are: (1) autonomy of the GCRS, (2) dumped energy (DE), (3) loss of power supply (LPSP), (4) customer satisfaction (CS), and (5) carbon emission (CE).

B) Design Constraints

The most important constraint is the power balance between generation and consumption sides of the GCRS. The import/export power from/to the main grid is generally limited in the distribution networks. As realistic examples, the single-phase and three-phase GCRS are not allowed to export more than 5 kW and 30 kW power to the main grid using rooftop solar PVs in South Australia. The constraint associated with the battery is the state-of-charge (SoC) level which should deviate between maximum and minimum rates. The rooftop availability to install the solar panels is another constraint for the optimal sizing in GCRS. In fact, the maximum capacity of solar PV should be selected based on the rooftop availability of the residential building. The budget limit for the component's investment is the next constraint. The optimisation model should consider the maximum budget to obtain the capacity of the components. The countries policies for installation of rooftop solar PV and BES should be considered as a constraint in the optimisation model. The renewable factor is considered as a constraint for the optimal sizing problems where higher load supply from the solar PV is preferable. Resiliency and flexibility are two new metrics that can be considered as constraints. The resiliency constraint is used to boost the robustness of the GCRS system with PV and BES against extreme events with low probability and high impact. The other metric is to increase the operation flexibility of the power system to manage the variability of renewable energies.

C) Electricity Pricing Programs

Electricity pricing programs are: (1) flat price, (2) TOU, (3) stepwise tariff, (4) critical peak pricing, and (5) RTP. Using the flat rates, the import/export power is charged by a constant price. In the TOU pricing, the electricity rates are usually divided into two or three time periods during a day. Higher rates are assigned to peak load times of the day. In the stepwise tariff, the electricity rate is increased due to increasing the electricity consumption of the GCRS. The critical peak pricing is based on the wholesale market. Once the utilities anticipate critical events in the power market, they may call for high prices during a time period. In RTP, the electricity rate is changed dynamically in an hourly basis. This means that the electricity rate is assigned by the operator based on the market price. The type of electricity pricing in the system is very important to develop the energy management to make the highest profit.

D) Home Energy Management Systems

Energy management system (EMS) is essential to monitor and control the power flow between generation and consumption sides in a PV-battery GCRS. The main target with EMS is a safe power supply while minimising the electricity cost. The EMS monitors the electricity rates, existent appliances for demand response, forecasted solar PV generation, battery's SOC and loads of the GCRS. Then, based on the monitored data, the EMS decides efficient energy management.

E) Optimisation Algorithms

The applicable optimisation algorithms are probabilistic, artificial intelligence, iterative, analytical, sensitivity analysis, and intuitive approaches. The probabilistic methods can observe the stochastic model of uncertainties and then solve the problem analytically. The artificial intelligence methods can efficiently overcome the nonlinearity of the optimisation model. The artificial intelligence methods can be used for single-objective and multi-objective optimisation problems. Particle swarm optimisation (PSO) method and genetic algorithm (GA) are two worthy examples of single-objective artificial intelligence approaches. The multi-objective (MO) artificial intelligence methods solve the problem in its nature by considering all objective functions and producing set of Pareto-fronts. The non-sorting genetic algorithm II (NSGA-II) and multi-objective particle swarm optimisation (MOPSO) are some substantial examples of these approaches.

In optimal planning by the iterative methods, optimisation problem should be repeated multiple times by random initial conditions. Methods based on sensitivity analysis can achieve the most sensitive capacities to the objectives. In classical mathematical methods, the computational and mathematical model of the system are used for the optimisation. These methods ensure the convergence of the solution to the optimal result. The intuitive methods are useful when exact information and data about the system are not available. The optimisation algorithm should be selected due to defined objective functions and the system model.

F) Software Tools

Software tools can be used for operation analysis, techno-economic analysis and optimal sizing of PV and BES in grid-connected residential sector. Some of the important software are: HOMER [46], TRNSYS [47], RETScreen [48], HYBRID2 [49], iHOGA [50] and Sunny Design [51] which can be used for sizing of PV and BES in GCRS. A comprehensive review on software tools is provided in [52]. The pros and cons of software tools are investigated in [53].

2.1.3 *Present Status and Technical Challenges in PV-battery Optimal Planning*

The present status of the existing studies and technical challenges in PV-battery optimal planning for GCRS are investigated in this section.

A) Present Status: Review of the Existing Studies

A review on state-of-the-art studies on optimal planning of PV-battery for GCRS are investigated in this section. The studies are classified into three groups: (1) optimal planning of only solar PV system, (2) optimal planning of only BES, and (3) optimal planning of PV and BES. Each group is investigated based on the objective function, design constraints, optimisation method, type of electricity rates, input data and the country in which the study was conducted. The first group is important for the households which are not equipped with solar PV. The second group of studies represents the optimal capacity of BES for the households who already equipped with PV panels. The third group of studies presents the optimal sizing of PV-battery for the households without any renewable resources.

According to the literature review, more than 80 studies were performed on optimal sizing of PV and BES for GCRS in all journals and conferences. Fig. 10 shows the number of publications per year from 2008 to 2020 in PV-battery optimal planning for GCRS. As illustrated in Fig. 2-5, the number of publications has increased from 2016. In 2017, the number of publications was 13 as the highest number per year.

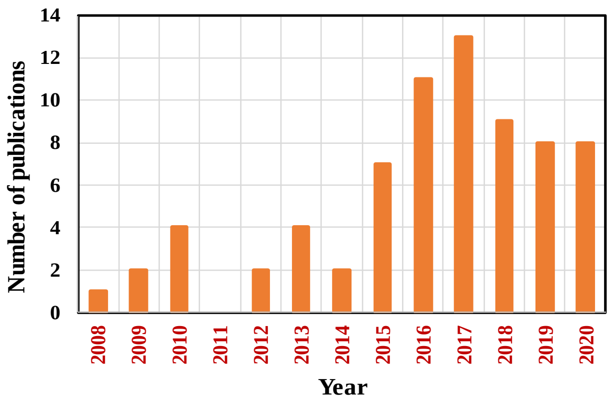

Figure 2-5. Number of publications per year from 2008 to 2020 in PV-battery optimal planning for grid-connected residential sector.

a) Optimal Planning of Only Solar PV System

Table 2-3 lists the reference number, optimisation method, objective function and design constraints, electricity tariff and the studied country for optimal sizing of only PV in GCRS. Several studies not only optimised the PV capacity but also optimised the other factors associated with the solar PV system. Various factors such as tracking system [54], inverter type [58], inverter capacity [61] and tilt angle [60]-[62]-[64] are optimised along with PV capacity. HOMER software, as the most used simulation tool, was employed by four studies to optimise the capacity of solar PV [54, 56, 60-61]. Other software tools like TRNSYS [55] and Sunny Design [63] are also used for optimal sizing. Although the NPV was used as the objective function by most of the studies, a few papers applied COE [55], IRR [65] and PV system energy [58] as the objective function. The flat electricity pricing program was considered in most of the studies. TOU and stepwise electricity pricing programs were only used by [54] and [56], respectively.

Table 2-3. Characteristics of studies on optimal planning of only solar PV for grid-connected residential sectors.

Ref.	Decision Variable	Optimisation Method	Objective Function	Design Constraints	Electricity Tariff	Country
[54]	PV capacity and its tracking system	HOMER	Net present value	Power balance, PV size	Time-of-use	Saudi Arabia
[55]	PV capacity	TRNSYS	Cost of electricity	Energy balance	Flat	United Kingdom
[56]	PV capacity	HOMER	Net present value	Not specified	Stepwise	Malaysia
[57]	PV capacity	GA and PSO	Net present value	Power outage schedules	Flat	Lebanon
[58]	PV module technology and inclination, the inverter type and the location	Energy approach	PV system energy	Not specified	Flat	France
[59]	PV capacity	PSO and GA	Net present value	Not specified	Flat	Greece
[60]	PV capacity and slop of array	HOMER	Net present value	Not specified	Flat	Australia
[61]	PV array and inverter size	HOMER	Net present value	Not specified	Flat	Saudi Arabia
[62]	Number, tilt angle and arrangement of PV modules, and inverters	GA	Net present value Payback period Internal rate of return	Not specified	Flat	Greece
[63]	PV capacity	Sunny Design	Net present value	Not specified	Flat	Morocco
[64]	PV capacity number, tilt angle and placement of PV modules	MOPSO	Net present value	Not specified	Flat	Greece
[65]	PV capacity	Self-developed	Internal rate of return	Not specified	Flat	Austria
[66]	PV capacity	Weighted Sum	Net present value Payback period Energy saving	Budget and rooftop limits	Not specified	South Africa

b) Optimal Planning of Only BES System

Table 2-4 lists the characteristics of studies on optimal sizing of only BES for grid-connected residential sector with PV. In [67-68], the system operation was also optimised alongside the BES capacity optimisation. The software simulation tools are not used for battery optimal sizing. Most of the studies developed the optimisation code using MATLAB or GAMS. In [67], a multi-objective optimal sizing was developed by considering NPV and self-efficiency ratio as the objective functions. In [78], the optimal planning of PV and battery was examined for three types of batteries known as lead-acid, lithium-iron-phosphate, and lithium-nickel-manganese-cobalt. The results of their study showed that the lithium-iron-phosphate has the best economic results for the GCRS if the customer has 6 kW solar PV and a load demand of higher than 6 MWh per year. In [81], various objective functions were optimised using NSGA-II. The constraints of power balance and SOC of battery were applied in most of the studies. Unlike the studies for only PV optimal sizing (Table 2-3), the TOU pricing program was frequently used for BES capacity optimisation. The studies mostly conducted for developed countries like Australia, Germany, etc.

Table 2-4. Characteristics of studies on optimal planning of only battery storage for grid-connected residential sectors.

Ref.	**Decision Variable**	**Optimisation Method**	**Objective Function**	**Design Constraints**	**Electricity Tariff**	**Country**
[67]	BES capacity and operation	NSGA-II	Net present value Self-sufficiency ratio	Power balance, SOC of battery	Time-of-use	Sweden
[68]	BES capacity and Charging/discharging regime	Stochastic mixed integer nonlinear programming	Annual electricity cost	Not specified	Flat	Not specified
[69]	BES capacity	Not specified	Internal rate of return	Not specified	Flat	Germany
[70]	BES and converter capacities	Not specified	Self-consumption	Not specified	Flat	Germany
[71]	BES capacity	GAMS	Net present value	Power balance, SOC of battery	Time-of-use	United States
[72]	BES capacity	Mixed integer linear programming CPLEX	Net present value	SOC and energy of BES, peak shaving limit	Time-of-use	United States
[73]	BES capacity	Self-developed in MATLAB	Net present value	Not specified	Flat	Italy Switzerland UK
[74]	BES capacity	Convex programming in MATLAB	Net present value	Power balance, SOC of battery, import/export power	Time-of-use	United States
[75]	BES capacity	Self-developed in MATLAB	Net present value	Power balance, SOC of battery, purchase/sell power	Time-of-use	Australia
[76]	BES capacity	Stochastic simulation using Monte Carlo	Lifecycle cost	Not specified	Not specified	United Kingdom
[77]	BES capacity	Off-line linear programming	Return of investment	Power balance, SOC of battery,	Not specified	Not specified

		in MATLAB		import/export power		
[78]	BES capacity	Dual-simplex algorithm in matlab	Net present value	Power balance, SOC of battery	Flat	Germany
[79]	BES capacity	Mixed integer programming with ILOG CPLEX	Annual net payment	Power balance, SOC of battery	Flat	Luxembourg
[80]	BES capacity	Mixed integer programming with CPLEX-MATLAB	Total annual cost	Bidirectional power flow and SOC of BES	Flat Time-of-use	Australia
[81]	BES capacity	TRNSYS and NSGA-II	Net present value CO_2 emission PV efficiency Load cover ratio	Power balance, SOC of battery	Time-of-use	China

c) Optimal Planning of PV-battery System

Table 2-5 lists the characteristics of studies on optimal sizing of PV and BES for grid-connected residential sector. A few studies considered the optimisation of operation [82], dispatch [83], energy scheduling [84] and energy flow [89] alongside the PV-battery optimal sizing. Genetic algorithm was used as the optimisation algorithm in [86]. Mixed-integer linear programming (MILP) was frequently used for optimal sizing. While financial objective functions were used in most of the studies, only in [90], maximising the amount of power fed back to the grid was considered as the objective function. Various design constraints such as power balance, battery, and grid limitations, as well as renewable factor were conducted in the existing studies. The flat and TOU were the most applied electricity pricing programs. Again, most of the PV-battery optimal sizing studies were conducted for developed countries.

Table 2-5. Characteristics of studies on optimal planning of solar PV and battery for grid-connected residential sectors.

Ref.	Decision Variable	Optimisation Method	Objective Function	Design Constraints	Electricity Tariff	Country
[82]	PV-BES capacity and operation	Mixed integer programming with CPLEX-GAMS	Net present value	Power balance, charging/ discharging and SOC limits of battery	Flat	Not specified
[83]	PV-BES capacity and dispatch	NREL's Renewable Energy Optimisation (REopt) model	Life cycle cost	Power balance	Time-of-use	United States
[84]	PV-BES capacity and energy schedule	Mixed integer programming, CPLEX	Net present value	Not specified	Time-of-use	Australia
[85]	PV-BES capacity	Mixed integer programming, GAMS	Net present value	Not specified	Flat	Australia

[86]	PV-BES capacity	GA	Net present value	Numbers of PV and BES Renewable factor	Not specified	Australia
[87]	PV-BES capacity	Mixed integer programming, CPLEX	Net present value	Not specified	Time-of-use	Australia
[88]	PV-BES capacity	HOMER	Cost of electricity	Not specified	Time-of-use	India
[89]	PV-BES capacity and energy flow	Mixed integer programming, Python	Net present value	Power balance Budget	Time-of-use	Australia Germany
[90]	PV-BES capacity	Probabilistic-based sizing tool	Maximise amount of power fed back to the grid	Not specified	Not specified	United States
[91]	PV-BES capacity	Self-developed in MATLAB	Cost of electricity	SOC of battery Budget	Not specified	United Kingdom
[92]	PV-BES capacity	DICOPT solver in GAMS	Annual operation cost	Power balance SOC of battery Import/export power	Time-of-use Stepwise Real time pricing	China
[93]	PV-BES capacity	Not specified	Self-consumption Annual electricity cost	Not specified	Flat	Germany
[94]	PV-BES capacity	Direct search method	Net present value	Not specified	Time-of-use	Australia
[95]	PV-BES capacity	Sensitivity tool	Life cycle cost	Not specified	Not specified	Turkey
[96]	PV-BES capacity	Mixed-integer linear optimisation	Operating and investment costs	Power balance SOC of battery	Flat	Germany
[97]	PV-BES capacity	Stochastic mixed integer optimisation in GAMS	Operating and investment costs	Power balance, charging/ discharging and SOC limits of battery	Time-of-use	United States
[98]	PV-BES capacity	Hybrid MILP and a heuristic optimisation algorithm	Electricity cost	Power balance SOC of battery	Flat	Germany
[99]	PV-BES capacity	Self-developed in MATLAB	Annual electricity cost	Power balance, SOC of battery, grid limits, renewable factor	Flat	Not specified

B) Technical Challenges

Although several papers have conducted studies on optimal sizing of PV and BES for grid-connected residential sector, there are multiple technical challenges in the present status. The flat and TOU electricity rates were frequently used by most of the studies. The stepwise electricity rate was employed only in two studies [56] and [92]. The RTP was used only in [92]. Please note that application of stepwise or RTP pricing is not a challenge alone. But new energy management systems should be developed to control the power flow in the GCRS based on the electricity price variations. For example, in a RTP program, the electricity price changes hourly or half-hourly. Hence, new EMSs should have the capability to receive the forecast data of solar insolation and load consumption to achieve the most efficient operation. Hence, the optimal sizing of PV and BES for GCRS under stepwise, dynamic, and critical peak pricing electricity rates should be adequately analyzed. The energy management systems were developed in several studies. A few of the developed EMS considered the demand side management [67]. The load shifting and curtailment as well as incentive demand response need further investigations. Several objective functions like grid dependency, dumped energy and customer satisfaction were neglected by the existing studies. Battery capacity degradation model in optimal planning is an important factor which was not adequately studied in the literature. Most of the studies are conducted based on hourly arranged yearly data. Investigations of long-period data (e.g., 10 years) or high resolution (e.g., 5 minutes) was not addressed. A high-resolution data can assist the designers to not only examine the planning but also validate dynamic performance at the meantime to achieve the most practical results. The robust optimisation and novel metaheuristic approaches were not examined for PV-battery optimal sizing in GCRS.

2.1.4 Recent Developments in Optimal Planning

A) Guideline for Customers

Guidelines can be provided for the customers to advise them to purchase the optimal capacity of solar PV and battery systems. Flat electricity rate can be considered for import/export energy from/to the main grid. The guidelines can be developed based on the available rooftop area and the average daily electricity consumption of residential households. It was shown that as the daily electricity demand of the household increases the integrated capacity of PV boosts. Based on the guidelines, it is understandable that the recent BES market price is not economically efficient for integration in the grid-connected households. Such guidelines are very helpful for customers to render the most economic capacity of PV and BES for their households in urban area. Guidelines based on the other electricity rates such as TOU or RTP are neglected in the literature.

B) Robust Optimal Planning

In [100], an adaptive robust optimal planning and operation was proposed for PV-BES in grid-connected homes. The polyhedral sets were used to model the uncertainties of solar PV generation and load consumption. The developed robust planning was based on the worst-case realization of uncertain parameters. The optimisation problem was solved by an outer min challenge known as "here-and-now" decisions for PV and BES sizing and an inner max-min challenge to determine the operation variables known as "wait-and-see" decisions. It was approved that the main features of robust optimisation for PV and BES sizing over conventional methods like scenario generation, Monte Carlo simulation, K-means data clustering and probability distribution functions are reliability and tractability of the method. The robust optimisation approach solves the planning problem based on bounded interval of uncertainty sets which eliminates the requirement of scenario generation. Robust planning based on the uncertainty in RTP is not studied in the literature.

C) Multi-objective Optimal Planning Considering the Autonomy

In [101], the MOPSO methodology was used for multi-objective optimal sizing of solar PV and BES in grid-connected households. Energy autonomy, power autonomy, payback period and lifetime capital cost were considered as the objective functions. The methodology optimally achieved the azimuth angle of PV panels and capacity of PV and BES. The lifetime of battery was estimated based on total capacity fade during the operation. Such multi-objective studies are very useful for the customers to not only consider the cost as an objective function, but also check the autonomy of the system operation for various capacities of PV and BES.

D) Detailed Model of Lead-acid Battery Lifetime Estimation

In [102], the optimal design conducted for a residential microgrid with lead-acid battery and solar PV based on the minimisation of COE. The decision variables were selected as the number of BES and PV panels, as well as the optimal value of battery depth-of-discharge (DOD) and the tilt angle of the photovoltaic panels. This paper deployed a detailed model of lead-acid battery based on the battery voltage, current and SOC performance. The developed model then considered the replacement of BES (battery lifetime estimation), in the project lifespan, based on the discharge current, SOC impacts, acid stratification, number of cycles and the sulfate-crystal structure. The study considered an annual loss of power supply based on the grid-interruptions to maximise the reliability of the designed PV-battery system. Because optimal planning problem is a long-period challenge, such studies are very useful to achieve an accurate lifetime of battery during the project lifespan. Based on the estimated lifetime of battery, more accurate economic results are attainable for the project.

E) Optimal Planning by Considering the Operation of Water Heater

In [103], a net zero energy home was investigated to optimally capacity the battery based on electric water heater operation. Based on the developed model with scheduling the charging/discharging of BES and power consumption of electric water heater, GCRS could operate like a dispatchable load or generator in the grid. Multiple objective functions including 1) minimising battery energy capacity, 2) minimising variations in grid output power, 3) maximising the rated power of battery, and 4) maximising the financial profit for the customer were considered. The results of the study showed that by coordinating the battery storage and electric water heater with the generated power of solar PV, smaller capacities of BES are attained for the customers.

2.1.5 Potential Direction for Research Works

Based on the aforementioned technical challenges and recent developments, the directions for future work are discussed in this section.

A) Demand Response and Optimal Planning

Demand response is an impressive factor in optimal sizing of a PV-battery system for GCRS. Forecasts of solar insolation, load consumption and electricity rates are important to render useful insights for the demand response action. Efficient demand response programs can effectively decrease the capacity of the PV and battery, and hence decrease the cost of the system. However, the DR programs diminish the satisfaction of the customers for the electricity availability. Objective function like customer satisfaction (i.e., user’s convenience/comfort level) is very helpful to be considered in the optimal sizing with a DR framework [104]. The CS objective function shows that how much the customers are satisfied by the demand response program. To achieve a maximum CS in GCRS, three strategies can be conducted (1) the time for load shifting can be minimised, (2) the load curtailment can be minimised, and (3) the incentive payments for contribution in DR program can be maximised. A multi-objective optimal planning of PV-battery system for a GCRS by considering the NPV and customer satisfaction is strongly recommended.

B) Dynamic Electricity Rates and Optimal Planning

Dynamic electricity rate (i.e., RTP) forces the customers to develop efficient energy management systems. In this case, demand response and charging/discharging of battery are of much important aspects in the energy management under RTP. The main aim is to maximise the profits by monitoring and controlling the energy flow in the GCRS based on the market prices [105]. This trend completely affects the optimal capacity of PV and BES for residential sector. A bilevel optimisation model is recommended to optimise (1) the capacity of PV and BES, and (2) the operation (energy management system) of the system.

C) Resilient PV-Battery Planning

A resilient PV-battery optimal planning is an opportunity to strengthen the load supply probability using the PV-battery system in grid outages [106]. Natural disasters are the main reasons for grid outages which can jeopardize the resiliency of the network. Since the natural disasters are mostly unpredictable, considering probability distribution functions based on the type of the disaster can be integrated into the optimal sizing problem. This can enhance the resiliency of the designed PV-battery system. New design factors like a limitation for the maximum load supply during the grid outage can be accounted for the resiliency in GCRS.

D) Grid Dependency in Optimal Planning

The customers tend to decrease their dependency on the main grid by the installed PV-battery system. In such condition, grid dependency (GD) can be identified as a new objective function. Grid dependency is the fraction of imported electricity from the main grid over the total electricity demand by the residential sector. It is notable that when the GD is zero, it means that the GCRS operates as a standalone system with PV and battery. Increasing the capacity of PV and BES can decrease the GD of the GCRS; however, this trend increases the system costs. Hence, a trade-off between the cost of electricity and grid dependency is important from the customer point of view.

E) Distribution Network Considerations in Optimal Planning

Increasing the number of embedded solar PV panels in low voltage distribution feeders may cause new challenges. One of the main challenges is voltage increase, which may result in restriction of the solar PV hosting capacity by the distribution feeders. Some remedies are efficient management of the battery storage and demand response in the GCRS [107]. Therefore, optimal sizing by considering the voltage increase crisis in distribution network is a new trend for the future studies.

F) Aggregator Viewpoint Optimal Planning

Aggregator entities have facilitated the participation of small-scale PV-battery system (e.g., in households) in electricity markets. In this case, customers are needed to control their power consumption based on the aggregator's requirements for demand response. In some cases, aggregators may encourage the customers in a localized area to use a central battery storage. Based on the contracts with the aggregators, the optimal capacity of PV and BES may be changed in GCRS.

G) Strategies for Planning in Households with EV

Recently, electric vehicles (EVs) have become popular transportation fleet due to environmental concerns. The EVs could be charged at the premises of the households. This would increase the electricity bill of the residential customer. When the EV is charged at home, the energy management system and subsequently the optimal planning of PV and BES are affected. Since the EV arrives home at evening time, the PV generation is not available and hence the BES can be discharged to not only supply the loads of the home but also charge the EV' battery. Hence, a larger capacity of the BES may be required for the residential households with EV. In addition, a higher capacity of PV may be needed to charge a large battery. On the other side, the vehicle-to-grid (V2G) and vehicle-to-home (V2H) capabilities of EV may increase the profitability of the PV-battery system in the GCRS. This makes the EMS of the household with EV more complicated. Therefore, the future studies can examine the consideration of EVs in the household while implementing the optimal planning of PV and BES.

2.1.6 Conclusion on the PV-Battery Optimal Sizing Review

This review investigated a survey on the state-of-the-art optimal sizing of solar PV and BES for GCRS. The problem was overviewed by classifying the important parameters which can affect the optimal capacity of PV and BES in a GCRS. The applied electricity pricing programs, objective functions, design constraints, home energy management systems, optimisation methodologies and input data were investigated. The existing studies were classified based on the decision variables: (1) only PV sizing, (2) only BES sizing, and (3) PV-BES sizing. The technical challenges were identified, and recent research developments were explained. The future directions were introduced to the researchers.

The main implications of this review are as follows:

- Practical guidelines would be useful for the customers in residential sector to purchase the optimal capacity of PV and battery based on all practical factors. However, only one practical guideline was published in the existing studies which provided the guideline based on Flat electricity price. More guidelines should be generated for the customers with other electricity prices.
- While several studies have been published on optimal planning by considering

Flat and TOU electricity prices, the variable tariffs have been rarely investigated. By the advancement of smart grid facilities, optimal planning of PV and battery needs careful investigation under real time pricing for electricity exchange between the customer and the network.

- Practical demand response strategies would be useful for customers to reduce the capacity of PV and battery and hence the costs of the system. This would be possible by load shifting or curtailment of controllable loads such as heating, ventilation, and air conditioning (HVAC) loads in the households.
- Optimal planning of the grid-connected customers with electric vehicle would be a hot topic for the researchers. This is a major implication because of the growing penetration level of EVs in the residential sector.
- New factors like grid dependency, distribution network limitations, and resiliency are among the hot topics recently. The customers would like to see how much autonomy could be achieved by different capacity of PV and battery in their household. In addition, which capacity of PV and battery could give them a resilient system against grid outages. The distribution networks face several challenges due to high penetration of rooftop solar PV systems.

References

[1] International Energy Agency, World Energy Outlook, 2018.

[2] M. Combe, et al., "Cost effective sizing of an AC mini-grid hybrid power system for a remote area in South Australia," *IET Generation, Transmission and Distribution*, vol. 13, iss. 2, pp. 277 – 287, 2019.

[3] M. Combe, et al., "Optimal Sizing of an AC-Coupled Hybrid Power System Considering Incentive-based Demand Response," *IET Generation, Transmission and Distribution*, vol. 13, iss. 15, pp. 3354 – 3361, 2019.

[4] Renewables 2020 Global Status Report, [Online], Available: https://www.ren21.net/reports/global-status-report/?gclid=CjwKCAjw1K75BRAEEiwAd41h1Dxzm8phSkeMwiySxt38eWF7g0Zo5GzfooKdq3f70lAU6Fd5PzeymhoCYRoQAvD_BwE

[5] A. Jäger-Waldau, A. PV Status Report 2019; Publications Office of the European Union: Luxembourg, 2019.

[6] A. Jäger-Waldau, "Snapshot of Photovoltaics—February 2020," *Energies*, vol. 13, pp. 930, Feb. 2020.

[7] M.A. Hayat, F. Shahnia, and GM Shafiullah, "Replacing flat rate feed-in tariffs for rooftop photovoltaic systems with a dynamic one to consider technical, environmental, social, and geographical factors," *IEEE Transactions on Industial Informatics*, vol. 15, no. 7, pp. 3831-3844, Jul. 2019.

[8] T. Georgitsioti, N. Pearsall and I. Forbes, "Simplified levelised cost of the domestic photovoltaic energy in the UK: the importance of the feed-in tariff scheme," *IET Renewable Power Generation*, vol. 8, no. 5, pp. 451-458, Jul. 2014.

[9] K. Jalilpour, et al., "Optimal sizing of energy storage system," Chapter 9, in *Variability, Scallability, and Stability of Microgrids* by S. M Muyeen, Syed Islam, and Frede Blaabjerg, The Institution of Engineering and Technology (IET), UK, June 2019, pp. 263–289.

[10] A. S. Hassan, L. Cipcigan, and N. Jenkins, "Optimal battery storage operation for PV systems with tariff incentives," *Applied Energy*, vol. 203, pp. 422-441, 2017.

[11] Y. Wu, J. Lin and H. Lin, "Standards and Guidelines for Grid-Connected Photovoltaic Generation Systems: A Review and Comparison," *IEEE Transactions on Indutry Applications*, vol. 53, no. 4, pp. 3205-3216, July-Aug. 2017.

[12] R. Panigrahi, S. K. Mishra, S. C. Srivastava, A. K. Srivastava and N. N. Schulz, "Grid Integration of Small-Scale Photovoltaic Systems in Secondary Distribution Network—A Review," *IEEE Transactions on Indutry Applications*, vol. 56, no. 3, pp. 3178-3195, May-June 2020.

[13] A. Anzalchi, and A. Sarwat, "Overview of technical specifications for grid-connected photovoltaic systems," *Energy conversion and management*, vol. 152, pp. 312-327, 2017.

[14] B. Parida, S. Iniyan, and R. Goic, "A review of solar photovoltaic technologies," *Renewable and sustainable energy reviews*, vol. 15, iss. 3, pp. 1625-1636, 2011.

[15] M. A. Eltawil, and Z. Zhao, "Grid-connected photovoltaic power systems: Technical and potential problems—A review," *Renewable and sustainable energy reviews*, vol. 14, iss. 1, pp. 112-129, 2010.

[16] C. Lupangu, and R. C. Bansal, "A review of technical issues on the development of solar photovoltaic systems. *Renewable and Sustainable Energy Reviews*, vol. 73, pp. 950-965, 2017.

[17] J. Jana, H. Saha, and K. D. Bhattacharya, "A review of inverter topologies for single-phase grid-connected photovoltaic systems," *Renewable and Sustainable Energy Reviews*, vol. 72, pp. 1256-1270, 2017.

[18] W. Xiao, M. S. El Moursi, O. Khan, and D. Infield, "Review of grid-tied converter topologies used in photovoltaic systems," *IET Renewable Power Generation*, vol. 10, iss.10, pp. 1543-1551, 2016.

[19] R. Luthander, J. Widén, D. Nilsson, and J. Palm, "Photovoltaic self-consumption in buildings: A review," *Applied Energy*, vol. 142, pp. 80-94, 2015.

[20] M.A. Omar, and M.M. Mahmoud, "Grid-connected PV-home systems in Palestine: A review on technical performance, effects and economic feasibility," *Renewable and Sustainable Energy Reviews*, vol. 82, pp. 2490-2497, 2018.

[21] H. Jr, de Faria, F. B. Trigoso, and J. A. Cavalcanti, "Review of distributed generation with photovoltaic grid connected systems in Brazil: Challenges and prospects," *Renewable and Sustainable Energy Reviews*, vol. 75, pp. 469-475, 2017.

[22] M. Senatla, R. C. Bansal, R. Naidoo, L. Chiloane and U. Mudau, "Estimating the economic potential of PV rooftop systems in South Africa's residential sector: a tale of eight metropolitan cities," *IET Renewable Power Generation*, vol. 14, no. 4, pp. 506-514, Mar. 2020.

[23] J. Liu, X. Chen, S. Cao, and H. Yang, "Overview on hybrid solar photovoltaic-electrical energy storage technologies for power supply to buildings," *Energy conversion and management*, vol. 187, pp. 103-121, 2019.

[24] V. Vega-Garita, L. Ramirez-Elizondo, G. R. C. Mouli, and P. Bauer, "Review of residential PV-storage architectures," *In 2016 IEEE International Energy Conference (ENERGYCON)*, pp. 1-6. IEEE, 2016.

[25] J. Hoppmann, J. Volland, T. S. Schmidt, and V. H. Hoffmann, "The economic viability of battery storage for residential solar photovoltaic systems–A review and a simulation model," *Renewable and Sustainable Energy Reviews*, vol. 39, pp. 1101-1118, 2014.

[26] E. O'Shaughnessy, D. Cutler, K. Ardani, and R. Margolis, "Solar plus: A review of the end-user economics of solar PV integration with storage and load control in residential buildings," *Applied Energy*, vol. 228, pp. 2165-2175., 2018.

[27] E. Tervo, K. Agbim, F. DeAngelis, J. Hernandez, H. K. Kim, and A. Odukomaiya, "An economic analysis of residential photovoltaic systems with lithium ion battery storage in the United States," *Renewable and Sustainable Energy Reviews*, vol. 94, pp. 1057-1066, 2018.

[28] O. M. Toledo, D. Oliveira Filho, and A. S. A. C. Diniz, "Distributed photovoltaic generation and energy storage systems: A review," *Renewable and Sustainable Energy Reviews*, vol. 14, iss. 1, pp. 506-511, 2010.

[29] D. Azuatalam, K. Paridari, Y. Ma, M. Förstl, A. C. Chapman, and G. Verbič, "Energy management of small-scale PV-battery systems: A systematic review considering practical implementation, computational requirements, quality of input data and battery degradation," *Renewable and Sustainable Energy Reviews*, vol. 112, pp. 555-570, 2019.

[30] S. Agnew, and P. Dargusch, "Consumer preferences for household-level battery energy storage," *Renewable and Sustainable Energy Reviews*, vol. 75, pp. 609-617, 2017.

[31] B. D. Olaszi, and J. Ladanyi, "Comparison of different discharge strategies of grid-connected residential PV systems with energy storage in perspective of optimal battery energy storage system sizing," *Renewable and Sustainable Energy Reviews*, vol. 75, pp. 710-718, 2017.

[32] A. Mellit, S. A. Kalogirou, L. Hontoria, and S. Shaari, "Artificial intelligence techniques for sizing photovoltaic systems: A review," *Renewable and Sustainable Energy Reviews*, vol. 13, iss. 2, pp. 406-419, 2009.

[33] T. Khatib, I. A. Ibrahim, and A. Mohamed, "A review on sizing methodologies of photovoltaic array and storage battery in a standalone photovoltaic system," *Energy Conversion and Management*, vol. 120, pp. 430-448, 2016.

[34] R. Rawat, S. C. Kaushik, and R. Lamba, "A review on modeling, design methodology and size optimization of photovoltaic based water pumping, standalone and grid connected system," *Renewable and Sustainable Energy Reviews*, vol. 57, pp. 1506-1519, 2016.

[35] M. P. HA, P. D. Huy, and V. K. Ramachandaramurthy, "A review of the optimal allocation of distributed generation: Objectives, constraints, methods, and algorithms," *Renewable and Sustainable Energy Reviews*, vol. 75, pp. 293-312, 2017.

[36] T. Khatib, A. Mohamed, and K. Sopian, "A review of photovoltaic systems size optimization techniques," *Renewable and Sustainable Energy Reviews*, vol. 22, pp. 454-465, 2013.

[37] R. Singh, and R. C. Bansal, "Review of HRESs based on storage options, system architecture and optimisation criteria and methodologies," *IET Renewable Power Generation*, vol. 12, iss. 7, pp. 747-760, Jun. 2018.

[38] Y. Yang, S. Bremner, Ch. Menictas, and M. Kay, “Battery energy storage system size determination in renewable energy systems: A review,” *Renewable and Sustainable Energy Reviews*, vol. 91, pp. 109–125, 2018.
[39] M. Zidar, P. S Georgilakis, N. D Hatziargyriou, T. Capuder, and D. Škrlec, “Review of energy storage allocation in power distribution networks: applications, methods and future research,” *IET Generation, Transmission and Distribution*, vol. 10, iss. 3, pp. 645 – 652, Feb. 2016.
[40] A. Dolatabadi and B. Mohammadi-Ivatloo, “Stochastic Risk-Constrained Optimal Sizing for Hybrid Power System of Merchant Marine Vessels,” *IEEE Transactions on Industrial Informatics*, vol. 14, no. 12, pp. 5509-5517, Dec. 2018.
[41] N. Amin, S.A. Shahahmadi, P. Chelvanathan, K.S. Rahman, M.I. Hossain, and M.D. Akhtaruzzaman, “Solar photovoltaic technologies: from inception toward the most reliable energy resource,” *Encyclopedia of sustainable technologies*, pp. 11-26, 2017.
[42] M. Faisal, M.A. Hannan, P.J. Ker, A. Hussain, M.B. Mansor, and F. Blaabjerg, “Review of energy storage system technologies in microgrid applications: Issues and challenges,” *IEEE Access*, vol. 6, pp. 35143-35164, 2018.
[43] S. Koohi-Fayegh, and M.A. Rosen, “A review of energy storage types, applications and recent developments,” *Journal of Energy Storage*, vol. 27, pp. 101047, 2020.
[44] M. Aneke, and M.H. Wang, “Energy storage technologies and real life applications - A state of the art review,” *Applied Energy*, vol. 179, pp. 350-377, 2016.
[45] H. Khorramdel, J. Aghaei, B. Khorramdel and P. Siano, “Optimal Battery Sizing in Microgrids Using Probabilistic Unit Commitment,” *IEEE Transactions on Industrial Informatics*, vol. 12, no. 2, pp. 834-843, April 2016.
[46] S. Bahramara, M. P. Moghaddam, and M. R. Haghifam, “Optimal planning of hybrid renewable energy systems using HOMER: A review,” *Renewable and Sustainable Energy Reviews*, vol. 62, pp. 609-620, 2016.
[47] Y. Rayl, C. Tammineedi, and J. R. Brownson, “PV Analyst: Coupling ArcGIS with TRNSYS to assess distributed photovoltaic potential in urban areas,” *Solar Energy*, vol. 85, iss. 11, pp. 2924-2939, 2011.
[48] A. B. Owolabi, B. E. K. Nsafon, J. W. Roh, D. Suh, and J. S. Huh, “Validating the techno-economic and environmental sustainability of solar PV technology in Nigeria using RETScreen Experts to assess its viability,” *Sustainable Energy Technologies and Assessments*, vol. 36, 2019.
[49] Manwell, J. F., Rogers, A., Hayman, G., Avelar, C. T., McGowan, J. G., Abdulwahid, U., & Wu, K. (2006). Hybrid2–a hybrid system simulation model–theory manual. Renewable Energy Research Laboratory, University of Massachusetts.
[50] P. Ganguly, A. Kalam and A. Zayegh, “Design an optimum standalone hybrid renewable energy system for a small town at Portland, Victoria using iHOGA,” *2017 Australasian Universities Power Engineering Conference (AUPEC)*, Melbourne, VIC, pp. 1-6, 2017.
[51] A. K. Shukla, K. Sudhakar, and P. Baredar, “Design, simulation and economic analysis of standalone roof top solar PV system in India,” *Solar Energy*, vol. 136, pp. 437-449, 2016.
[52] S. Sinha, and S. S. Chandel, “Review of software tools for hybrid renewable energy systems,” *Renewable and Sustainable Energy Reviews*, vol. 32, pp. 192-205, 2014.
[53] R. Singh and R. C. Bansal, “Optimization of an Autonomous Hybrid Renewable Energy System Using Reformed Electric System Cascade Analysis,” *IEEE Transactions on Industrial Informatics*, vol. 15, no. 1, pp. 399-409, Jan. 2019.H. Z. Al
[54] Garni, A. Awasthi, and M. A. Ramli, “Optimal design and analysis of grid-connected photovoltaic under different tracking systems using HOMER,” *Energy conversion and management*, vol. 155, pp. 42-57, 2018.
[55] J. D. Mondol, Y. G. Yohanis, and B. Norton, “Optimising the economic viability of grid-connected photovoltaic systems,” *Applied Energy*, vol. 86, pp. 985-999, 2009.
[56] K. Y. Lau, N. A. Muhamad, Y. Z. Arief, C. W. Tan, and A. H. M. Yatim, “Grid-connected photovoltaic systems for Malaysian residential sector: Effects of component costs, feed-in tariffs, and carbon taxes,” *Energy*, vol. 102, pp. 65-82, 2016.
[57] J. Khoury, R. Mbayed, G. Salloum, and E. Monmasson, “Optimal sizing of a residential PV-battery backup for an intermittent primary energy source under realistic constraints,” *Energy and Buildings*, vol. 105, pp. 206-216, 2015.
[58] G. Notton, V. Lazarov, and L. Stoyanov, “Optimal sizing of a grid-connected PV system for various PV module technologies and inclinations, inverter efficiency characteristics and locations,” *Renewable Energy*, vol. 35, iss. 2, pp. 541-554, 2010.
[59] A. Kornelakis, and Y. Marinakis, “Contribution for optimal sizing of grid-connected PV-systems using PSO,” *Renewable Energy*, vol. 35, iss. 6, pp. 1333-1341, 2010.
[60] G. Liu, M. G. Rasul, M. T. O. Amanullah, and M. M. K. Khan, “Techno-economic simulation and optimization of residential grid-connected PV system for the Queensland climate,” *Renewable Energy*, vol. 45, pp. 146-155, 2012.
[61] M. A. Ramli, A. Hiendro, K. Sedraoui, and S. Twaha, “Optimal sizing of grid-connected photovoltaic energy system in Saudi Arabia,” *Renewable Energy*, vol. 75, pp. 489-495, 2015.
[62] A. Kornelakis and E. Koutroulis, “Methodology for the design optimisation and the economic analysis of grid-connected photovoltaic systems,” *IET Renewable Power Generation*, vol. 3, no. 4, pp. 476-492, Dec. 2009.

[63] M. Khanfara, R. El Bachtiri, M. Boussetta, and K. El Hammoumi, “Economic Sizing of a Grid-Connected Photovoltaic System: Case of GISER research project in Morocco,” *In IOP Conference Series: Earth and Environmental Science* (Vol. 161, No. 1, p. 012006). IOP Publishing, 2018.

[64] A. Kornelakis, “Multiobjective particle swarm optimization for the optimal design of photovoltaic grid-connected systems,” *Solar Energy*, vol. 84, iss. 12, pp. 2022-2033, 2010.

[65] M. Hartner, D. Mayr, A. Kollmann, and R. Haas, “Optimal sizing of residential PV-systems from a household and social cost perspective: A case study in Austria,” *Solar Energy*, vol. 141, pp. 49-58, 2017.

[66] Y. Fan, and X. Xia, “A multi-objective optimization model for energy-efficiency building envelope retrofitting plan with rooftop PV system installation and maintenance,” *Applied energy*, vol. 189, pp. 327-335, 2017.

[67] Y. Zhang, A. Lundblad, P. E. Campana, F. Benavente, and J. Yan, “Battery sizing and rule-based operation of grid-connected photovoltaic-battery system: A case study in Sweden,” *Energy conversion and management*, vol. 133, pp. 249-263, 2017.

[68] R. Hemmati, and H. Saboori, “Stochastic optimal battery storage sizing and scheduling in home energy management systems equipped with solar photovoltaic panels,” *Energy and Buildings*, vol. 152, pp. 290-300, 2017.

[69] M. Naumann, R. C. Karl, C. N. Truong, A. Jossen, and H. C. Hesse, “Lithium-ion battery cost analysis in PV-household application,” *Energy Procedia*, vol. 73, pp. 37-47, 2015.

[70] J. Weniger, T. Tjaden, J. Bergner, and V. Quaschning, “Sizing of battery converters for residential PV storage systems,” *Energy Procedia*, vol. 99, pp. 3-10, 2016.

[71] M. Gitizadeh, and H. Fakharzadegan, “Effects of electricity tariffs on optimal battery energy storage sizing in residential PV/storage systems,” *In 2013 International Conference on Energy Efficient Technologies for Sustainability*, pp. 1072-1077, IEEE, 2013.

[72] Y. Ru, J. Kleissl and S. Martinez, “Storage Size Determination for Grid-Connected Photovoltaic Systems,” *IEEE Transactions on Sustainable Energy*, vol. 4, no. 1, pp. 68-81, Jan. 2013.

[73] S. Barcellona, L. Piegari, V. Musolino and C. Ballif, “Economic viability for residential battery storage systems in grid-connected PV plants,” *IET Renewable Power Generation*, vol. 12, no. 2, pp. 135-142, Feb. 2018.

[74] X. Wu, X. Hu, X. Yin, C. Zhang, and S. Qian, “Optimal battery sizing of smart home via convex programming,” *Energy*, vol. 140, pp. 444-453, 2017.

[75] X. Zhang, Y. Li, M. Skyllas-Kazacos, and J. Bao, “Optimal sizing of vanadium redox flow battery systems for residential applications based on battery electrochemical characteristics,” *Energies*, vol. 9, iss. 10, pp. 857, 2016.

[76] C. W. Tan, T. C. Green, and C. A. Hernandez-Aramburo, “A stochastic method for battery sizing with uninterruptible-power and demand shift capabilities in PV (photovoltaic) systems,” *Energy*, vol. 35, iss. 12, pp. 5082-5092, 2010.

[77] H. Turker and P. Favre-Perrod, “Management, optimal sizing and technical-economic analysis of batteries for constant production in photovoltaic systems,” *IEEE International Conference on Renewable Energy Research and Applications (ICRERA)*, Birmingham, pp. 1055-1061, 2016.

[78] H. C. Hesse, R. Martins, P. Musilek, M. Naumann, C. N. Truong, and A. Jossen, “Economic optimization of component sizing for residential battery storage systems,” *Energies*, vol. 10, iss. 7, pp. 835, 2017.

[79] M. Mehrtash, F. Capitanescu and P. K. Heiselberg, “An Efficient Mixed-Integer Linear Programming Model for Optimal Sizing of Battery Energy Storage in Smart Sustainable Buildings,” *IEEE Texas Power and Energy Conference (TPEC)*, College Station, TX, USA, pp. 1-6, 2020.

[80] U. G. K. Mulleriyawage and W. X. Shen, “Optimally sizing of battery energy storage capacity by operational optimization of residential PV-Battery systems: An Australian household case study,” *Renewable Energy*, 2020.

[81] J. Liu, X. Chen, H. Yang, and Y. Li, “Energy storage and management system design optimization for a photovoltaic integrated low-energy building,” Energy, vol. 190, pp. 116424, 2020.

[82] O. Erdinc, N. G. Paterakis, I. N. Pappi, A. G. Bakirtzis, and J. P. Catalão, “A new perspective for sizing of distributed generation and energy storage for smart households under demand response,” *Applied Energy*, vol. 143, pp. 26-37, 2015.

[83] E. O'Shaughnessy, D. Cutler, K. Ardani, and R. Margolis, “Solar plus: Optimization of distributed solar PV through battery storage and dispatchable load in residential buildings,” *Applied Energy*, vol. 213, pp. 11-21, 2018.

[84] J. Koskela, A. Rautiainen, and P. Järventausta, “Using electrical energy storage in residential buildings–Sizing of battery and photovoltaic panels based on electricity cost optimization,” *Applied Energy*, vol. 239, pp. 1175-1189, 2019.

[85] K. R. Khalilpour, and A. Vassallo, “Technoeconomic parametric analysis of PV-battery systems,” *Renewable Energy*, vol. 97, pp.757-768, 2016.

[86] O. Talent, and H. Du, “Optimal sizing and energy scheduling of photovoltaic-battery systems under different tariff structures,” Renewable energy, vol. 129, pp. 513-526, 2018.

[87] J. Abushnaf, and A. Rassau, “Impact of energy management system on the sizing of a grid-connected PV/Battery system,” *The Electricity Journal*, vol. 31, iss. 2, pp. 58-66, 2018.

[88] K. R. Khalilpour, and A. Vassallo, “Planning and operation scheduling of PV-battery systems: A novel methodology,” *Renewable and Sustainable Energy Reviews*, vol. 53, pp. 194-208, 2016.

[89] Tomar, V., & Tiwari, G. N. (2017). Techno-economic evaluation of grid connected PV system for

households with feed in tariff and time of day tariff regulation in New Delhi–A sustainable approach. Renewable and Sustainable Energy Reviews, 70, 822-835.

[90] J. von Appen, J. H. Braslavsky, J. K. Ward and M. Braun, "Sizing and grid impact of PV battery systems - a comparative analysis for Australia and Germany," *International Symposium on Smart Electric Distribution Systems and Technologies (EDST)*, Vienna, pp. 612-619, 2015.

[91] Xiangqi Zhu, Jiahong Yan and Ning Lu, "A probabilistic-based PV and energy storage sizing tool for residential loads," *IEEE/PES Transmission and Distribution Conference and Exposition (T&D)*, Dallas, TX, pp. 1-5, 2016.

[92] Y. Khawaja, D. Giaouris, H. Patsios and M. Dahidah, "Optimal cost-based model for sizing grid-connected PV and battery energy system," *IEEE Jordan Conference on Applied Electrical Engineering and Computing Technologies (AEECT)*, Aqaba, pp. 1-6, 2017.

[93] L. Zhou, Y. Zhang, X. Lin, C. Li, Z. Cai, and P. Yang, "Optimal sizing of PV and BESS for a smart household considering different price mechanisms," *IEEE Access*, vol. 6, pp. 41050-41059, Jun. 2018.

[94] J. Weniger, T. Tjaden, and V. Quaschning, "Sizing and grid integration of residential PV battery systems," *In 8th International Renewable Energy Storage Conference and Exhibition (IRES 2013)*, Berlin, 2013.

[95] G. Mokhtari, G. Nourbakhsh, and A. Gosh, "Optimal Sizing of Combined PV-Energy Storage for a Grid-connected Residential Building," *Advances in Energy Engineering*, vol. 1, iss. 3, pp. 53-65, 2013.

[96] A. N. Celik, T. Muneer, and P. Clarke, "Optimal sizing and life cycle assessment of residential photovoltaic energy systems with battery storage," *Progress in Photovoltaics: Research and Applications*, vol. 16, iss. 1, pp. 69-85, 2008.

[97] T. Beck, H. Kondziella, G. Huard, and T. Bruckner, "Assessing the influence of the temporal resolution of electrical load and PV generation profiles on self-consumption and sizing of PV-battery systems," Applied energy, vol. 173, pp. 331-342, 2016.

[98] J. Cervantes, and F. Choobineh, "Optimal sizing of a nonutility-scale solar power system and its battery storage," *Applied Energy*, vol. 216, pp. 105-115, 2018.

[99] H. Wolisz, T. Schütz, T. Blanke, M. Hagenkamp, M. Kohrn, M. Wesseling, and D. Müller, "Cost optimal sizing of smart buildings' energy system components considering changing end-consumer electricity markets," *Energy*, vol. 137, pp. 715-728, 2017.

[100] M. Aghamohamadi, A. Mahmoudi, and M. H. Haque "Two-stage Robust Sizing and Operation Co-optimization for Residential PV-battery Systems Considering the Uncertainty of PV Generation and Load," *IEEE Transactions on Industrial Informatics*, Early Access, Apr. 2020.

[101] M. Alramlawi, and P. Li, "Design optimization of a residential PV-Battery microgrid with a detailed battery lifetime estimation model," *IEEE Transactions on Indutry Applications*, vol. 56, no. 2, pp. 2020-2030, Mar.-Apr. 2020.

[102] S. Bandyopadhyay, G. R. C. Mouli, Z. Qin, L. R. Elizondo and P. Bauer, "Techno-Economical Model Based Optimal Sizing of PV-Battery Systems for Microgrids," *IEEE Transactions on Sustainable Energy*, vol. 11, no. 3, pp. 1657-1668, July 2020.

[103] H. Gong, V. Rallabandi, D. M. Ionel, D. Colliver, S. Duerr and C. Ababei, "Dynamic Modeling and Optimal Design for Net Zero Energy Houses Including Hybrid Electric and Thermal Energy Storage," *IEEE Transactions on Industry Applications*, Early Access, 2020.

[104] H. Li, Z. Wan and H. He, "Real-Time Residential Demand Response," *IEEE Transactions on Smart Grid*, Early Access, 2020.

[105] S. S. Barhagh, M. Abapour, and B. Mohammadi-Ivatloo, "Optimal scheduling of electric vehicles and photovoltaic systems in residential complexes under real-time pricing mechanism," *Journal of Cleaner Production*, vol. 246, pp. 119041, 2020.

[106] P. K. C. Wong, A. Kalam and R. Barr, "Modelling and analysis of practical options to improve the hosting capacity of low voltage networks for embedded photo-voltaic generation," *IET Renewable Power Generation*, vol. 11, no. 5, pp. 625-632, Apr. 2017.

[107] S. Hashemi and J. Østergaard, "Efficient Control of Energy Storage for Increasing the PV Hosting Capacity of LV Grids," *IEEE Transactions on Smart Grid*, vol. 9, no. 3, pp. 2295-2303, May 2018.

2.2 Capacity Optimisation of Remote Area Electricity Supply Systems

Optimal sizing of a remote area electricity supply (RAES) system is a vital challenge to achieve a reliable, clean, and cost-effective system. Diesel generators, renewable energy resources, and energy storage systems are essential components for RAES systems. This review presents an overview on the fundamental of optimal sizing procedure in RAES systems by considering the important parameters, methods, and data. It is necessary to summarise the lessons from the existing studies on RAES optimal sizing and detect future opportunities for researchers. Hence, a timely review on the state-of-the-art is presented and the applied objective functions, design constraints, system components, optimisation algorithms, type of system and studied country are specified for the existing studies. The existing challenges in the field are recognized and discussed. Recent trends and developments on the problem are explained in detail. Eventually, this review paper renders the recommendations of the future scopes for researchers intending to explore the optimal sizing of components in RAES systems.

The contribution of this review is presented in one published review paper.
R. Khezri, A. Mahmoudi, H. Aki, and SM Muyeen, "Optimal Planning of Remote Area Electricity Supply System: Comprehensive Review, Recent Developments and Future Scopes," *Energies*, 2021.

The student has developed the conceptualization and necessity of this review study. Analysis and review of research data has been done by him and the co-author. The student prepared a draft of the review paper. Revisions and comments were provided by the co-author so as to contribute to the interpretation.

2.2.1 Introduction

Globally, it is estimated that 17% of the world's population (about 1.2 billion people) lacks access to national electricity [1]. Around 1.1 billion of these people live in Asia and Africa. The remaining 0.1 billion live in the Middle East, Latin America, and the developed countries. In Asia, 512 million people suffer from electricity inaccessibility, where 244 million live in India, 41 million in Indonesia, and 11 million in Philippines [1]. Worldwide, deploying remote area electricity supply (RAES) systems is the main solution to provide and maintain electrification of remote areas [2]. Indeed, a RAES system is a desirable alternative for national grid extensions. Fig. 2-6 shows important sites with the necessity to develop RAES systems. The community or villages, residential buildings, islands, and rural areas are in essential need to provide the human welfare by electrification. Telecommunication, water pumping system, desalination, and agriculture are the requirements for people in remote areas that can be considered for electrification by distributed RAES systems. Mining sites and railways in remote areas also need to be equipped by RAES systems.

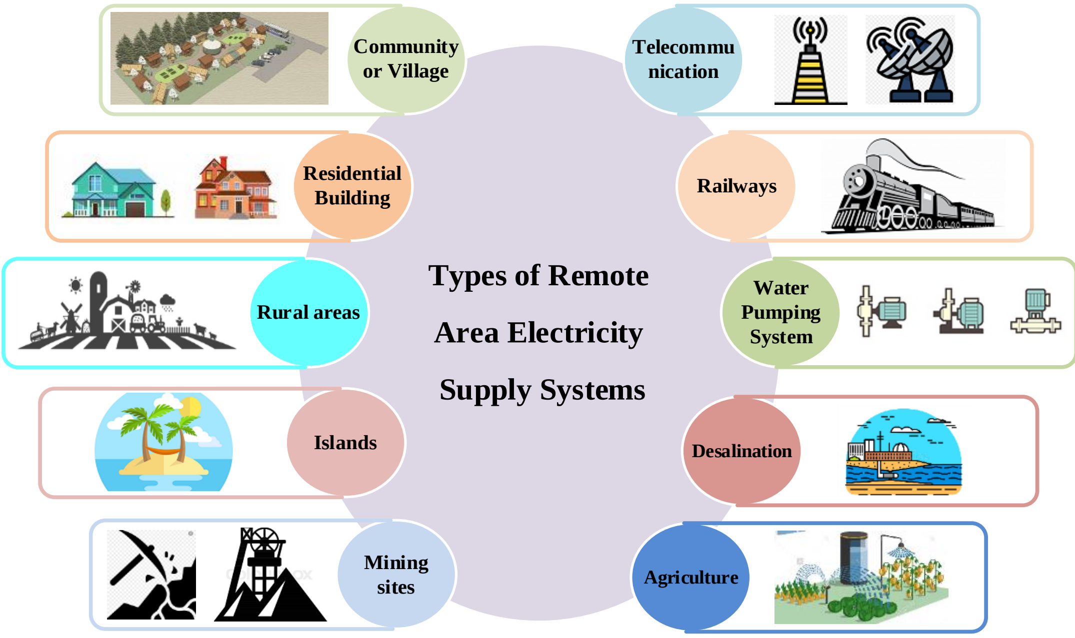

Figure 2-6. Important sites with the necessity to develop RAES systems.

Conventionally, the RAES systems are designed based on diesel generators [3]. Reserves of fossil fuels are, however, limited and depleted rapidly which need urgent attention and appropriate manners to eschew potential energy crisis in the future [4]. In addition, the harmful emission of fossil, including greenhouse gasses (GHGs), contributes to the global warming challenge [5]. Furthermore, the petroleum price is severely fluctuating, especially after the COVID-19 pandemic. National grid's inaccessibility, air pollution and high cost are the other challenges. Generally, remote areas are located far from capital cities. Hence, fuel transportation is another major concern to deliver on time and with the lowest cost. Reliability is the other challenge since the current RAES systems are mostly run with diesel generators as a single source system.

To overcome the aforementioned challenges, distributed renewable energy resources (DRERs) are competent options. The DRERs use the straight environment resources to generate power which will not run out. The DRERs emit little to no greenhouse gases or pollutants into the air. In most cases, DRERs require less maintenance than conventional generators which use traditional fuel sources. On the other side, using DRERs not only decreases the maintenance cost but also reduces the operation cost of the system. Despite all the advantages, DRERs suffer from higher upfront cost, geographic limitations, and high intermittency [6]. Even though the market prices are dropping for DRERs, energy storage systems (ESSs) are essential to overcome the intermittency problem [7]. It is worth noting that the ESS cost is not in a favourable range yet especially when a high capacity is needed in large-scale renewable power plants. Hence, a hybrid diesel generator-DRER-ESS configuration is recommended to achieve an environmental-friendly system with a low cost. A hybrid RAES system with multiple components is, however, a complicated system and optimal sizing of the system is the utmost important part.

Literature survey indicates several review papers on hybrid energy systems (HESs). In [8], the developments of HESs with diesel generators, solar PV, WT, and ESS were reviewed. The study investigated the types of converters and controllers without highlighting the methodology and software for solving the problem. In [9], the PV-WT hybrid renewable systems were reviewed without highlighting any technical challenges in the field. Software tools for hybrid systems based on DRERs were discussed in [10] without highlighting the methodologies. In [11], only the optimisation techniques for HES were investigated without any system challenges. The energy management systems of HESs were explained in [12]. However, it was not addressed that how the management systems can be integrated with optimal sizing. Configurations and control of HESs were investigated in [13] and [14] with less focus on sizing. A comprehensive review on storage options and architectures for HESs was provided in [15] without highlighting their role in RAES. In [16], the HESs were investigated by addressing the model of components without addressing the sizing basics. Microgrid planning by focusing on operation strategies was studied in [17]. However, these studies did not consider HESs for remote areas. The RAES systems should receive greater attention due to critical electrification issues.

Several studies have specifically focused on standalone and remote area systems. In [18], standalone systems with solar PV, WT, and fuel cell (FC) technologies were interrogated for energy management systems. The role of diesel generator, which is highly integrated in RAES systems, was neglected. Applications and technologies of components for RAES were analyzed in [19]. The benefits of designing a HES for off-grid systems was discussed in [20] by briefly describing the models. Different configurations of HESs for off-grid systems with describing the available components were introduced in [21]. Modelling, applications, and control of HESs for electricity supply in standalone systems were considered in [22]. The benefits of decentralized electrification of rural areas were described in [23] by discussing the electricity demand in remote communities. In [24], the development and classification of HESs for electrification in rural areas were discussed. The implementation of HESs in small communities was reviewed in [25]. Performance evaluation of HES in rural areas was conducted in [26]. The optimisation techniques suitable for HESs in standalone systems were discussed in [27] without addressing the advantages and disadvantages of each technique. The mathematical and artificial intelligence methods for optimising the HESs were studied in [28]. However, none of those studies investigated the optimal sizing issue.

In [29], the configuration and sizing of standalone systems were discussed without addressing any critical challenges. In [30], the optimisation process and algorithms were studied. A comprehensive review for topologies, methods, and models was presented in [31]-[32]. In [33], a complimentary review was conducted on the HOMER software tool for optimal sizing. Multi-objective optimal sizing of system components in HESs was overviewed in [34]. Optimal allocation of distributed generation (DG) units were reviewed in [35]-[36]. Reviews on optimal sizing and siting of ESS in distribution networks were conducted in [37] and [38]. Capacity determination of ESS in renewable energy systems and microgrids was reviewed in [39] and [40], respectively. The planning and operation of remote area power supply was discussed in [41]. However, the study in [41] focused more on the control levels of the system without discussing the sizing challenges, trends, and developments.

2.2.2 Overview on Optimal Sizing of RAES Systems

Optimal sizing problem of RAES systems is to determine the best capacity of system components (decision variables) by minimising/maximising objective functions considering feasibility constraints. The optimal sizing algorithms for RAES system design are commenced with input data of the system. Then, the system configuration of the RAES system should be specified. Optimisation algorithm initializes the sizing problem. The operation of the RAES system is evaluated in the next step. Satisfaction of the feasibility constraints is checked after the operation of the RAES system. If all the constraints are satisfied, the objective function is calculated to finalize the optimisation problem.

The first factor to be assigned is the generation and storage components of the system. The necessary input data to start the optimisation needs to be designated. Then, the objective of the project and feasibility constraints should be clearly identified and formulated. Based on the components and constraints, the operation strategy should be developed as an important item. Efficient optimisation methodology should be selected based on the formulated problem. All these items will be deeply discussed in this section.

A) System Components

There are several system components that can be utilized for power supply in remote areas. Fig. 2-7 classifies the components into three groups: (1) fuel-based components, (2) renewable energy components and (3) energy storage components. The fuel-based components like diesel generators or gas generators generate power using fossil fuels and they have high impact on greenhouse gas emission. Recently, there is a variety of renewable energy components that can be integrated with RAES systems. Solar PV, WT, hydropower, tidal power, and biogas generator are the most available and applicable components which can be applied in RAES. However, their application highly depends on the geographical location of the studied site [42]. For example, using tidal power is appropriate for islands. Solar PV systems have a wider application because of sun availability in most locations, easy installation on rooftops, and availability in different scales (from W to MW). The WT systems need a wide land with an acceptable wind to be installed. Hydro power needs to be installed in a location that we have access to dams or almost we can pump water from rivers to reservoirs. Biogas generators will receive higher attention soon because of biomass availability in remote areas [43]. The applicable storage components in RAES systems are battery energy storage (BES), hydrogen energy, thermal storage, and flywheel. The characteristics of different types of ESSs were well explained in the literature [44].

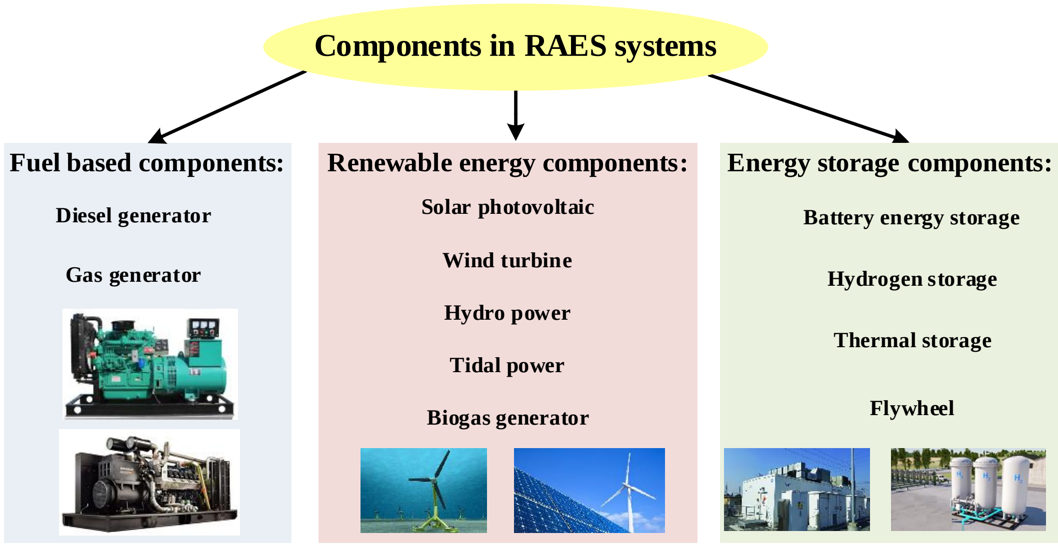

Figure 2-7. System components in remote area electricity supply systems.

B) *Input Data*

Technical and economic data of system components are needed based on the availability in the market of the studied country. The economic data contains the capital cost, maintenance cost and replacement cost of the components. Technical data involves the specifications like the capacity and efficiency of the components. The electricity demand should be available for a long period. The available loads for demand response should be specified in the case system if it contains demand side management [45]. Weather data contains the ambient temperature, solar irradiance, wind speed, water availability in the reservoir and wave speed, which like electricity demand, should be available for a long period. Project data for the study involves the project lifespan, interest/discount rate and escalation rate of fuel. All data should be properly arranged to achieve an accurate optimal sizing study. Any improper input data may result in a nonreliable and expensive system.

C) *Objective Functions*

The most important objective functions for RAES optimal sizing problem are demonstrated in Fig. 2-8. Financial and reliability objective functions are the major types of targets which have been considered. The other objective functions are related to emission and some technical issues. Selection of the objective function depends on the type of study. In most of the cases, financial objective functions are the priorities. Reliability is another concern if the project financial is limited. In some cases, emission is under high attention. Due to different natures of the objectives, optimal sizing in RAES systems can be done by solving a single-objective or sometimes multi-objective optimisation problem. In multi-objective problems, the results are shown in the form of Pareto-fronts and a compromise between the objective functions need to be done.

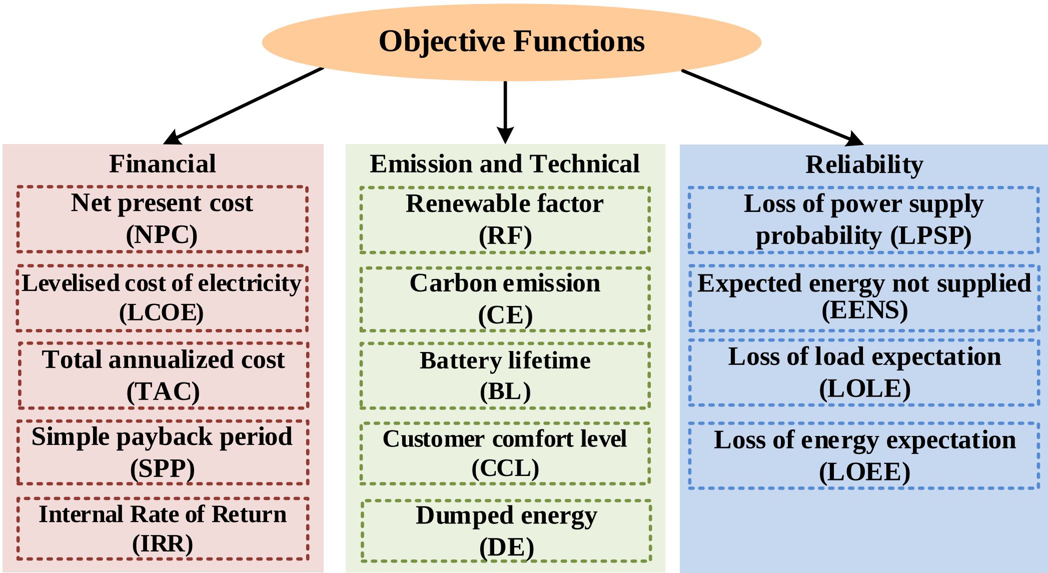

Figure 2-8. Objective functions for optimal sizing of RAES systems.

a) Financial Objective Functions

Net present cost (NPC), levelised cost of electricity (LCOE), total annual cost (TAC), simple payback period (SPP) and internal rate of return (IRR) are the functions that can be used as financial objectives. The NPC is the summation of total present costs of capital, maintenance, replacement, and salvage of components, as well as the present cost of fuel consumption in the case that diesel generator is integrated. The LCOE is calculated by multiplication of NPC by capital recovery factor over the annual energy demand of the system. The TAC is the sum of annual capital and maintenance costs and annual fuel cost. The SPP is the number of years to pay back the capital cost of components by the annual profits. The IRR is the discount rate that makes the NPC of all cash flows equal to zero.

b) Reliability Objective Functions

Loss of power supply probability (LPSP) expected energy not supplied (EENS), loss of load expectation (LOLE), and loss of energy expectation (LOEE) are the most common measures and objective functions for the reliability of RAES systems. The LPSP is the probability of the unmet load over the total energy demand of the RAES. The EENS is the expected energy that is not supplied by the RAES system. The number of hours of the year in which the RAES load exceeds the generation system is known as LOLE or loss of load probability (LOLP). The LOEE is the total energy not supplied by the RAES system.

c) Emission and Technical Objective Functions

The other groups of objective functions are emission and technical objectives which contain renewable factor (RF), carbon emission (CE), battery lifetime (BL), customer comfort level (CCL) and dumped energy (DE). The RF shows that how much of the energy demand in RAES system is supplied by renewable resources. The CE is the amount of carbon emission by the designed RAES system during the project lifetime. The BL is the lifetime of the integrated battery in RAES which is affected by the degradation. A suitable operation strategy should be developed to decrease the degradation of battery and hence increase its lifetime. The CCL is applied when demand response is integrated in the optimal sizing problem. The extra energy of the DRERs and diesel generators after supplying the load is known as DE which should be curtailed by inverter or dumped by resistors. It is notable that formulation of CCL depends on the demand response solution in the study. For example, if load shifting is examined, then the number of hours in which the load shifting applied can be minimised to reach the maximum CCL. The EFR can be formulated by considering the control system of inverters to minimise the power fluctuations and hence the minimum disruption in power supply.

D) Feasibility Constraints

There are two major types of feasibility constraints: (1) constraints associated with components, (2) technical constraints of the system.

The components constraints can be related to diesel generators, DRERs or ESSs. The constraint can be applied on the number of the components based on their unit capacity. Land availability is an important constraint to install PVs, WTs and ESSs. The diesel generator’s output power must be constrained between minimum and maximum generation limits. The fuel consumption and tank capacity can be considered as a constraint to limit the obtained emission from diesel generators. Hub height and blade diameter are considered as constraints to limit the size of WT. The constraint of PV panel's tilt-angle is considered to extract higher power. There are several constraints on ESSs like the energy of pump-storage hydro, energy at hydrogen tank, as well as battery SOC and power limits.

The most important technical constraint is the power balance of RAES system which means that the equilibrium between load and generation should be maintained. The power reserve of the RAES system should always be maintained using diesel generators or ESSs. The budget of the project to invest in the system components is an important constraint. The LPSP index can be used as a constraint to limit the amount of load curtailment. A part of the load can be limited to be supplied using the renewable generation; this is the renewable energy fraction. In some cases, the sizing of RAES systems is constrained by the countries policies. If DR is applied, then constraints should be considered to limit the DR strength.

E) Operation Strategies

The essence of the operational strategy is to control the power flow between components and loads in the RAES system. The main aim of the operation strategies is to achieve a reliable and clean energy supply while reaching the minimum cost. The operation strategy can receive the forecasting data of renewable generation and load consumption, the state-of-charge (SOC) of battery and the amount of remained fuel in the site to decide for the best operation in the system. It can change the load consumption using demand side management approaches [46].

F) Solving the RAES Optimal Sizing

Optimal sizing problem of RAES systems can be solved using a wide range of optimisation algorithms. The most applied methods are metaheuristic algorithms. Using software to solve the problem is also conducted in the literature.

a) Metaheuristic Methods

The metaheuristic methods are powerful optimization algorithms which can handle the nonlinearity and complexity of optimisation problems [47]. Another advantage of metaheuristic is the ability to use for optimal sizing of single-objective and multi-objective optimisation problems. A wide range of metaheuristic methods is developed by the researchers. Some of the best-known metaheuristic methods are particle swarm optimisation (PSO) algorithm, genetic algorithm (GA) and artificial bee colony (ABC).

b) Other Optimisation Methods

Probabilistic, sensitivity analysis, classic mathematical, and iterative algorithms are the other methods that have been used for optimal sizing of components in RAES systems. Probabilistic methods have the capability to consider the unpredictability of the parameters in the optimisation model [48]. The methods based on sensitivity analysis measure the sensitivity of the component's capacities against the defined objective functions in the problem [49]. In classic methods, the optimisation problem is mathematically solved [50].

c) HOMER Software

Hybrid Optimisation Model for Electric Renewables (HOMER) software is one of the most powerful tools for optimal sizing of components in energy systems. HOMER was developed by National Renewable Energy Laboratory (NREL) [51]. The software includes a broad range of components like PV, WT, converters, diesel generator, BES, etc. To solve the optimal sizing problems, HOMER minimises the net present cost of the energy systems. HOMER software shows a wide range of results like optimal sizes, sensitivity analysis, cash flows, and other economic and technical analysis.

2.2.3 Review on Existing Studies and Technical Challenges

A review on the existing studies is conducted in this section. The studies are first classified based on their conduced case system: (1) hybrid, and (2) clean RAES systems. Then, each category is classified based on the optimisation model: (i) HOMER software optimisation, (ii) metaheuristic methods, and (iii) non-metaheuristic (i.e., mathematical, iterative, probabilistic, etc.) methods. All the existing studies are investigated by specifying system components, the type of RAES system (i.e., rural areas, building, etc.), the used objective functions, feasibility constraints, country, and publication year.

A) Hybrid RAES Systems with/without ESS

The hybrid RAES systems are based on diesel generator power plants and renewable energy sources. The energy storage systems can also be integrated. These systems have a higher level of reliability because of the controllability of dispatchable diesel generator units. However, the emission and high cost are the main challenges. Several studies are developed for optimal sizing of hybrid RAES systems. The studies are reviewed based on HOMER software as well as metaheuristic and other methods.

a) HOMER Software for Hybrid RAES Systems

Two studies were conducted on optimal sizing of hybrid RAES systems without ESS for Saudi Arabia [52]. Optimal sizing of diesel generator-PV-BES system was investigated in [53] for remote communities. Optimal sizing of diesel generator-PV-WT-BES system was developed for islands [54], remote agriculture [55], telecommunication [56], and off-grid villages [57]. The Diesel generator-PV-WT-FC system was optimally sized in [58] for a village and mining site. In [59], hydropower was used alongside Diesel generator-PV-WT system for optimal sizing of a rural area in Iraq. A hybrid energy storage system (BES with hydro) was optimally sized with Diesel generator-PV-WT in [60]. In [61], a biogas generation unit is optimised for a hybrid RAES system with Diesel generator-PV-WT-BES in a remote community of Bangladesh.

b) Metaheuristic Methods for Hybrid RAES Systems

The metaheuristic methods are widely used for optimal sizing of hybrid RAES systems. The existing studies of metaheuristic methods are classified based on single- and multi-objective optimisation studies. Table 2-6 shows the reference number, applied methods, system components, RAES type, objective functions, and feasibility constraints, as well as the country and publication year of the existing studies on single-objective optimal sizing of hybrid RAES with metaheuristic methods. A range of metaheuristic methods was used for optimal sizing in RAES systems. In some studies, the applied method was compared with other methodologies. The hybrid Diesel generator-PV-WT-BES system was mostly sized by metaheuristic methods. All the applied objective functions are the economic type like NPC, LCOE, TAC and life cycle cost. The number of components and power balance between generation and consumption were the most used feasibility constraints. In some studies, like [95], the LPSP was considered as a constraint to improve the reliability. The constraints related to renewable energy were considered as a contribution by renewable factor [98], and renewable energy portion [100].

Table 2-6. Characteristics of studies on single-objective optimal sizing for hybrid RAES systems.

Ref.	Applied Method	System Components	RAES Type	Objective Function	Feasibility Constraints	Country	Year
[62]	Levy flight-based particle swarm optimisation	Diesel generator-PV	Not Specified	NPC	Output Power of Diesel generator, available area for PV, LPSP	Iran	2017
[63]	Particle swarm optimisation	Diesel generator-PV-BES	Island	Total system cost	Power balance, node voltage, number of components	Indonesia	2018
[64]	Several algorithms	Diesel generator-PV-WT-BES	Remote village	LCOE	LPSP, power balance, SOC	Egypt	2019
[65]	Hybrid simulated annealing–tabu search	Diesel generator-Biodiesel-PV-WT-BES-FC	Educational Institute	LCOE	Initial cost, unmet load, capacity shortage, fuel consumption, renewable factor, components' size	Greece	2012
[66]	Particle swarm optimisation	Diesel generator-PV-BES-EV	Residential	Lifetime cost	Size of components, unit commitment constraints	India	2019
[67]	Crow search algorithm	Diesel generator-PV-FC	Remote area community	NPC	LPSP, renewable energy portion	Iran	2020

Table 2-7 shows the reference number, applied methods, system components, RAES type, objective functions, and feasibility constraints, as well as the country and publication year of the existing studies on multi-objective optimal sizing of hybrid RAES with metaheuristic methods. The multi-objective optimal sizing of RAES systems was investigated by 18 papers. A range of objective functions were used along with economic objectives to optimise the capacity of components. The emission and reliability related objective functions were the most applied after economic objectives. The grid voltage deviation as a technical objective function was applied in [73]. A tidal power generator was used in [70] for Flinders Island in Australia.

Table 2-7. Multi-objective capacity optimisation for hybrid RAES with metaheuristic methods.

Ref.	Applied Method	System Components	RAES Type	Objective Function	Feasibility Constraints	Country	Year
[68]	Multi-objective crow search algorithm	Diesel generator-PV-FC	Not specified	NPC and LPSP	Number of components, tank energy	Iran	2019
[69]	Multi-objective particle swarm optimisation	Diesel generator-PV-WT-BES	Remote community with 15 houses	COE, LPSP, renewable factor	Not specified	Iran	2014
[70]	Multi-objective grey wolf algorithm	Diesel generator-PV-WT-Tidal-BES	Flinders island	LCOE, emission	Number of components, operating reserve	Australia	2018
[71]	Multi-objective genetic algorithm	Diesel generator-PV-BES	Remote village	LCOE, carbon footprint of energy	Not specified	Russia	2015
[72]	Fuzzy artificial bee colony	Diesel generator-PV-	An edge region	Annualized cost,	Number of components,	USA	2020

	optimisation mechanism	WT-BES		emission	battery's energy		
[73]	Non-dominated sorting genetic algorithm II	Diesel generator-PV-BES	Island	LCOE, CE, grid voltage deviation	Number of components, battery's energy	Indonesia	2018

c) Non-Metaheuristic Optimisation Algorithms for Hybrid RAES Systems

The existing studies which optimised the capacity of components based on methodologies rather than metaheuristic and HOMER for hybrid RAES systems are categorised in Table 2-8. The applied method is specified for each study and the other characteristics are represented in Table 6. As illustrated in the table, various optimisation techniques were used for optimal sizing. In [78], a dynamic programming algorithm was used for optimal sizing of vanadium redox battery in a Diesel generator-PV-BES system. The dynamic programming algorithm was utilized to overcome the challenge of optimal scheduling by considering the operating and efficiency characteristics of vanadium redox battery. In [79], a stochastic mixed integer non-linear programming (MINLP) optimisation was conducted for optimal sizing which was solved with GAMS software.

Table 2-8. Hybrid RAES system optimal sizing studies with non-metaheuristic methods.

Ref.	Applied Method	System Components	RAES Type	Objective Function	Feasibility Constraints	Country	Year
[74]	MILP with CPLEX	Diesel generator-WT-BES	Island	Cost over the project lifetime	Power balance, Diesel generator output power, operating reserve, power, and energy of BES	Vietnam	2018
[75]	CPLEX optimiser in JAVA	Diesel generator-PV-BES	Ten households in rural area	Capacity of battery	SOC, Diesel generator's output power	Australia	2018
[76]	Reformed electric system cascade analysis	Diesel generator-PV-WT-BES	Residential community with 100 homes	Defined based on constraints	Final Excess Energy, Renewable Energy Fraction, LPSP, Annual System Cost	USA	2019
[77]	MINLP in GAMS using BARON solver	Diesel generator-PV-BES	A remote 38-bus distribution network	Annualized costs	Power flow, active and reactive power mismatch constraints, system frequency	Not specified	2019
[78]	Dynamic programming algorithm	Diesel generator-PV-BES	Not specified	Total cost per day	Power and energy of BES	USA	2015
[79]	Stochastic MINLP optimisation with GAMS	Diesel generator-PV-WT-BES	Not specified	NPC	Power balance, Diesel generator constraints, operating reserve, BES constraints, budget constraint	Not specified	2018

B) Clean (Renewable-Storage) RAES Systems

In clean power systems, all the electricity demand will be supplied using renewable energies and ESSs, hence, there is no diesel generator unit.

a) HOMER Software for Renewable-Storage RAES Systems

The optimal sizing of renewable-storage RAES systems using HOMER software was conducted by 13 papers. The NPC was the only objective function, and the feasibility constraints were not specified in most of the studies. The PV-WT-BES system was the most considered system for clean RAES [80]. FC, supercapacitor (SC), biogas, and hydro were the other technologies which used along with PV and WT in clean RAES. In [81], optimal sizing of PV-FC system was investigated for small communities. Hybrid energy storage systems for clean RAES systems was broadly examined. In [82], a hybrid FC-SC storage system was employed with solar PV for a remote commercial load in South Africa. A combination of BES and FC was optimally sized with PV and WT in [83]. Biogas generation unit was used with PV-WT-BES system to build a clean hybrid system with higher flexibility in electricity supply [84]. The application of biogas generation units with hydropower in clean RAES systems was also investigated by HOMER in [85].

b) Metaheuristic Methods for Renewable-Storage RAES Systems

The metaheuristic methods are applied as single-objective and multi-objective for optimal sizing of clean RAES systems. However, due to the lack of diesel generators in clean RAES systems, the emission objective functions are eliminated in the optimal sizing. Hence, the number of objective functions is limited. Table 2-9 presents the characteristics (applied method, system components, type of RAES, objective functions, feasibility constraints, country, and publication year) of the existing studies on single-objective optimal sizing of clean RAES with metaheuristic methods. A wide range of studies have investigated the optimal sizing problem of clean RAES systems using metaheuristic methods. Like Table 1, the particle swarm optimisation was the most applied algorithm. In [96], a PV-WT-PHS system was designed to supply the loads in a coastline community. Such a system is very efficient in coastline communities due to water availability for PHS.

Table 2-9. Single-objective metaheuristic capacity optimisation for clean RAES systems.

Ref.	Applied Method	System Components	RAES Type	Objective Function	Feasibility Constraints	Country	Year
[86]	Particle swarm optimisation	PV-WT-Tidal-BES	Remote house	NPC	Number of components, reliability, SOC	France	2019
[87]	Hybrid grey wolf optimiser-sine cosine algorithm	PV-WT-FC	Residential-commercial center	lifespan cost of hybrid system	Load interruption probability, number of components, energy at tank	Iran	2020
[88]	Genetic algorithm	PV-WT-BES	Forty households	Total cost of ownership	Number of components, tilt angle of PV, height of WT	New Zealand	2016
[89]	Improved bee algorithm	PV-WT-BES-FC-Reverse Osmosis Desalination	Desalination systems and community load	Total life cycle cost	LPSP, energy at hydrogen tank, SOC, number of components	Iran	2018
[90]	Simulated annealing algorithm	PV-WT-BES-FC	Remote region	Total life cycle cost	SOC, number of components, energy in tank	Iran	2018
[91]	Particle swarm optimisation	PV-WT-BES	Single house	NPC	Power balance, number of components	Australia	2019
[92]	Particle swarm optimisation	Biogas-PV-BES	Residential	LCOE	Constraint on deficit power of PV	Kenya	2017
[93]	Artificial bee colony	PV-Biomass	Rural area	LCOE	Number of components, output power of biogas	India	2016
[94]	Whale optimisation algorithm	PV-WT-FC-Tidal	Remote region	NPC	Load deficit probability Size of components	Iran	2020
[95]	Four algorithms	PV-WT-BES-PHS	Remote island	NPC	Number of components, battery's energy and SOC	China	2020
[96]	Genetic algorithm	PV-WT-PHS	Coastline communities	Life cycle cost	Not specified	Nigeria	2020

The existing studies on RAES optimal sizing with multi-objective methods are categorised based on applied method, system components, type of RAES, objective functions, feasibility constraints, country, and publication year. Table 2-10 presents the classification of the existing studies. Multi-objective particle swarm optimisation algorithm was the most applied method for optimal sizing of clean RAES systems. In [98], the PV-WT-BES system was combined with pumped hydro storage (PHS). A combination of FC and BES was considered in [99]. In [97], a PV-WT-BES system was optimised for electricity supply to a rural telecom tower in India. A range of economic and reliability objective functions were applied. Only two studies were conducted for multi-objective optimal sizing of RAES systems with more than three components: PV-WT-BES-FC in [99] and PV-WT-BES-PHS in [98].

Table 2-10. Clean RAES systems optimal sizing with multi-objective metaheuristic methods.

Ref.	Applied Method	System Components	RAES Type	Objective Function	Feasibility Constraints	Country	Year
[97]	Multi-objective grey wolf algorithm	PV-WT-BES	Rural telecom tower	COE, LPSP, DE	SOC	India	2020
[98]	Multi-objective grey wolf algorithm	PV-WT-BES-PHS	Isolated farmstead	COE, LPSP	Energy of battery and pump-storage hydro	Algeria	2019
[99]	Multi-objective genetic algorithm	PV-WT-BES-FC	Not specified	NPC, excess energy, life cycle emission	Number of components, energy of tank	Australia	2015
[100]	Multi-objective genetic algorithm	PV-WT-BES	A residential home with four occupants	Life cycle cost, embodied energy, LPSP	SOC	USA	2014
[101]	Multi-objective particle swarm optimisation	PV-WT-FC	Not specified	TAC, LOEE, LOLE	Energy at tank, number of components, PV tilt angle	Not specified	2016
[102]	Non-dominated sorting genetic algorithm II	PV-BES-FC	Residential (10 houses)	LPSP, system cost, potential energy waste	Number of components	China	2019
[103]	Mutation adaptive differential evolution	PV-BES	Rural area	Life cycle cost, LOLP, LCOE	SOC	Malaysia	2020

c) Non-Metaheuristic Optimisation Algorithms for Renewable-Storage RAES Systems

Table 2-11 lists the characteristics of the studies on capacity optimisation for clean RAES systems with other methods rather than HOMER and metaheuristic methods. To solve the multi-objective problem by the methods rather than metaheuristic approaches iterative technique [106] and power pinch analysis [107] were developed by the existing studies. Most of the optimal sizing studies were conducted on PV-WT-BES system.

Table 2-11. Studies on optimal sizing of clean RAES systems with non-metaheuristic methods.

Ref.	Applied Method	System Components	RAES Type	Objective Function	Feasibility Constraints	Country	Year
[104]	Sensitivity analysis	PV-WT-BES-PHS	Remote island	Life cycle cost	Not specified	Hong Kong	2014
[105]	Simulink Design Optimisation	PV-BES-FC	Not specified	Cost	Not specified	Spain	2013
[106]	Iterative technique	PV-WT-BES	Remote residential household	LPSP and LCOE	SOC, number of components	Algeria	2011
[107]	Power Pinch Analysis	PV-BES	Remote community	Cost	Not specified	Bhutan	2017
[108]	Object-Oriented Programming	PV-WT-BES	Not specified	NPC	LPSP, SOC	Algeria	2014
[109]	Iterative simulation-	PV-WT-BES-FC	Not specified	LCOE	LOLE	Iran	2016

	optimisation						
[110]	MILP	PV-WT-BES	Remote area mountain lodge	NPC	Energy of BES, power balance	Italy	2020
[111]	An iterative method	PV-WT-BES	Ten houses in a remote island	NPC	LPSP, COE	China	2019
[112]	Logical approach	PV-WT-BES	Remote community	NPC	Number of components	South Korea	2016
[113]	Enumerative method	PV-BES	House	LCOE	Unmet load percentage, number of days of autonomy	Spain	2018
[114]	Sensitivity based method	PV-WT-FC-PHS	University	RES fraction	Not specified	Cyprus	2020

C) Discussion

Regarding the used objective functions in the existing studies, the priority goes to cost objectives in most of the studies. Then, the reliability objectives have obtained more attention than the emission aims because of grid absence in remote areas systems. Finally, due to global concern, emission objective functions have been attained enough attention by the researchers after cost and reliability targets. The number of publications per continent for RAES optimal sizing is demonstrated in Fig. 2-9. It is observed that most of the studies (about 100 papers) were conducted for Asian case studies. After Asia, optimal sizing for African case studies was attracted the highest attention with more than 30 papers. Fig. 2-16 also shows the number of publications per country in Asia. It is observed that a high contribution of studies was developed in Iran and India. China is the next country with about 15 studies on RAES optimal sizing.

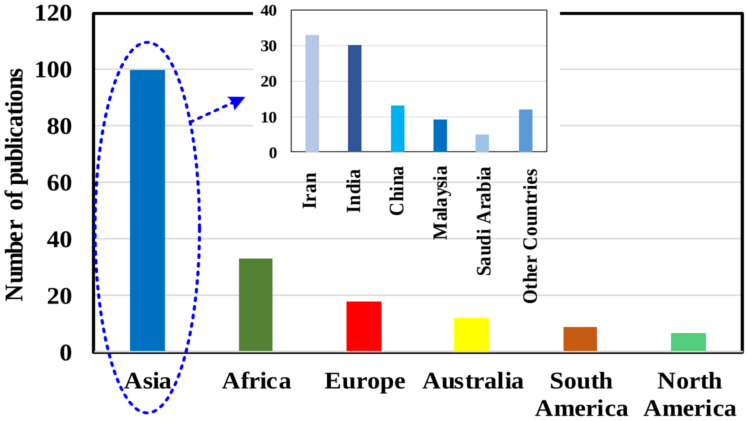

Figure 2-9. Number of publications per countries for RAES optimal sizing.

D) Discussions on Methods and Uncertainties

Metaheuristic methods have been broadly used for optimal sizing of RAES systems because of good potential to escape from local optimal point, freeness from gradient calculation, and simple implementation. These methods could effectively prevail over the nonlinearity and complexity of optimisation formulation. The other merit of these algorithms over the classical optimisation methods is the possibility of reaching/finding the global optima solution and capability to deal with non-convex optimal sizing problems that is hardly possible when classical methods are utilized. For optimal sizing problems of RAES systems, the metaheuristic methods have the capability to reach the near-optimal solutions effectively. Since the problem of optimal sizing for RAES systems with several components deal with a fact that many results may be found as possible solutions, it may not be required to find the exact optimal result and hence the near-optimal result by satisfying the design constraints can be a potential solution. Literature has reported that more than 70% of the existing papers have used metaheuristic methods for RAES optimal sizing. Particle swarm optimisation has the highest contribution among the applied methods for single-objective optimal sizing.

As the number of objectives is increased, solving the optimal sizing problem of RAES system in a multi-objective basis becomes more popular. On the other hand, the number of constraints is also increased, and the types of constraints become more complicated. Hence, the multi-objective metaheuristic methods can be used as an appropriate method for such problems. These methods are able to generate several solutions in form of Pareto-front in each run of simulation. This is the main advantage of multi-objective metaheuristic methods over the classic methods. The multi-objective genetic algorithm is the most applied method for optimal sizing.

In optimal sizing of RAES systems with HOMER software, NPC is the only objective function which was considered by all existing studies. This is one of the main deficiencies of using HOMER for optimal sizing that the objective function cannot be changed. The design constraints are generally improvised in the block of the components in HOMER and the designer cannot define new constraints or models. This is the main reason that the design constraints are not specified in most of the studies by the HOMER. Another deficiency by HOMER is the incapability to run multi-objective optimisation.

Among the non-metaheuristic methods, solving the RAES optimal sizing problem with MILP using commercial software was the most utilized one. In such a method, the mathematical formulation of the problem is modelled. High computational burden and inability to handle the nonlinearities are the main shortcomings of such classic methods. The iterative methods may trap in local solutions and hence the global optimal solution may not attain. To overcome this challenge, the iterative approach should be repeated multiple times by random initial conditions. Hence, the best local solution obtained by the approach is chosen as the optimal solution. It should be noted that repeating the simulation for different initial conditions increases the calculation time of the approach.

Analytical approaches evaluate the performance of the system for a set of feasible configurations for the specific capacity of the components in the RAES system. Then, the best system configuration is selected by evaluating single or multiple performance indices. Probabilistic methods develop suitable models for the generation of resources and/or load demand and they create a risk model by a combination of the developed models. Using the probabilistic methods for sizing of RAES systems was conducted by a few studies. This is because the probabilistic methods cannot characterize the dynamic changing nature of hybrid RAES systems.

E) Technical Challenges

Due to the intermittency of renewable energy, a large mismatch may happen between generation and consumption in clean RAES systems. To compensate the power deficiency, a large capacity of BES is required. This high capacity of battery is a technical challenge due to the high cost of the battery. To reduce the capacity of the battery, demand response programs should be developed. Although the DR strategies have been developed for grid-connected systems, the application of DRs in optimal sizing of remote areas systems was neglected. Due to high intermittency of renewable energies and load, a robust optimal sizing of a clean RAES system can guarantee the energy supply. However, a robust optimal sizing in the RAES system was neglected. Guidelines for customers in RAES systems to purchase PV, WT, and BES was neglected in the existing literature. If the customers are equipped with renewable-storage systems, the high pressure of energy supply can be efficiently reduced in RAES systems. Only limited studies considered some distribution network indices in the sizing process. However, the distribution network constraints like voltage and frequency constraints can highly affect the optimal sizing problem.

2.2.4 Recent Developments in Optimal Sizing

Recently, some research developments have been performed for optimal sizing of RAES systems which are discussed in this section.

A) EV Charging Stations and Diesel Generator

In [115], an optimal sizing methodology was developed for allocation of EV charging station and DGs in a remote community. A multi-objective optimisation problem was developed to minimise emission and cost of the microgrid. It was assumed that by substituting EVs with fossil-fuelled vehicles, the pollutant emission from driving would be zero. It was found that it will be both economic and clean for investors to construct EV charging stations in remote communities.

B) Integrated Energy System with Solar PV and Biogas

In [116], optimal sizing of an integrated energy system with solar PV, battery, and biogas was proposed for a remote area residential load. The main purpose of adding the biogas system was in twofold: 1) to decrease the capacity of the battery, and 2) to design a system for thermal, electricity, and gas supply in remote areas. The study showed that the proposed system resulted in a low LCOE for the case study. Such studies by considering a multi-energy system for remote areas are highly recommended to not only supply the electricity but also thermal and gas demands.

C) Hybrid Energy Storage and PV

In [117], a standalone system was developed based on solar PV, ice-thermal energy storage (TES), and BES for an islanded building. This study achieved valuable developments in twofold. First, optimal sizing of a RAES system. Second, deployment of the dynamic model of the system to show the system operation in a real-time simulation on the OPAL-RT platform. A coordinated operation between BES and TES was proposed to decrease the capacity of BES. It was found that the system based on hybrid energy storage is more economical than the system with only BES. Such studies are valuable to validate both the sizing and operation.

D) Optimal Configuration

In [118], optimal sizing of standalone microgrids was modelled with full identification of the system topology. In this model, the optimal type of microgrid (AC, DC, or hybrid AC/DC) as well as the capacity optimisation of the DGs, storages, capacitors, and the power electronic converters were assigned by minimising the total sizing cost. If a hybrid topology was found as the best, the model calculated the optimal size of interlinking converters. Such studies by considering control, sizing, and topology of the RAES system is in interest.

E) Accurate Battery Lifetime Estimation and Technology Selection

In [119], a two-stage methodology was developed to determine the optimal capacity, maximum depth of discharge, and the service lifetime in years of BES for a remote microgrid. The different performance of full and half cycles was investigated. It was found that the higher capacity of BES results in lower DODs and hence a higher estimated lifetime for RAES microgrids.

F) Concentrating Solar Power Plant

In [120], a renewable-storage system was proposed for a remote area electricity and water supply system based on WT, concentrating solar power (CSP) plant and BES. By using the CSP plant, superheated steam was generated to run generators to produce electricity. The low/medium temperature exhaust steam of the CSP was used in desalination units to produce freshwater. A TES was also considered in the CSP plant to reduce the BES capacity. Integrated CSP-desalination unit could be very useful for RAES systems. Such a system would give more flexibility for energy scheduling.

G) Cooperation of Diesel Generator and Flywheel with Incentive DR

In [121], flywheel (FW) was examined for optimal sizing of RAES system. The authors optimised a Diesel generator-FW-PV-WT-BES system by considering an incentive DR program. The FW reduced the number of offline diesel generators to supply the loads. By the incentive DR, customers received a financial benefit to contribute to load shedding. The study has opened some good views on the optimal sizing problem; however, a flat incentive was selected.

2.2.5 Potential Directions for Research Works on RAES Optimal Planning

This paper facilitates future scopes on optimal sizing of RAES systems.

A) Distribution network constraints

Optimal sizing of RAES systems by considering distribution network constraints obtains more practical results. Generally, the households are located far from each other in remote and rural areas which causes long distribution lines between customers in RAES systems. Hence, the distribution network in RAES system needs higher attention due to power losses as well as voltage and frequency deviations [122]. The optimal sizing should be accomplished by considering all distribution constraints. Optimal allocation of components should be investigated in by considering the distribution network and components requirements.

E) Guidelines for RAES Customers

Guidelines in RAES systems should be rendered for the customers to purchase renewable-storage systems. The guidelines can help electricity consumers to invest the right cost on solar PV, WT and BES for their properties. The guideline can be based on the budget, the available area for PV and WT installation, and the possibility of DR application. Such guidelines can reduce the electricity cost and increase the reliability of the electricity supply of customers in RAES systems.

F) Feed-in-tariff in RAES

An effective incentive for the customers in RAES systems is to assign feed-in-tariff for exporting electricity from their PV and WT systems to the distribution network. The feed-in-tariff can be based on flat rate or time-of-use rates [123]. When the feed-in-tariff is assigned, the customer exports the power to supply the electricity demand of the other electricity consumers in the system. Using feed-in-tariff, the electricity bill of the customers is reduced and the high pressure of electricity supply by the main grid will be lifted. An efficient feed-in-tariff program for customers in RAES systems is a good policy in the future.

G) Robust Optimal Sizing

To achieve a clean reliable RAES system to supply the load uninterruptedly, a robust optimisation is essential. Optimal sizing with robust strategies can overcome the intermittency of consumption and generation sides as well as the demand variations subjected by population change. The robust strategies can consider the worst-case scenario of renewable generation and load consumption to generate the optimal capacities [124]. Due to robustness of these methods, the designed system can supply the load in the days with lower renewable generation and higher load variations. Robust optimal sizing is an efficient future direction.

2.2.6 Conclusion on the Review for RAES Optimal Planning

This paper investigated the state-of-the-art optimal sizing of remote area electricity supply (RAES) systems. A problem identification was accomplished to highlight the most important aspects of optimal sizing in RAES systems. These aspects included the type of components, necessary input data, objective functions, feasibility constraints, operation strategies and optimisation methods. The existing studies on the field were classified based on hybrid or clean systems, optimisation methodologies or software (HOMER) optimisation, and single- or multi- objective problem. The existing challenges were explained and the latest developments in optimal sizing of RAES systems were discussed. The future perspectives were introduced to highlight the potential research ideas for the researchers. It was found that feed-in-tariffs and guidelines should be introduced for customers in RAES systems in order to reduce of the electricity cost. New software tools are necessary to optimise the capacity of components based on various objective functions.

References

[1] International Energy Agency, World Energy Outlook, 2018.

[2] ME. Khodayar, "Rural electrification and expansion planning of off-grid microgrids," *The Electricity Journal*, vol. 30, iss. 4, pp. 68-74, 2017.

[3] M. Combe M, et al., "Cost-effective sizing of an AC mini-grid hybrid power system for a remote area in South Australia," *IET Generation, Transmission & Distribution*, vol. 13, iss. 2, pp. 277-87, 2019.

[4] Akuru UB, Onukwube IE, Okoro OI, Obe ES. Towards 100% renewable energy in Nigeria. Renewable and Sustainable Energy Reviews. 2017 May 1;71:943-53.

[5] Hansen K, Mathiesen BV, Skov IR. Full energy system transition towards 100% renewable energy in Germany in 2050. Renewable and Sustainable Energy Reviews. 2019 Mar 1;102:1-3.

[6] Child M, Kemfert C, Bogdanov D, Breyer C. Flexible electricity generation, grid exchange and storage for the transition to a 100% renewable energy system in Europe. Renewable Energy. 2019;139:80-101.

[7] K. Jalilpour, et al. Optimal sizing of energy storage system. Chapter 9, in *Variability, Scallability, and Stability of Microgrids* by S. M Muyeen, Syed Islam, and Frede Blaabjerg, The Institution of Engineering and Technology (IET), UK, June 2019, pp. 263–289.

[8] A. Mahesh, Sandhu KS. Hybrid wind/photovoltaic energy system developments: Critical review and findings. *Renewable and Sustainable Energy Reviews*. 2015 Dec 1;52:1135-47.

[9] V. Khare, Nema S, Baredar P. Solar–wind hybrid renewable energy system: A review. *Renewable and Sustainable Energy Reviews*. 2016 May 1;58:23-33.

[10] S. Sinha, Chandel SS. Review of software tools for hybrid renewable energy systems. *Renewable and Sustainable Energy Reviews*. 2014 Apr 1;32:192-205.

[11] S. Sinha, S. Chandel, "Review of recent trends in optimization techniques for solar photovoltaic–wind based hybrid energy systems," *Renewable and Sustainable Energy Reviews*, vol. 50, pp, 755-69, 2015.

[12] L. Olatomiwa, Mekhilef S, Ismail MS, Moghavvemi M. Energy management strategies in hybrid renewable energy systems: A review. *Renewable and Sustainable Energy Reviews*. 2016;62:821-35.

[13] M. H. Nehrir *et al*., "A Review of Hybrid Renewable/Alternative Energy Systems for Electric Power Generation: Configurations, Control, and Applications," in *IEEE Transactions on Sustainable Energy*, vol. 2, no. 4, pp. 392-403, Oct. 2011.

[14] M. Rezkallah, A. Chandra, B. Singh and S. Singh, "Microgrid: Configurations, Control and Applications," in *IEEE Transactions on Smart Grid*, vol. 10, no. 2, pp. 1290-1302, March 2019.

[15] R. Singh, Bansal RC. Review of HRESs based on storage options, system architecture and optimisation criteria and methodologies. *IET Renewable Power Generation*. 2018 Jan 11;12(7):747-60.

[16] AH Fathima, Palanisamy K. Optimization in microgrids with hybrid energy systems–A review. *Renewable and Sustainable Energy Reviews*. 2015 May 1;45:431-46.

[17] C. Gamarra, Guerrero JM. Computational optimization techniques applied to microgrids planning: A review. *Renewable and Sustainable Energy Reviews*. 2015 Aug 1;48:413-24.

[18] AL Bukar, Tan CW. A review on stand-alone photovoltaic-wind energy system with fuel cell: System optimization and energy management strategy. *Journal of cleaner production*. 2019 Jun 1;221:73-88.

[19] JC Rojas-Zerpa, Yusta JM. Methodologies, technologies and applications for electric supply planning in rural remote areas. *Energy for Sustainable Development*. 2014 Jun 1;20:66-76.

[20] YS Mohammed, Mustafa MW, Bashir N. Hybrid renewable energy systems for off-grid electric power: Review of substantial issues. *Renewable and Sustainable Energy Reviews*. 2014 Jul 1;35:527-39.

[21] A. Chauhan, Saini RP. A review on integrated renewable energy system based power generation for stand-alone applications: configurations, storage options, sizing methodologies and control. *Renewable and Sustainable Energy Reviews*. 2014 Oct 1;38:99-120.

[22] R. Siddaiah, Saini RP. A review on planning, configurations, modeling and optimization techniques of hybrid renewable energy systems for off grid applications. *Renewable and Sustainable Energy Reviews*. 2016 May 1;58:376-96.

[23] AA Lahimer, Alghoul MA, Yousif F, Razykov TM, Amin N, Sopian K. Research and development aspects on decentralized electrification options for rural household. *Renewable and Sustainable Energy Reviews*. 2013 Aug 1;24:314-24.

[24] S. Mandelli, Barbieri J, Mereu R, Colombo E. Off-grid systems for rural electrification in developing countries: Definitions, classification and a comprehensive literature review. *Renewable and Sustainable Energy Reviews*. 2016 May 1;58:1621-46.

[25] D. Neves, Silva CA, Connors S. Design and implementation of hybrid renewable energy systems on micro-communities: A review on case studies. *Renewable and Sustainable Energy Reviews*. 2014 Mar 1;31:935-46.

[26] S. Goel, Sharma R. Performance evaluation of stand alone, grid connected and hybrid renewable energy systems for rural application: A comparative review. *Renewable and Sustainable Energy Reviews*. 2017 Oct 1;78:1378-89.

[27] T. Tezer, Yaman R, Yaman G. Evaluation of approaches used for optimization of stand-alone hybrid renewable energy systems. *Renewable and Sustainable Energy Reviews*. 2017 Jun 1;73:840-53.

[28] S. Twaha, Ramli MA. A review of optimization approaches for hybrid distributed energy generation systems: Off-grid and grid-connected systems. *Sustainable Cities and Society*. 2018 Aug 1;41:320-31.

[29] MD Al-Falahi, Jayasinghe SD, Enshaei HJ. A review on recent size optimization methodologies for standalone solar and wind hybrid renewable energy system. *Energy conversion and management*. 2017 Jul 1;143:252-74.

[30] M. Faccio, Gamberi M, Bortolini M, Nedaei M. State-of-art review of the optimization methods to design the configuration of hybrid renewable energy systems (HRESs). *Frontiers in Energy*. 2018 Dec 1;12(4):591-622.

[31] K. Anoune K, Bouya M, Astito A, Abdellah AB. Sizing methods and optimization techniques for PV-wind based hybrid renewable energy system: A review. *Renewable and Sustainable Energy Reviews*. 2018 Oct 1;93:652-73.

[32] O. M. Babatunde, J. L. Munda and Y. Hamam, "A Comprehensive State-of-the-Art Survey on Hybrid Renewable Energy System Operations and Planning," in *IEEE Access*, vol. 8, pp. 75313-75346, 2020.

[33] S. Bahramara, Moghaddam MP, Haghifam MR. Optimal planning of hybrid renewable energy systems using HOMER: A review. *Renewable and Sustainable Energy Reviews*. 2016 Sep 1;62:609-20.

[34] L. Ali, SM Muyeen, H. Bizhani, A. Ghosh "A multi-objective optimization for planning of networked microgrid using a game theory for peer-to-peer energy trading scheme," *IET Generation, Transmission & Distribution*, 2021.

[35] HA M. Pesaran, Huy PD, Ramachandaramurthy VK. A review of the optimal allocation of distributed generation: Objectives, constraints, methods, and algorithms. Renewable and Sustainable Energy Reviews. 2017 Aug 1;75:293-312.

[36] A. Keane *et al*., "State-of-the-Art Techniques and Challenges Ahead for Distributed Generation Planning and Optimization," in *IEEE Transactions on Power Systems*, vol. 28, no. 2, pp. 1493-1502, May 2013.

[37] LA Wong, Ramachandaramurthy VK, Taylor P, Ekanayake JB, Walker SL, Padmanaban S. Review on the optimal placement, sizing and control of an energy storage system in the distribution network. *Journal*

of Energy Storage. 2019 Feb 1;21:489-504.

[38] M. Zidar, Georgilakis PS, Hatziargyriou ND, Capuder T, Škrlec D. Review of energy storage allocation in power distribution networks: applications, methods and future research. *IET Generation, Transmission & Distribution*. 2016 Feb 18;10(3):645-52.

[39] Y. Yang, Bremner S, Menictas C, Kay M. Battery energy storage system size determination in renewable energy systems: A review. *Renewable and Sustainable Energy Reviews*. 2018 Aug 1;91:109-25.

[40] MA Hannan, Faisal M, Ker PJ, Begum RA, Dong ZY, Zhang C. Review of optimal methods and algorithms for sizing energy storage systems to achieve decarbonization in microgrid applications. *Renewable and Sustainable Energy Reviews*. 2020 Oct 1;131:110022.

[41] Y. Tan, Meegahapola L, Muttaqi KM. A review of technical challenges in planning and operation of remote area power supply systems. *Renewable and Sustainable Energy Reviews*. 2014 Oct 1;38:876-89.

[42] J. Benedek, Sebestyén TT, Bartók B. Evaluation of renewable energy sources in peripheral areas and renewable energy-based rural development. *Renewable and Sustainable Energy Reviews*. 2018 Jul 1;90:516-35.

[43] B. Zhou *et al*., "Optimal Scheduling of Biogas–Solar–Wind Renewable Portfolio for Multicarrier Energy Supplies," in *IEEE Transactions on Power Systems*, vol. 33, no. 6, pp. 6229-6239, Nov. 2018.

[44] M. Faisal, M. A. Hannan, P. J. Ker, A. Hussain, M. B. Mansor and F. Blaabjerg, "Review of Energy Storage System Technologies in Microgrid Applications: Issues and Challenges," in *IEEE Access*, vol. 6, pp. 35143-35164, 2018.

[45] L. Bhamidi and S. Sivasubra, "Optimal Sizing of Smart Home Renewable Energy Resources and Battery Under Prosumer-Based Energy Management," *IEEE Systems Journal*, vol. 15, no. 1, pp. 105-113, 2021.

[46] R. Deng, Z. Yang, M. Chow and J. Chen, "A Survey on Demand Response in Smart Grids: Mathematical Models and Approaches," *IEEE Transactions on Industrial Informatics*, vol. 11, no. 3, pp. 570-582, 2015.

[47] Cuevas E, Espejo EB, Enríquez AC. Metaheuristics Algorithms in Power Systems. Springer; 2019.

[48] YM Atwa, El-Saadany EF. Probabilistic approach for optimal allocation of wind-based distributed generation in distribution systems. *IET Renewable Power Generation*. 2011 Jan 1;5(1):79-88.

[49] AR Jordehi. Allocation of distributed generation units in electric power systems: A review. *Renewable and Sustainable Energy Reviews*. 2016 Apr 1;56:893-905.

[50] WS Tan, Hassan MY, Majid MS, Rahman HA. Optimal distributed renewable generation planning: A review of different approaches. *Renewable and Sustainable Energy Reviews*. 2013 Feb 1;18:626-45.

[51] ⟨http://www.nrel/gov/HOMER⟩.

[52] MA Baseer, Alqahtani A, Rehman S. Techno-economic design and evaluation of hybrid energy systems for residential communities: Case study of Jubail industrial city. *Journal of Cleaner Production*. 2019 Nov 10;237:117806.

[53] S. Yilmaz, Dincer F. Optimal design of hybrid PV-Diesel-Battery systems for isolated lands: A case study for Kilis, Turkey. *Renewable and Sustainable Energy Reviews*. 2017 Sep 1;77:344-52.

[54] L. J. Olatomiwa, S. Mekhilef and A. S. N. Huda, "Optimal sizing of hybrid energy system for a remote telecom tower: A case study in Nigeria," *2014 IEEE Conference on Energy Conversion (CENCON)*, 2014, pp. 243-247.

[55] E. A. Al-Ammar *et al*., "Residential Community Load Management Based on Optimal Design of Standalone HRES With Model Predictive Control," in *IEEE Access*, vol. 8, pp. 12542-12572, 2020.

[56] L. Ali, Shahnia. Determination of an economically-suitable and sustainable standalone power system for an off-grid town in Western Australia. *Renewable energy*. 2017 Jun 1;106:243-54.

[57] S. Rehman, N. Natrajan, M. Mohandes, L. M. Alhems, Y. Himri and A. Allouhi, "Feasibility Study of Hybrid Power Systems for Remote Dwellings in Tamil Nadu, India," in *IEEE Access*, vol. 8, pp. 143881-143890, 2020.

[58] V. Khare, Nema S, Baredar P. Optimization of hydrogen based hybrid renewable energy system using HOMER, BB-BC and GAMBIT. *International Journal of Hydrogen Energy*. 2016;41(38):16743-51.

[59] AS Aziz, Tajuddin MF, Adzman MR, Azmi A, Ramli MA. Optimization and sensitivity analysis of standalone hybrid energy systems for rural electrification: A case study of Iraq. *Renewable Energy*. 2019 Aug 1;138:775-92.

[60] O. Hafez, Bhattacharya K. Optimal planning and design of a renewable energy based supply system for microgrids. *Renewable Energy*. 2012 Sep 1;45:7-15.

[61] BK Das, Hoque N, Mandal S, Pal TK, Raihan MA. A techno-economic feasibility of a stand-alone hybrid power generation for remote area application in Bangladesh. *Energy*. 2017 Sep 1;134:775-88.

[62] A. Askarzadeh. Solution for sizing a PV/diesel HPGS for isolated sites. *IET Renewable Power Generation*. 2016 Aug 15;11(1):143-51.

[63] C. D. Rodríguez-Gallegos *et al*., "A Siting and Sizing Optimization Approach for PV–Battery–Diesel Hybrid Systems," in *IEEE Transactions on Industry Applications*, vol. 54, no. 3, pp. 2637-2645, May-June 2018.

[64] A. A. Z. Diab, H. M. Sultan, I. S. Mohamed, O. N. Kuznetsov and T. D. Do, "Application of Different Optimization Algorithms for Optimal Sizing of PV/Wind/Diesel/Battery Storage Stand-Alone Hybrid Microgrid," in *IEEE Access*, vol. 7, pp. 119223-119245, 2019.

[65] Y. A. Katsigiannis, P. S. Georgilakis and E. S. Karapidakis, "Hybrid Simulated Annealing–Tabu Search Method for Optimal Sizing of Autonomous Power Systems With Renewables," in *IEEE Transactions on Sustainable Energy*, vol. 3, no. 3, pp. 330-338, July 2012.

[66] DR Prathapaneni, Detroja KP. An integrated framework for optimal planning and operation schedule of microgrid under uncertainty. *Sustainable Energy, Grids and Networks*. 2019 Sep 1;19:100232.

[67] A. Ghaffari, Askarzadeh A. Design optimization of a hybrid system subject to reliability level and renewable energy penetration. *Energy*. 2020 Feb 15;193:116754.

[68] M. Jamshidi, Askarzadeh A. Techno-economic analysis and size optimization of an off-grid hybrid photovoltaic, fuel cell and diesel generator system. *Sustainable Cities and Society*. 2019;44:310-20.

[69] H. Borhanazad, Mekhilef S, Ganapathy VG, Modiri-Delshad M, Mirtaheri A. Optimization of micro-grid system using MOPSO. *Renewable Energy*. 2014 Nov 1;71:295-306.

[70] K. S. El-Bidairi, H. Duc Nguyen, S. D. G. Jayasinghe, T. S. Mahmoud and I. Penesis, "Impact of Tidal Energy on Battery Sizing in Standalone Microgrids: A Case Study," *2018 IEEE International Conference on Environment and Electrical Engineering*, 2018, pp. 1-6.

[71] M. Bortolini, Gamberi M, Graziani A, Pilati F. Economic and environmental bi-objective design of an off-grid photovoltaic–battery–diesel generator hybrid energy system. *Energy Conversion and Management*. 2015 Dec 1;106:1024-38.

[72] R. Wang R. Multi-objective configuration optimization method for a diesel-based hybrid energy system. *Energy Reports*. 2020 Nov 1;6:2146-52.

[73] CD Rodríguez-Gallegos, Yang D, Gandhi O, Bieri M, Reindl T, Panda SK. A multi-objective and robust optimization approach for sizing and placement of PV and batteries in off-grid systems fully operated by diesel generators: An Indonesian case study. *Energy*. 2018 Oct 1;160:410-29.

[74] N. Nguyen-Hong, H. Nguyen-Duc and Y. Nakanishi, "Optimal Sizing of Energy Storage Devices in Isolated Wind-Diesel Systems Considering Load Growth Uncertainty," in *IEEE Transactions on Industry Applications*, vol. 54, no. 3, pp. 1983-1991, May-June 2018.

[75] R. Morsali, Kowalczyk R. Demand response based day-ahead scheduling and battery sizing in microgrid management in rural areas. *IET Renewable Power Generation*. 2018 Aug 8;12(14):1651-8.

[76] R. Singh and R. C. Bansal, "Optimization of an Autonomous Hybrid Renewable Energy System Using Reformed Electric System Cascade Analysis," in *IEEE Transactions on Industrial Informatics*, vol. 15, no. 1, pp. 399-409, Jan. 2019.

[77] S. Mohamed, M. F. Shaaban, M. Ismail, and K. A. Qaraqe, "An Efficient Planning Algorithm for Hybrid Remote Microgrids," *IEEE Transactions on Sustainable Energy*, vol. 10, no. 1, pp. 257-267, 2019.

[78] T. A. Nguyen, M. L. Crow and A. C. Elmore, "Optimal Sizing of a Vanadium Redox Battery System for Microgrid Systems," in *IEEE Transactions on Sustainable Energy*, vol. 6, no. 3, pp. 729-737, July 2015.

[79] H. Alharbi and K. Bhattacharya, "Stochastic Optimal Planning of Battery Energy Storage Systems for Isolated Microgrids," in *IEEE Transactions on Sustainable Energy*, vol. 9, no. 1, pp. 211-227, Jan. 2018.

[80] T. Ma, Yang H, Lu L. A feasibility study of a stand-alone hybrid solar–wind–battery system for a remote island. *Applied Energy*. 2014 May 15;121:149-58.

[81] O. H. Mohammed, Y. Amirat, M. Benbouzid and A. A. Elbaset, "Optimal design of a PV/fuel cell hybrid power system for the city of Brest in France," *2014 First International Conference on Green Energy ICGE 2014*, 2014, pp. 119-123.

[82] DN Luta, Raji AK. Optimal sizing of hybrid fuel cell-supercapacitor storage system for off-grid renewable applications. *Energy*. 2019 Jan 1;166:530-40.

[83] F. Fazelpour, Soltani N, Rosen MA. Economic analysis of standalone hybrid energy systems for

application in Tehran, Iran. *International Journal of Hydrogen Energy*. 2016 May 25;41(19):7732-43.

[84] K. Murugaperumal, Raj PA. Feasibility design and techno-economic analysis of hybrid renewable energy system for rural electrification. *Solar Energy*. 2019 Aug 1;188:1068-83.

[85] R. Sen, Bhattacharyya SC. Off-grid electricity generation with renewable energy technologies in India: An application of HOMER. *Renewable Energy*. 2014 Feb 1;62:388-98.

[86] OH Mohammed, Amirat Y, Benbouzid M. Particle swarm optimization of a hybrid wind/tidal/PV/battery energy system. Application to a remote area in Bretagne, France. *Energy Procedia*. 2019;162:87-96.

[87] M. Jahannoosh, Nowdeh SA, Naderipour A, Kamyab H, Davoodkhani IF, Klemeš JJ. New Hybrid Meta-Heuristic Algorithm for Reliable and Cost-Effective Designing of Photovoltaic/Wind/Fuel Cell Energy System Considering Load Interruption Probability. *Journal of Cleaner Production*. 2020 Aug 8:123406.

[88] SR Tito, Lie TT, Anderson TN. Optimal sizing of a wind-photovoltaic-battery hybrid renewable energy system considering socio-demographic factors. *Solar Energy*. 2016 Oct 15;136:525-32.

[89] A. Maleki. Design and optimization of autonomous solar-wind-reverse osmosis desalination systems coupling battery and hydrogen energy storage by an improved bee algorithm. *Desalination*. 2018 Jun 1;435:221-34.

[90] W. Zhang, Maleki A, Rosen MA, Liu J. Optimization with a simulated annealing algorithm of a hybrid system for renewable energy including battery and hydrogen storage. *Energy*. 2018 Nov 15;163:191-207.

[91] N. AfsariArdabilil, S. SeyedShenava and H. Shayeghi, "Price and Reliability-Based Planning of Hybrid Power System in Off-Grid Mode," *2018 Smart Grid Conference (SGC)*, 2018, pp. 1-7.

[92] C. S. Lai and M. D. McCulloch, "Sizing of Stand-Alone Solar PV and Storage System With Anaerobic Digestion Biogas Power Plants," in *IEEE Transactions on Industrial Electronics*, vol. 64, no. 3, pp. 2112-2121, March 2017.

[93] S. Singh, Kaushik SC. Optimal sizing of grid integrated hybrid PV-biomass energy system using artificial bee colony algorithm. *IET Renewable Power Generation*. 2016 May 1;10(5):642-50.

[94] A. Naderipour, Abdul-Malek Z, Nowdeh SA, Kamyab H, Ramtin AR, Shahrokhi S, Klemeš JJ. Comparative evaluation of hybrid photovoltaic, wind, tidal and fuel cell clean system design for different regions with remote application considering cost. *Journal of Cleaner Production*. 2020 Oct 13:124207.

[95] MS Javed, Ma T, Jurasz J, Ahmed S, Mikulik J. Performance comparison of heuristic algorithms for optimization of hybrid off-grid renewable energy systems. *Energy*. 2020 Nov 1;210:118599.

[96] EN Nyeche, Diemuodeke EO. Modelling and optimisation of a hybrid PV-wind turbine-pumped hydro storage energy system for mini-grid application in coastline communities. *Journal of Cleaner Production*. 2020 Mar 20;250:119578.

[97] R. Kaur, V. Krishnasamy, N. K. Kandasamy and S. Kumar, "Discrete Multiobjective Grey Wolf Algorithm Based Optimal Sizing and Sensitivity Analysis of PV-Wind-Battery System for Rural Telecom Towers," in *IEEE Systems Journal*, vol. 14, no. 1, pp. 729-737, March 2020.

[98] M. Guezgouz, et al. Optimal hybrid pumped hydro-battery storage scheme for off-grid renewable energy systems. *Energy Conversion and Management*. 2019 Nov 1;199:112046.

[99] A. Brka, Al-Abdeli YM, Kothapalli G. The interplay between renewables penetration, costing and emissions in the sizing of stand-alone hydrogen systems. International Journal of Hydrogen Energy. 2015 Jan 5;40(1):125-35.

[100] D. Abbes, Martinez A, Champenois G. Life cycle cost, embodied energy and loss of power supply probability for the optimal design of hybrid power systems. *Mathematics and Computers in Simulation*. 2014 Apr 1;98:46-62.

[101] HR Baghaee, Mirsalim M, Gharehpetian GB, Talebi HA. Reliability/cost-based multi-objective Pareto optimal design of stand-alone wind/PV/FC generation microgrid system. *Energy*. 2016 Nov 15;115:1022-41.

[102] Z. Huang, Xie Z, Zhang C, Chan SH, Milewski J, Xie Y, Yang Y, Hu X. Modeling and multi-objective optimization of a stand-alone PV-hydrogen-retired EV battery hybrid energy system. *Energy Conversion and Management*. 2019 Feb 1;181:80-92.

[103] HM Ridha, Gomes C, Hazim H, Ahmadipour M. Sizing and implementing off-grid stand-alone photovoltaic/battery systems based on multi-objective optimization and techno-economic (MADE) analysis. *Energy*. 2020 Sep 15;207:118163.

[104] T. Ma, Yang H, Lu L. Feasibility study and economic analysis of pumped hydro storage and battery storage for a renewable energy powered island. *Energy Conversion and Management*. 2014;79:387-97.

[105] M. Castaneda, Cano A, Jurado F, Sánchez H, Fernández LM. Sizing optimization, dynamic modeling and energy management strategies of a stand-alone PV/hydrogen/battery-based hybrid system. *International Journal of Hydrogen Energy*. 2013 Apr 1;38(10):3830-45.

[106] A. Kaabeche, Belhamel M, Ibtiouen R. Sizing optimization of grid-independent hybrid photovoltaic/wind power generation system. *Energy*. 2011 Feb 1;36(2):1214-22.

[107] S. Norbu, Bandyopadhyay S. Power Pinch Analysis for optimal sizing of renewable-based isolated system with uncertainties. *Energy*. 2017 Sep 15;135:466-75.

[108] H. Belmili, Haddadi M, Bacha S, Almi MF, Bendib B. Sizing stand-alone photovoltaic–wind hybrid system: Techno-economic analysis and optimization. *Renewable and Sustainable Energy Reviews*. 2014 Feb 1;30:821-32.

[109] R. Hosseinalizadeh, Shakouri H, Amalnick MS, Taghipour P. Economic sizing of a hybrid (PV–WT–FC) renewable energy system (HRES) for stand-alone usages by an optimization-simulation model: Case study of Iran. *Renewable and Sustainable Energy Reviews*. 2016 Feb 1;54:139-50.

[110] JC Alberizzi, Rossi M, Renzi M. A MILP algorithm for the optimal sizing of an off-grid hybrid renewable energy system in South Tyrol. *Energy Reports*. 2020 Feb 1;6:21-6.

[111] T. Ma, Javed MS. Integrated sizing of hybrid PV-wind-battery system for remote island considering the saturation of each renewable energy resource. *Energy Conversion and Management*. 2019 Feb 15;182:178-90.

[112] A. Ahadi, Kang SK, Lee JH. A novel approach for optimal combinations of wind, PV, and energy storage system in diesel-free isolated communities. *Applied Energy*. 2016 May 15;170:101-15.

[113] M. Astaneh, Roshandel R, Dufo-López R, Bernal-Agustín JL. A novel framework for optimization of size and control strategy of lithium-ion battery based off-grid renewable energy systems. *Energy Conversion and Management*. 2018 Nov 1;175:99-111.

[114] L. Al-Ghussain, R. Samu O. Taylan, M. Fahrioglu, “Sizing renewable energy systems with energy storage systems in microgrids for maximum cost-efficient utilization of renewable energy resources,” *Sustainable Cities and Society*, vol. 55, pp. 102059, 2020.

[115] M. F. Shaaban, S. Mohamed, M. Ismail, K. A. Qaraqe and E. Serpedin, "Joint Planning of Smart EV Charging Stations and DGs in Eco-Friendly Remote Hybrid Microgrids," in *IEEE Transactions on Smart Grid*, vol. 10, no. 5, pp. 5819-5830, Sept. 2019.

[116] C. Li *et al*., "Optimal Planning of Islanded Integrated Energy System With Solar-Biogas Energy Supply," in *IEEE Transactions on Sustainable Energy*, vol. 11, no. 4, pp. 2437-2448, Oct. 2020.

[117] B. Mohandes, S. Acharya, M. S. E. Moursi, A. S. Al-Sumaiti, H. Doukas and S. Sgouridis, "Optimal Design of an Islanded Microgrid With Load Shifting Mechanism Between Electrical and Thermal Energy Storage Systems," in *IEEE Transactions on Power Systems*, vol. 35, no. 4, pp. 2642-2657, July 2020.

[118] A. A. Hamad, M. E. Nassar, E. F. El-Saadany and M. M. A. Salama, "Optimal Configuration of Isolated Hybrid AC/DC Microgrids," in *IEEE Transactions on Smart Grid*, vol. 10, no. 3, pp. 2789-2798, May 2019.

[119] T. M. Masaud and E. F. El-Saadany, "Correlating Optimal Size, Cycle Life Estimation, and Technology Selection of Batteries: A Two-Stage Approach for Microgrid Applications," in *IEEE Transactions on Sustainable Energy*, vol. 11, no. 3, pp. 1257-1267, July 2020.

[120] Z. Wang, X. Lin, N. Tong, Z. Li, S. Sun, C. Liu, “Optimal planning of a 100% renewable energy island supply system based on the integration of a concentrating solar power plant and desalination units,” *International Journal of Electrical Power & Energy Systems*, vol. 117, pp. 105707, 2020.

[121] M. Combe, et al., “Optimal sizing of an AC-coupled hybrid power system considering incentive-based demand response,” *IET Generation, Transmission & Distribution*, vol. 13, iss. 15, pp. 3354-61, 2019.

[122] A. Ehsan, Q. Yang, “Optimal integration and planning of renewable distributed generation in the power distribution networks: A review of analytical techniques,” *Applied Energy*, vol. 210, pp. 44-59, 2018.

[123] M. A. Hayat, F. Shahnia and G. Shafiullah, "Replacing Flat Rate Feed-In Tariffs for Rooftop Photovoltaic Systems With a Dynamic One to Consider Technical, Environmental, Social, and Geographical Factors," in *IEEE Transactions on Industrial Informatics*, vol. 15, no. 7, pp. 3831-3844, July 2019.

[124] M. Aghamohamadi, A. Mahmoudi and M. H. Haque, "Two-Stage Robust Sizing and Operation Co-Optimization for Residential PV–Battery Systems Considering the Uncertainty of PV Generation and Load," in *IEEE Transactions on Industrial Informatics*, vol. 17, no. 2, pp. 1005-1017, Feb. 2021.

2.3 Multi-Objective Optimal Sizing of Hybrid Standalone/Grid-Connected Electricity Systems

Integration of renewable and energy storage components in standalone/grid-connected energy systems, which results in hybrid energy systems, is increasing nowadays. Optimisation of hybrid energy systems is an essential matter for economic, clean, convenient, and reliable energy supply. Since the optimal design should satisfy multiple objectives, application of multi-objective optimisation is preferred rather than single-objective solution. By multi-objective optimisation, a trade-off among different objectives can be obtained. This review presents a timely survey on the state-of-the-art in multi-objective optimal design of hybrid standalone/grid-connected energy systems. The existing literature is categorised by various indices: (1) standalone or grid-connected mode, (2) number and type of objective functions, (3) completely renewable-based or diesel-renewable-based hybrid systems, and (4) multi-energy systems. The applied objective functions, design constraints and decision variables in optimisation of hybrid energy systems are addressed.

The contribution of this review is presented in one published review paper.

R. Khezri, and A. Mahmoudi, "Review on the state-of-the-art multi-objective optimisation of hybrid standalone/grid-connected energy systems," ***IET Generation, Transmission & Distribution***, vol. 14, iss. 20, pp. 4285–4300, Oct. 2020.

The student has developed the conceptualization and necessity of this review study. Analysis and review of research data has been done by him and the co-author. The student prepared a draft of the review paper. Revisions and comments were provided by the co-author so as to contribute to the interpretation.

2.3.1 Background and Motivation for Hybrid Energy System Research

Integration of distributed renewable energy resources (DRERs) in standalone and grid-connected energy systems is developed worldwide. Feed-in-tariffs in grid-connected systems, fuel delivery troubles for standalone remote area systems, and air pollution problems are some significant reasons for such a high-level development of renewable energy system [1]. However, the uncertain nature and high initial cost of DRERs are the main challenges for reliable and cost-effective power supply in standalone and grid-connected electrical systems. The uncertainty of renewable energies is compensated by diesel generators (DGs) integration in standalone systems, and the main grid in grid-connected systems. However, high fuel cost, green-house gas emission and high electricity cost are the barriers to use only DGs for renewable energies. The alternative remedies for the integration of DRERs are energy storage and demand response [2].

Energy storage systems (ESSs), as significant remedies, store the extra power of DRERs and release it whenever required by the power system. They improve the reliability of standalone system by discharging at the times that the DRERs do not generate power. In addition, ESSs can increase the profitability of DRERs in grid-connected systems by saving the extra energy at the periods that electricity price is low and sell it back to the main grid at the periods that electricity price is high. However, the price of energy storage systems is still high for a beneficial integration [3].

The other remedy for DRER integration is demand response (i.e., demand side management). By demand response, the customer's power consumption can be rescheduled or curtailed to match with the DRERs output power. The demand response can make the renewable energies more profitable by using the generated power of DRERs in high electricity price periods.

The electrical systems with DGs, DRERs, ESSs and demand response in standalone or grid-connected modes are known as hybrid energy systems (HESs). The HES is a complex system with various components and complex energy management. High investigations should be provided in terms of operation, control and optimisation of standalone/grid-connected HESs. There are numerous review and survey papers on generation and transmission expansion planning [4], hybrid renewable energy systems [5], mathematical modelling [6], hybrid energy storage application [7], software tool for modelling [8], and development [9] of HES. Several review papers have studied the optimisation aspect like optimal operation [10], optimisation of distributed energy systems [11], microgrids optimisation [12], and application of artificial intelligence [13] for HES.

Among the various topics associated with HESs, optimal sizing of the components is an important subject for researchers to explore the optimal design of the system. Such a decision-making problem can be accomplished to achieve a range of objectives: decreasing the costs of HES, reducing the air pollution, increasing the reliability, boosting the customer satisfaction, decreasing the excess energy in the system, etc. Considering the variety of objectives, the HES optimisation problem has been solved by single-objective or multi-objective algorithms in the literature.

In a primary level, studies have investigated the optimal sizing problem with a single-objective optimisation model. Several review papers investigated the optimal sizing problem for standalone HES [14], DRERs [15], planning of microgrid [16] and power system [17], different configurations of HES [18], and ESS in distribution network [19]. The single-objective optimisation suffers from considering only one target to maximise or minimise. Although the single-objective optimisation is a useful tool to render insights into the nature of the problem for the decision makers, but generally cannot render a set of alternative solutions that trade various objectives against each other.

In a multi-objective optimisation model, which consists of conflicting objectives, there is no single optimal solution. The interaction among different objectives is shown as a set of compromised solutions, mostly known as the trade-off, non-dominated, non-inferior or Pareto-optimal front solutions. There is only one review study for multi-objective optimisation in HES [20]. The main deficiencies in [20] are: (i) only standalone HES is investigated, (ii) only the evolutionary algorithms were investigated, (iii) overall optimisation (not only optimal sizing) of HESs was investigated, and (iv) only a few studies were considered.

A) *Objective Functions*

a) *Energy cost*

The most important objective function in the first group (minimisation) is the electricity cost of the HES. The electricity cost can be applied using the net present cost (NPC), annual energy cost, and cost of energy (COE) or levelised cost of energy (LCOE).

b) *Air Pollution*

Minimisation of air pollution depends on the mode of the HES (standalone or grid-connected). In standalone HES, the air pollution can be minimised by decreasing the fuel consumption of the diesel generators (DGs). The concept is different in grid-connected HES. Since most of the electricity in the grid-connected HES is supplied through large-scale fossil fuel generators, the air pollution can be minimised by decreasing the imported energy from the grid. In both modes, renewable factor (RF) is an important factor to decrease the air pollution.

c) Dumped Energy

Dumped energy, also recognised as excess energy, has different definitions in standalone and grid-connected HES. In the standalone HES, dumped energy is the remaining energy of renewable energies after feeding the loads and charging the energy storages. However, the dumped energy in the grid-connected HES is the excess energy after feeding loads, charging energy storages, and selling electricity to the main grid.

d) Supply Reliability

The supply reliability objective function is generally used in standalone HES. Since the customers are supplied through the main grid in the grid-connected HES, the supply reliability is not a concern as an objective function for such systems. Maximising the supply reliability means to reduce the supply interruptions in the system. To supply entire loads in the standalone HES, the system needs high capacity of energy storages to be used alongside the renewable energies. Supply interruption is used to decrease the capacity of energy storages and decrease the cost of HES. Conventionally, this objective function is used with cost of system to reach a trade-off between cost and reliability in the standalone energy systems.

The most common ways for considering this objective function are minimising loss of power supply probability (LPSP), and loss of load probability (LOLP).

e) Autonomy

Grid autonomy can be used as an objective function for the grid-connected HES. There are two factors for grid autonomy, known as energy autonomy and power autonomy, which can be used in the optimisation.

B) Design Constraints

The constraints are categorised based on their applications for standalone, grid-connected or both standalone/grid-connected HESs.

Grid constraints should be considered based on the limitations on import/export power from/to the grid for the grid-connected HESs. If demand response is considered in the optimisation of grid-connected HES, then load limitations should be applied to allow a specified value of load to contribute to demand response. Power balance between generation and consumption of HES is the main constraint during the optimisation of standalone HES. Then, reliability constraints can be considered to allow for a specified load reduction to decrease the system costs.

There are several common constraints between standalone and grid-connected HESs. Battery, which is widely considered in both systems, has a limitation on the state-of-charge (SoC). SoC of battery should remain in an interval between the minimum and maximum SoCs. The land and rooftop availability are important constraints for WT and PV installation due to the swept area by these components. Investment limitations in the HES design projects are considered as budget limits. The policies enforced by countries are the other possible constraints. Master planning of the areas is the other limitation in urban areas which should be considered as a constraint in optimal sizing of power systems. Technical constraints are the other types of common limitations in the optimal sizing procedure. Scalability factor is a technical constraint which can be considered to make the optimal sizing scalable. Resiliency constraints are applied to increase the robustness of the designed system against extreme disturbances such as grid outage or natural disasters. Flexibility in operation is an important index because of high penetration of renewable energies in the power systems.

C) Decision Variables

The decision variables in optimisation of HES are the capacities of the components. There are different components which have been considered for the HES design: DG, WT, PV, BSS, super-capacitor (SC) and fuel cell (FC). The decision variables should be optimised to reach the minimum/maximum objective functions. In general, constrains are applied to the size of components (as the decision variables) in the optimisation problem to restrict the capacities.

D) Multi-objective Optimisation Principles

The problem formulation, dominance concept, Pareto-optimal front, and solution algorithms in multi-objective optimisation problems are discussed in this section. A multi-objective optimisation problem can mathematically be presented as follows:

$$\text{Minimise/Maximise} \quad \boldsymbol{F_m(X_i), i = 1, 2, \ldots, M}$$

$$\text{Subject to:} \quad \begin{cases} \boldsymbol{G_k(X_i) \geq 0}, & \boldsymbol{k = 1, 2, \ldots, K} \\ \boldsymbol{H_j(X_i) = 0}, & \boldsymbol{j = 1, 2, \ldots, J} \\ \boldsymbol{X_i = (x_1, x_2, \ldots, x_n)} \end{cases}$$

where $\boldsymbol{F_m}$ and *M* are the *m*th objective function and the number of objectives, respectively. $\boldsymbol{G_k}$ and *K* are the *k*th inequality constraint and the number of inequality constraints, respectively. $\boldsymbol{H_j}$ and *J* are the *j*th equality constraint and the number of equality constraints, respectively. $\boldsymbol{X_i}$ is the *i*th decision variables vector and *n* is the number of decision variables.

Optimisation problems with a single-objective are definitely solvable by finding the *best solution* (minimum or maximum objective function). Inversely, the multi-objective optimisation problems do not have an individual solution and there are a set of optimal solutions. In such a condition, a new concept known as *dominance* needs to be defined. Once the following two conditions are true, it can be concluded that a solution *b* is dominated by a solution *a*:

$$\text{Solution } b \text{ is dominated by a solution } a\text{:} \quad \boldsymbol{a \preccurlyeq b}$$

$$\text{if :} \quad \begin{cases} \forall\, \boldsymbol{i} : \ \boldsymbol{a_i \leq b_i} \\ \exists\, \boldsymbol{i} : \ \boldsymbol{a_{i_0} < b_{i_0}} \end{cases}$$

It means that *b* is not better than *a* in all objectives and *a* is better than *b* in at least one objective. When the dominance concept is applied for a solution in a coordinate table, four different areas can be defined. Fig. 2-10 demonstrates the dominance condition of solution *X* compared to four different areas.

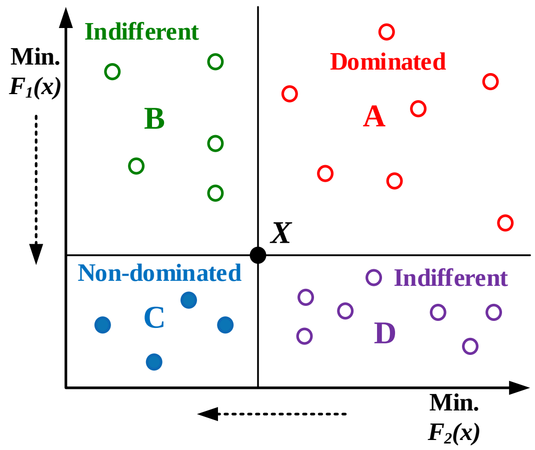

Figure 2-10. Dominance condition of solution X compared to four different areas.

- All the solutions in area A are dominated by the solution *X*.
- Solution *X* is dominated by all the solutions in area C.
- Solutions in areas B and D are indifferent to the solution *X*.

Pareto-optimal Front

Pareto-optimal front is a set of non-dominated solutions to the multi-objective optimisation problem [21]. Generally, it is a curve based on the non-dominated solutions. The solutions in the Pareto-optimal front set are the optimal solutions; means that any improvement is impossible in one objective without losing in any other objectives. The Pareto-optimal front curve should be determined based on the objective functions. The Pareto-optimal front is generally divided into four categories based on the trade-offs between the objective functions. Fig. 2-11 shows a Pareto-optimal front curve for a Max-Min compromise between two objective functions. The other three compromises (Max-Max, Min-Min and Min-Max) can be obtained by translating “max” into “-min” and vice versa [22]. The yellow zone shows the infeasible region of the problem. The solutions placed on the Pareto-optimal front curve are known as “non-dominated solutions” which are not dominated by the other solutions.

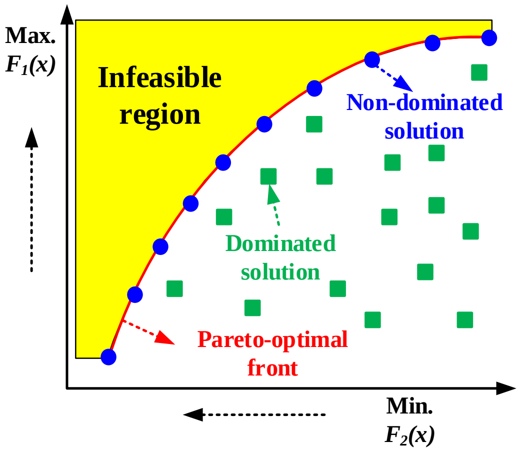

Figure 2-11. Pareto-optimal front curves a Max-Min compromise between two objective functions.

Practically, it is impossible to find all the solutions on the Pareto-optimal front of the optimisation problem. Because of that, a subset of the Pareto-optimal front set is generally sought. Hence, as much as solutions on the Pareto-optimal front should be found for solving a multi-objective optimisation problem; and these solutions should satisfy accuracy and diversity based on the Pareto-optimal front. Fig. 2-21 illustrates four different conditions of accuracy and diversity of solutions considering the Pareto-optimal front.

E) Solving Methods

Solving a multi-objective optimisation problem means finding an appropriate Pareto-optimal front based on the objective functions [22]. Fig. 2-12 shows that, in general, the multi-objective optimisation problems (finding the Pareto-optimal fronts) can be solved by two types of methods: (1) by converting the problem into a single-objective problem, and (2) by directly solving as a multi-objective problem (evolutionary algorithms). Some of the most applied decomposition methods and evolutionary algorithms are shown in Fig. 2-13.

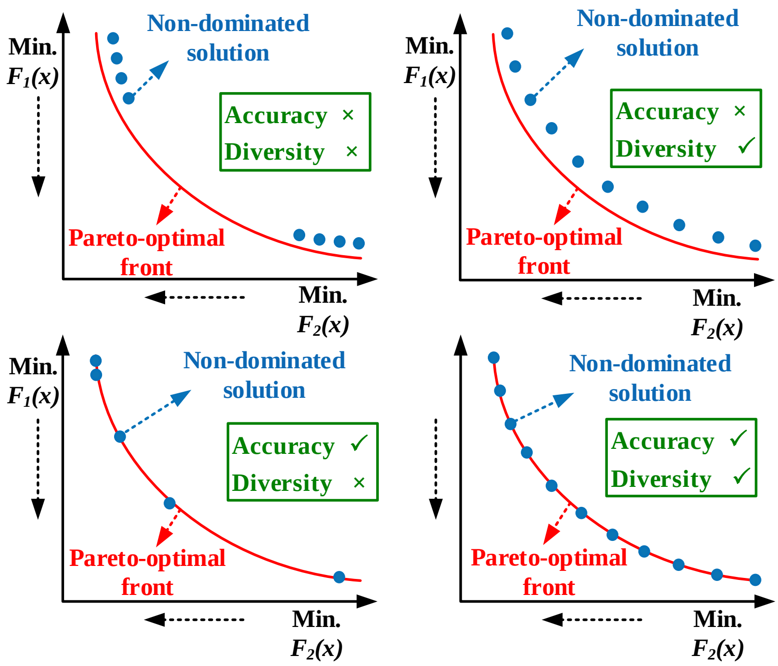

Figure 2-12. Four different conditions of the accuracy and diversity of solutions considering the Pareto-optimal front.

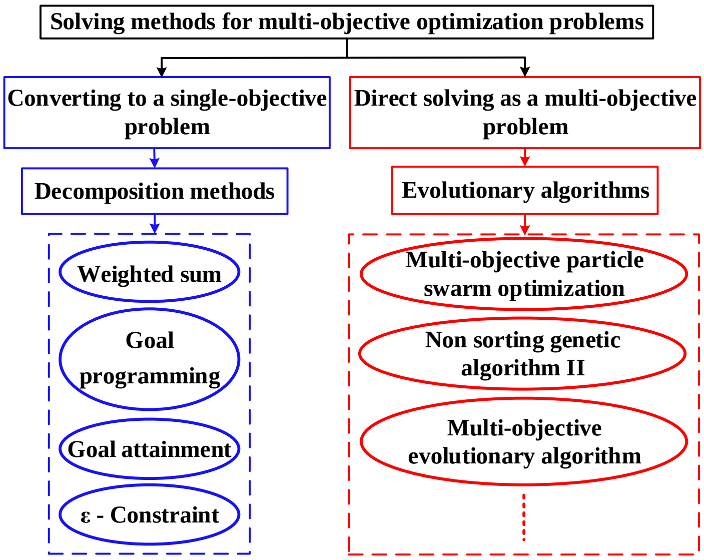

Figure 2-13. Solving methods for multi-objective optimisation problems.

In the first group, decomposition methods are used to convert the problem into a single-objective optimisation model [23]. The first group of methods are known as classic or conventional methods. The applied approaches for the classic method are weighted sum [24], goal programming [25], goal attainment [26], and epsilon-constraint [27]. The main advantage of these methods is that the problem is finally solved as a single-objective problem. However, there are some drawbacks within these methods: (i) the decomposition methods give an individual solution by each run; then, it needs to run the system many times to have an appropriate Pareto-optimal front, and (ii) Such methods require expert knowledge and prior information about the system.

In the second group, evolutionary algorithms are used to solve the problem in a multi-objective optimisation model. Generally, solving multi-objective optimisation problem by the evolutionary algorithms overcome the deficiencies of the first group. For instance, each run of evolutionary algorithms results in a bunch of solutions in the Pareto-optimal front. Multi-objective particle swarm optimisation algorithm (MOPSO) and non-sorting genetic algorithm II (NSGA-II) are the most common multi-objective evolutionary algorithms applied for grid-connected/standalone HESs.

2.3.2 Multi-objective Optimisation of Hybrid Standalone/Grid-Connected Energy Systems

Multi-objective optimisation of standalone/grid-connected HES has been done by previous studies to make a trade-off between different objective functions. In all the previous studies, energy cost is considered as the main objective function and the other objectives are selected based on the requirements of the system model. It is illustrated that minimisation of HES cost is conflicted with all the other objective functions except the dumped energy which has a design dependent relationship with the system cost. Maximising the HES reliability has a conflicting relationship with emission. The relationships between the objective functions show that the multi-objective optimisation of HES is a challenging problem.

The literature review shows that this challenging problem has been investigated for standalone/grid-connected HES by around 69 publications. Fig. 2-14 demonstrates the number of publications per year from 2006 to 2020 in multi-objective optimisation of standalone/grid-connected HES. This shows that most of the publications per year is for 2018, and the topic is more studied in the recent years between 2014 and 2020.

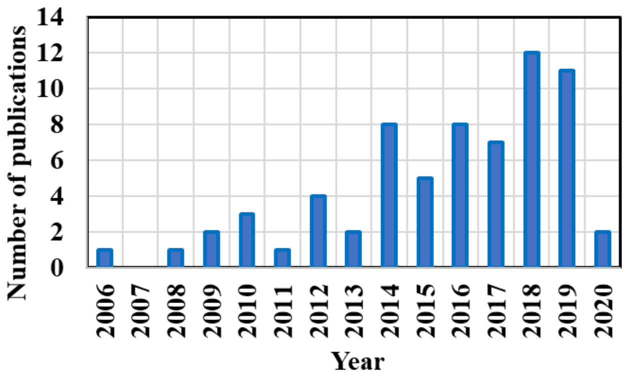

Figure 2-14. Number of publications per year from 2006 to 2020 in multi-objective optimisation.

The previous studies on electrical HESs are categorised into three groups for grid-connected and standalone HES: (1) two-objective HES optimisation problems, (2) three-objective HES optimisation problems, and (3) four-objective HES optimisation problems. Each group is discussed for grid-connected and standalone modes in separate. The studies on standalone mode are also divided in renewable-diesel and completely-renewable based systems.

The existing studies on multi-objective optimal planning of HES by considering multi-energy (electricity, thermal, gas, etc.) system concept are also reviewed in this section.

A) Two-objective Optimisation of HES

The two-objective (or bi-objective) HES optimisation studies have investigated a compromise between electricity cost and another objective function. These studies have been categorised into two groups: grid-connected and standalone.

Grid-connected Hybrid Energy Systems

Table 2-12 shows the applied methods, design constraints, components (decision variables), and objective functions for two-objective optimisation problems of grid-connected HES. CO_2 emission, availability, reliability, customer satisfaction, and grid absorption probability are the objective functions that have been maximised/minimised alongside the cost minimisation.

Table 2-12. Two-objective optimisation studies on grid-connected HES.

Reference	Method	Design constraint	Components (decision variables)	Objective functions
[28]	MOPSO	- Capacity of components	PV	- NPV - CO_2 emission
[29]	MOGA	- Available area - Imported power from grid	PV+WT+BSS	- Cost - Availability

		- Power balance		
[30]	MOPSO	- Capacity of components - LPSP	PV+WT+BSS	- Annualized cost - Imported energy
[31]	NSGA-II	- Not specified	PV+BSS	- Life-cycle cost - Carbon emission
[32]	MOPSO	- Limitations on BSS	BSS	- Total cost - Reliability
[33]	NSGA-II	- Not specified	DG+PV+BSS	- Cost - Emission
[34]	Weighting sum	- Not specified	PV	- Total life cycle cost - LPSP

In [28], using a multi-objective genetic algorithm (MOGA), an availability index has maximised alongside minimising the cost of a grid-connected microgrid. Availability is defined as a fraction of the time when energy is available.

Standalone Hybrid Energy Systems

Studies on bi-objective optimisation of standalone HESs are classified into renewable-diesel based and completely renewable-based systems.

Renewable-Diesel Based Standalone HES

Table 2-13 shows the two-objective optimisation of renewable-diesel standalone HESs. These types of optimisation problems are the major parts of the literature for the multi-objective studies on hybrid energy systems. Various optimisation methods have been applied, such as mixed method [35], robust multi-objective (RMO) methodology [36], strength Pareto evolutionary algorithm (SPEA) [37], multi-objective self-adaptive differential evolution algorithm (MOSADEA) [38], multi-objective crow search algorithm (MOCSA) [39], and multi-objective evolutionary algorithm (MOEA) [42].

Table 2-13. Two-objective optimisation studies on renewable-diesel based standalone HES.

Reference	**Method**	**Design constraint**	**Components (decision variables)**	**Objective functions**
[35]	MODE-NBI-DEA	- Not specified	PV+DG	- LCOE - CO_2 emission
[36]	RMO	- Not specified	PV+WT+DG	- Cost - Reliability
[37]	SPEA	- Not specified	PV+WT+BSS+DG	- LCOE - CO_2 emission
[38]	MOSADEA	- Renewable Factor	PV+WT+BSS+DG	- COE - LPSP
[39]	MOCSA	- Capacity of components	PV+FC+DG	- NPC - LPSP
[40]	MOPSO	- Renewable Factor	PV+WT+BSS+DG	- LCOE - LPSP
[41]	NSGA-II	- Not specified	PV+WT+BSS+DG	- NPC - Emission
[42]	MOEA	- Not specified	PV+WT+BSS+DG	- NPC

				- Unmet load
[43]	NSGA-II	- Limits on the BSS - Unmet load	DG+WT+BSS	- Internal rate of return - Generation cost
[44]	MOPSO	- Not specified	DG+PV+WT+BSS	- LPSP - Price of electricity
[45]	MOPSO	- Not specified	DG+PV+WT	- Cost - Emission

In [35], a mixture design of experiments (MDOE) methodology is used to define the model of objective functions. Normal boundary intersection (NBI) is employed to generate the Pareto-optimal front for the optimisation problem. Data envelopment analysis (DEA) is then applied for the decision making between the optimal non-dominated results.

Completely Renewable Based Standalone HES

The second type of two-objective optimisation problems for standalone HESs is a completely renewable-based energy system. Since the renewable energies are intermittent and unreliable resources, energy storage systems play an important role for such systems. In general, the optimal design of completely renewable-based standalone HES results in a high capacity of energy storage. Several types of energy storages are examined in the design process, such as BSS, FC and SC. Table 2-14 demonstrates the two-objective optimisation studies on completely renewable-based standalone HES.

Table 2-14. Two-objective optimisation studies on completely renewable based standalone HES.

Reference	**Method**	**Design constraint**	**Components (decision variables)**	**Objective functions**
[46]	MOPSO	- Not specified	PV+WT+BSS	- Cost - Reliability
[47]	NSGA-II	- Limits on the BSS	PV+WT+BSS	- Cost - Reliability
[48]	ε-constraint method	- Limits on the BSS - Limits on the hydrogen	PV+WT+BSS+FC	- Cost - Reliability
[49]	NSGA-II	- Limits on the BSS	PV+WT+BSS	- Cost - Reliability
[50]	MOPSO	- Not specified	PV+WT+BSS+FC	- Cost - Reliability

B) Three-objective Optimisation of HES

Generally, 3D representation or 2D curves of the Pareto-optimal front for different objective functions are analyzed for the tri-objective optimisation problems. The tri-objective optimisation problems are divided into grid-connected and standalone systems.

Grid-connected Hybrid Energy Systems

Based on the literature review, there are only six studies on the three-objective optimisation for grid-connected HESs (Table 2-15). In [51], a modified PSO known as constrained mixed-integer MOPSO is used for optimal sizing of the components of a hybrid generation system. In [52], the optimal capacities of PV and WT are analyzed by adopting different multicriteria decision analysis (MCDA) optimisation approaches. A new objective function known as social acceptability, which shows the social resistance to the installation of PV and WT, is included as a social performance evaluation criterion.

Table 2-15. Three-objective optimisation studies on grid-connected HES.

Reference	Method	Design constraint	Components (decision variables)	Objective functions
[51]	Modified PSO	- Power balance - Bounds of design variables	PV+WT+BSS	- Cost - Reliability - Emission
[52]	MCDA	- Total energy lost	PV+WT	- Economic - Emission - Social
[53]	NSGA-II	- Load flow - Components - DG constraint	PV+WT+BSS	- Investment cost - EENS - Power loss
[54]	NSGA-II	- Power flow - Voltage limits - Active power ramp - Storage constraints	BSS	- Total cost - Reliability - Self-adequacy

Standalone Hybrid Energy Systems

The tri-objective optimisation problems of standalone HESs are divided into renewable-diesel- and completely renewable based studies.

Renewable-Diesel Based Standalone HES

Table 2-16 shows that most of the studies on three-objective optimisation of renewable-diesel based standalone HES have considered cost of system, emission and reliability as the objective functions.

Table 2-16. Three-objective optimisation studies on renewable-diesel based standalone HES.

Reference	Method	Design constraint	Components (decision variables)	Objective functions
[55]	MOCSA	- Not specified	PV+DG	- Cost - Reliability - Emission
[56]	MOGA	- Power balance	PV+WT+BSS+DG	- Life cycle cost

				- Dumped energy - CO_2 emission
[57]	MOPSO	- Not specified	PV+WT+BSS+DG	- LCOE - LPSP - Renewable factor
[58]	MOEA	- Not specified	PV+WT+BSS+ FC+DG	- Cost - Environmental - Reliability
[59]	MOPSO	- Limits on the BSS - Limits on the hydrogen - Type of the components	PV+WT+BSS+ FC+DG	- Cost - LPSP - CO_2 emission
[60]	Response surface methodology	- Power balance - Reserve capacity	DG+PV+WT+BSS +FC	- Load curtailment - Operation cost - Emission

Completely Renewable Based Standalone HES

Studies on three-objective completely renewable based standalone HES are shown in Table 2-17. Since these systems are completely renewable based, the emission is not considered as the objective function. In [63], a multi-objective grey wolf algorithm (MOGWA) is applied to optimise the size of components for efficient electricity supply of rural telecom towers.

Table 2-17. Three-objective optimisation studies on completely renewable based standalone HES.

Reference	**Method**	**Design constraint**	**Components (decision variables)**	**Objective functions**
[61]	NSGA-II	- Capacity of components	PV+FC	- Cost - Reliability - Potential energy waste possibility
[62]	NSGA-II	- Not specified	PV+WT+BSS	- Cost - Excess energy - Reliability
[63]	MOGWO	- Not specified	PV+WT+BSS	- Cost - Excess energy - Reliability
[64]	Improved NSGA-II)	- Capacity of components - Limits on the BSS	PV+WT+BSS	- Cost - Environmental - Reliability
[65]	Iterative filter selection approach	- Limits on the BSS - Swept area by the PV and WT	PV+WT+BSS	- Total Cost - Reliability - Dump power
[66]	NSGA-II	- Limits on the BSS	PV+BSS	- LOLP - COE - Battery index

C) Four-objective Optimisation of HES

The studies on quad-objective optimisation of HESs are very limited. Same as the tri-objective problems, these studies used both 2D and 3D representations of objective functions to analyze the non-dominated Pareto-optimal front solutions.

Grid-connected Hybrid Energy Systems

Table 2-18 shows the considered objective functions, components, constraints, and applied methodologies in the four-objective optimisation studies. In [67], a multi-objective artificial bee colony (MOABC) algorithm is used for optimal sizing of WT, PV and FC in a grid-connected HES. The results of the MOABC have shown a better diversity in Pareto-optimal front compared to NSGA-II and MOPSO. The MOPSO approach is used in [68] to optimise the size of PV and BSS in residential buildings based on different objective functions.

Table 2-18. Four-objective optimisation studies on grid-connected HES.

Reference	**Method**	**Design constraint**	**Components (decision variables)**	**Objective functions**
[67]	MOABC	- Active and reactive power generation constraint - Bus voltage limitation - DG penetration level limitation - Thermal limit - Reliability	PV+WT+FC	- Total power loss - Total cost - Emission - Voltage stability index
[68]	MOPSO	- Not specified	PV+BSS	- Energy autonomy - Power autonomy - Payback period - Lifetime cost

Standalone Hybrid Energy Systems

Table 2-19 lists the previous studies on four-objective optimisation problem of standalone HESs. Multi-criterion decision making (MCDM) and normalized weighted constrained multi-objective (NWCMO) algorithms are used for optimal sizing of components in standalone HESs in [142].

Table 2-19. Four-objective optimisation studies on standalone HES.

Reference	**Method**	**Design constraint**	**Components (decision variables)**	**Objective functions**
[69]	MCDM	- Not specified	PV+WT+BSS	- LCOE - Unmet load fraction - Wasted energy - Fuel consumption
[70]	Triangular Aggregation Model and the Levy-Harmony Algorithm	- SOC of battery - Number of components	DG+PV+WT+BSS	- COE - LPSP - Emission - LOLP

Multi-Objective Optimal Planning in Multi-Energy Hybrid Systems

This subsection summarises the application of multi-objective optimal planning in multi-energy hybrid systems. The planning problem of energy systems is more complexed when the interactions among various energy systems are considered. Multi-energy system is a combination of various forms of energies such as electricity, gas, water, thermal, etc. The application of gas turbines in power system has increased the interactions between electricity and gas networks. Hence, the planning of gas-electricity multi-carrier system has attracted the most attention. The planning studies on multi-energy water-electricity systems can investigate the interactions between electricity supply, hydropower, water pumping and water desalination systems. The interactions between cooling, heating and electricity systems are investigated in thermal-electricity multi-energy system

The multi-objective co-expansion planning of gas and electricity networks was investigated by [71]. The decision variables were selected as the transmission lines, generation units, as well as gas compressors and pipelines. In gas-electricity systems, the total cost, as an objective function, not only considers the electricity economics but also the gas operation and investment costs.

In [72], a multi-objective optimal planning was proposed for an electricity-water system considering a resilience index to make the system robust against earthquakes. In [73], the influence of hydropower unit on downstream riverine ecosystem was considered as an objective function for multi-objective design of an electricity-water system. In [74], water storage tank was used as a decision variable in the optimisation model. In water-electricity systems, cost of water is not an issue compared to water storage level/size and ecosystem issues.

All the studies for electricity-thermal system [75] used NSGA-II as the optimisation method. Solar thermal collector, thermal energy storage and fuel cell are the additional components considered in electricity-thermal system optimisation. In [76], a multi-energy vector was investigated considering electricity, gas, hydrogen and syngas energies. The transmission and distribution lines as well as the generation units were considered as the decision variables.

2.3.3 Discussion and New Trends

Literature survey revealed a diversity in the considered objective functions that have been applied in multi-objective optimisation problem of components sizing in hybrid energy systems. This section summarises the classification of existing studies, shortcomings and limited applications, and potential future directions in multi-objective optimal planning of hybrid energy systems.

A) Shortcomings and Limited Applications

Several objective functions in the multi-objective optimisation problem have not investigated accurately and sufficiently by the previous studies. For example, the objective functions associated with demand response in the HES were neglected by the existing multi-objective studies. An objective function, known as customer satisfaction, is used for the optimal sizing programs which include demand response in the optimisation procedure. However, solving such a problem using an evolutionary multi-objective method is neglected in the literature.

Regarding the demand side management in optimal planning, other objective functions like incentive demand response and comfort level of customers are not considered by the existing studies. There is a lack of study for these potential objective functions since the transition from grid-connected system to standalone HES requires an accurate analysis of these indices. Dumped/excess energy is very important objective function in a standalone HES. However, the existing studies have not used this objective function as significant as it is. Only six studies have considered the dumped energy in an optimal planning with three objective functions.

B) Potential Future Directions

The existing studies are classified, and the shortcomings are identified. The potential future directions are provided based on the deficiencies in multi-objective optimal planning of HES. The new trends can be discussed in five categories.

Due to demand response development in hybrid energy systems, considering the customer satisfaction needs more investigation in optimal sizing. The objective functions should maximise the satisfaction of the customers who participate in the demand response program. Since the demand response is generally modelled by load shifting in HESs, the customer satisfaction index should minimise the number of times and appliances which are affected by the demand response program. This index is also addressed as the user’s convenience/comfort level. On the other hand, demand responses with peak shaving needs incentives for the participants. In this case, customer satisfaction can be considered by maximising the incentive payment to the participants. This conflicts with the total cost minimisation of the HES. Therefore, a compromise is required between customer satisfaction and total system cost as the objective functions.

The recent trend in design of grid-connected hybrid energy systems is to decrease the dependency on the main grid. For this purpose, a new objective function is proposed named “grid-dependency (GD)” which is a fraction of imported energy from the grid over the total load demand. Hence, the transition of HES between grid-connected and standalone modes can be discussed based on the concept of GD. Decreasing GD is achievable by integrating distributed renewable energies (PV and WT) to supply the load in grid-connected HES. However, because of intermittency problem of renewable energies, battery energy storage is required to supply the load uninterruptedly. It is notable that as the grid-dependency factor decreases, the size of battery increases and hence the cost of system increases. The highest battery capacity is required when the HES operates as a standalone system (i.e. GD is zero and the transition of HES from grid-connected to standalone mode is completed). A multi-objective optimisation based on the cost and GD factor is an interesting topic of future research on grid-connected HES.

The other group of indices, which can be considered in multi-objective optimisation, are the battery characteristics. Recently, batteries are widely used as a component for the HESs. The battery cost is high, and its lifetime is short. Battery lifetime depends on its operation characteristics in the system. It is generally measured by the number of cycles and the depth of discharge (DOD) of the cycles. Hence, considering the battery operation characteristics to increase its lifetime can achieve lower costs in the system.

2.3.4 Conclusion on the Review of Multi-objective Planning of HES

This paper has presented a survey on the state-of-the-art multi-objective optimisation of hybrid standalone/grid-connected energy systems. The applied objective functions, optimisation algorithms and design constraints in the previous studies were investigated. The methods to solve multi-objective optimisation problems were discussed. The previous studies were categorised by various indices: (1) standalone or grid-connected mode, (2) the number and type of objective functions, and (3) completely renewable-based or diesel-renewable-based hybrid energy systems. It was found that a range of evolutionary algorithms have been applied for the multi-objective optimisation problems. MOPSO and NSGA-II are the most applied algorithms in the previous studies. The customer satisfaction, grid-dependency, battery indices and resiliency as the recent objective functions need further investigation in the multi-objective design procedure.

References

[1] M.A. Hayat, F. Shahnia, and GM Shafiullah, "Replacing flat rate feed-in tariffs for rooftop photovoltaic systems with a dynamic one to consider technical, environmental, social, and geographical factors," *IEEE Trans. Indust. Infor.*, vol. 15, no. 7, pp. 3831-3844, Jul. 2019.

[2] H. Nezamabadi, and V. Vahidinasab, "Market bidding strategy of the microgrids considering demand response and energy storage potential flexibilities," *IET Gene., Trans. Dist.*, vol. 13, iss. 8, pp. 1346 – 1357, Apr. 2019.

[3] M. Stecca, L. R. Elizondo, T. B. Soeiro, P. Bauer and P. Palensky, "A Comprehensive Review of the Integration of Battery Energy Storage Systems Into Distribution Networks," in *IEEE Open Journal of the Industrial Electronics Society*, vol. 1, pp. 46-65, 2020.

[4] M. Navidi, S. M. M. Tafreshi, and A. Anvari-Moghaddam, "A game theoretical approach for sub-transmission and generation expansion planning utilizing multi-regional energy systems," *Int. J. of Electr. Power and Energy Syst.*, vol. 118, Jun. 2020.

[5] R. Singh, and R. C. Bansal, "Review of HRESs based on storage options, system architecture and optimisation criteria and methodologies," *IET Renew. Power Gener.*, vol. 12, iss. 7, pp. 747-760, Jun. 2018.

[6] B. Bhandari, S.R. Poudel, KT. Lee, and SH. Ahn, "Mathematical modeling of hybrid renewable energy system: A review on small hydro-solar-wind power generation," *Int. J. of Precis. Eng. and Manuf.-Green Tech.*, vol. 1, pp. 157-173, 2014.

[7] S. Hajiaghasi, A. Salemnia, and M. Hamzeh, "Hybrid energy storage system for microgrids applications: A review," *Journal of Energy Storage*, vol. 21, pp. 543-570, Feb. 2019.

[8] S. Sinha, and S.S. Chandel, "Review of software tools for hybrid renewable energy systems," *Renew. Sustain. Energy Rev.*, vol. 32, pp. 192-205, Apr. 2014.

[9] A. Mahesh, K.S. Sandhu, "Hybrid wind/photovoltaic energy system developments: Critical review and findings," *Renew. Sustain. Energy Rev.*, vol. 52, pp. 1135-1147, Dec. 2015.

[10] M. Pourbehzadi, T. Niknam, J. Aghaei, G. Mokryani, M. Shafie-khah, an J. P.S.Catalão, "Optimal operation of hybrid AC/DC microgrids under uncertainty of renewable energy resources: A comprehensive review,"*Int. J. of Electr. Power and Energy Syst.*, vol. 109, pp. 139-159, Jul. 2019.

[11] W. L. Theo, J. S. Lim, W. S. Ho, H. Hashim, and C. T. Lee, "Review of distributed generation (DG) system planning and optimisation techniques: Comparison of numerical and mathematical modelling methods" *Renew. Sustain. Energy Rev.*, vol. 67, pp. 531–573, 2017.

[12] A. H. Fatima, and K. Palanisamy, "Optimization in microgrids with hybrid energy systems – A review," *Renew. Sustain. Energy Rev.*, vol. 43, pp. 431-446, May 2015.

[13] S. M. Zahraee, M. K. Assadi, and R. Saidur, "Application of artificial intelligence methods for hybrid energy system optimization," *Renew. Sustain. Energy Rev.*, vol. 66, pp. 617-630, Dec. 2016.

[14] T. Khatib, I.A. Ibrahim, and A. Mohamed, "A review on sizing methodologies of photovoltaic array and storage battery in a standalone photovoltaic system," *Energy Conversion and Management*, vol. 120, pp. 430-448, 2016.

[15] F. A. Khan, N. Pal, and S.H. Saeed, "Review of solar photovoltaic and wind hybrid energy systems for sizing strategies optimization techniques and cost analysis methodologies," *Renew. Sustain. Energy Rev.*, vol. 92, pp. 937-947, Sep. 2018.

[16] J. Jung, and M. Villaran, "Optimal planning and design of hybrid renewable energy systems for microgrids," *Renew. Sustain. Energy Rev.*, vol. 75, pp. 180-191, Aug. 2017.

[17] X. Deng, and T. Lv, "Power system planning with increasing variable renewable energy: A review of optimization models," *Journal of Cleaner Production*, vol. 246, Feb. 2020.

[18] K. Anoune, M. Bouya, A. Astito, and A.B. Abdellah, "Sizing methods and optimization techniques for PV-wind based hybrid renewable energy system: A review," *Renew. Sustain. Energy Rev.*, vol. 93, pp. 652-673, 2018.

[19] M. Zidar, P. S Georgilakis, N. D Hatziargyriou, T. Capuder, and D. Škrlec, "Review of energy storage allocation in power distribution networks: applications, methods and future research," *IET Gene., Trans. Dist.*, vol. 10, iss. 3, pp. 645 – 652, Feb. 2016.

[20] M. Fadaee, and M.A.M. Radzi, "Multi-objective optimization of a standalone hybrid renewable energy system by using evolutionary algorithms: A review," *Renew. Sustain. Energy Rev.*, vol. 16, pp. 3364-3369, 2012.

[21] C.A. Coello, D.A.V. Veldhuizen, G.B. Lamont, *Evolutionary Algorithms for Solving Multi-objective Problems*, Kluwer Aca, New York, 2002.

[22] Deb K. *Multi-Objective Optimization Using Evolutionary Algorithms*. John Wiley and Sons: Chichester, England.

[23] A. A. Rodriguez, G. Ault, and S. Galloway, "Multi-objective planning of distributed energy resources: A review of the state-of-the-art," *Renew. Sustain. Energy Rev.*, vol. 14, pp. 1353–1366, Jan. 2010.

[24] R. T. Marler, and J. S. Arora, "The weighted sum method for multi-objective optimization: new insights," *Structural and Multidisciplinary Optimization*, vol. 41, pp. 853–862, 2010.

[25] M. Tamiz, D. F. Jones, and E. El-Darzi, "A review of Goal Programming and its applications," *Annals*

of Operations Research, vol. 48, pp. 39-53, 1995.

[26] F. Gembicki, and Y. Haimes, “Approach to performance and sensitivity multi-objective optimization: The goal attainment method,” *IEEE Trans. on Automatic Control*, vol. 20, iss. 6, pp. 769-771 Dec. 1975.

[27] A.E. Nezhad, A. Ahmadi, M.S. Javadi, and M. Janghorbani, “Multi-objective decision-making framework for an electricity retailer in energy markets using lexicographic optimization and augmented epsilon-constraint,” *Int. Trans. Electr. Energ. Syst.*, vol. 28, pp. 3660-3680, 2015.

[28] A. Kornelakis, “Multiobjective Particle Swarm Optimization for the optimal design of photovoltaic grid-connected systems,” *Solar Energy*, vol. 84 pp. 2022–2033, 2010.

[29] M. B. Shadmand, and R. S. Balog, “Multi-objective optimization and design of photovoltaic-wind hybrid system for community smart DC microgrid,” *IEEE Trans. Smart Grid*, vol. 5, iss. 5, pp. 2635–2643, 2014.

[30] J. L. Duchaud, G. Notton, C. Darras, and C. Voyant, “Multi-Objective Particle Swarm optimal sizing of a renewable hybrid power plant with storage,” *Renewable Energy*, vol. 131, pp. 1156-1167, 2019.

[31] R. D. Bingham, M. Agelin-Chaab, and M. A. Rosen, “Whole building optimization of a residential home with PV and battery storage in The Bahamas,” *Renewable Energy*, vol. 132, pp. 1088-1103, 2019.

[32] H. B. Yamchi, H. Shahsavari, N. T. Kalantari, A. Safari, and M. Farrokhifar, “A cost-efficient application of different battery energy storage technologies in microgrids considering load uncertainty,” *Journal of Energy Storage*, vol. 22, pp. 17-26, 2019.

[33] M. L. D. Silvestre, G. Graditi, and E. R. Sanseverino, “A generalized framework for optimal sizing of distributed energy resources in micro-grids using an indicator-based swarm approach,” *IEEE Trans. Indust. Infor.*, vol. 10, iss. 1, pp. 152 - 162, 2014.

[34] K. Ndwali, J. G. Njiri, and E. M. Wanjiru, “Multi-objective optimal sizing of grid connected photovoltaic batteryless system minimizing the total life cycle cost and the grid energy,” *Renewable Energy*, vol. 148, pp. 1256-1265, 2020.

[35] M. N. Fonseca, E. D. Pamplona, A. R. Queiroz, V. E. M. Valerio, G. Aquila, and S. R. Silva, “Multi-objective optimization applied for designing hybrid power generation systems in isolated networks,” *Solar Energy*, vol. 161, pp. 207-219, 2018.

[36] A. Maheri, “Multi-objective design optimisation of standalone hybrid wind-PV diesel systems under uncertainties,” *Renewable Energy*, vol. 66, pp. 650-661, 2014.

[37] R. Dufo-López, J. L. Bernal-Agustín, J. M. Yusta-Loyo, J. A. Domínguez-Navarro, I. J. Ramírez-Rosado, J. Lujano, and I. Aso, “Multi-objective optimization minimizing cost and life cycle emissions of stand-alone PV–wind–diesel systems with batteries storage,” *Applied Energy*, vol. 88, pp. 4033–4041, 2011.

[38] M. A. M. Ramli, H. R. E. H. Bouchekara, and A. S. Alghamdi, “Optimal sizing of PV/wind/diesel hybrid microgrid system using multi-objective self-adaptive differential evolution algorithm,” *Renewable Energy*, vol. 121, pp. 400-411, 2018.

[39] M. Jamshidi, and A. Askarzadeh, “Techno-economic analysis and size optimization of an off-grid hybrid photovoltaic, fuel cell and diesel generator system,” *Sustainable Energy, Grids and Networks*, vol. 44, pp. 310–320, 2019.

[40] H. Borhanazad, S. Mekhilef, V.G. Ganapathy, M. Modiri-Delshad, and A. Mirtaheri, “Optimization of micro-grid system using MOPSO,” *Renewable Energy*, vol. 71, pp. 295-306, 2014.

[41] L. Guo, W. Liu, B. Jiao, B. Hong, and C. Wang, “Multi-objective stochastic optimal planning method for stand-alone microgrid system,” *IET Gener. Trans. Distr.*, vol. 8, iss. 7, pp. 1263–1273, 2014.

[42] J.L. Bernal-Agustı´n, and R. Dufo-Lo´pez, “Multi-objective design and control of hybrid systems minimizing costs and unmet load,” *Electric Power Systems Research*, vol. 79, pp. 170–180, 2009.

[43] L. Guo, N. Wang, H. Lu, X. Li, and C. Wang, “Multi-objective optimal planning of the stand-alone microgrid system based on different benefit subjects,” *Energy*, vol. 116, pp. 353-363, 2016.

[44] M. Jayachandran, and G. Ravi, “Design and optimization of hybrid micro-grid system,” *Energy Procedia*, vol. 117, pp. 95-103, 2017.

[45] P. Machado, R.S. Netto, L. E. Souza, and JC. Maun, “Probabilistic and multi-objective approach for planning of microgrids under uncertainty: a distributed architecture proposal,” *IET Gene., Trans. Dist.*, vol. 13, iss. 7, pp. 1025-1035, 2019.

[46] N. Ghorbani, A. Kasaeian, A. Toopshekan, L. Bahrami, and A. Maghami, “Optimizing a hybrid wind-PV-battery system using GA-PSO and MOPSO for reducing cost and increasing reliability,” *Energy*, vol. 154, pp. 581-591, 2018.

[47] M. Belouda, M. Hajjaji, H. Sliti, and A. Mami, “Bi-objective optimization of a standalone hybrid PV–Wind–battery system generation in a remote area in Tunisia,” *Sustainable Energy, Grids and Networks*, vol. 16, pp. 315–326, 2018.

[48] H. Bakhtiari, and R.A. Naghizadeh, “Multi-criteria optimal sizing of hybrid renewable energy systems including wind, photovoltaic, battery, and hydrogen storage with ε–constraint method,” *IET Renew. Power Gener.*, vol. 12, iss. 8, pp. 883–892, 2018.

[49] A. Kamjoo, A. Maheri, A.M. Dizqah, and G.A. Putrus, “Multi-objective design under uncertainties of hybrid renewable energy system using NSGA-II and chance constrained programming,” *Int. J. of Electr. Power and Energy Syst.*, vol. 74, pp. 187–194, 2016.

[50] A. Parizad, and K. J. Hatziadoniu, “Multi-objective optimization of PV/Wind/ESS hybrid microgrid system considering reliability and cost indices,” *North American Power Symposium (NAPS)*, Wichita, KS, USA, 2019.

[51] L. Wang and C. Singh, “Multicriteria design of hybrid power generation systems based on a modified

particle swarm optimization algorithm," *IEEE Trans. Energy Convers.*, vol. 24, no. 1, pp. 163–172, Mar. 2009.

[52] M. Alsayed, M. Cacciato, G. Scarcella, and G. Scelba, "Multicriteria optimal sizing of photovoltaic-wind turbine grid connected systems," *IEEE Trans. Energy Convers.*, vol. 28, no. 2, pp. 370–379, Jun. 2013.

[53] W. Sheng, K. Liu, X. Meng, X. Ye, and Y. Liu, "Research and practice on typical modes and optimal allocation method for PV-Wind-ES in Microgrid," *Electric Power Systems Research*, vol. 120, pp. 242-255, 2015.

[54] F. Moghateli, S. A. Taher, A. Karimi, and M. Shahidehpour, "Multi-objective design method for construction of multi-microgrid systems in active distribution networks," *IET Smart Grid*, Feb. 2020.

[55] Z. Movahediyan, and A. Askarzadeh, "Multi-objective optimization framework of a photovoltaic-diesel generator hybrid energy system considering operating reserve," *Sustainable Cities and Society*, vol. 41, pp. 1–12, 2018.

[56] A.S.O. Ogunjuyigbe, T.R. Ayodele, and O.A. Akinola, "Optimal allocation and sizing of PV/Wind/Split-diesel/Battery hybrid energy system for minimizing life cycle cost, carbon emission and dump energy of remote residential building," *Applied Energy*, vol. 171, pp. 153–171, 2016.

[57] M. Azaza, and F. Wallin, "Multi objective particle swarm optimization of hybrid micro-grid system: A case study in Sweden," *Energy*, vol. 123, pp. 108-118, 2017.

[58] R. Dufo-Lo´pez, and J.L. Bernal-Agustı´n, "Multi-objective design of PV– wind– diesel– hydrogen– battery systems," *Renewable Energy*, vol. 33, pp. 2559–2572, 2008.

[59] M. Sharafi, and T.Y. Mekkawy, "Multi-objective optimal design of hybrid renewable energy systems using PSO-simulation based approach," *Renewable Energy*, vol. 68, pp. 67–79, 2014.

[60] X. Cao, J. Wang, and Z. Zhang, "Multi-objective optimization of preplanned microgrid islanding based on stochastic short-term simulation," *Int. Trans. Electr. Energ. Syst.*, vol. 27, pp. 1–16, 2017.

[61] Z. Huang, Z. Xie, C. Zhang, S.H. Chan, J. Milewskic, Y. Xie, Y. Yang, and X. Hu, "Modeling and multi-objective optimization of a stand-alone PV-hydrogen retired EV battery hybrid energy system," *Energy Conversion and Management*, vol. 181, pp. 80–92, 2019.

[62] R. Kaur, V. Lrishnasamy, and N.K. Kandasamy, "Optimal sizing of wind-PV-based DC microgrid for telecom power supply in remote-areas," *IET Renew. Power Gener.*, vol. 12, iss. 7, pp. 859–866, 2018.

[63] R. Kaur, V. Lrishnasamy, N.K. Kandasamy, and S. Kumar, "Discrete Multi-objective Grey Wolf Algorithm Based Optimal Sizing and Sensitivity Analysis of PV-Wind-Battery System for Rural Telecom Towers," *IEEE Systems Journal*, vol. 14, iss. 1, pp. 729 - 737, 2020.

[64] H. Shayeghi, and Y. Hashemi, "Application of fuzzy decision-making based on INSGA-II to designing PV–wind hybrid system," *Engineering Applications of Artificial Intelligence*, vol. 45, pp. 1–17, 2015.

[65] S. Hussain, R. Al-ammar, A. Iqbal, M. Jafar, and S. Padmanaban, "Optimisation of hybrid renewable energy system using iterative filter selection approach," *IET Renew. Power Gener.*, vol. 11, iss. 11, pp. 1440-1445, 2017.

[66] M. I. Hlal, V. K. Ramachandaramurthy, A. Sarhan, A. Pouryekta, and U. Subramaniam, "Optimum battery depth of discharge for off-grid solar PV/battery system," *Journal of Energy Storage*, vol. 26, 2019.

[67] H. Nasiraghdam, and S. Jadid, "Optimal hybrid PV/WT/FC sizing and distribution system reconfiguration using multi-objective artificial bee colony (MOABC) algorithm," *Solar Energy*, vol. 86, pp. 3057–3071, 2012.

[68] S. Bandyopadhyay, G.R. Mouli, Z. Qin, L.R. Elizondo, and Pavol Bauer, "Techno-economical model based optimal sizing of PV-Battery systems for microgrids," *IEEE Trans. Sustain. Energy*, Early Access, Aug. 2019.

[69] A.T.D. Perera, R.A. Attalage, K.K.C.K. Perera, and V.P.C. Dassanayake, "A hybrid tool to combine multi-objective optimization and multi-criterion decision making in designing standalone hybrid energy systems," *Applied Energy*, vol. 107, pp. 412–425, 2013.

[70] P. Li, R. Li, Y. Cao, D. Li and G. Xie, "Multi-objective Sizing Optimization for Island Microgrids Using a Triangular Aggregation Model and the Levy-Harmony Algorithm," *IEEE Trans. on Indust. Infor.*, vol. 14, no. 8, pp. 3495-3505, Aug. 2018.

[71] H. Cong, X. Wang, and C. Jiang, "Two-stage nested bilevel model for generation expansion planning in combined electricity and gas markets," *IET Gene., Trans. Dist.*, vol. 13, iss. 15, pp. 3443 – 3454, 2019.

[72] J. Najafi, A. Peiravi, and A. Anvari-Moghaddam, "Enhancing Integrated Power and Water Distribution Networks Seismic Resilience Leveraging Microgrids," *Sustainability*, vol. 12, no. 6, pp. 1-16, Mar. 2020.

[73] W. Liu, F. Zhu, J. Chen, H. Wang, B. Xu, P. Song, et al., "Multi-objective optimization scheduling of wind–photovoltaic–hydropower systems considering riverine ecosystem," *Energy Conversion and Management*, vol. 196, pp. 32-43, Jun. 2019.

[74] D. H. Muhsen, A. B. Ghazali, T. Khatib, I. A. Abed, and E. M. Natsheh, "Sizing of a standalone photovoltaic water pumping system using a multi-objective evolutionary algorithm," *Energy*, vol. 109, pp. 961-973, 2016.

[75] J. Assaf, and B. Shabani, "Multi-objective sizing optimisation of a solar-thermal system integrated with a solar-hydrogen combined heat and power system, using genetic algorithm," *Energy Conversion and Management*, vol. 164, pp. 518-532, Mar. 2018.

[76] S. Samsatli, and N. J. Samsatli, "A multi-objective MILP model for the design and operation of future integrated multi-vector energy networks capturing detailed spatio-temporal dependencies," *Applied Energy*, vol. 220, pp. 893–920, 2018.

Chapter 3
Optimal Capacity of Rooftop Solar PV and Battery for Grid-Connected Households

This chapter investigates the optimal sizing problem of rooftop solar PV and battery storage for grid-connected households in Australia. Two system configurations (PV-only and PV-battery) are optimally sized. Practical guidelines are presented for the customers in South Australia to purchase the correct capacity of PV and battery based on their available roof area and average electricity consumption.

The contribution of this chapter is presented in one published research article. **R. Khezri**, A. Mahmoudi and M. H. Haque, "Optimal Capacity of Solar PV and Battery Storage for Australian Grid-Connected Households," ***IEEE Transactions on Industry Applications***, vol. 56, no. 5, pp. 5319-5329, Sept.-Oct. 2020.

The student has developed the conceptualization. He designed the optimisation model. Analysis and interpretation of research data has been done by him and the co-authors. A draft of the paper was prepared by the student. Revisions and comments were provided by the co-authors so as to contribute to the interpretation.

3.1 Introduction

Rooftop solar photovoltaic (PV) systems are increasingly integrated in Australian households. According to an Australian clean energy report [1], five rooftop solar PV systems were installed in each hour of 2018. At the end of June 2019, more than one-third of Australian dwellings had rooftop solar PV systems [2].

Such a high penetration of PV systems is the result of high retail price, falling PV system costs and incentives from the government in forms of feed-in-tariff (FiT) and rebates [3].

In a grid-connected system, the installed PV system feeds the load and sells the excess power to the grid [4]. This reduces the annual electricity bills of the household. Since the FiT is much lower than the retail price (RP) in South Australia (SA) [5], integration of battery storage in grid-connected households becomes an attractive option. With battery integration, the excess power generated by the PV during daytime can be stored [6]. The battery then releases the stored energy in the evenings during the peak hours [7].

Currently, battery energy storage (BES) is an expensive technology and its viability for economic integration in households needs investigation. Rooftop PV system, if not selected optimally, may not offer economic benefits [8]. Thus, the selection of optimal capacity of PV and BES is an important issue for a grid-connected household to achieve the maximum technical and economic benefits.

The main scope of this chapter is optimal planning of solar PV and battery for grid-connected residential households. In this study, two different rule-based home energy management system (HEMS) techniques are developed for two configurations: PV only and PV with BES. The HEMS techniques ensure the accurate operation of the configurations by considering the grid constraint and dumped power. The real annual meteorological and load data, PV, and BES capital expenditure (Capex) and Opex, and appropriate interest/escalation rates are incorporated which makes the model more realistic. The optimisation model for optimal sizing of PV and BES is extended for other Australian States.

The main contributions of this study compared to previous works are summarised as follows:

- Development of a practical optimisation technique for two different configurations of grid-connected households to determine the optimal capacity of PV and BES using realistic data.
- Study the effect of grid constraint on the optimal capacity of components and cost of electricity (COE).
- Investigate the effects of electricity demand, RP, FiT, and costs of PV and BES on COE and optimal sizing.

- Development of annual cash flow analysis for each configuration of a grid-connected household.
- Evaluate the optimal results by conducting an uncertainty analysis of solar insolation and ambient temperature using 10 years real data.
- Provide a practical guideline for the consumers to select the right capacities of PV and BES based on the average daily electricity demand and the available rooftop space for PV installation.

3.2 Operating Strategies

Fig. 3-1 shows two different configurations for a grid- connected household. In the first configuration, only a PV system is integrated with the household. In the second configuration, an ac coupled BES is added in parallel with the PV system. Note that a third configuration (series connection of PV and BES) is also investigated. However, the corresponding results are found to be economically unattractive.

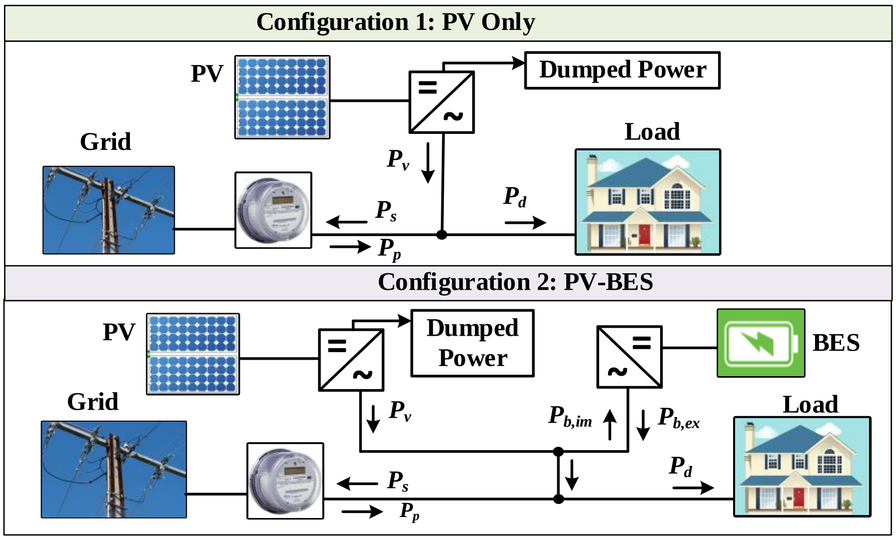

Figure 3-1. Two system configurations of a grid-connected house: (1) PV only, and (2) PV with BES.

The real-time rule-based HEMS of both configurations is shown on right hand side of Fig. 3-2 which is discussed in this section. Rule-based HEMSs are easy to understand and user-friendly. In this method, all the rules are explicit for the designers and customers. These rules can be simply updated if the customers use time-of-use or real time pricing tariffs.

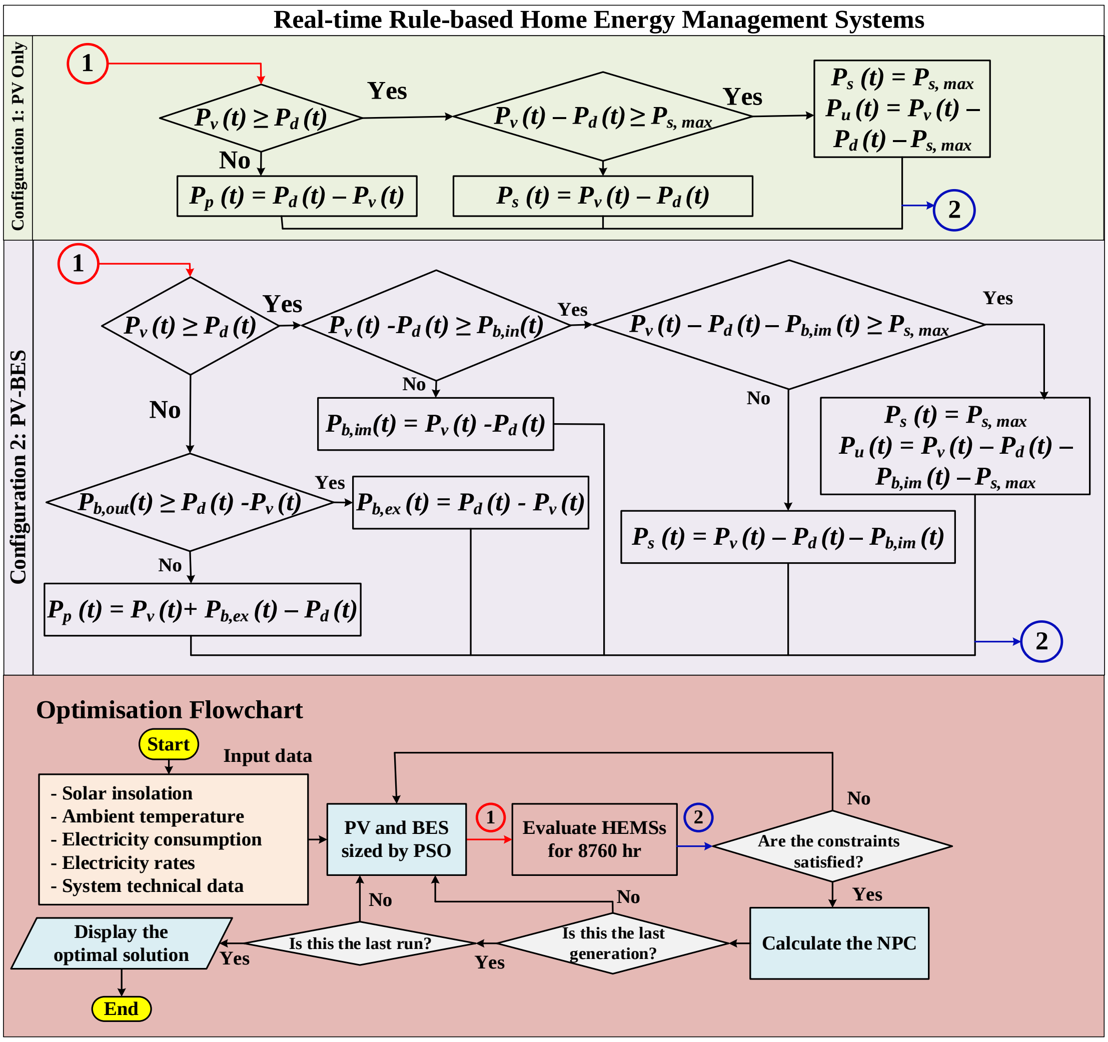

Figure 3-2. Optimisation flowchart and HEMS for the proposed system configurations.

3.2.1 Configuration 1: PV Only

The first configuration supplies power from the rooftop PV to the household. When the PV power exceeds the demand of the household, the excess power/energy is exported or sold to the grid at feed-in-tariff. In general, there is a maximum export power limit $P_{s,max}$ imposed by the utility. With the notations shown in Fig. 1, the export or sold power can be expressed as:

$$P_s(t) = \min\left(P_{s,max}, P_v(t) - P_d(t)\right) \tag{3-1}$$

If the difference between the PV power and the household demand exceeds the maximum export power limit, the extra power is dumped using the control system of PV. Thus, the dumped power can be written as:

$$P_u(t) = P_v(t) - P_d(t) - P_{s,max} \tag{3-2}$$

When the PV power is less the household demand, the system imports or purchases power from the grid. Thus, the purchase power can be expressed as:

$$P_p(t) = P_d(t) - P_v(t) \tag{3-3}$$

3.2.2 Configuration 2: PV and BES

In the second configuration, an ac coupled battery is added in parallel with the PV. When the PV power exceeds the household demand, first the BES will be charged (if the state of charge (SOC) level and input power of the BES are within the limits) and then the extra power, if any, will be exported or sold to the grid. Thus, exported or sold power to the grid is:

$$P_s(t) = \min\left(P_{s,max}, P_v(t) - P_d(t) - P_{b,im}(t)\right) \tag{3-4}$$

Like Configuration 1, the dumped power is:

$$P_u(t) = P_v(t) - P_d(t) - P_{b,im}(t) - P_{s,max} \tag{3-5}$$

If the PV power is less than the household demand, first the BES will discharge to meet the demand (if the SOC level and output power of the BES are within the limit) and then the shortage power, if any, will be imported from the grid. Thus, the import or purchase power P_p can be written as:

$$P_p(t) = P_d(t) - P_v(t) - P_{b,ex}(t) \tag{3-6}$$

The SOC of battery in each time interval is calculated by:

$$SOC(t + \Delta t) = SOC(t) + \frac{P_{b,im}(t).\,\eta_{b,im} - P_{b,ex}(t)/\eta_{b,ex}}{E_b/\mathrm{h}} \tag{3-7}$$

The available input and output power for charging/discharging of BES are calculated as:

$$P_{b,in}(t) = \min\left(P_{b,max}\,, (E_b/\mathrm{h}).\left(SOC_{max} - SOC(t)\right)\right) \tag{3-8}$$

$$P_{b,out}(t) = \min\left(P_{b,max}\,, (E_b/\mathrm{h}).\,(SOC(t) - SOC_{min})\right) \tag{3-9}$$

3.3 Optimisation Model

This section describes the optimisation model for the planning problem. The optimisation process is shown in a flow chart on left hand side of Fig. 3.2. The formulated problem can be solved using different solvers (available in MATLAB optimisation toolbox), but the particle swarm optimisation approach is used in this study. The PSO algorithm is successfully applied to solve the power system optimisation problems [9]. Among the evolutionary algorithms, PSO is a well-known method due to its suitable convergence rate, simplicity, less requirement of storage and minimum initial points dependency [10]. To guarantee the global optimal solution by the PSO algorithm, high number of populations (300) and generations (500) are considered in this study. In addition, the PSO optimisation has been done in 20 runs to achieve global optimal results for the systems.

3.3.1 Objective Function

The net present cost (NPC) over 20-year project lifespan is considered as the objective function. It is calculated from the components (PV and BES) net present cost and the electricity net present cost. The total NPC is:

$$NPC_t = NPC_s + NPC_e \tag{3-10}$$

The components net present cost is calculated as follows:

$$\begin{gathered} NPC_s = N_b \cdot \left(PC_{x(b)} + PC_{y(b)} + PC_{z(b)}\right) + \\ N_v \cdot \left(PC_{x(v)} + PC_{y(v)} + PC_{z(v)}\right) \end{gathered} \tag{3-11}$$

Indices *b* and *v* represent BES and PV, respectively. The present cost for a series of fixed annual maintenance over the component's lifetime at an interest rate *i* is calculated by:

$$PC_y = C_y.\frac{(1+i)^M - 1}{i(1+i)^M} \tag{3-12}$$

The present cost of a component replacement, every Y years of the system lifetime is:

$$PC_z = C_z.\sum_{t=1}^{tY<M} \frac{1}{(1+i)^{tY}} \tag{3-13}$$

It is considered that electricity cost escalates at a rate (e) above the interest rate *i*. Thus, the real interest rate is:

$$r = \frac{i-e}{1+e} \tag{3-14}$$

The net present cost for an annual electricity cost is:

$$NPC_e = C_e.\frac{(1+r)^n - 1}{r(1+r)^n} \tag{3-15}$$

$$C_e = \sum_{t=1}^{8760} RP(t).P_p(t).\Delta t - \sum_{t=1}^{8760} FiT(t).P_s(t).\Delta t \tag{3-16}$$

3.3.2 Design Constraints

Design constraints are considered as follows:

$$0 \leq P_v(t) \leq P_{v,max} \tag{3-17}$$

$$0 \leq P_{b,im}(t), P_{b,ex}(t) \leq P_{b,max} \tag{3-18}$$

$$SOC_{min} \leq SOC(t) \leq SOC_{max} \tag{3-19}$$

$$P_b(t) + P_v(t) + P_p(t) - P_s(t) \geq P_d(t) \tag{3-20}$$

$$0 \leq P_s(t) \leq P_{s,max} \tag{3-21}$$

Equations (3-17) and (3-18) are the constraints on PV and BES output powers, respectively. Equation (3-19) is the SOC constraint of battery. Equation (3-20) is a constraint for power balance at each time period. Equation (3-21) is the grid constraint to limit the export power from the PV to the grid.

3.3.3 Cost of Electricity

The cost of electricity (COE) is the ratio of net annual payment to the net annual electricity consumption. The COE (¢/kWh) is calculated based on the components and electricity net present costs, associated capital recovery factor (CRF), and the annual load demand:

$$\mathrm{COE} = \frac{NPC_s.\mathrm{CRF_s} + NPC_e.\mathrm{CRF_e}}{E_{annual}} \tag{3-22}$$

$$\mathrm{CRF}_s = \frac{d(1+d)^n}{(1+d)^n - 1} \tag{3-23}$$

$$\mathrm{CRF}_e = \frac{q(1+q)^n}{(1+q)^n - 1} \tag{3-24}$$

$$\mathrm{E}_{annual} = \sum_{t=1}^{8760} P_d(t).\Delta t \tag{3-25}$$

It is to be noted that *d* and *q* are the same as *i* and *r*, respectively.

The COE is typically used to compare the cost of different electricity systems. In the absence of PV and BES, the COE of the household is the same as the RP.

3.4 Case Study

The developed HEMSs and optimisation model are general and can be applied to all standard networks. In this chapter, a grid-connected household in SA is considered as the case study to investigate the proposed optimisation model. Input data used in the case study is explained in this section. This includes two different data sets: (1) economic and technical data of components and main grid; (2) load and meteorological data.

3.4.1 Economic and Technical Data

Table 3-1 lists the component costs and parameters, RP and FiT of electricity, and the interest and escalation rates. The above values are selected based on the actual market price in SA. In this study, all prices are in Australian dollar. The project lifespan is considered as 20 years. The degradation of the BES due to aging is indirectly included by considering the round-trip efficiency as 76% during the project lifespan.

Table 3-1. System components costs, electricity prices and economic rates.

PV [12]	Capital cost = $1,500/kW Replacement cost = $300/kW Maintenance = $50/kW/year	PV lifetime = 25 years Inverter lifetime = 10 years Solar cell efficiency = 20%	
BES [13]	Capital cost = $700-1,000/kWh Replacement cost = $400/kWh BES lifetime = 10 years	SOC_{min} = 20% SOC_{max} = 100%	
Electricity prices	Retail price = 48 ¢/kWh Feed-in-tariff = 17 ¢/kWh	**Economic rates**	i = 8% e = 2%

In 2017, SA power network imposed the maximum export power limit of single-phase households to 5 kW [11]. By the grid constraint, the local electricity networks can be protected from overloading problem.

3.4.2 Load Profile and Meteorological Data

The box plot of load consumption for a typical household in SA is shown in Fig. 3-3 [3]. The maximum and average load consumptions during a year are 1.647 kW and 0.651 kW, respectively. Daily average and annual energy consumptions are 15.63 kWh and 5,704.9 kWh, respectively.

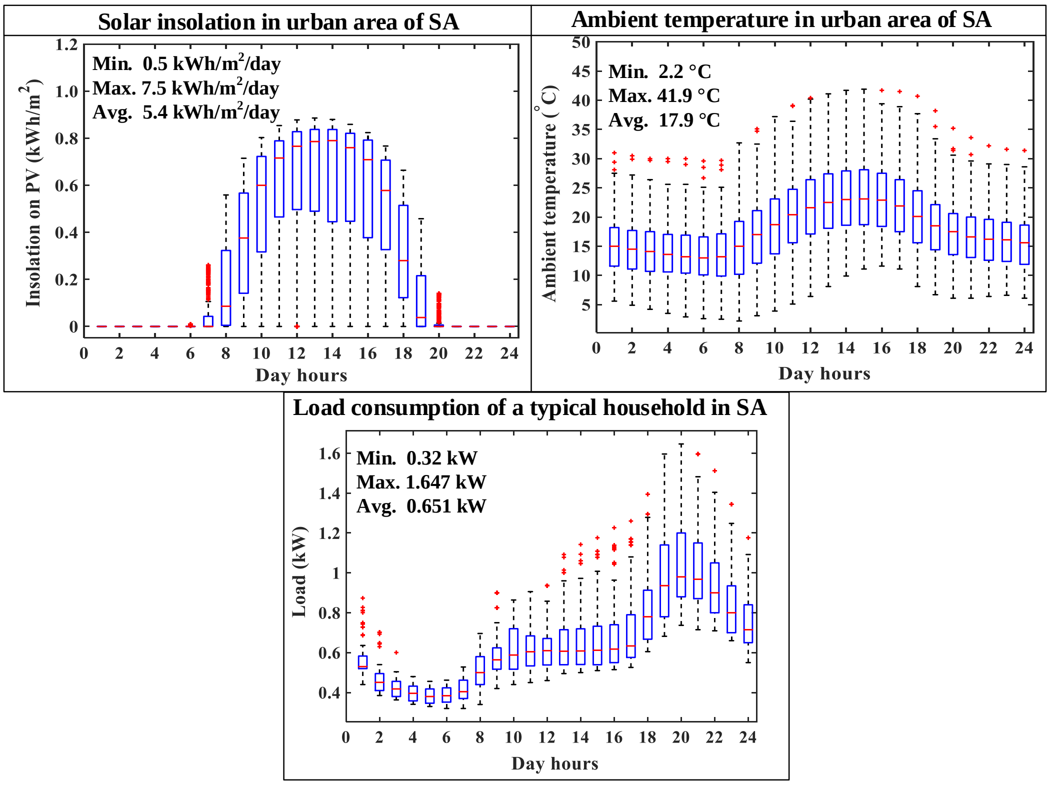

Figure 3-3. Daily box plot of the load, insolation, and temperature of a typical household in SA.

In Australia, the annual solar radiation is around 58 million peta-joules (PJ) which is approximately 10,000 times of the Australia's annual energy consumption [14]. The daily average solar insolation and ambient temperature in SA are 5.4 kWh/m^2/day and 17.9°C, respectively [15]. This results in 4.3 kWh daily generation for a 1 kW$_p$ PV system. Daily box plot of solar insolation and ambient temperature in urban area of SA in 2018 are also shown in Fig. 3.3.

3.5 Results and Discussions

The proposed optimisation technique is applied to a typical grid-connected household in SA. Various simulation results obtained for both configurations (as shown in Fig. 1) are discussed. The results of sensitivity analysis, cash flows analysis, and uncertainty analysis are also presented. A practical guideline is presented for the customers in SA.

3.5.1 Rooftop PV and BES Capacity Optimisation

Table 3-2 lists the optimal capacity of PV and BES, NPC$_t$, COE, annual dumped energy (ADE), annual export energy to grid (AEEG), and annual import energy from grid (AIEG) for both configurations. For the first configuration, the optimised PV capacity is found as 9 kW. The COE is obtained as 28.08 ¢/kWh that means 42% reduction compared to the case of without any solar PV. Since there is no battery in this configuration, the extra power of PV after feeding the demand is sold to the grid. By a 9 kW PV, 11.13 MWh energy is sold to the main grid. The AIEG is 3.21 MWh which means that the solar PV supplies 2.49 MWh of the annual electricity demand of the household. Because of relatively large capacity of PV, there is an annual dumped energy of 0.52 MWh.

Table 3-2. Optimisation results for both System configurations.

Configuration	PV (kW)	BES (kWh)	NPC_t ($)	COE (¢/kWh)	AIEG (MWh)	AEEG (MWh)	ADE (MWh)
Only PV	9	-	15,113	28.08	3.21	11.13	0.52
PV-BES (BES cost: $350/kWh)	9	11	12,021	24.73	0.59	7.76	0.42

For the second configuration, the proposed optimisation technique provided a zero BES capacity indicating that the current BES price ($700-1000/kWh) is not economically viable. Thus, the results of this configuration are the same as that of the first configuration. However, the SA government is currently providing a subsidy of $500-600/kWh of BES capacity to some eligible customers [16]. With the above subsidy, the present market price of BES is around $350/kWh. When the proposed optimisation technique is applied to the second configuration with a BES price of $350/kWh, the optimal battery size is found as 11 kWh. Other optimised results of the system are shown in Table 3-2 (last row). In this case, the COE reduction is around 48% compared to the system without any PV. The AEEG is decreased by 3.37 MWh compared to configuration 1. However, the PV-BES configuration supplies around 90% of the household demand. The effect of BES price on COE is separately shown in sensitivity analysis.

3.5.2 Annual Payment Cashflow Analysis

Annual payment cash flow analysis illustrates the customer payment in each year during the project lifetime. In SA, the capital/replacement costs of the inverter, BES, and PV are generally sourced from a financial institution in a low interest rate. The total annual payment (TAP) of the household is:

$$TAP = AP_{Capex} + AP_{Opex} + AP_{Electricity} \tag{3-26}$$

For the grid-connected household without any solar PV, the annual electricity bill (i.e., annual energy consumption at RP) is the total annual payment. The annual benefit (AB) and the total benefit (TB) of each system configuration (SC) are then calculated as follows:

$$AB_{sc} = TAP_g - TAP_{sc} \tag{3-27}$$

$$TB_{sc} = \sum_{y=1}^{20} AB_{sc}(y) \tag{3-28}$$

Fig. 3-4 shows the 20-year annual payment cash flow analysis results for both configurations. Replacement loan payment (for the BES and inverter) from the 10th year has increased the TAP for both configurations. In both configurations, the annual revenue from selling electricity to the grid is higher than the annual payment for the purchased electricity from the grid. The TAP of both configurations is much lower than that of the grid alone system. The differences between the blue and red lines demonstrates the annual benefits of each system.

The annual and total benefits of the household with PV only, and PV-BES are shown in Fig. 3-4. The annual benefits for each year during the project lifetime are more than $1,500 (for the PV only system) and $2,000 (for PV-BES system). The average of TAP difference in 20-year is $2,100 for the PV only system, and $2,500 for the PV-BES system. This means that the customer can save an average of $2,100 and $2,500 for the annual payment with configurations 1 and 2, respectively. The total benefit in PV-BES system is $7,735.65 more than that of the PV only system.

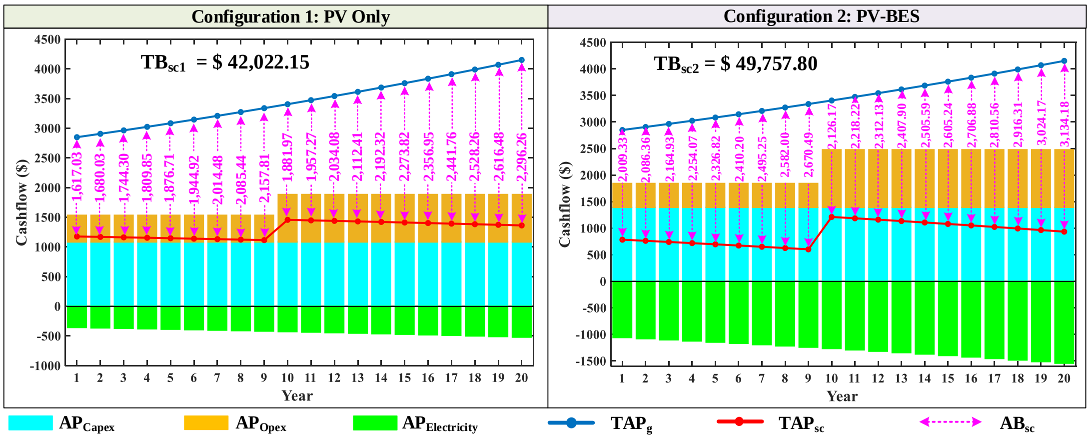

Figure 3-4. Cash flow during the project lifetime including the annual and total benefits for both studied system configurations.

3.5.3 Daily Operational Analysis

The power flow of both configurations needs to be investigated to analyse the operation of the systems. Fig. 3-5 shows the variation of various power (solar PV, load, grid, battery and dumped) in four sample days: (1) two consecutive sunny days (48 hr) in summer, and (2) two consecutive cloudy days (48 hr) in winter. During the sunny days of summer, there is no import power from 9:00 am to 5:00 pm, and PV feeds the total load and sells the extra power to the grid in both configurations. As shown, most of the PV power is exported to the grid and the export power does not exceed the maximum allowable limit 5 kW at any time.

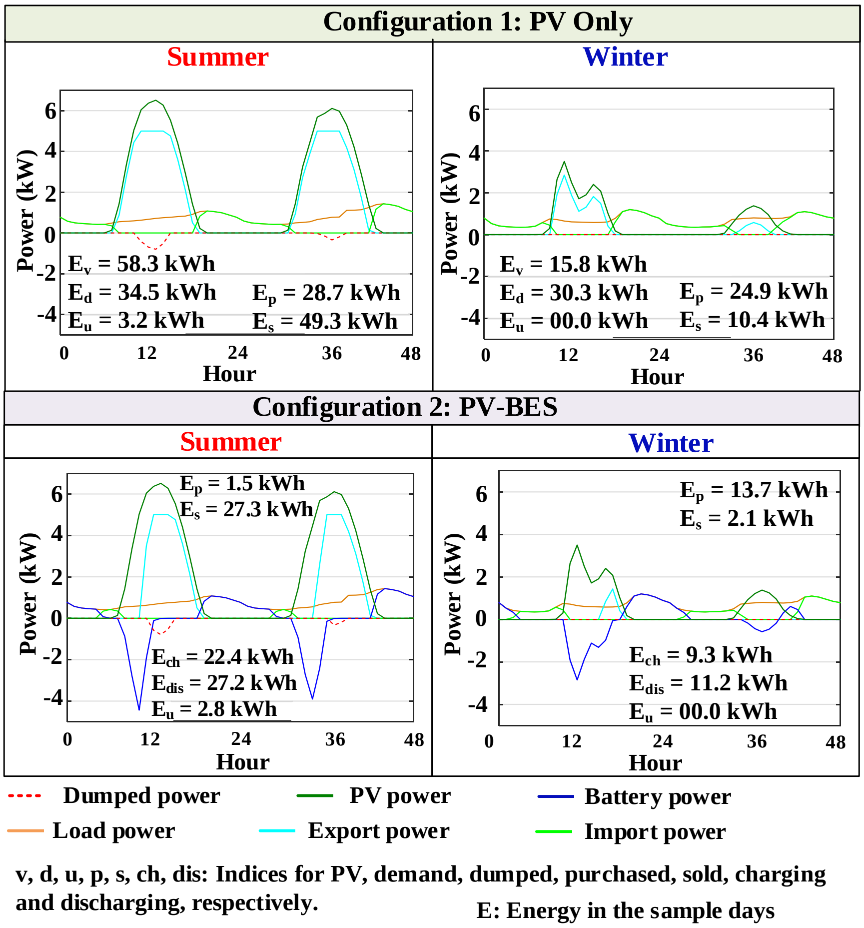

Figure 3-5. Daily power flow for both studied system configurations in four sample days (two sunny days in summer and two cloudy days in winter).

In the evening, the load power is supplied through import power from the grid for configuration 1. However, in configuration 2, the BES supplies the load power in the evening time and the import power from the grid is almost zero. The PV energy during the summer is higher than the demand of the household (it operates like a zero net energy home). In winter, the PV generation is limited to a few hours and the import power is increased for configuration 1. However, BES supplies most of the remaining load and the import power from the grid is less for configuration 2.

3.5.4 Sensitivity Analysis

In SA, as well as other Australian States, there is a maximum export power limit from a residential home to the grid. It is important to analyse the effect of a range of export power limit on the COE and capacities of PV and BES. Fig. 3-6 shows the variation of optimal capacity of system component(s) and COE against the export power limit for both configurations.

A 2-kW solar PV is the optimal capacity in Configuration 1 when the PV is prohibited of exporting power to the grid (point A). When the BES is added (in Configuration 2), the optimal PV capacity is increased to 4 kW (point B) without exporting any power. In both configurations, the optimal PV capacity increases, and the value of COE decreases with the increase in export power limit. In Configuration 1, the annual dumped energy fluctuates between 0.21 MWh and 1.18 MWh for different values of export power limit. However, the use of BES in Configuration 2 reduces the dumped energy fluctuation between 0.34 MWh and 0.93 MWh.

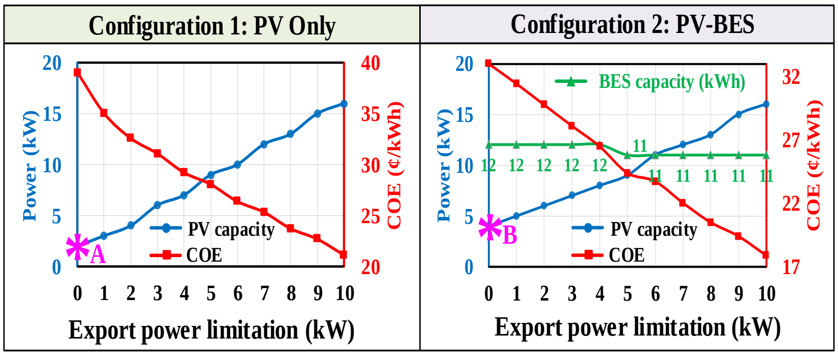

Figure 3-6. Sensitivity analysis for the limitation on the export power to the grid.

The effects of various factors (such as, a range of PV and BES costs, daily average electricity demand, PV and BES capacities, RP and FiT) on the COE are also investigated. Fig. 3-7a shows the value of COE (colour bars) of configuration 1 when the PV cost and the daily average electricity demand are changed. In this case, PV installation is more beneficial with low electricity demand. For example, in a household with 10 kWh of daily electricity demand and a PV cost of \$1200/kW (point A), the customer can collect some revenue by exporting more power to the grid. Fig. 3-7b shows the effect of RP and FiT on the COE of configuration 1. It is found that the minimum COE occurs where the RP is minimum, and the FiT is maximum (point B). In other words, for a given FiT, COE increases with the increase of RP. Inversely, for a given RP, COE decreases with the decrease in FiT.

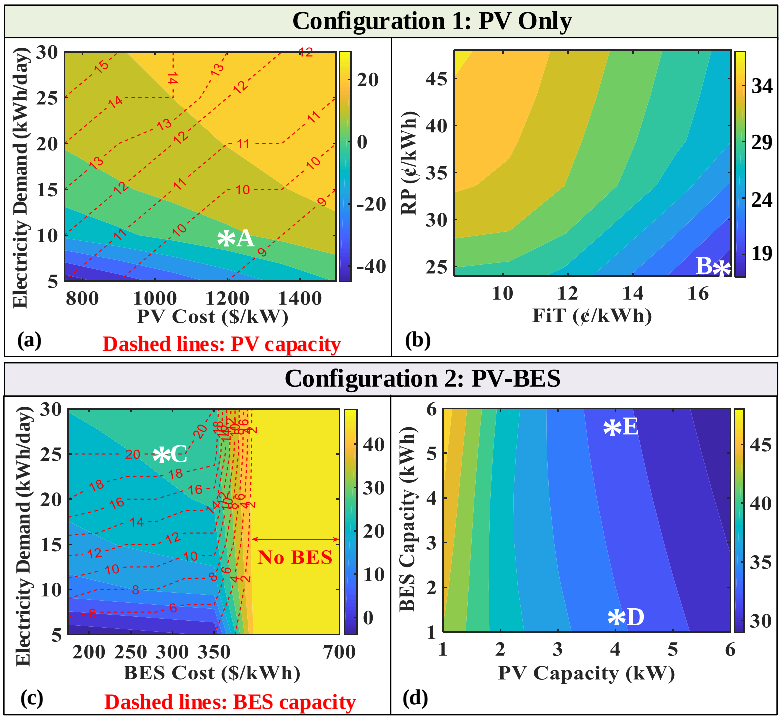

Figure 3-7. Sensitivity analysis of COE. (a) Average electricity demand per day versus PV cost. (b) Average electricity demand per day versus BES cost. (c) RP versus FiT for the typical household. (d) BES capacity versus PV capacity for the typical home.

Fig. 3-7c shows the value of COE (colour bars) for Configuration 2 when the cost of BES and the household daily average electricity demand are changed. For BES price of more than $400/kWh, the optimal size of BES is found as zero indicating that BES is not economically beneficial. When the BES price varies between $350 and $400/kWh, BES is not much effective in reducing the value of COE. For BES price of less than $350/kWh, both the BES capacity and COE increase with the increase in daily average electricity demand. For example, for a daily average demand of 25 kWh and a BES cost of $300/kWh (point C), the optimal capacity of BES is found as 20 kWh and the corresponding COE is 30 ¢/kWh.

Fig. 3-7d shows the effect of BES and PV capacities on the COE for a typical household in SA (daily average energy of 15.6 kWh). The value of COE, for a given PV capacity, is very insensitive to the variations in BES capacity. For example, a 4 kW PV system with a 1 kWh BES (point D) has almost the same value of COE with a 6 kWh BES (point E). On the other hand, for a given BES capacity, COE decreases significantly with the increase of PV capacity.

3.5.5 *Uncertainty Analysis Based on 10-Year Real Data*

To investigate the robustness of the proposed methodology, an uncertainty analysis is conducted. The uncertainty in solar insolation and ambient temperature on the optimal capacities is investigated using real data in SA urban area over a period of 10 years (2009-2018). Fig. 3-8a shows the annual average ambient temperature and the daily average solar insolation for the above period. The optimal capacities of PV (in Configurations 1 and 2) and BES (in Configuration 2) found by the proposed method are shown in Fig. 3-8b. It can be noticed in Fig. 8b that the optimal PV capacity in Configuration 1 is obtained as 7 kW for three years, 8 kW for three years, and 9 kW for four years. In Configuration 2, the optimal capacity of PV is found as 9 kW for five years, 8 kW for four years and 7 kW for only one year. The optimal BES capacity (with a battery price of $350/kWh) is obtained as 11 kWh for nine years and 10 kWh for one year. The above analysis confirms that the optimal capacities obtained in section V.A are reasonable for a typical household with a daily average energy consumption of 15.6 kWh/day.

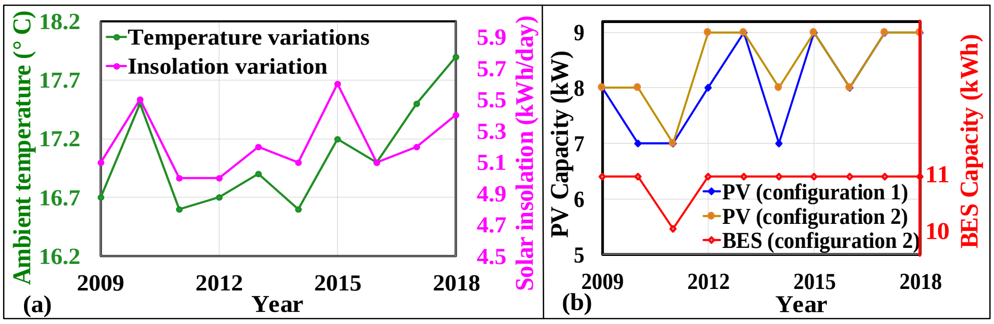

Figure 3-8. Uncertainties analysis from 2009-2018. (a) Ambient temperature and solar insolation. (b) Optimal capacities for each year based on the data.

3.5.6 Practical Guideline

This study facilitates a practical guideline for a residential consumer in SA to select optimal capacities of rooftop PV and BES to reduce the electricity cost. The practical guideline is based on the available rooftop space and daily average electricity demand for the customers without PV as well as the customers with an existing fixed size PV but need only BES. The maximum PV capacity for a given rooftop area can be calculated based on the solar cell efficiency as follow:

$$P_{v,max} = 1\,\mathrm{kW/m^2} \times A(\mathrm{m^2}) \times \eta_v \tag{3-29}$$

Fig. 3-9 shows the practical guideline for the residential customers in SA. First it is checked whether the household already has a PV or not. If the PV is already installed, the capacity of BES needs to be optimised with the existing PV capacity. This is shown with green lines in Fig. 3-9a. It is found that for a given PV capacity, the BES capacity increases when average daily load demand is increased. However, for a given electricity demand, BES size is less sensitive to PV size (beyond a certain capacity). For example, a household with 15 kWh daily load demand and a 5 kW PV (point A), needs the same BES capacity for a household with the same daily load demand and an 11 kW PV (point B).

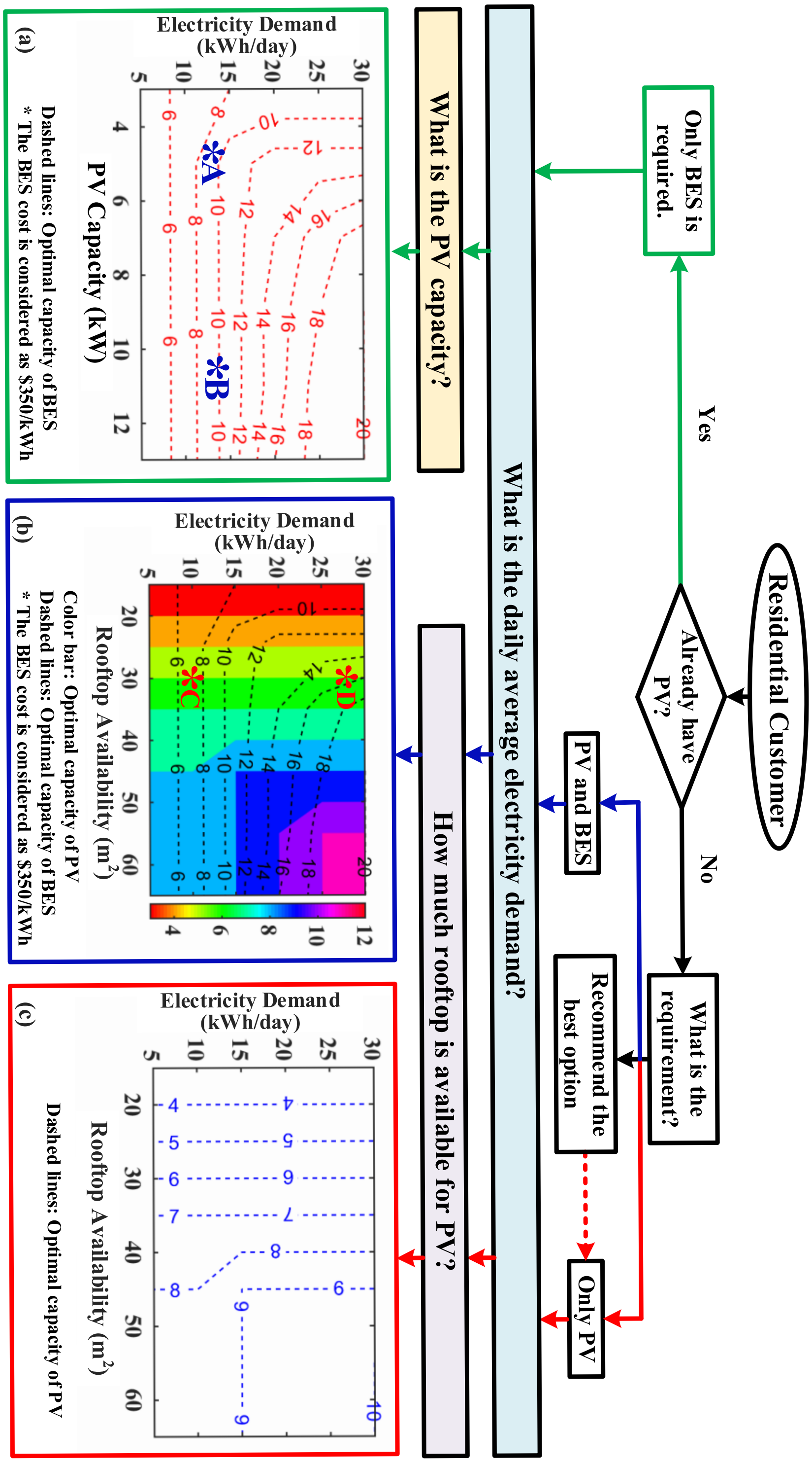

Figure 3-9. Practical guideline for a costumer in SA. (a) Customer already has PV and needs BES. (b) Customer needs PV-BES. (c) Customer only needs PV.

For customers without a PV system, the guideline advises whether the customer needs PV only, or PV with BES, or has no idea and needs a recommendation. In this case, the optimal capacities of PV and BES are determined based on the average daily electricity demand, available rooftop space for PV installation, as well as RP and FiT. If the customer has no idea, the recommendation is the only PV system because the BES cost (without subsidy) is not economical for the integration in grid-connected households.

Fig. 3-9b shows the practical guideline for the customers who need both PV and BES. For a limited rooftop space, the PV capacity is almost constant when the daily load demand increases. However, the BES capacity increases with the increase in daily load demand. For example, a household with 30 m^2 available rooftop space and 10 kWh daily load demand (point C), needs the same PV capacity for a household with same rooftop and 20 kWh daily load demand (point D). However, the optimal BES capacity for household (point C) is 7 kWh less than the BES for household (point D). Fig. 3-9c demonstrates the optimal capacity of PV for the customer who only needs PV. For a given daily load demand, the PV capacity increases with the increase in available rooftop space.

3.6 Optimal Systems in Australian States

The proposed optimisation technique with system configurations is also applied to the households of different Australian States (New South Wales (NSW), Queensland (QLD), South Australia (SA), Tasmania (TAS), Victoria (VIC), and Western Australia (WA)). The optimisation technique used real data of the respective state including solar insolation, air temperature, RP and FiT in urban area [4]. Table 3-3 lists the average solar insolation, air temperature, RP and FiT for Australian States. TAS has the minimum RP of 25 ¢/kWh, and the WA has the minimum FiT of 7 ¢/kWh. SA has the highest RP among all states. The FiT is almost the same for SA and QLD. The annual average solar insolation is the highest in SA and QLD (5.4 kWh/m^2), and the annual average ambient temperature is the highest for QLD (25°C). Thus, SA and QLD are likely to get more benefit from PV installation.

Table 3-3. Real metrological data and electricity rates in Australian States.

	Daily average temperature (°C)	Daily average solar insolation (kWh/m^2)	RP (¢/kWh)	FiT (¢/kWh)
NSW	18.6	5	31	13
QLD	25	5.4	33	16
SA	17.9	5.4	48	17
TAS	15.9	4.6	25	9
VIC	16.4	4.7	26	12
WA	20.1	5.5	26	7

Fig. 3-10 shows the comparison of optimal PV size and COE of configuration 1 for various states. The lowest PV capacity is obtained in WA, since the state has the minimum FiT. Solar PV has the minimum effect on the COE in TAS and VIC, because of lower solar insolation. The lowest COE is found in QLD (22 ¢/kWh) but the highest COE reduction occurred in SA (from 48 to 28 ¢/kWh). Because of relatively high solar insolation and RP, SA is the best state for PV installation.

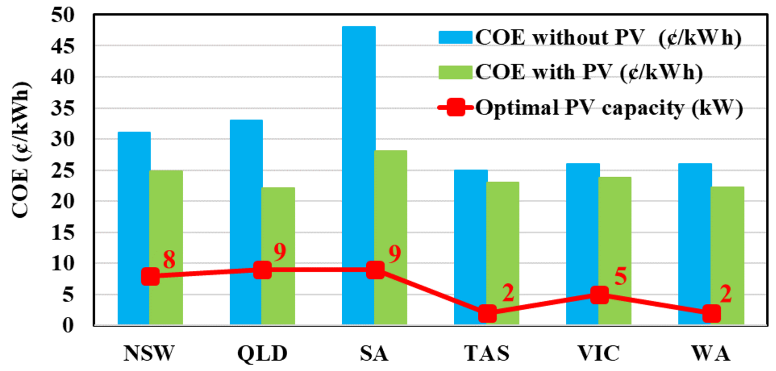

Figure 3-10. COE comparison of configuration 1 for different Australian States.

In configuration 2 (when the BES is added), optimisation results illustrate that the current market price of BES in Australia is not economic for none of the states. The minimum cost of BES for an efficient integration to the grid-connected household of Australian States is shown in Table 3-4. For NSW, the minimum cost of BES for economic integration is found as $190/kWh which is one-fourth of the current market price of battery. SA has the highest potential for BES integration among the other states. Therefore, it is more appropriate to install the BES for grid-connected households in SA in near future.

Table 3-4. Efficient BES cost for economic integration in different states.

State	NSW	QLD	SA	TAS	VIC	WA
BES Cost ($/kWh)	190	300	350	220	200	240

3.7 Conclusions

This chapter determined the optimal capacity of solar PV and BES for grid-connected households in Australia. The optimal results are obtained for two different configurations: (a) PV only, and (b) PV with BES, using the real annual data of load consumption, solar insolation, and ambient temperature. For a typical home in SA, the optimal capacity of the PV system is found as 9 kW that can decrease the COE by about 40%.

In SA, the current market price of battery is found to be unattractive for economic integration of BES in a grid-connected household. The battery price should decrease to \$350/kWh to become economically attractive. The total benefit from the PV only and the PV-BES (with a BES cost of \$350/kWh) systems during the project lifespan was found around \$42,000 and \$50,000, respectively.

The uncertainty analysis based on 10-year real data confirmed that the optimised PV (9 kW) and BES (11 kWh) capacities remain almost the same over a period of 10 years. A practical guideline was also presented for the households in SA to invest on the right capacity of PV and BES. It was found that the optimal PV capacity should be determined based on not only the available rooftop space but also on daily energy consumption. For a typical household (5,705 kWh electricity demand per year), 9-kW is the most optimal capacity of solar PV system.

Optimal system capacities for two different configurations were also investigated for various states of Australia and it was found that the PV only system (without battery subsidy) is the most beneficial for households in SA because of highest RP. SA has the highest potential for BES integration among the other states.

Nomenclature

A. Parameters:

A	Available rooftop area (m^2)
C_y	Annual maintenance cost of components (\$)
C_z	Replacement cost of components (\$)
CRF_s	Components capital recovery factor
CRF_e	Electricity capital recovery factor
e	Escalation rate (%)
h	Hour
i, d	Interest/discount rates (%)
M	Component's lifetime (year)

n	Project lifetime (year)
$P_{b,max}$	Maximum allowable power of battery (kW)
$P_{s,max}$	Maximum export power limit to the grid (kW)
$P_{v,max}$	Maximum allowable power of PV (kW)
PC_x	Capital present cost of components ($)
PC_y	Maintenance present cost of components ($)
PC_z	Replacement present cost of components ($)
r, q	Electricity interest/discount rates (%)
SOC_{max}, SOC_{min}	Maximum and minimum SOC of battery (%)
y	Year
Δt	Time interval (hr)
$\eta_{b,im}, \eta_{b,ex}$	Import/export efficiency of battery (%)
η_v	Solar cell efficiency (%)

B. Variables:

AB_{sc}	Annual benefit of system configurations ($)
AP_{capex}	Annual payment for the loan of Capex ($)
$AP_{Electricity}$	Annual electricity payment ($)
AP_{opex}	Annual payment for the loan of Opex ($)
C_e	Annual cost of electricity trade with grid ($)
E_b	Battery capacity (kWh)
E_{annual}	Annual electricity demand (MWh)
N_b	Number of batteries
N_v	Number of PVs
NPC_s	Net present cost of components ($)
NPC_e	Net present cost of electricity trade with grid ($)
NPC_t	Total net present cost of system configurations ($)
$P_{b,im}, P_{b,ex}$	Import/export power of battery (kW)
$P_{b,in}, P_{b,out}$	Available input/output power of battery (kW)
P_d	Load power (kW)
P_s, P_p	Export/import power to/from grid (kW)
P_u	Dumped power (kW)
P_v	Output power of solar PV (kW)
TAP_g	Total annual payment with only grid ($)
TAP_{sc}	Total annual payment of configurations ($)
TB_{sc}	Total benefit of configurations ($)

References

[1] Clean Energy Council. “Clean Energy Australia Report,” [Online]. Available:https://assets.cleanenergycouncil.org.au/documents/resources/reports/clean-energy-australia/clean-energy-australia-report-2019.pdf Accessed on: Apr. 2019.

[2] Australian Renewable Energy Agency, “Australian PV Institute Solar Map,” [Online]. Available:

pv-map.apvi.org.au. Accessed on: Jun. 2019.

[3] Australian Energy Market Operator. “South Australian Electricity Report,” [Online]. Available: https://www.aemo.com.au/media/Files/ Electricity/ NEM/Planning_and_Forecasting/SA_Advisory/2018/2018-South-Australian-Electricity-Report.pdf. Accessed on: Nov. 2018.

[4] T. Khalili, S. Nojavan, and K. Zare, “Optimal performance of microgrid in the presence of demand response exchange: A stochastic multi-objective model,” *Comput. Elect. Eng.*, vol. 74, pp. 429-450, Mar. 2019.

[5] Australian Energy Council. “Solar Report,” [Online]. Available: https://www.energycouncil.com.au/media/16114/australian-energy-council-solar-report_-q1-2019_final.pdf, Accessed on: Apr. 2019.

[6] B. Ke, T. Ku, Y. Ke, C. Chung, and H. Chen, “Sizing the battery energy storage system on a university campus with prediction of load and photovoltaic generation,” *IEEE Trans. Ind. Appl.*, vol. 2, no. 2, pp. 1136–1147, Apr. 2016.

[7] A. Ibarra, E. Laserna, D. Stroe, M. Swierczynski, and P. Rodriguez, “Sizing study of second life Li-ion batteries for enhancing renewable energy grid integration,” *IEEE Trans. Ind. Appl.*, vol. 52, no. 6, pp. 4999 -5008, Dec. 2016.

[8] A. Sangwongwanich, Y. Yang, D. Sera, F. Blaabjerg, and D. Zhou, “On the impacts of PV array sizing on the inverter reliability and lifetime,” *IEEE Trans. Ind. Appl.*, vol. 54, no. 4, pp. 3656-3667, Jul.-Aug. 2018.

[9] M. Combe, et al., “Cost effective sizing of an AC mini-grid hybrid power system for a remote area in South Australia,” *IET Gene., Trans. Dist.*, vol. 13, iss. 2, pp. 277–287, Jan. 2019.

[10] M. Combe, et al., “Optimal sizing of an AC-coupled hybrid power system considering incentive-based demand response,” *IET Gene., Trans. Dist.*, vol. 13, iss. 15, pp. 3354 – 3361, Sep. 2019.

[11] SA Power Network. https://www.sapowernetworks. com.au/data/17901/update-to-small-embedded-generation-inverter-limits-and-theredevelopment-of-our-forms/ Accessed on: Apr. 2018.

[12] Sonnen Batterie. https://sonnen.com.au/sonnenbatterie/ Accessed on: Nov. 2019.

[13] Tesla Powerwall. https://www.tesla.com/en_AU/powerwall Accessed on: Nov. 2019.

[14] Australian Government, Geoscience Australia. Solar Energy [Online] https://www.ga.gov.au/scientific-topics/energy/resources/other-renewable-energy-resources/solar-energy Accessed on: May 2019.

[15] Australian Government. Bureau of Meteorology. Climate Data Online. http://www.bom.gov.au/climate/data/index.shtml?bookmark=200 Accessed on: May 2019.

[16] South Australian Government's Home Battery Scheme: https://homebatteryscheme.sa.gov.au/. Accessed on: Oct. 2019.

Chapter 4

Impact of Optimal Sizing of Wind Turbine and Battery for a Grid-Connected Household with and without an Electric Vehicle

This chapter investigates the capacity optimisation problem of small wind turbine and battery storage for grid-connected households with and electric vehicles.

The contribution of this chapter is presented in one submitted research article.

R. Khezri, A. Mahmoudi, and M. Haque, "Impact of Optimal Sizing of Wind Turbine and Battery Energy Storage for a Grid-Connected Household With/Without an Electric Vehicle," ***IEEE Transactions on Industrial Informatics***, Under Revision, 2020.

The student has developed the conceptualization. He designed the optimisation model. Analysis and interpretation of research data has been done by him and the co-authors. A draft of the paper was prepared by the student. Revisions and comments were provided by the co-authors so as to contribute to the interpretation.

4.1 Introduction

Integration of renewable distributed generators to grid-connected households (GCHs) is an effective way of reducing the electricity cost. Taking advantages of compact design, simple structure, portability, low noise and reasonable capital cost, small wind turbine (SWT) is one of the appropriate candidates for distributed generators in GCHs [1]. The installed SWT can supply the household load and export the excess power, if any, to the grid at a feed-in-tariff (FiT) rate to reduce the annual electricity cost of the household. The FiT rate is considerably lower than the retail price (RP) for residential customers in most of the developed countries like Australia. Therefore, integration of battery energy storage (BES) in GCHs with SWT may become an economically attractive solution. On the other hand, Australia is planning to ban the sale of internal combustion engine (ICE) vehicles by 2035 and that will increase the growth of electric vehicle (EV) significantly in near future [2]. Hence, if the homeowner owns an EV, the SWT can also charge the EV and reduce the electricity cost further by reducing the imported electricity from the grid.

The SWT and BES may not offer economic benefits if their capacity is not selected optimally. To achieve the maximum economic and technical benefits, selection of optimal capacities of SWT and BES is very important. The determination of optimal capacities in a GCH depends on various factors: (1) real data of economic factors and wind-load profiles, (2) technical factors such as grid constraint and components data, (3) energy management system (EMS) and (4) uncertainty of EV, load and renewable.

The key contribution of this chapter is to develop a practical capacity optimisation model for SWT and BES in a GCH with/without an EV by analysing all uncertainties associated with wind, load and EV. The optimisation model minimises the actual electricity cost of two different configurations of the GCH: (i) with only SWT, and (ii) with SWT and BES. Novel rule-based home EMSs (HEMSs), with grid constraints, are developed for all possible cases (with/without BES as well as with/without EV) of the GCH. All uncertainties of EV's arrival/departure time and initial SOC are incorporated in the optimal sizing model. While the proposed method is very general and applicable to any system, the actual data (real annual wind speed and load profile, components cost, and electricity rates) in South Australian context are used in this study to make the optimisation model more realistic. Effects of household load, costs of SWT, BES, RP, FiT, and grid constraint on the optimal sizing and COE are also investigated.

4.2 Home Energy Management Systems

Two different configurations of the GCH, as shown in Fig. 4-1, are investigated in this study. In the first configuration, only SWTs are connected to the

GCH and in the second configuration, both SWTs and BES are connected to the GCH. Both configurations are then investigated for two cases: with and without an EV in the premises of the GCH. The operation strategies are developed for these system configurations. Fig. 4-2 shows the rule-based HEMSs for the GCH with and without EV of both configurations.

For the GCH with an EV, it is assumed that the charging of the EV will start immediately after arrival until the battery is fully charged. It may be mentioned here that flat rates are considered for electricity tariffs. It is also assumed that the EV does not operate in V2H or V2G mode.

4.2.1 Configuration 1

As mentioned, only SWTs are integrated to this configuration of the GCH, and the composite system is then analysed for two cases – with and without an EV in the premises. The energy management systems of both cases are briefly described in the following.

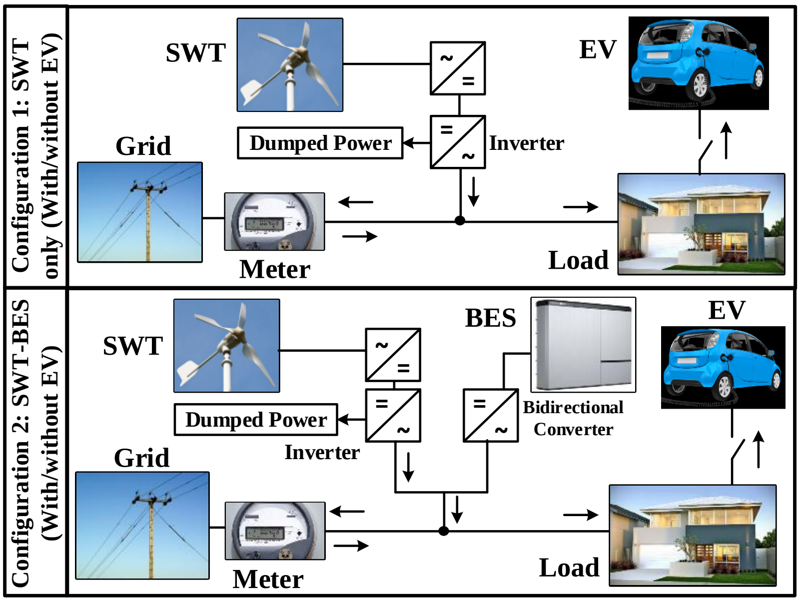

Figure 4-1. Two configurations of a GCH: (1) SWT only (with/without EV), and (2) WT-BES (with/without EV).

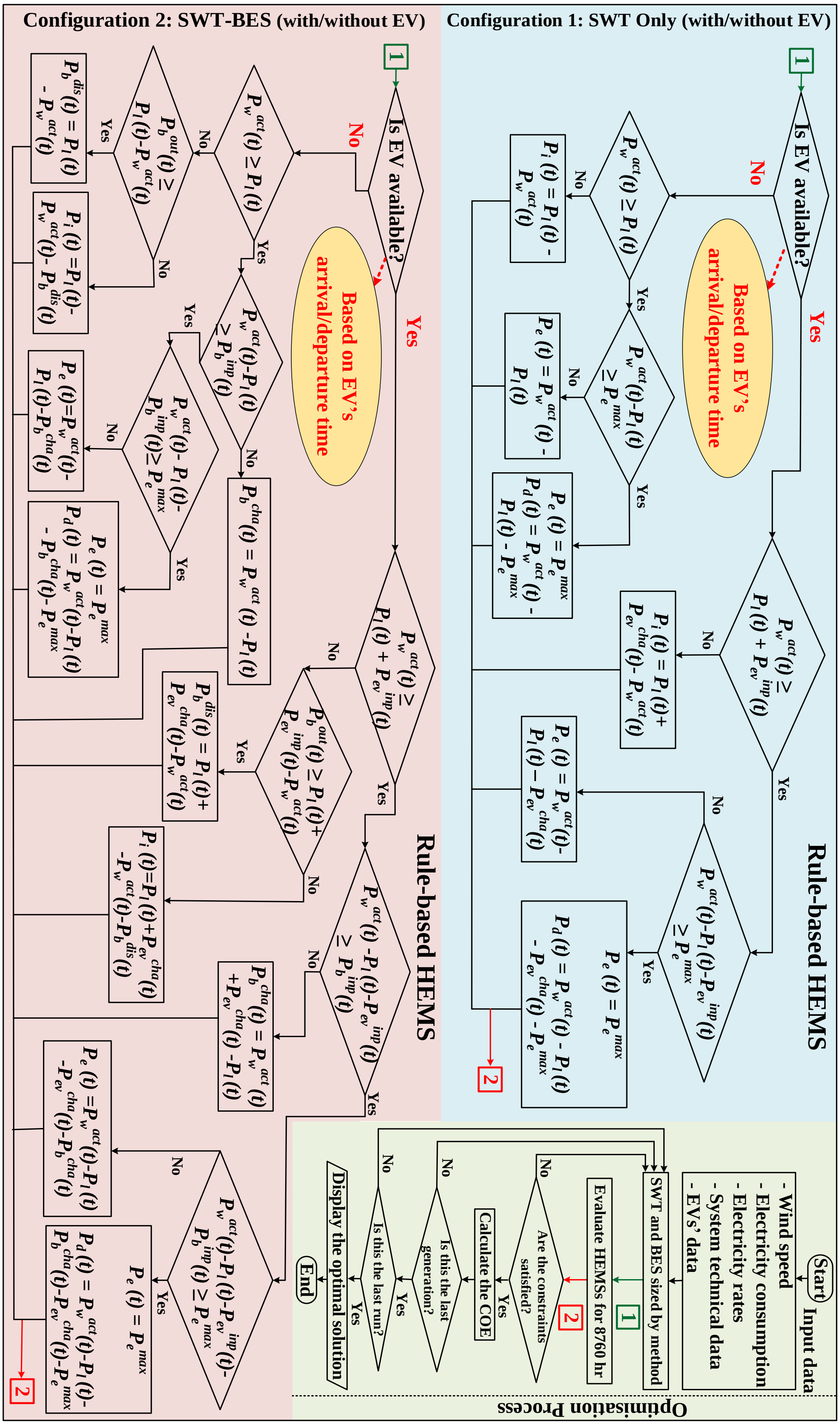

Figure 4-2. Optimisation procedure and rule-based HEMS for both configurations with/without EV.

A) Without an EV

In the absence of an EV, any power produced by the SWT first feeds the load and then exports the excess power, if any, to the grid within the export power limit at a FiT rate. Thus, the export power P_e can be written as:

$$P_e(t) = \min\left(P_e^{max}, P_w^{act}(t) - P_l(t)\right) \tag{4-1}$$

where P_w^{act} is the actual power generated by all wind turbines.

$$P_w^{act}(t) = N_w . P_w(t) \tag{4-2}$$

In this study, it is assumed that any excess power beyond the export power limit will be dumped using the inverter control system of the SWTs. The excess power of the SWT can be controlled using a voltage feedback loop in the control system of the inverter [3]. This means that no physical dump load is considered in the designed system. The dumped power can be calculated as:

$$P_d(t) = P_w^{act}(t) - P_l(t) - P_e^{max} \tag{4-3}$$

If the SWTs' power is less than the load, the power shortage is imported from the grid. Thus, the imported power is:

$$P_i(t) = P_l(t) - P_w^{act}(t) \tag{4-4}$$

B) With an EV

In the presence of an EV, the operation of HEMS depends on the availability of the EV (an uncertain parameter). In this case, the excess power of SWT (after feeding the load) first charges the EV within the charging power limit of the EV battery, if the EV in the premises. Any further excess power is then exported to the grid within the maximum export power limit.

$$P_e(t) = \min\left(P_e^{max}, P_w^{act}(t) - P_l(t) - P_{ev}^{cha}(t)\right) \tag{4-5}$$

In this case, the dumped power is calculated as:

$$P_d(t) = P_w^{act}(t) - P_l(t) - P_{ev}^{cha}(t) - P_e^{max} \tag{4-6}$$

When the SWT power is less than the sum of load and EV charging power, the shortage power is imported from the grid.

$$P_i(t) = P_l(t) + P_{ev}^{cha}(t) - P_w^{act}(t) \tag{4-7}$$

The SOC of EV (when parked at home) in each time interval is calculated as:

$$S_{ev}(t+\Delta t) = S_{ev}(t) + \frac{P_{ev}^{cha}(t).\eta_{ev}^{cha}.\Delta t}{E_{ev}} \tag{4-8}$$

The available input power limit (which is basically inverter size) for EV charging is considered as follows:

$$P_{ev}^{inp}(t) = \min\left(P_{ev}\ ,(E_{ev}/\Delta t).\left(S_{ev}^{max} - S_{ev}(t)\right)\right) \tag{4-9}$$

Since it is assumed that the EV is not discharged in the premises of the GCH, the discharging power of EV and hence its effect on the SOC is not considered in the optimisation model.

4.2.2 Configuration 2

In this configuration, SWT and BES are integrated to the GCH, and the composite system is again analysed for two cases – with and without an EV in the premises.

A) Without an EV

In the absence of an EV, any power produced by the SWTs first feeds the load and then the excess power, if any, is used to charge the BES (within the charging power limit and the maximum SOC level). Any further excess power is exported to the grid within the maximum export power limit. Thus, P_e can be expressed as:

$$P_e(t) = \min\left(P_e^{max}, P_w^{act}(t) - P_l(t) - P_b^{cha}(t)\right) \tag{4-10}$$

In this case, the dumped power is calculated as:

$$P_d(t) = P_w^{act}(t) - P_l(t) - P_b^{cha}(t) - P_e^{max} \tag{4-11}$$

When the power of the SWTs is less than the load, first the BES will discharge (if its power and SOC level are within the limits) to meet the load. Any further shortage of power will then be imported from the grid. Thus, the imported power is:

$$P_i(t) = P_l(t) - P_w^{act}(t) - P_b^{dis}(t) \tag{4-12}$$

The SOC and available input/output powers for charging/discharging of BES are calculated as:

$$S_b(t+\Delta t) = S_b(t) + \frac{\left(P_b^{cha}(t).\eta_b^{cha} - P_b^{dis}(t)/\eta_b^{dis}\right).\Delta t}{E_b^{max}} \tag{4-13}$$

$$P_b^{inp}(t) = \min\left(P_b^{max}\ ,(E_b^{max}/\Delta t).\left(S_b^{max} - S_b(t)\right)\right) \tag{4-14}$$

$$P_b^{out}(t) = \min\left(P_b^{max}, (E_b^{max}/\Delta t).\left(S_b(t) - S_b^{min}\right)\right) \tag{4-15}$$

The maximum charging/discharging power and maximum energy of the BES are calculated as follows:

$$P_b^{max} = N_b.P_b, \qquad E_b^{max} = N_b.E_b \tag{4-16}$$

B) With an EV

In the presence of an EV, the excess power of the SWTs (after feeding the load) first charges the EV and then charges the BES within their respective charging power limits. Any further excess power is exported to the grid within the maximum export power limit.

$$P_e(t) = \min\left(P_e^{max}, P_w^{act}(t) - P_l(t) - P_b^{cha}(t) - P_{ev}^{cha}(t)\right) \tag{4-17}$$

Dumped power is calculated as follows:

$$P_d(t) = P_w^{act}(t) - P_l(t) - P_b^{cha}(t) - P_{ev}^{cha}(t) - P_e^{max} \tag{4-18}$$

When the power of the SWTs is less than the sum of the load and EV charging power, the BES will be discharged (within its power and SOC limits) to meet the shortfall. Any further shortfall will then be imported from the grid.

$$P_i(t) = P_l(t) + P_{ev}^{cha}(t) - P_w^{act}(t) - P_b^{dis}(t) \tag{4-19}$$

4.3 Optimisation Model

This section presents the problem formulation and the optimisation process.

4.3.1 Problem Formulation

The cost of electricity (COE) is calculated through the net present cost (NPC) and capital recovery factors (CRFs) of system components and electricity as well as the annual electricity demand.

$$COE = \frac{NPC_c.\mathrm{CRF_c} + NPC_g.\mathrm{CRF}_g}{E_l}$$
$$E_l = \sum_{t=1}^{T} P_l(t).\Delta t \tag{4-20}$$

The CRF depends on discount rate and de-escalation factor, and can be expressed as:

$$\mathrm{CRF}_c = \frac{d.(1+d)^n}{(1+d)^n - 1}, \quad \mathrm{CRF}_g = \frac{q.(1+q)^n}{(1+q)^n - 1}$$
$$q = \frac{d-j}{1+j} \tag{4-21}$$

The total NPC of the system is calculated as:

$$NPC_t = NPC_c + NPC_g \tag{4-22}$$

The NPC of components can be calculated as follows:

$$NPC_c = N_w \cdot \left(PC_w^{cap} + PC_w^{mai} + PC_w^{rep}\right) + N_b \cdot \left(PC_b^{cap} + PC_b^{mai} + PC_b^{rep}\right) \tag{4-23}$$

The present value of maintenance and replacement costs of the components are given by:

$$PC^{mai} = C^{mai}.\frac{(1+i)^M - 1}{i(1+i)^M} \tag{4-24}$$

$$PC^{rep} = C^{rep}.\sum_{t=1}^{ty<M} \frac{1}{(1+i)^{ty}} \tag{4-25}$$

The net present cost of electricity trading with grid is:

$$NPC_g = C_g.\frac{(1+r)^n - 1}{r(1+r)^n}$$
$$r = \frac{i-e}{1+e} \tag{4-26}$$

The annual electricity trading cost with grid is calculated as:

$$C_g = \sum_{t=1}^{T} RP(t).P_i(t).\Delta t - \sum_{t=1}^{T} FiT(t).P_e(t).\Delta t \tag{4-27}$$

The objective function and the design constraints of the optimisation problem are as follows:

$$f = \mathrm{Minimise}(COE) \tag{4-28}$$

Subject to:

$$0 \le N_w \le N_w^{max} \tag{4-29}$$

$$0 \le N_b \le N_b^{max} \tag{4-30}$$

$$P_w^{act}(t) + P_i(t) + P_b^{dis}(t) - P_e(t) - P_b^{cha}(t) - P_{ev}^{cha}(t) = P_l(t) + P_d(t) \tag{4-31}$$

$$S_b^{min} \le S_b(t) \le S_b^{max} \tag{4-32}$$

$$S_{ev}^{min} \le S_{ev}(t) \le S_{ev}^{max} \tag{4-33}$$

$$0 \le P_e(t) \le P_e^{max} \tag{4-34}$$

$$S_b(T) \ge S_b(t=0) \tag{4-35}$$

$$S_{ev}(t=dep) \ge S_{ev}^{max} \tag{4-36}$$

Eqn. (4-28) represents that the COE of the GCH is selected as the objective function. Eqns. (4-29) and (4-30) represent the size constraints on SWT and BES. Eqn. (4-31) represents the power balance equation. Eqns. (4-32) and (4-33) represent the SOC constraints of BES and EV, respectively. Eqn. (4-34) represents the grid export power constraint. Eqn. (4-35) ensures that the SOC of BES at the end of time horizon is higher than that at the beginning of the project. Eqn. (4-36) ensures that the SOC level of EV at the departure time is at the maximum value.

4.3.2 Optimisation Process

The optimisation process for the optimal sizing of SWT and BES is shown in the top right corner of Fig. 4-2. The optimisation process starts with input data which is discussed in next section. The operation of the HEMS for different configurations (as shown in top and bottom parts of Fig. 4-2) is then inserted between points $\boxed{1}$ and $\boxed{2}$. Finally, the optimisation model is implemented to obtain the optimal capacity of components. The numbers of SWT and BES are the decision variables of the optimisation model. It may be mentioned here that the main aim of this study is to determine the optimal size of system components and analyse the steady-state performance of various system configurations. Thus, the dynamic analysis like control strategy, proof of stability, and control robustness are not investigated.

While the formulated problem can be solved using different solvers in MATLAB software, the particle swarm optimisation (PSO) approach is used in this study. The PSO method has been successfully implemented to solve the optimal sizing problems of power systems. Hence, comparison of the performance of PSO with other methods is not within the scope of this study. The main advantages of the PSO compared to other methods are appropriate rate of convergence, minimum dependency on initial points, low storage requirement, and simplicity. In the PSO optimisation procedure, it has been ascertained that selecting higher numbers of population, generation, and runs can ensure the optimality of the results [4]. Hence, in this study, 300 populations and 500 generations are considered. In addition, the PSO approach has been repeated in 20 runs to obtain global optimal results for the configurations. It may be noted that the same results are obtained for all 20 runs of the simulation.

4.4 Case Study

The proposed technique described in Sections II and III is then applied to a grid-connected household in South Australia (SA). The various input data including technical and financial parameters required for this purpose are discussed in the following sub-sections.

4.4.1 Load Consumption and Wind Speed

Fig. 4-3a shows the actual hourly load pattern of a typical GCH in SA [5]. The daily average and annual energy consumption of the house are 15.6 kWh and 5,705 kWh, respectively. The actual wind speed data of Adelaide airport (urban area of SA capital city) at a height of 10 m is collected for the entire year of 2018 [5] and its hourly pattern is shown in Fig. 4-3b. Using the above wind speed, the annual energy generated by a 1-kW wind turbine is found as 2,146.2 kWh.

4.4.2 Electricity Rates and Grid Constraint

In this study, flat electricity tariffs are considered as most of the residential houses in SA are under this tariff structure. However, the optimisation model described in this chapter can also be used for other tariff structures. The RP and FiT are considered as 48 ¢/kWh and 17 ¢/kWh, respectively [5]. Note that all prices in this study are in Australian dollar.

SA Power Network has a restriction of maximum export power limit of 5 kW for customers with a single-phase inverter [6].

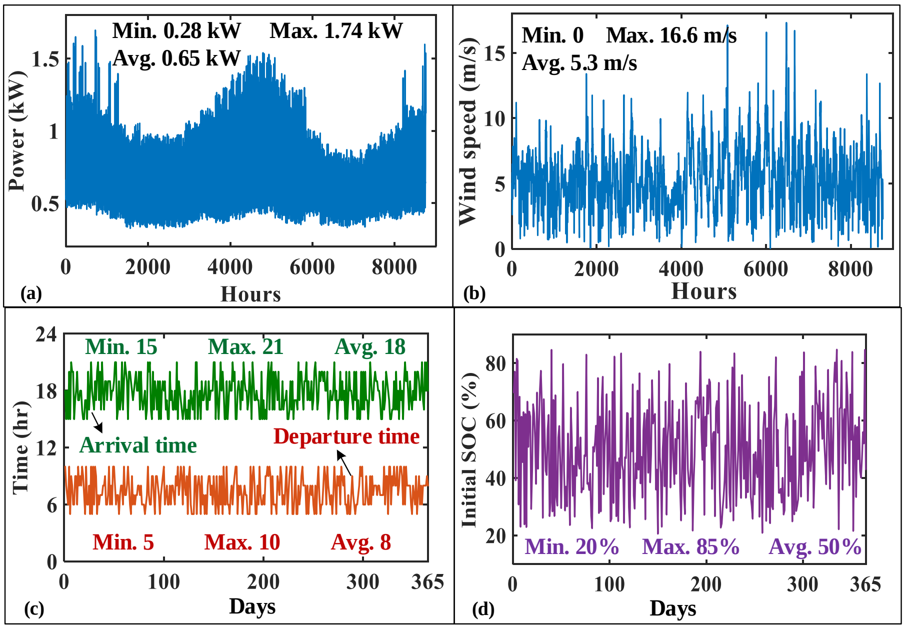

Figure 4-3. Annual data. (a) Electricity demand. (b) Urban area wind speed. (c) Stochastic arrival/departure time of EV. (d) Stochastic initial SOC level of EV.

4.4.3 Battery Energy Storage and Small Wind Turbine

Lithium-ion batteries are widely used for residential applications in South Australia. The market price of the battery is around $700/kWh. However, a subsidy of $300-400/kWh has recently been introduced by the SA government to customers [7]. Table 4-1 lists the cost and characteristics of the BES used in this study. The unit size of BES is considered as 0.5kW/1kWh. The charging and discharging efficiencies are considered as the square root of the round-trip efficiency. The total energy throughput of the battery is used to measure the BES lifetime. The estimated lifetime of BES, which does not exceed the calendar lifetime, is calculated as:

$$L_b(\text{year}) = \min\left(CL_b, \frac{ET_{tot}}{ET_{bs}}\right) \tag{4-37}$$

The calendar lifetime and total energy throughput of lithium-ion battery are obtained from [8].

Roof mounted SWTs are used in this study. Table 4-1 also lists the cost and lifetime of the roof mounted SWT.

Table 4-1. Battery Energy Storage and Small Wind Turbine Data.

BES	Capital cost = $300-400/kWh Replacement cost = $300/kWh	S_b^{min} = 20% S_b^{max} = 95% Round-trip efficiency=90%
SWT	Capital cost = $3,000/kW Inverter replacement cost = $300/kW Maintenance = $50/kW/yr	SWT lifetime = 20 yr Inverter lifetime = 10 yr

4.4.4 Electric Vehicle Data

Renault Zoe 22-kWh (2016) EV with a 3-kW charging power (single-phase) is considered in this study. The stochastic models of EV's availability at the premise (arrival and departure times) and initial SOC level at arrival are obtained from a truncated Gaussian distribution [9]. Table 4-3 lists the stochastic parameters of probability distributions for the EV's availability and initial SOC. Figs. 4-3c and 4-3d illustrate the generated stochastic data of EV. The maximum/minimum SOC levels and efficiency of the EV battery are the same as that of the BES.

Table 4-2. Stochastic Parameters for Probability Distributions of Electric Vehicle Availability and Initial SOC Data.

	Mean	**Standard deviation**	**Min.**	**Max.**
Arrival SOC of EV (%)	50	30	20	85
Arrival time (h)	18	3	15	21
Departure time (h)	8	3	5	10

4.4.5 General Parameters

The project lifetime is considered as 20 years. For the GCH with an EV, it is considered that the homeowner owns the EV during entire lifetime of the project. The interest/discount and escalation/de-escalation rates are considered as 8% and 2%, respectively. The maximum capacities of SWT and BES are considered as 10-kW and 20-kWh, respectively. The simulation time interval is 1-hr.

4.5 Results and Discussions

The simulation results obtained by the proposed method for both configurations are described in the following.

It may be mentioned that, without the SWT, the GCH imports all its energy from the grid. In such a case, the COE, NPC_t and annual imported energy from grid (AIEG), without the EV, are 48¢/kWh, $31,710 and 5.7MWh, respectively. However, with the EV, the COE, NPC_t and annual imported energy from grid (AIEG) are 48¢/kWh, $52,928 and 9.52MWh, respectively.

4.5.1 Configuration 1

Table 4-3 lists the optimal capacity of SWT, and the COE found by the proposed technique for both cases (with and without an EV) of configuration 1. The respective NPC_t, AIEG, annual exported energy to grid (AEEG), and annual dumped energy (ADE) are also shown in the Table.

Table 4-3. Optimisation Results for Configuration 1 With/Without EV.

Configuration 1 (Only SWT)	SWT (kW)	COE (¢/kWh)	NPC_t ($)	AIEG (MWh)	AEEG (MWh)	ADE (kWh)
Without EV	6	31.07	16,618	2.50	9.68	5.69
With EV	6	34.81	34,517	5.39	8.74	5.65

The results of Table 4-3 indicate that the optimal capacity of the SWT is 6 kW for both cases (with and without the EV). The SWT reduces the COE of the GCH by 16.93¢/kWh (without the EV) and 13.19¢/kWh (with the EV). Without the EV, most of the energy generated by the SWT is exported to the grid and only 3.2 MWh of annual energy generated by the SWT is used to meet the demand of the GCH. In the presence of the EV, the annual exported energy is reduced by 0.94 MWh and the annual imported energy is increased by 2.89 MWh to meet the additional demand of the EV. The annual dumped energy in both cases (with and without the EV) is very insignificant and less than 6 kWh.

4.5.2 Configuration 2

When the proposed optimisation technique is applied to the GCH of configuration 2 with a battery cost of $300-400/kWh (as shown in Table 4-1), the optimal battery size for both cases (with and without the EV) is found as zero. This indicates that the current battery price even with SA government subsidy is not economically viable. However, with some repeated simulations, it was found that the battery price should reduce to 250/kWh for its economic integration to the GCH.

Table 4-4 shows various optimal results obtained by the proposed optimisation technique with the reduced battery cost. The optimal capacity of the SWT in this case is found to be the same as that of configuration 1 for both cases (with and without the EV). The optimal battery size, at a cost of $250/kWh, with and without the EV is found as only 1 kWh and 2 kWh, respectively. Because of smaller battery sizes, the change in the rest of results (COE, NPC_t, AIEG, AEEG and ADE) is not significant compared to that of configuration 1.

Table 4-4. Optimisation Results for Configuration 2 With/Without EV.

Configuration 2 (SWT-BES)	SWT (kW)	BES (kWh)	COE (¢/kWh)	NPC_t ($)	AIEG (MWh)	AEEG (MWh)	ADE (kWh)
Without EV (BES cost: $250/kWh)	6	2	30.87	16,367	2.24	9.39	5.53
With EV (BES cost: $250/kWh)	6	1	34.80	34,451	5.28	8.62	5.53

4.5.3 Additional Results of Both Configurations

Some additional results of both configurations are presented in the following.

A) Computational Time

The computational time for optimisation changes when the system configuration changes. Table 4-5 lists the required computational time for solving the optimal sizing problem for 1 and 20 runs implemented on Intel® Core™ i7-7700 CPU @ 3.60 GHz, RAM 16.0 GB computer. It is notable that MATLAB uses only one core of CPU to execute the user-written codes. Configuration 2 with EV requires the highest computational time due to complexity of the developed home energy management system in the proposed configuration.

Table 4-5. Computational Time for Optimisation of Each Configuration.

System Configurations	Configuration 1 without EV	Configuration 1 with EV	Configuration 2 without EV	Configuration 2 with EV
Computational time (for 1 run)	43.874 s	133.819 s	106.880 s	140.574 s
Computational time (for 20 run)	832.451 s	2,611.229 s	2,096.411 s	2,778.664 s

B) Daily Operation for Five Successive Sample Days

The daily operation of the GCH for various possible scenarios is investigated for five successive days (days 1-3 with low wind and days 4-5 with high wind). Fig. 4-4 shows the hourly power variation of SWT, BES, EV, and load, as well as import/export power and dumped power for both configurations with/without an EV. The negative power of BES indicates the charging state of the storage. The dumped energy is almost zero in all sample days. Fig. 4-4a shows that the SWT power of configuration 1 (without EV), after feeding the load, is completely exported to the grid. Point A in day-1 of configuration 1 (with EV) shows that when there is no output power of the SWT, both the load and EV demand are supplied by the imported power from the grid. Point B in day-3 of configuration 2 (without EV) shows that the BES is efficiently charged by the SWT when its power exceeds the load. Fig. 4-4d shows that the BES charging power is less than 1 kW, and the EV charging power does not exceed 3 kW because of the maximum charging power limit of the EV.

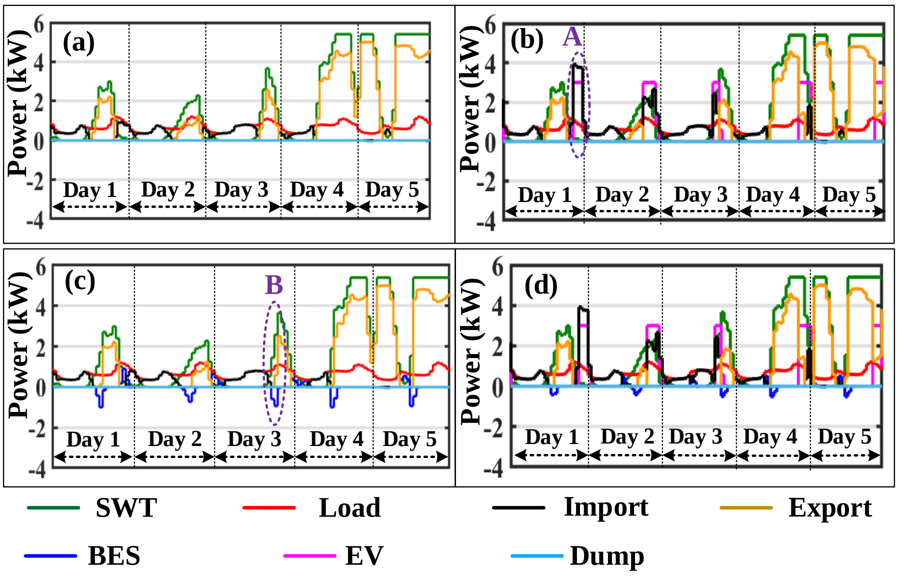

Figure 4-4. Daily operation of the GCH for five sample successive days. (a) Configuration 1 without EV. (b) Configuration 1 with EV. (c) Configuration 2 without EV. (d) Configuration 2 with EV.

C) Sensitivity Analysis

In SA, the maximum export power limit to the grid is applied to all residential customers. The impacts of various export power limits on the optimal capacity of SWT and BES as well as the COE of the GCH without the EV is shown in Fig. 4-5. In case of zero export power limit, the optimal capacity of SWT for configuration 1 is found as only 1 kW (point A) and the corresponding COE is around 40 ¢/kWh (point B). When the export power limit is increased to 10 kW, the optimal capacity of SWT increases to 10 kW (point C) and the COE decreases to 30 ¢/kWh (point D). In configuration 2, it was found the optimal battery capacity is very insensitive to the export power limit, but the optimal SWT capacity increases and the COE decreases as the export power limit is increased.

The impacts of SWT cost and daily electricity demand of the household as well as retail price and feed-in-tariff on the COE and optimal SWT capacity are also investigated for the first configuration of the GCH without an EV and the results found are shown in Fig. 4-6. The optimal SWT capacity is shown by dotted line. It can be seen in Fig. 4-6a that, for a given SWT cost, the value of COE decreases with the decrease in electricity demand. In fact, for a daily electricity demand of 6 kWh and SWT cost of $200/kW, the optimal capacity of SWT was found as 6 kW for which the value of COE is -10¢/kWh (point A). On the other hand, Fig. 4-6b indicates the value of COE decreases with the decrease in retail price and increase in feed-in-tariff. Point B shows the minimum COE, and it occurs at the lowest retail price and the highest feed-in-tariff.

The impacts of BES cost and daily electricity demand as well as SWT and BES capacities on the COE and battery size are also investigated for the second configuration of the GCH without an EV and the results are shown in Fig. 4-7. The optimal BES capacity is shown by dotted line in Fig. 4-7a. Fig. 4-7a indicates that, for a battery cost of \$300-\$700/kWh, the optimal battery capacity was found as zero. For a battery cost of \$250-\$300/kWh, installation of battery is not very effective in reducing the COE. Fig. 4-7a also indicates that, at a lower battery cost, the optimal battery capacity increases with the increase of daily electricity demand. On the other hand, Fig. 4-7b indicates that, for a given BES capacity, the value of COE for a typical GCH (with daily electricity demand of 15.6 kWh) decreases with the increase in SWT capacity.

D) Uncertainty Analysis Based on 10-Year Real Data

To check the robustness of the proposed optimisation models, the impact of uncertainties in wind speed, load consumption, and EV data on the optimal capacities is investigated for 10 different scenarios. The actual wind speed data in an urban area of SA over a period of 10 years (2009-2018) is used for this purpose. The uncertainties of EV's availability at the premise (arrival and departure times) and initial SOC level at arrival are separately generated for each scenario in the configurations with EV. The load in the above scenarios (or years) are obtained by adding an uncertainty as follows:

$$P_l^y(t) = P_l(t) + P_l(t).\beta.ran(t) \tag{4-38}$$

where P_l^y is the randomly generated load profile for y^{th} year, β is a deviation factor and '*ran*' is a random number generator. The value of β is in the range of 10%-50% and the range of the random numbers is considered in between -1 and +1.

Fig. 4-8 shows the annual average value of wind speed and load data for 24 hrs over the period of 10 years (2009-2018). The optimal capacity of SWT and the corresponding COE found by the proposed method for the first configuration of the GCH with and without EV is shown in Fig. 4-9a for all scenarios. Without the EV, the optimal capacity of SWT is found as 6 kW for five years, 5 kW for two years, and 4 kW for three years. With the EV, the optimal capacity of SWT is obtained as 6 kW for six years, 5 kW for three years, and 7 kW for one year. In all cases, the COE varies between 30¢/kWh and 44¢/kWh.

The BES capacity and price for economic integration in the second configuration of the GCH, with and without EV, are shown in Fig. 4-9b. It is seen that, for economic integration of BES without an EV, the price of BES should reduce to $300/kWh for three years, $250/kWh for six years, and $200/kWh for one year. On the other hand, the average battery cost and optimal BES capacity, with the EV, are found as $250/kWh and 1 kWh, respectively. The above uncertainty analysis confirms that the optimal capacities obtained in Section V.A are reasonable for a GCH with a daily average energy consumption of 15.6 kWh.

E) Comparison of Operating Cost of EV and ICE Vehicle

Consider that the house owner has an option of selecting either an EV or an ICE type vehicle. The approximate operating cost of the above two vehicles are compared in this sub-section. It is assumed that the EV (Renault Zoe) can travel 7 km of distance using 1 kWh of energy [10]. In configurations 1 and 2, the cost of energy (COE), with an EV, was found as 34.81¢/kWh and 34.75¢/kWh, respectively. Thus, the operating cost of the EV is around 5¢/km. However, in the absence of SWT, the EV needs to charge from the grid at a retail price of 48¢/kWh and that would provide an operating cost of the EV as 6.86¢/km. On the other hand, the fuel consumption of the ICE vehicle is assumed as 13 km/liter. With the average fuel cost $1.30/liter in SA, the operating cost of an ICE vehicle is 10¢/km. Thus, the operating cost of an EV, when the premise has an optimal size SWT, is about 50% lower than that of an ICE vehicle.

F) Analysis of Available EVs in the Market

It is important to present an economic analysis and optimal capacity of SWT and BES for GCHs with other available EVs. The most popular EVs in Australian market for 2020 were BMW i3 (2019), Nissan Leaf (2019), Renault Zoe R135 (2019), and Tesla Model 3 (2020) [13]. Table 4-6 lists the battery capacity and charging power for those EVs.

Table 4-6. Type, Battery Capacity, and Charging Power for Most Popular EVs in Australian Market

EV Type	**BMW i3 (2019)**	**Nissan Leaf (2019)**	**Renault Zoe (2019)**	**Tesla Model 3 (2020)**
Battery Capacity	42 kWh	62 kWh	54 kWh	75 kWh
Charging power	7.4 kW	6.6 kW	7.4 kW	7.4 kW

Table 4-7 lists the optimal capacity of SWT and BES, COE, and total NPC for both system configurations with different EV types. The capacity of SWT is obtained as 7 kW for Nissan Leaf and Tesla Model 3 because of higher capacity of their batteries. However, the capacity of SWT is 6 kW for BMW i3 and Renault Zoe. As the battery capacity of EV increases, the total NPC and COE increase. For example, the COE and total NPC of a GCH with Tesla Model 3 are about 1.64 ¢/kWh and $ 28,259 higher than those of GCH with BMW i3 for configuration 1. The capacity of BES is obtained as 1 kWh for all EV types in the second configuration.

Table 4-7. Optimisation Results for Configuration With EV.

System Configurations	EV Type	SWT (kW)	BES (kWh)	COE (¢/kWh)	NPC_t ($)
Configuration 1 (Only SWT)	**BMW i3**	6	-	38.17	53,599
	Nissan Leaf	7	-	39.01	69,928
	Renault Zoe R135	6	-	38.96	64,209
	Tesla Model 3	7	-	39.81	81,858
Configuration 2 (SWT-BES)	**BMW i3**	6	1	38.16	53,555
	Nissan Leaf	7	1	38.99	69,891
	Renault Zoe R135	6	1	38.95	64,147
	Tesla Model 3	7	1	39.80	81,822

4.6 Conclusion

A method of determining the optimal capacity of SWT and BES system for a GCH, with and without EV, to minimise the overall COE has been proposed in this chapter. New rule-based HEMS have been developed for the optimisation model. The EV’s arrival/departure time, and initial SOC (when arriving at home parking) are modelled with uncertainty. Actual annual load and wind speed profiles, electricity tariff rates, and grid constraints in South Australian context are used in the optimisation process. The optimisation method and the HEMS are applied to a South Australian GCH with two configurations: (a) integrated with SWT only, and (b) integrated with SWT and BES. The effects of stochastic behaviour of SWT power generation and load consumption on the optimal capacities of SWT and BES are also investigated.

It was found that a 6-kW wind turbine is the optimal capacity for a typical GCH in SA. The optimal size SWT can decrease the COE by 35% (without an EV) and 27% (with an EV). The current BES price is unable to reduce the COE further. To obtain any further financial benefit, the net BES price, after the SA government subsidy, should reduce to 250 $/kWh. Using load uncertainty in SA and actual wind speed data for 10 years, it was found that the optimal capacity of both SWT and BES remains almost the same over the above period. It was found that when the GCH has an optimal capacity of SWT, the operating cost of an EV is about 50% lower than that of an internal combustion engine vehicle.

Nomenclature

A. Superscripts:

act	Actual
ari	Arrival
cap	Capital
cha	Charging
dep	Departure
dis	Discharging
inp	Input
mai	Maintenance
max	Maximum
min	Minimum
rep	Replacement
out	Output

B. Parameters:

C	Annual cost ($)
CL_b	Battery calendar lifetime (year)
CRF_c	Components capital recovery factor
CRF_g	Grid capital recovery factor
e, j	Escalation/de-escalation rates (%)
E_{ev}	Nominal capacity of EV (kWh)
ET_{tot}	Nominal battery total energy throughput (kWh)
h	Hour (hr)
i, d	Interest/discount rates (%)
M	Component lifetime (year)
n	Project lifetime (year)
PC_b	Present cost related to battery ($)
PC_w	Present cost related to SWT ($)
r, q	Real interest/ discount rates (%)
T	Total hours of a year (hr)
y	Year
Δt	Time interval (hr)
η_b	Efficiency of battery (%)
η_{ev}	Efficiency of EV (%)

C. Variables:

C_g	Annual cost of electricity trade with grid ($)

E_b	Nominal battery capacity (kWh)
E_l	Annual electricity demand (MWh)
ET_{bs}	Annual energy throughput of battery (kWh)
L_b	Actual lifetime of battery (year)
N_b	Number of batteries
N_w	Number of wind turbines
NPC_c	Net present cost of components ($)
NPC_g	Net present cost of electricity exchange with grid ($)
NPC_t	Total net present cost of system configurations ($)
P_b	Nominal power rating of the battery inverter (kW)
P_{ev}	Nominal power rating of the EV inverter (kW)
P_l	Load power (kW)
P_e, P_i	Export/ import power to/ from grid (kW)
P_d	Dumped power (kW)
P_w	Active power of wind turbine (kW)
S_b	State-of-charge of battery (%)
S_{ev}	State-of-charge of EV (%)

References

[1] N.A. Orlando, M. Liserre, R.A. Mastromauro, and A. Dell'Aquila, "A survey of control issues in PMSG-based small wind-turbine systems," *IEEE Trans. Indust. Infor.*, vol. 9, no. 3, pp. 1211-1221, Aug. 2013.

[2] Australia urged to copy UK ban on new fossil fuel cars by 2035. https://thedriven.io/2020/02/06/australia-urged-to-copy-uk-ban-on-new-fossil-fuel-cars-by-2035/ Accessed on: Apr. 2020.

[3] T. Hirose, and H. Matsuo, "Standalone Hybrid Wind-Solar Power Generation System Applying Dump Power Control Without Dump Load," *IEEE Trans. Ind. Electron.*, vol. 59, no. 2, pp. 988-997, Feb. 2012.

[4] M. Combe, et al., "Cost effective sizing of an AC mini-grid hybrid power system for a remote area in South Australia," *IET Gene., Trans. Dist.*, vol. 13, iss. 2, pp. 277–287, Jan. 2019.

[5] Australian Government. Bureau of Meteorology. Climate Data Online. http://www.bom.gov.au/climate/data/index.shtml?bookmark=200 Accessed on: May 2019.

[6] SA Power Network. https://www.sapowernetworks.com.au/data/17901/ update-to-small-embedded-generation-inverter-limits-and-the redevelopment-of-our-forms/ Accessed on: Apr. 2020.

[7] South Australian Government's Home Battery Scheme: https://homebatteryscheme.sa.gov.au/home-battery-scheme-subsidy-changes. Accessed on: June. 2020.

[8] M. Zheng, et al., "Smart households: Dispatch strategies and economic analysis of distributed energy storage for residential peak shaving," *Appl. Energy,* vol. 147, pp. 246–257, Jun. 2015.

[9] M. Shafie-Khah, and P. Siano, "A stochastic home energy management system considering satisfaction cost and response fatigue," *IEEE Trans. Indust. Infor.,* vol. 14, no. 2, pp. 629-638, Feb. 2018.

[10] Renault Zoe Driving Range Battery and Charging. https://www.ren ault.co.uk/electric-vehicles/zoe/battery.html. Accessed on: Mar. 2020.

[11] Electric car sales 2020: https://www.budgetdirect.com.au/car-insurance/research/electric-car-sales-australia.html Accessed on: April 2021.

Chapter 5
A Demand Side Management Approach for Optimal Sizing of Standalone Renewable Battery Systems

Demand side management is an efficient strategy to reduce the electricity cost in residential sector. This is implemented by shifting or curtailing some of the loads in the household according to energy and cost forecasts. In this chapter, the effect of demand side management on cost of electricity of standalone households is investigated. For this purpose, a novel DSM strategy is proposed to reduce the electricity demand in the days with lower generation from renewable energy sources.

The contribution of this chapter is presented in one published research article. **R. Khezri**, A. Mahmoudi, and M. Haque, "A Demand Side Management Approach for Optimal Sizing of Standalone Renewable-Battery Systems," ***IEEE Transactions on Sustainable Energy***, Early Access, May 2021.

The student has developed the conceptualization. He designed the optimisation model. Analysis and interpretation of research data has been done by him and the co-authors. A draft of the paper was prepared by the student. Revisions and comments were provided by the co-authors so as to contribute to the interpretation.

5.1 Introduction

Worldwide, 1.2 billion people do not have access to grid electricity as they live in remote areas and extension of national grid to such areas is not economically feasible [1]. Around 93% of this population is in Asia and Africa. The remaining 7% is located in Latin America, the Middle East, and the developed countries [1]. In Australia, as a developed country, remote area electricity supply (RAES) comprises 5% of annual electricity demand [2]. In South Australia (SA), the RAES covers a wide geographical area in which the farthest system is 1,600 km away from the capital city (Adelaide) [3]. In these areas, RAES supplies electricity to approximately 3,400 customers in 13 remote towns (15GWh/year) and 11 aboriginal communities (9GWh/year) [3].

The RAES systems are predominantly supplied by diesel generators (DGs). The main problems with DGs are air pollution, difficulty in fuel transportation and centralized supply. Distributed renewable energy (RE) sources, such as wind turbine (WT) and solar photovoltaic (PV) are attractive options of supplying clean energy to remote communities. Intermittency is one of the main concerns with renewable sources. However, this problem can be addressed by using suitable battery storage (BS). To obtain a reliable power supply, a large capacity of BS may be needed. However, the BS capacity and hence the total cost of the RAES system can be reduced by implementing an appropriate demand side management (DSM) strategy. Therefore, designing a clean RAES system is a complicated process which integrates BS with renewable energy sources and implements DSM to obtain a reliable and cost-effective energy system.

From a practical point of view, this chapter addresses a timely topic of practicing engineering problem for a real case study. The main novelty of this chapter is to develop a new practical DSM strategy for a comprehensive and practical optimal sizing of standalone renewable-battery systems. A new fuzzy-based DSM strategy is developed based on day-ahead forecasted renewable generation and battery state-of-charge (SOC) level. All essential parameters like operating reserve, salvation cost and battery capacity degradation are considered. A certain level of operating reserve based on the day-ahead forecasted errors of renewable generation and load consumption is maintained in the standalone system. Three system configurations: PV-BS, WT-BS and PV-WT-BS are optimally sized and compared.

The objective is to minimise the net present value (NPV) of the system and hence the levelised cost of energy (LCOE) over the project lifespan. Salvation cost of components is applied in the calculation of NPV. Two cases, with and without DSM strategy, are considered and compared for all system configurations. The optimal planning is investigated by considering capacity degradation of the battery based on the annual operation. A standalone household in South Australia is considered as the case study by incorporating real annual meteorological and load data, as well as real market price of system components.

5.2 System Model

This section describes the studied system configurations, model of various components, and household load.

5.2.1 System Configurations

Three different system configurations of electricity system of a standalone household with various combinations of PV, WT and BS are considered. Fig. 5-1 shows the studied system configurations: (1) PV-BS, (2) WT-BS and (3) PV-WT-BS. In all configurations, a DC interface is considered. That is, the above components are connected to a common DC bus. A DC interface has been chosen for the studied system configurations as it has some beneficial features, such as easy interconnection between components, high efficiency, acceptable reliability, lower cost, and absence of synchronization problems [4]–[5]. The AC loads of the household are connected to the DC bus through an inverter (INV).

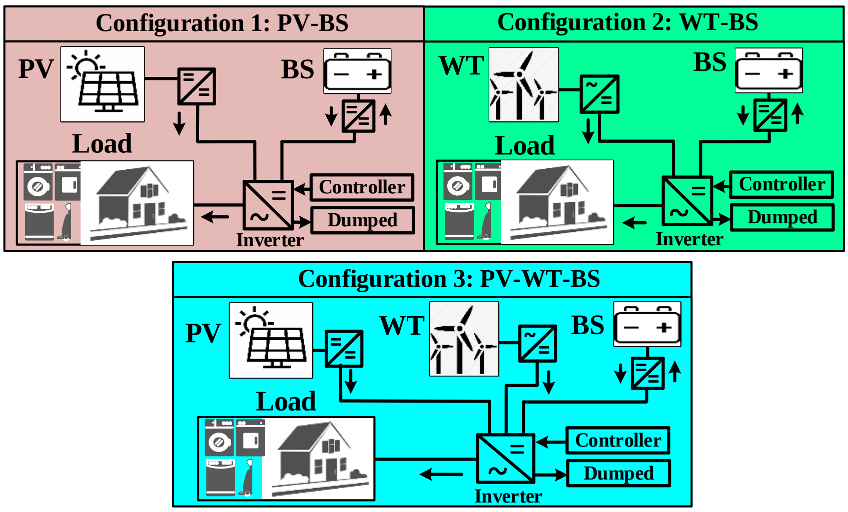

Figure 5-1. Three studied renewable-storage system configurations based on the PV, WT and BS for a remote area standalone household.

5.2.2 Solar Photovoltaic

The output power of a single PV module (P_p) is calculated as [6]:

$$P_p(t) = \eta_p P_{p,r} I_c \big(1 - 0.004(T_a - 25)\big) \tag{5-1}$$

where T_a(°C) is the ambient temperature, I_c (kW/m^2) is the solar insolation on the PV module collector, $P_{p,r}$ is the rated output power of the PV module, and η_p is the PV converter efficiency including losses in the cable.

5.2.3 Wind Turbine

The output power (P_w) of a WT is considered as a piecewise function of wind speed v [6]:

$$P_w(t) = \begin{cases} 0 & v < v_c \ or \ v > v_f \\ P_{w,r}\left(\dfrac{v - v_c}{v_t - v_c}\right)^3 & v_c \le v < v_t \\ P_{w,r} & v_t \le v \le v_f \end{cases} \tag{5-2}$$

where v_c, v_t and v_f are the cut-in, rated and cut-out wind speeds, respectively, and $P_{w,r}$ is the rated power of the WT.

5.2.4 Battery Storage

When the power generated by the renewable sources exceeds the load power, the excess power is used to charge the battery. On the other hand, when the power of the renewable sources is less than the load power, the shortage of power is met by discharging the battery. The SOC level of the battery at each time interval depends on the SOC level of the previous time interval and the amount of charging or discharging energy of battery [7]. By considering Δt as the simulation time interval, the SOC of battery at time $t + \Delta t$ can calculated by:

$$SOC(t + \Delta t) = SOC(t) + \Delta SOC(t) \tag{5-3}$$

ΔSOC is the deviation of SOC due to charging/discharging of battery which can be calculated as follows:

$\Delta SOC(t) = \frac{E_{ch}(t).\eta_{ch}}{E_b^{max}}$, when BS is charging.

$$\Delta SOC(t) = -\frac{E_{dis}(t)}{E_b^{max}.\eta_{dis}}$$, when BS is discharging.

where E_{ch}, E_{dis} and E_b^{max} are the charging, discharging and rated energy of the battery, respectively. η_{ch} and η_{dis} are the charging and discharging efficiencies, respectively.

The E_{ch} and E_{dis} are calculated based on the operational strategy of the selected configuration and will be discussed with system operation in next section. In general, the charging or discharging energy depends on the charged or discharged power. In addition, the amount of charged or discharged power is limited based on the available battery input power. The available BS input power limit ($P_{b,i}$) at each time interval cannot exceed the maximum rate of charge/discharge power of battery (P_b^{max}) and it is calculated as:

$$P_{b,i}(t) = \min\left(P_b^{max}, (E_b^{max}/\Delta t)\left(SOC^{max} - SOC(t)\right)\right) \qquad (5\text{-}4)$$

SOC^{max} is the maximum SOC level of the battery.

5.2.5 Household Loads

Two types of loads are considered for the household: controllable and uncontrollable. The uncontrollable loads should be supplied uninterruptedly. The controllable loads are inferred to the appliances that have adjustable operating time, or rarely curtailed, if required. Table 5-1 shows various controllable appliances including their energy consumption, usage frequency, duration, and operating window. There are six appliances for which the operating time can be adjusted. Only the dish washer (DW) is used daily, and the rest are used once or twice a week.

Table 5-1. Controllable loads characteristics.

Appliance	Energy (kWh)	Usage Frequency	Duration (h)	Operation window
Washing machine	0.8	Twice a week	1	[09:00−23:00]
Cloth dryer	1.1	Twice a week	1	[09:00−23:00]
Dish washer	1.2	Every day	2	[15:00−23:00]
Electric oven	2.1	Twice a week	1	[11:00−21:00]
Iron	1.0	Once a week	1	[11:00−20:00]
Vacuum cleaner	0.7	Once a week	2	[10:00−19:00]

5.3 Methodology

The day-ahead forecasting method, operating reserve, DSM strategy, system operation, and battery capacity degradation are discussed in this section.

5.3.1 Day-ahead Forecasting Method

In this study, an artificial neural network (ANN) is used to forecast both the solar insolation and wind speed. A feed-forward neural network is developed with a back-propagation mechanism using Levenberg-Marquardt optimisation [8].

For solar insolation forecasting, the time of the day, day of the month, historical irradiance (for two years), and ambient temperature are used as input data to the input layer. The output layer provides the forecasted solar insolation for the studied/candidate day. For wind speed forecasting, two years of historical wind speed data is used as input. The output layer provides the forecasted wind speed for the studied day.

Once the day-ahead forecasted data for wind speed and solar insolation are generated, the output powers of the PV and WT are calculated from eqns. (1) and (2), respectively. The forecasting error in terms of mean absolute percentage error (MAPE) is then evaluated as [9]:

$$\text{MAPE (\%)} = \frac{100}{K}\sum_{j=1}^{K}\left|\frac{P_f^j - P_a^j}{P_a^j}\right| \tag{5-5}$$

Here, P_a is the actual generation, P_f is the forecasted generation, and K is the data size.

5.3.2 Operating Reserve

Since renewable energy is stochastic and household load demand is unpredictable, an operating reserve must be maintained by the available discharging power of the battery. Using the forecasting errors, the operating reserve (P_r) is calculated as follows:

$$P_r(t) \geq \text{MAPE}_w . P_w(t) + \text{MAPE}_p . P_p(t) + \delta . P_l(t) \tag{5-6}$$

where, P_l is the household load demand (sum of controllable and uncontrollable loads), and δ is the load forecasting error. MAPE_w and MAPE_p are the forecasting errors of WT and PV, respectively.

5.3.3 Demand Side Management

The main aim of DSM in this study is to reduce the electricity consumption for the days with low energy generation from PV and WT. The SOC of battery, which shows the amount of remained charge in the BS, can also be effective in making decision for DSM. This can be achieved by designing a DSM strategy which uses not only the day-ahead forecasts of PV and WT but also the SOC of BS.

Fig. 5-2 shows the DSM and operating strategies deployed in this study. The DSM strategy is developed based on the day-ahead forecasts of wind speed and solar insolation, as well as the received data from battery power conditioning system. So, the total day-ahead generation of renewable resources ($E_{pw,dh}$) is calculated and the battery SOC level is monitored. To identify the days with low renewable generation, the average daily generation ($E_{pw,a}$) of the site by PV and WT is first obtained based on the historical data. The days for which the forecasted renewable generation are less than the half of $E_{pw,a}$ are then considered as low generation days. By monitoring the SOC, two threshold values SOC_{ts1} and SOC_{ts2} (where SOC_{ts1} > SOC_{ts2}) are considered. The level of DSM decision is decided based on all these parameters.

A fuzzy logic method is used as the core of the DSM strategy for decision making. The fuzzy logic receives the $E_{pw,dh}$ and SOC as inputs and generates the demand response strategy for the day-ahead as the output. Fig. 5-3 illustrates the fuzzy characteristics (membership functions and rules table) for the developed DSM strategy.

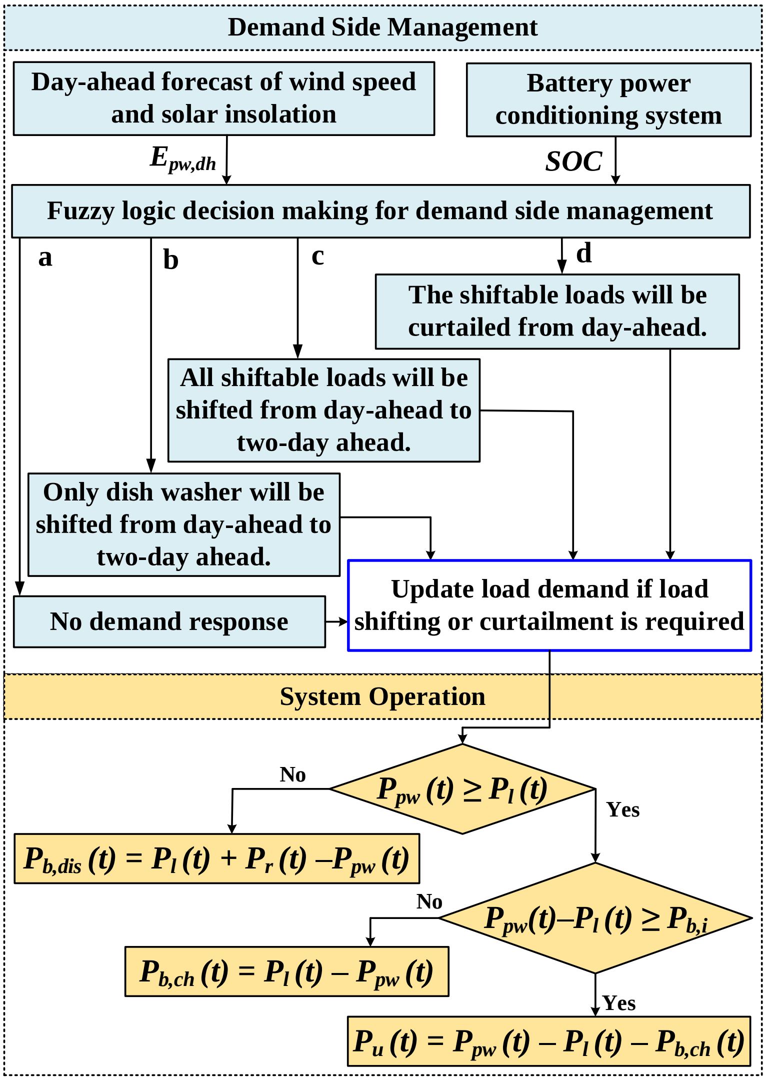

Figure 5-2. Demand side management strategy and system operation.

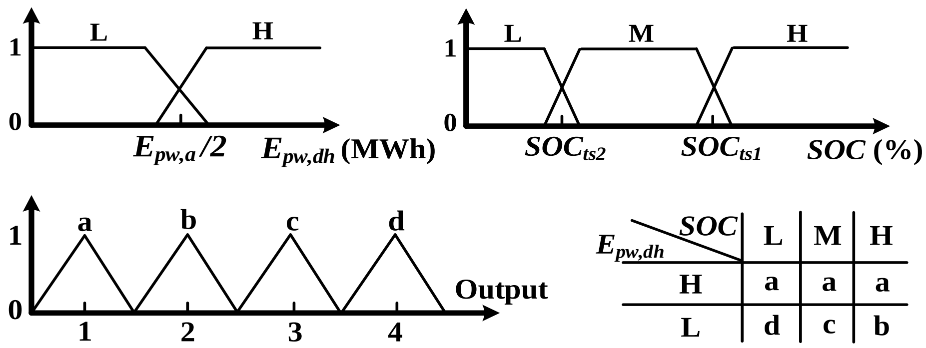

Figure 5-3. Fuzzy logic membership functions and rules table for DSM.

The fuzzy logic first compares the $E_{pw,dh}$ with the average daily generation of the site ($E_{pw,a}$) at 12am. If the total day-ahead generation is higher than half of the average daily generation, no demand response is required (path '*a*' in Fig. 5-3). If the $E_{pw,dh}$ is less than half of $E_{pw,a}$, SOC of the battery should be analysed. If the SOC of battery is higher than the SOC_{ts1}, only operation of the DW will be shifted from day-ahead to two-day ahead (path 'b' in Fig. 3):

$$\begin{cases} P_{l,1dh}(t) = P_l(t) - P_{dw,1dh}(t) \\ P_{l,2dh}(t) = P_l(t) + P_{dw,1dh}(t) \end{cases} \tag{5-7}$$

where $P_{l,1dh}$ and $P_{l,2dh}$ are one day-ahead and two day-ahead loads of the household, and $P_{dw,1dh}$ is the DW load demand in the day-ahead.

If the SOC of battery is in between the SOC_{ts1} and SOC_{ts2}, all the shiftable loads in day-ahead ($P_{s,1dh}$) will be shifted from day-ahead to two-day ahead (path 'c' in Fig. 3):

$$\begin{cases} P_{l,1dh}(t) = P_l(t) - P_{s,1dh}(t) \\ P_{l,2dh}(t) = P_l(t) + P_{s,1dh}(t) \end{cases} \tag{5-8}$$

Finally, if the SOC is lower than the SOC_{ts2}, all shiftable loads in day-ahead will be curtailed (path 'd' in Fig. 5-3):

$$\begin{cases} P_{l,1dh}(t) = P_l(t) - P_{s,1dh}(t) \\ P_{l,2dh}(t) = P_l(t) \end{cases} \tag{5-9}$$

The above demand response strategies represented by eqns. (5-7)-(5-9) are activated by the output of the fuzzy logic as shown in Fig. 5-3.

5.3.4 System Operation

In all three system configurations, if the generated power by renewable sources (P_{pw}) is greater than the load, the extra power of renewable sources charges the battery within the input power limit of the BS ($P_{b,i}$). Hence, the battery charging power ($P_{b.ch}$) can be written as:

$$P_{b,ch}(t) = \min\left(P_{b,i}(t), P_{pw}(t) - P_l(t)\right) \tag{5-10}$$

$$P_{pw}(t) = P_p(t) + P_w(t) \tag{5-11}$$

If the extra power is more than the battery input power limit, the surplus power is dumped. Thus, the dumped power (P_u) can be expressed as:

$$P_u(t) = P_{pw}(t) - P_l(t) - P_{b,ch}(t) \tag{5-12}$$

If the generated power by renewable sources is less than the load, the battery supplies the shortfall. The discharging power ($P_{b,dis}$) of the battery can be written as:

$$P_{b,dis}(t) = P_l(t) + P_r(t) - P_{pw}(t) \tag{5-13}$$

In this case, the BS must have adequate stored energy to supply not only the shortfall but also maintain the operating reserve.

5.3.5 Battery Capacity Degradation

The battery CD and subsequently battery lifetime can be calculated based on the number of cycles and associated depth of discharge (DOD) of each cycle. At the end of annual operation, the annual SOC of the battery is extracted. The number of charge/discharge cycles and the corresponding DOD ($= 1 - SOC$) of the battery are then obtained using Rainflow Counting Algorithm (RCA) [10]. The Li-ion battery is used in this study for which the CD in each full cycle can be calculated as:

$$CD(c) = \frac{20}{33000.\,e^{-0.06576.DOD(c)} + 3277} \tag{5-14}$$

The RCA extracts the number of full cycles and half cycles in the DOD of the battery. It is assumed that the CD is half of eqn. (14) for the half cycles. A filtering procedure is implemented on the SOC to disregard the adjacent local max/min points below a threshold (<1Wh) [11]. The annual capacity degradation (ACD) of battery can be calculated by:

$$ACD = \sum_{c=1}^{\mathcal{C}} CD(c) \tag{5-15}$$

where $\mathcal{C}$ is the total number of cycles of the year obtained by the RCA. Once the total CD of battery exceeds 20%, the battery should be replaced.

5.4 Optimisation Model

The optimisation model investigates the objective function, design constraints and optimisation algorithm. Decision variables of the optimisation model are the capacities of PV, WT, BS, and INV.

5.4.1 Problem Formulation

The NPV of the system over the project lifespan is a function of capital present value (C^a), replacement present value (C^e), maintenance present value (C^m) and salvation value (C^s) of the system components.

$$\begin{aligned} \text{NPV} = \left(C_p^a + C_p^m - C_p^s\right).\alpha_p + (C_w^a + C_w^m).\alpha_w \\ +(C_b^a + C_b^e + C_b^m - C_b^s).\alpha_b + (C_v^a + C_v^e).\alpha_v \end{aligned} \tag{5-16}$$

Eqn. (5-16) represents the NPV of the system where α is the number of components as the decision variables. Subscripts *p*, *w*, *b*, and *v* represent PV, WT, BS, and INV, respectively.

The capital payment of components takes place at the beginning of the project and is the same as capital present value C^a. The present value of maintenance cost C^m is calculated from annual maintenance cost (M), interest rate (i), and project lifespan (n).

$$C^m = M\frac{(1+i)^n - 1}{i(1+i)^n} \tag{5-17}$$

The replacement cost is applicable to only those components that have lower lifetime (less than project lifespan). Thus, replacement cost is not applicable to PV and WT as their lifetime is higher than or equal to the project lifespan. The present value of replacement cost C^e is calculated from component replacement cost (R), interest rate (*i*) and component replacement year (*G*).

$$C^e = R\frac{1}{(1+i)^G} \tag{5-18}$$

The salvation value C^s is the remaining value of the component at the end of the project lifespan and is applicable to only solar PV and battery.

$$C_p^s = C_p^a.\frac{H_p}{L_p}\ , \qquad C_b^s = C_b^e.\frac{H_b}{L_b} \tag{5-19}$$

where L_p and L_b are the lifetime of PV and BS, respectively. H_p and H_b are the remaining life (in years) of PV and BS, respectively, at the end of project lifespan.

Once the NPV is obtained, the levelised cost of electricity (LCOE) can be calculated:

$$LCOE = \frac{NPV}{E_l}.\overbrace{\left(\frac{i(1+i)^n}{(1+i)^n-1}\right)}^{CRF} \tag{5-20}$$

where E_l is the annual load of system and CRF is the capital recovery factor.

The objective function and design constraints of the optimisation problem are formulated as follows:

$$f = \text{minimise (NPV)} \tag{5-21}$$

Subject to:

$$0 \leq \alpha_k \leq \alpha_k^{max}, \qquad \alpha_k \epsilon \{\alpha_p, \alpha_w, \alpha_b, , \alpha_v\} \tag{5-22}$$

$$P_w(t) + P_p(t) + \ P_{b,dis}(t) = P_l(t) + P_u(t) + P_{b,ch}(t) \tag{5-23}$$

$$SOC^{min} \leq SOC(t) \leq SOC^{max} \tag{5-24}$$

$$SOC(T) \geq SOC(t = 0) \tag{5-25}$$

Eqn. (5-21) represents the NPV as the objective function. Eqn. (5-22) ensures that the number of system components (α_k) are within their maximum limits. Eqn. (5-23) represents the power balance constraint. Eqn. (5-24) guarantees that the battery SOC level is within the upper and lower limits. Finally, eqn. (5-25) ensures that the SOC of BS at the end of time horizon is higher than the initial SOC of BS at the beginning of project.

5.4.2 Optimisation Algorithm

In real-world applications, the capacity of battery is degraded due to system operation. The capacity is not updated by consumer or operator as it is in the nature of the battery that the initial capacity will not be available due to degradation. When the capacity degradation reaches 20% of the initial capacity, the battery should be replaced. The most efficient method to calculate the battery degradation is the degradation per cycle. However, the cycles and their associated DODs are not available at the beginning of project (before the system operation), and they are different for various system configurations. For example, in a WT-BS system, the battery may experience lower charging/discharging cycles with lower DODs and thus lower degradation can be obtained. In contrary, the number of charging/discharging cycles and their DODs may increase for another system and hence higher degradation can be obtained. To overcome this challenge in our study, the system is first operated for one year and then the DOD data is extracted. After that, the Rainflow cycling algorithm is used to extract the number of cycles from the annual DOD data. Finally, an experimental method, stated in equation (14), is adopted to calculate the degradation due to each cycle of battery.

Fig. 5-4 shows the flowchart of the optimisation procedure. In this study, the operation of the system is carried out in two stages. At the first stage, the optimisation of the system is carried out and the value of ACD is extracted from eqn. (15). At the second stage, the obtained ACD from the first stage is used to update the BS capacity and repeat the calculations. The battery lifetime is calculated based on the obtained ACD of the second stage. This is a simple way to obtain a more realistic battery CD during the operation.

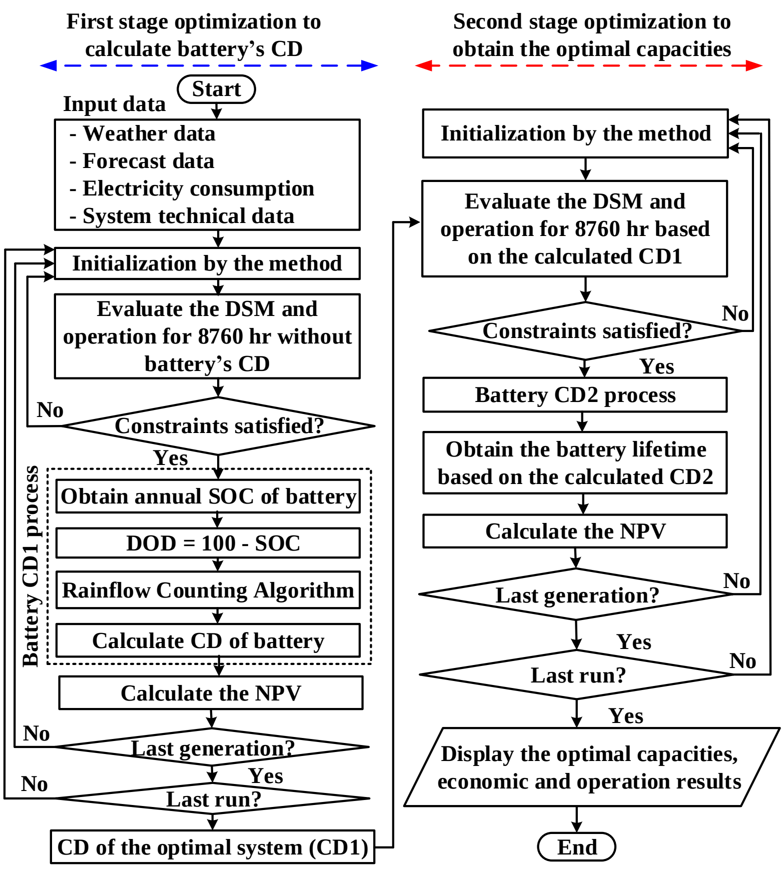

Figure 5-4. Optimisation procedure for optimal sizing of components.

Different solvers, available in MATLAB optimisation toolbox, can be used to solve the formulated problem. Particle swarm approach is used in this study because of its simple concept, suitability in rate of convergence, computational efficiency, easy implementation, and minimum dependency on initial points [6]. This algorithm is extensively used to solve the optimal sizing problems in power systems. To guarantee of global optimal result achievement by the algorithm, high number of populations (300) and generations (500) have been run in 20 repetitions.

5.5 System Data

A typical household in SA is considered as the case study. It is assumed that the project lifespan is 20 years. The financial/technical parameters of system components as well as load and weather data are discussed in this section.

5.5.1 System Components Data

Table 5-2 shows the capital cost, replacement cost, and maintenance cost of various system components [12]. All prices are in Australian dollar (AUD). The lifetimes of PV, WT and INV are assumed as 25, 20 and 10 years, respectively.

Table 5-2. Capital, Replacement, and Maintenance Costs of PV, WT and BS [12].

Component	Unit size	Capital cost	Replacement cost	Maintenance cost
PV	1 kW	$ 1,200/kW	N/A	$25
WT	1 kW	$ 2,500/kW	N/A	$50
BS	0.3kW/1kWh	$ 500/kWh	$ 350	$10
INV	1 kW	$ 1,000/kW	$ 500	N/A

The round-trip efficiency of BS is considered as 92%. The values of $SOC_{\min}$ and $SOC_{\max}$ are considered as 20% and 95%, respectively. The initial value of SOC at the beginning of simulation is assumed as 60%. It may be mentioned here that a lower value of initial SOC cannot supply the load uninterruptedly. The higher value of initial SOC does not affect the optimisation results. The value of SOC_{ts1} and SOC_{ts2} are considered as 60% and 35%, respectively.

An annual capacity degradation of solar PV is considered as 0.95% over its lifetime. The cut-in, cut-out and rated wind speeds of the WT are considered as 3m/s, 22m/s, and 8m/s, respectively.

5.5.2 Load and Weather Data

The operation of the controllable appliances is randomly distributed during the year according to their operating time window and usage frequency (as shown in Table II). The annual, maximum daily, and average daily energy demands of the household are 6,205 kWh, 24 kWh and 17 kWh, respectively. The forecasted data has only generated for renewable generation in this study. It is, however, not that simple to generate the forecasted data of customers electricity consumption due to some main reasons which can be described by several factors. The availability of historical data is the first factor. For this study, the load data of the standalone household was only available for one year. On the other hand, residential load forecasting depends on several other factors like customer lifestyle, working hours, days of the week, and the number of people in the household. These factors vary from one household to another, and it is not easy to access them. Therefore, the day-ahead load forecast error in literature is used in this study. The considered load forecasting error ($\delta = 25\%$) is taken from [9].

The actual wind speed and solar insolation data of Nundaroo (31.48 S, 131.84 E), a remote town located along the South Australian coast, are used to analyse the annual operation of the systems [7]. The average solar insolation and wind speed of the site are found as 5.4 kWh/m^2/day and 4.3 m/s, respectively. The average daily generation of a 1-kW PV and a 1-kW WT are calculated as 4.7 kWh and 6.9 kWh, respectively [7].

The MAPE for WT and PV generation forecasts of the site are obtained as 10.8% and 8.2%, respectively. Fig. 5-5 shows the comparison of actual and ANN-based forecasted day-ahead wind speed and solar insolation of the site for the first week of July. By considering the forecast errors, the average daily generation ($E_{pw,a}$) of the site for various system configurations is updated as follows:

PV-BS system: $$E_{pw,a} = \left(1 - MAPE_p/100\right) \times 4.7 \qquad (5\text{-}26)$$

WT-BS system: $$E_{pw,a} = (1 - MAPE_w/100) \times 6.9 \qquad (5\text{-}27)$$

PV-WT-BS system: $$E_{pw,a} = \left(\left(1 - MAPE_p/100\right) \times 4.7 + (1 - MAPE_w/100) \times 6.9\right)/2 \qquad (5\text{-}28)$$

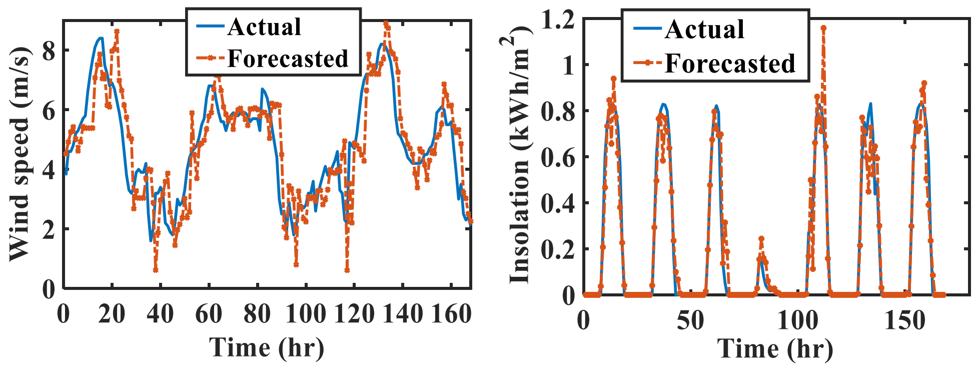

Figure 5-5. Actual and forecasted wind speed and solar insolation.

5.6 Results and Discussion

To demonstrate the benefits of the proposed DSM strategy, various results of all three system configurations of Fig. 5-1 are evaluated using the proposed DSM and compared with that found without using the DSM. Some of the results (NPV, LCOE and CO_2 emission) of the best configuration are compared with that reported in [6] and [7], as well as the actual electricity rate in SA.

5.6.1 Without DSM

The optimal capacity of various system components and the corresponding economic results of all three configurations are evaluated without considering the DSM and the results found are summarised in Table 5-3. The third configuration (PV-WT-BS) is the best system as it has the lowest value of NPV and LCOE. This system is supplied by 8 kW of PV and 2 kW of WT and has the lowest capacity of BS (35 kWh). The second configuration (WT-BS) is the most expensive system as it has the highest capacity of battery (193 kWh). The results (NPV, LCOE and BS capacity) of the first configuration (PV-BS) are in between that of the second and the third configurations.

Table 5-3. Optimal Capacity and Economical Results Without DSM.

System	Components' capacities				NPV ($)	LCOE (¢/kWh)
	PV (kW)	WT (kW)	BS (kWh)	INV (kW)		
PV-BS	10	-	83	4	73,807	123
WT-BS	-	12	193	4	125,321	210
PV-WT-BS	8	2	35	4	38,659	65

The battery capacity in WT-BS system is found to be much higher than that of other configurations. This is because of the stochastic variations of wind speed and successive days of low wind speed (or low wind energy). It has been observed that, for some months of the year, the wind generation was less than 1 kWh for four successive days and that requires higher battery capacity to supply the load uninterruptedly. However, in the PV-BS and PV-WT-BS systems, the PV system did not have low generation for more than two successive days and thus required lower battery capacity.

The annual generated energy can be divided into three components: feeding the load directly, charging the battery, and dumping by the inverter control. The pie charts of the above components of all configurations are shown in Fig. 5-6. The PV-WT-BS system used the highest percentage (27%) of its generated energy to feed the load directly followed by the PV-BS system (22%) and the WT-BS system (14%). The percentage of generated energy used to charge the battery varies between 11% (for the WT-BS system) and 26% (for the PV-BS system). A high percentage of generated energy is dumped (52% for the PV-BS system, 58% for the PV-WT-BS system and 75% for the WT-BS system). The WT-BS system has the highest annual renewable generation (25.17 MWh) and hence the highest annual dumped energy (almost 75% of the renewable generation). It may be mentioned here that the dumped energy is basically uncollected energy by the inverters but not physically dumped to a resistor.

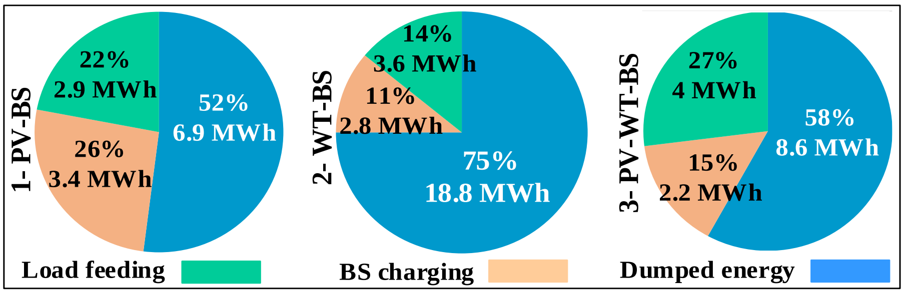

Figure 5-6. Breakdown of generated energy without DSM.

5.6.2 *With DSM*

The optimal capacity of system components and economic results for all configurations with the proposed DSM strategy are listed in Table 5-4. In this case, the capacity of renewable energy sources (PV and WT) is found to be the same as that of without DSM. However, the battery capacity for all configurations has reduced due to the implementation of DSM. For the PV-BS system, the BS capacity has decreased by 13 kWh and that reduces the value of NPV and LCOE by $8,900 and 14 ¢/kWh, respectively. The lowest LCOE (57 ¢/kWh) is found for the PV-WT-

BS system for which the BS capacity is reduced by 11 kWh.

Table 5-4. Optimal Capacity and Economical Results by Considering DSM.

System	Components' capacities				NPV ($)	LCOE (¢/kWh)
	PV (kW)	WT (kW)	BS (kWh)	INV (kW)		
PV-BS	10	-	70	4	64,907	109
WT-BS	-	12	179	4	119,191	200
PV-WT-BS	8	2	24	4	34,120	57

The fraction (or percentage) of energy used to charge the battery and feeding the load as well as dumped by the inverters is shown in Fig. 5-7. Comparison of Figs. 5-6 and 5-7 indicates that the proposed DSM has very little effect on the distribution of energy among the above three components.

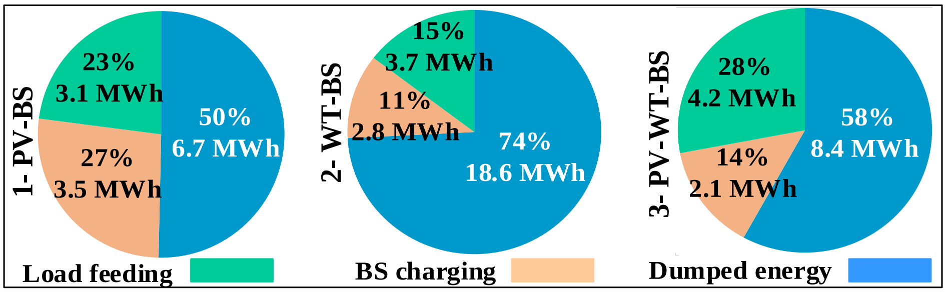

Figure 5-7. Breakdown of generated energy with DSM.

Fig. 5-8 shows the annual CD and lifetime of BS for all configurations. The BS lifetime is calculated from its ACD [8]. The shortest and longest lifetimes of the BS are found as 10 years (PV-BS system) and 15 years (WT-BS system), respectively. The BS lifetime for the optimal system (PV-WT-BS) is found as 13 years.

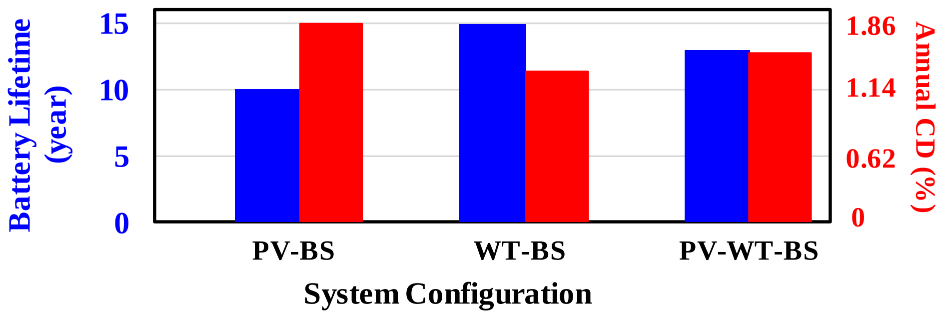

Figure 5-8. Battery CD and lifetime of all three system configurations with DSM.

The effects of the proposed DSM on load shifting and load curtailment are shown in Table 5-5. It can be noticed in the table that, for the optimal system configuration (PV-WT-BS), the DSM causes to shift loads for 21 days per year (as the day-ahead forested generation was less than half of daily average generation). The annual load shifting was only 66.5 kWh. However, there were only 6 days (out of 21 days of load shifting) for which load shifting was not adequate to maintain the energy balance and a drastic action or load curtailment was required. The annual load curtailment was only 22.7 kWh. The main reason for higher load curtailment in the PV-WT-BS system is the low capacity of battery. As seen in Table VI, the number of the days with low generation of renewable energies is 27 days (the days with load shifting and load curtailment). However, due to the low capacity of battery, only 6 out of those 27 days the SOC of battery is lower than 35% which is the threshold of SOC for load curtailment. This means that in those 6 days the available charge of battery is lower than 35% of its optimal capacity (24 kWh). For the other two system configurations, even though load shifting is required for a greater number of days, the annual load curtailment and the corresponding number of days are less because of the use of much higher capacity of BS.

Table 5-5. Load Shifting and Load Curtailment Caused by the DSM.

System	Number of days for load shifting	Amount of load shifting (kWh)	Number of days for load curtailment	Amount of load curtailment (kWh)
PV-BS	43	131.9	3	12.2
WT-BS	24	75.1	1	4.3
PV-WT-BS	21	66.5	6	22.7

5.6.3 Effects of Salvation Value and Battery Degradation

It is important to investigate the effects of salvation value and battery degradation on optimal sizing of system configurations. In this context, Fig. 5-9 demonstrates the impacts of salvation value and battery CD on LCOE and BS capacity of the studied system configurations. All results are obtained for the systems with the proposed DSM strategy. By neglecting the salvation value, the LCOE of system configurations has increased, however, the BS capacity is almost the same as the proposed models of this study. It is illustrated that when the battery CD is neglected, lower capacity of BS is obtained with slightly lower LCOE. However, degradation is the natural process of batteries, and it causes capacity drop during the operation. Hence, it is found that if the salvation value or battery degradation is neglected in the optimisation model, the optimal sizing results may not be accurate and reliable.

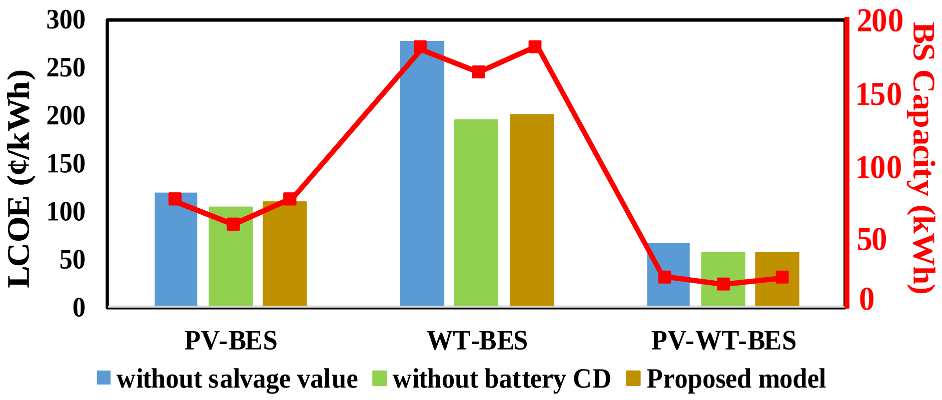

Figure 5-9. Comparison of the proposed model with the systems without considering salvation value and battery CD.

5.6.4 Comparison with Actual and Previously Studied Systems

In order to demonstrate the effectiveness of the proposed method, some of the results obtained in this study (for the optimal configuration) are compared with that of the actual (or existing) system as well as found by two previous studies [6] and [7]. The actual system is based on diesel generators (DG) which has a LCOE of 70-78 ¢/kWh (with an average of 74 ¢/kWh) [3]. In [7], a hybrid generating system consisting of DG-WT-PV-BS was found as the optimal system configuration for a standalone community in the same area. In [6], an incentive-based demand response was implemented in the above hybrid generating system. For comparison purpose, some of the results (NVP and CO_2 emission) of the above two methods were proportionally converted to match the load demand (6,205 kWh/yr) used in this study. Table 5-6 compares the LCOE, NPV and CO_2 emission of the above-mentioned systems. The systems investigated in this study (with and without DSM) are 100% renewable and thus have no CO_2 emission. The actual REAS system is 100% fossil fuel (or DG) based and thus has the highest CO_2 emission of 5.83 tonne/yr. The CO_2 emission of the hybrid systems is about half the DG-based system. It can be noticed in the table that actual DG-based system has the highest LCOE and NPV because of high fuel cost. The lowest value of LCOE and NPV is found for the proposed PV-WT-BS system with DSM. The LCOE and NPV for the hybrid systems [6], [7] are slightly higher than that found in this study. However, unlike the present study systems, the operating reserve for the renewable generation uncertainty was not considered in the previously reported hybrid systems.

Table 5-6. Comparison of Results of Various Systems.

System	LCOE (¢/kWh)	NPV ($)	CO_2 Emission (tonne/year)
Proposed PV-WT-BS without DSM	65	38,659	0
Proposed PV-WT-BS with DSM	57	34,120	0
Actual RAES rate in SA [3]	74	44,217	5.83
DG-WT-PV-BS without DR [7]	61	36,449	2.47
DG-WT-PV-BS with DR [6]	59	35,254	2.46

5.7 Conclusion

In this chapter, a novel practical DSM approach was developed for optimal sizing of renewable sources and battery storage. The proposed DSM strategy used battery SOC and day-ahead forecasted renewable generation, to implement the most efficient load shifting and/or load curtailment. A fuzzy logic technique was used as the core of DSM for decision making. The main feature of the developed DSM is its easy implementation in households. Three different system configurations (PV-BS, WT-BS and PV-WT-BS) have been formed and investigated for a standalone household. The optimal results obtained by the proposed method are then compared with that found and reported in two recent articles.

Without the proposed DSM strategy, it has been found that the WT-BS system configuration required the highest battery capacity and that caused the highest LCOE. However, the battery capacity degradation is found to be the lowest because of its less utilization. The PV-WT-BS configuration was found to be the most optimal having the lowest value of BS capacity and the LCOE. The LCOE of the PV-BS is found to be in between that of the WT-BS and PV-WT-BS configurations.

When the proposed DSM strategy was applied, the BS capacity of all configurations is reduced while the capacity of renewable sources remained the same. Because of the reduction of BS capacity, the NPV and hence the LCOE of all configurations are decreased compared to that found without applying the DSM. For the optimal configuration (PV-WT-BS), the BS capacity is found as 24 kWh (a reduction of 11 kWh) and LCOE of 57 ¢/kWh (a reduction of 8 ¢/kWh). In previous studies, the LCOE with hybrid generating system is found as 61 ¢/kWh (without demand response) and 59 ¢/kWh (with demand response). The actual or existing system, based on diesel generator, has a LCOE of 74 ¢/kWh. Note that both hybrid and existing systems emit CO_2 because of the use of diesel generators. However, the optimal configuration found by the proposed method not only has the lowest LCOE but also has no CO_2 emission as it is completely renewable-storage based. The lowest LCOE is achieved at an expense of annual load shifting of 66.5 kWh for six days and an annual load curtailment of 22.7 kWh.

References

[1] M. Arriaga, C. A. Cañizares and M. Kazerani, "Northern Lights: Access to Electricity in Canada's Northern and Remote Communities," *IEEE Power and Energy Magazine*, vol. 12, no. 4, pp. 50-59, July-Aug. 2014.

[2] Australian Infrastructure Audit 2019 [Online]. Available: https://www.infrastructureaustralia.gov.au/sites/default/files/201908/Australian%20Infrastructure%20Audit%202019.pdf,Accessed on: Jul. 2020.

[3] Government of South Australia, Department of Energy and Mining. Remote Area Energy Supply, [Online]. Available: https://www. energymining.sa.gov.au/energy_and_technical_regulation/energy_resources_and_supply/remote_area_energy_supply, Accessed on: July 2020.

[4] M. B. Shadmand and R. S. Balog, "Multi-Objective Optimization and Design of Photovoltaic-Wind Hybrid System for Community Smart DC Microgrid," *IEEE Trans. Smart Grid*, vol. 5, no. 5, pp. 2635-2643, Sept. 2014.

[5] M.D.A. Al-falahi, S.D.G. Jayasinghe, and H. Enshaei, "A review on recent size optimization methodologies for standalone solar and wind hybrid renewable energy system," *Energy Conversion and Management*, vol. 143, pp. 252-274, Jul. 2017.

[6] M. Combe, et al., "Optimal sizing of an AC-coupled hybrid power system considering incentive-based demand response," *IET Gene., Trans. Dist.*, vol. 13, iss. 15, pp. 3354 – 3361, Jun. 2019.

[7] M. Combe, et al., "Cost effective sizing of an AC mini-grid hybrid power system for a remote area in South Australia," *IET Gene., Trans. Dist.*, vol. 13, iss. 2, pp. 277–287, Jan. 2019.

[8] M. Yousefi, A. Hajizadeh, and M. N. Soltani, "A comparison study on stochastic modeling methods for home energy management system," *IEEE Trans. Indust. Infor.*, vol. 15, no. 8, pp. 4799 - 4808, Aug. 2019.

[9] S. Chen, H. Gooi, and M. Wang, "Sizing of energy storage for micr-ogrids," *IEEE Trans. Smart Grid*, vol. 3, iss. 1, pp. 142–151, Mar. 2012.

[10] M. Musallam and C. M. Johnson, "An Efficient Implementation of the Rainflow Counting Algorithm for Life Consumption Estimation," *IEEE Trans. Reliability*, vol. 61, no. 4, pp. 978-986, Dec. 2012.

[11] C. A. Correa, A. Gerossier, A. Michiorri and G. Kariniotakis, "Optimal scheduling of storage devices in smart buildings including battery cycling" *2017 IEEE Manchester PowerTech*, Manchester, 2017, pp. 1-6.

[12] GenCost 2020-21 – CSIRO [Online]. Available: https://www.csiro.au/-/media/News-releases/2020/renewables-cheapest/GenCost2020-21.pdf Accessed on: March 2021.

Chapter 6
Optimal Design Framework for a Residential Grid-Connected Renewable Battery System

This chapter develops a long-term operation model for planning studies of a renewable-battery system for a residential grid-connected house. The optimal planning is conducted on a multi-objective basis by considering cost of electricity, grid dependency, and dumped energy as the objective functions. It is found that the developed long-term operation achieves higher accuracy for the obtained results compared to those of short-term operation. In addition, the multi-objective sizing presents better guidelines for the customers to select the capacity of components based on different objective functions.

The contribution of this chapter is presented in one submitted research article. **R. Khezri**, A. Mahmoudi, and H. Aki, "Optimal Design Framework for a Residential Grid-connected Renewable-Battery System," ***IEEE Transactions on Industry Applications***, 2021.

The student has developed the conceptualization. He designed the optimisation model. Analysis and interpretation of research data has been done by him and the co-authors. A draft of the paper was prepared by the student. Revisions and comments were provided by the co-authors so as to contribute to the interpretation.

6.1 Introduction

Integration of renewable energy (RE) and battery storage (BS) systems is becoming a viable option for grid-connected households (GCHs). In GCHs with RE and BS, optimal planning of components is the utmost important aspect which must meet multiple objectives. Minimising cost of electricity (COE) is the main factor for the customers [1]. Decreasing dependency on the main grid is the other target in GCHs [2]. On the other side, increasing the curtailed energy from REs in GCHs is not desirable. Curtailed energy is the wasted energy of RE resources after feeding load, charging BS and exporting power to the main grid. Hence, there are several objective functions that could be considered for optimal planning of RE sources and BS in a grid-connected households.

Although single- objective scheme has been extensively used for optimal sizing, multi-objective (MO) optimal sizing/planning is a valuable substitution that can give wider ideas to the designer. In the single- objective sizing, the electricity cost is considered as the target and hence this type of optimisation is unable to render insights into the trade-offs between objective functions. However, by the MO optimisation several objective functions like grid dependency (GD), which shows the energy dependency of the GCH, and the curtailed energy can be considered alongside the electricity cost.

Generally optimal planning is a long period problem. On the other hand, the lifetimes of components are disparate and may mismatch the project lifespan. Considering the salvation cost which is the value of the components at the end of project lifespan realizes a precise optimisation model. Capacity degradation (CD) of PV and BS is the other challenge for optimal sizing problems. Due to CD, the initial capacity of components is not usable during the project lifespan because it degrades due to operation or the environmental issues. In addition, the CD may decrease the lifetime of BS. There is a lack of study to apply CD for both long-period operation and lifetime estimation. Most studies have conducted a short period of operation for optimal planning. However, to achieve a realistic model of the operation and battery's CD, as well as stochastic nature of the REs and load, a long-period operation is indispensable.

Based on the challenges in the literature, this chapter develops a comprehensive optimal design framework. The capacities of PV, WT and BS are optimised in a residential GCH based on three objective functions: (1) cost of electricity, (2) grid dependency, and (3) total curtailed energy (TCE). An operation strategy based on home energy management system and degradations of PV and BS is developed. The method uses 10-year data rather than yearly data. While the proposed optimisation framework is applicable to any GCH, the actual data (weather data, load profile, as well as PV, WT, BS, and electricity prices) in South Australia are used for a realistic optimisation study. The results of this study can be used as a guideline for: (*i*) customers to select the capacity of PV, WT and BS based on a compromise between COE and GD, (*ii*) designers to get insights into the BS degradation and TCE for various designs. The main contributions of this paper compared to previous studies are:

- Develop an optimisation model based on a long-period (10-year) operation for a GCH with PV, WT and BS by incorporating real data.
- Incorporate solar PV and battery capacity degradations in the long-period operation of the residential GCH.
- Optimise the capacity of PV, WT and BS based on electricity cost, grid dependency and curtailed energy.
- Compare the long-period optimal sizing framework with short-period optimisation.

6.2 Operation of Energy System

Fig. 6-1 demonstrates the system configuration for a grid-connected household. The components (PV, WT and BS) are parallelly connected to the household using an AC interface. The energy management system and degradations of PV and battery during the project lifespan (10 years) of the GCH are discussed in this section.

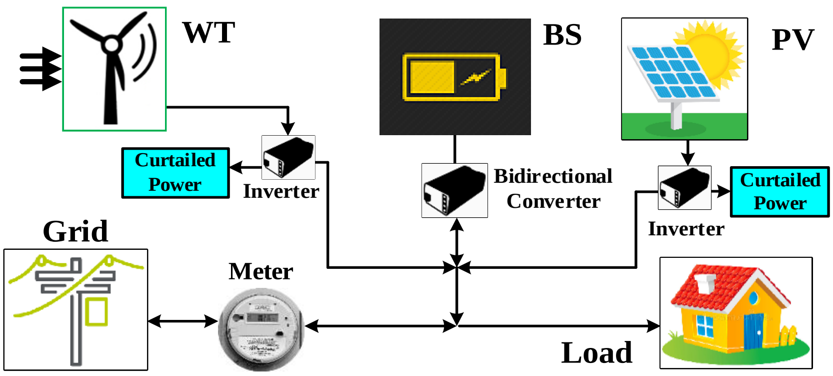

Figure 6-1. System configuration of the studied grid-connected household.

6.2.1 Energy Management System

In this study, a rule-based power management approach is considered for the GCH due to user-friendliness, low computational requirement, practicality, and simple implement in real-life. The developed power management and optimisation model of this study are general and can be implemented to all standard electricity rates (e.g., flat rate).

Fig. 6-2a illustrates the home energy management system of the GCH. The energy management commences by comparing the RE generation to the household's load demand. Once the output power of REs exceeds the load, the extra power first charges the BS considering the limitations of state of charge (SOC) and available input power of the battery.

$$P_{\beta}^{ch}(t) = \min\left(P_{\beta}^{in}(t), P_{re}(t) - P_{h}(t)\right) \tag{6-1}$$

$$P_{re}(t) = P_{\rho,y}(t) + P_{\omega}(t) \tag{6-2}$$

Battery's SOC at charging time interval and available input power limit are formulated as:

$$S(t + \Delta t) = S(t) + \left(P_{\beta}^{ch}(t).\eta_{\beta}^{ch}\right)/\left(E_{\beta,y}/\mathrm{h}\right) \tag{6-3}$$

$$P_{\beta}^{in}(t) = \min\left(P_{\beta}^{max}, \left(E_{\beta,y}/\mathrm{h}\right).\left(S^{max} - S(t)\right)\right) \tag{6-4}$$

If there is extra power of REs, it will be sold to the main grid considering the maximum allowable export power.

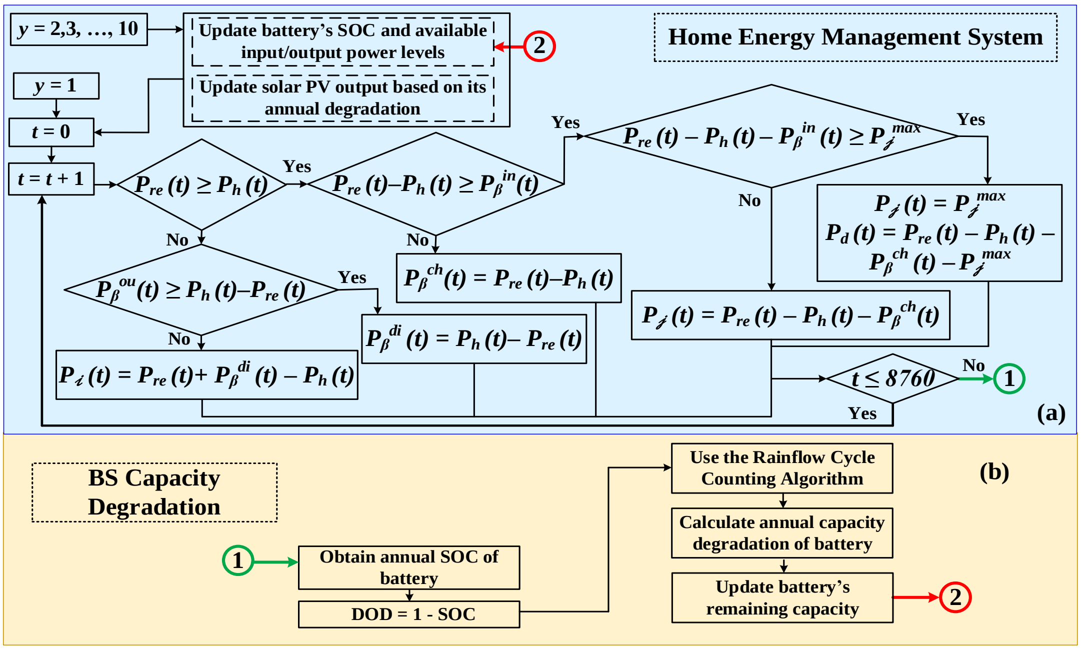

Figure 6-2. Operation of the electricity system for a grid-connected household. (a) Home energy management system, and (b) Battery capacity degradation.

$$P_{\jmath}(t) = \min\left(P_{\jmath}^{max}, P_{re}(t) - P_h(t) - P_\beta^{ch}(t)\right) \tag{6-5}$$

Any excess power of REs will be curtailed using the control system of inverters.

$$P_d(t) = P_{re}(t) - P_h(t) - P_\beta^{ch}(t) - P_{\jmath}^{max} \tag{6-6}$$

When the REs output power is lower than the load, the BS starts discharging to supply the household demand considering the limits of SOC level and available output power of battery.

$$P_\beta^{di}(t) = \min\left(P_\beta^{out}(t), P_h(t) - P_{re}(t)\right) \tag{6-7}$$

Battery's SOC at discharging time interval and available output power are calculated by:

$$S(t+\Delta t) = S(t) - \left(P_\beta^{di}(t)/\eta_\beta^{di}\right)\left(E_{\beta,y}/\mathrm{h}\right) \tag{6-8}$$

$$P_\beta^{ou}(t) = \min\left(P_\beta^{max}, \left(E_{\beta,y}/\mathrm{h}\right).\left(S(t) - S^{min}\right)\right) \tag{6-9}$$

If the load is still not fully supplied, then the unmet load is fed by the imported power from the main grid.

$$P_i(t) = P_h(t) - P_{re}(t) - P_\beta^{di}(t) \tag{6-10}$$

The output power of solar PV, as well as available input/output powers and SOC level are updated after each year based on the capacity degradations.

6.2.2 Degradation of Components

In real world applications, the capacity of PV and BS is degraded due to system operation and environmental issues. After degradation, the capacities are not updated by consumer or operator; but it is in the nature of the components that initial capacity will not be available due to degradation. It should be noted that the contribution of this paper is not a detailed model of battery or PV degradation, but it aims to obtain an accurate model to consider the degradations in a long-period operation.

A) Battery Capacity Degradation

The lifetime of battery is estimated based on the capacity degradation. Battery's CD affects the operation of the system in planning studies. The CD of BS depends on the number of charge/discharge cycles and their depth of discharge (DOD). Fig. 6-2b shows the procedure to calculate battery's CD and integrate it in the operation. The capacity of BS is updated at the end of each year based on the calculated degradation from the cycling of the last year. It should be noted that the CD can be calculated in shorter timeframes (e.g., monthly). However, the value of degradation will be rather small to be incorporated in the system design procedure. As the number of cycles in shorter timeframes are lower, smaller battery CD will obtain. The impact of smaller battery CD is insignificant and can be neglected for short timeframes.

After the annual operation of the GCH, the SOC of battery is extracted. Then, the annual DOD is obtained ($\mathrm{DOD} = 1 - \mathrm{SOC}$). Afterwards, the Rainflow Cycle Counting Algorithm (RCCA) is used to extract the number of cycles and associated DODs [3]. The RCCA is generally used to analyze the fatigue data. In this study, this method is conducted to obtain the irregular charging/discharging cycles that the battery experiences during the operation. The fundamentals of Rainflow Cycle Counting Algorithm to estimate the number of cycles and their DOD are deeply explained in [3]. The capacity degradation in each full cycle (φ) of a Li-ion battery is obtained by [4]:

$$\pi(\varphi) = \frac{20}{33000.\, e^{-0.06576.DoD(\varphi)} + 3277} \tag{6-11}$$

The Rainflow Cycle Counting Algorithm classifies the DOD cycles in twofold: full cycles and half cycles. It is assumed that for the half cycles, battery's CD is half of $\pi(\varphi)$. To disregard the adjacent local max/min points below a threshold (<1Wh), a filtering procedure is implemented on the SOC [5]. The total CD of each year can be calculated by (ϕ is total number of cycles of the year):

$$\pi_y = \sum_{\varphi=1}^{\phi} \pi(\varphi) \tag{6-12}$$

Once the annual CD of battery is obtained after each year of operation, the BS capacity is updated for the next year.

$$E_{\beta,y} = \left[\overbrace{\widetilde{E_\beta}}^{\substack{y=1 \\ E_{\beta,1}=}} , \overbrace{\left(1 - \frac{\pi_1}{100}\right) E_{\beta,1}}^{\substack{y=2 \\ E_{\beta,2}}} , \overbrace{\left(1 - \frac{\pi_2}{100}\right) E_{\beta,2}}^{\substack{y=3 \\ E_{\beta,3}=}} , \dots , \overbrace{\left(1 - \frac{\pi_9}{100}\right) E_{\beta,9}}^{\substack{y=10 \\ E_{\beta,10}=}} \right] \tag{6-13}$$

The total battery CD in 10-year operation is calculated by:

$$\pi_Y = \sum_{y=1}^{10} \pi_y \tag{6-14}$$

Battery should be replaced once the CD exceeds 20%.

B) Solar PV Degradation

The degradation of solar PV is highly associated with the discoloration of the PV panels. The degradation depends on weather conditions, and it varies in different locations with a range of 0.62%-1.45% per year [6]. In planning studies, it is a common practice to consider a constant value for the PV degradation [6], [7]. The output power of PV in the operation period by considering the degradation is as follows:

$$P_{\rho,y}(t) = \left[\overbrace{P_\rho(t)}^{\substack{y=1 \\ P_{\rho,1}=}}, \overbrace{\left(1-\frac{\sigma}{100}\right) P_\rho(t)}^{\substack{y=2 \\ P_{\rho,2}=}}, \overbrace{\left(1-\frac{\sigma}{100}\right)^2 P_\rho(t)}^{\substack{y=3 \\ P_{\rho,3}=}}, \dots, \overbrace{\left(1-\frac{\sigma}{100}\right)^9 P_\rho(t)}^{\substack{y=10 \\ P_{\rho,10}=}} \right] \tag{6-15}$$

Equation (6-15) shows the updated solar PV capacity after each year of operation. For example, in the second year of project, the solar PV capacity decreases to $\left(1-\frac{\sigma}{100}\right)$ of its initial capacity at the beginning of the operation. Please note that σ (%) is the annual degradation of solar PV. Since σ has a constant value during whole project lifespan, the capacity degradation of PV system will be $\left(1-\frac{\sigma}{100}\right)^9$ in the last year of operation.

6.3 Optimisation Framework

This section presents the problem formulation for optimal sizing of PV, WT and BS for the studied grid-connected household. This involves the objective functions, system constraints and the optimisation algorithm.

6.3.1 Objective Functions

Three important parameters: COE, GD and DE are considered as the objective functions.

A) Cost of Electricity

The first objective function is COE of the GCH. The COE is calculated based on the net present value (NPV), the capital recovery factors and the total load demand.

$$f_1 = \min_{(\theta_k)} COE \ (¢/\text{kWh}) = \frac{\mathbb{N}_k}{\mathbb{E}_h}.\psi_k + \frac{\mathbb{N}_g}{\mathbb{E}_h}.\psi_g \tag{6-16}$$

$$\mathbb{E}_h = \sum_{t=1}^{87,600} P_h(t).\Delta t \tag{6-17}$$

$$\psi_k = \frac{\gamma.(1+\gamma)^Y}{(1+\gamma)^Y - 1}, \quad \psi_g = \frac{\xi.(1+\xi)^Y}{(1+\xi)^Y - 1} \tag{6-18}$$

where ψ_k and ψ_g are the capital recovery factors of components and electricity, respectively. The electricity interest rate (ξ) is a function of interest and escalation rates.

$$\xi = \frac{\gamma - \varepsilon}{1 + \varepsilon} \tag{6-19}$$

NPV of each component in the system is calculated based on the capital, replacement, maintenance, and salvage values of the component at present.

$$\mathbb{N}_k = \sum_{k \in (\rho,\omega,\beta)} (\mathbb{C}_k^a + \mathbb{C}_k^e + \mathbb{C}_k^m - \mathbb{C}_k^s).\,\theta_k \tag{6-20}$$

The present values of replacement and maintenance costs are calculated by:

$$\mathbb{C}_k^m = \mathcal{M}_k.\frac{(1+\gamma)^Y - 1}{\gamma(1+\gamma)^Y} \tag{6-21}$$

$$\mathbb{C}_k^e = \mathcal{R}_k.\frac{1}{(1+\gamma)^{L_k}} \tag{6-22}$$

The PV and WT components have a constant lifetime. The battery lifetime, however, is obtained based on the operation of the system. Thus, the salvation values are calculated as:

$$\begin{aligned} &\text{For PV and WT: } \mathbb{C}_k^s = (\mathbb{C}_k^a - \mathbb{C}_k^e).\frac{Z_k}{L_k} \\ &\text{For battery: } \mathbb{C}_k^s = \mathbb{C}_k^a.\frac{Z_k}{L_\beta} \end{aligned} \tag{6-23}$$

The NPV of electricity trade with the main grid is calculated based on the total imported and exported electricity costs during the project lifespan.

$$\mathbb{N}_g = \sum_{y=1}^{Y} \sum_{t=1}^{8760} P_{\imath}(t).\,I_y(t).\,\Delta t - \sum_{y=1}^{Y} \sum_{t=1}^{8760} P_{\jmath}(t).\,\mathcal{J}_y(t).\,\Delta t \tag{6-24}$$

The import/export electricity rates are updated in each operation year based on the real interest rate.

$$\mathcal{I}_y(t) = \left[\overbrace{\frac{\mathcal{I}(t)}{1+\xi}}^{y=1}, \overbrace{\frac{\mathcal{I}(t)}{(1+\xi)^2}}^{y=2}, \overbrace{\frac{\mathcal{I}(t)}{(1+\xi)^3}}^{y=3}, \dots, \overbrace{\frac{\mathcal{I}(t)}{(1+\xi)^{10}}}^{y=10}\right] \tag{6-25}$$

$$\mathcal{J}_y(t) = \left[\overbrace{\frac{\mathcal{J}(t)}{1+\xi}}^{y=1}, \overbrace{\frac{\mathcal{J}(t)}{(1+\xi)^2}}^{y=2}, \overbrace{\frac{\mathcal{J}(t)}{(1+\xi)^3}}^{y=3}, \dots, \overbrace{\frac{\mathcal{J}(t)}{(1+\xi)^{10}}}^{y=10}\right] \tag{6-26}$$

B) Grid-Dependency

The second objective function indicates the dependency of the GCH on the main grid. Grid dependency is calculated based on the total imported electricity from the main grid over the total electricity demand of the household.

$$f_2 = \min_{(\theta_k)} GD\ (\%) = \frac{\mathbb{E}_{\imath}}{\mathbb{E}_h} \times 100 \tag{6-27}$$

Grid dependency concept can show the energy autonomy of the consumer. Lower percentages of GD show higher energy autonomy of the grid-connected households which means higher home energy supply through the PV-WT-BES system.

C) Total Curtailed Energy

The third objective function is the total curtailed energy of the GCH over the 10-year project lifespan. The TCE of the household is calculated based on the total RE generation plus imported energy from the grid and discharging energy of BS, minus the total load demand, exported energy and battery charging energy during the project lifespan.

$$f_3 = \min_{(\theta_k)} TCE\ (\text{MWh}) = \mathbb{E}_{re} + \mathbb{E}_{\imath} + \mathbb{E}_{\beta}^{di} - \mathbb{E}_h - \mathbb{E}_{\jmath} - \mathbb{E}_{\beta}^{ch} \tag{6-28}$$

1. System Constraints

The following system constraints are considered in the optimisation model.

$$0 \le \theta_k \le \theta_k^{max} \tag{6-29}$$

$$P_{re}(t) + P_{\imath}(t) + P_{\beta}^{di}(t) = P_h(t) + P_d(t) + P_{\jmath}(t) + P_{\beta}^{ch}(t) \tag{6-30}$$

$$S^{min} \leq S(t) \leq S^{max} \tag{6-31}$$

$$0 \leq P_{j}(t) \leq P_{j}^{max} \tag{6-32}$$

The constraint on the number of the components (PV, WT and BS) is indicated in equation (6-29). Equation (6-30) represents that the power balance between generation and consumption sides should be maintained at any time. Equation (6-31) represents that the SOC of BS should vary in a specified range. The main grid constraint to limit the export power from the GCH is indicated in equation (6-32).

6.3.2 Optimisation Algorithm

The multi-objective optimisation approaches are broadly categorised as evolutionary (metaheuristic) methods and mathematical optimisation [8]. Simultaneous deal with a set of possible optimal solutions (namely the population) is the main advantage of the multi-objective evolutionary methods (MOEMs). Hence, the MOEMs can attain several solutions of the Pareto-optimal front in each single run. However, a series of separate runs are mandatory in mathematical optimisation to achieve a set of optimal solutions. Moreover, the MOEMs take advantage of lower sensitivity to the continuity or shape of the Pareto-optimal front. Therefore, discontinuity and concavity of Pareto-optimal fronts are not concerns for MOEMs and can be easily handled. Furthermore, the MOEMs take benefits of easy implementation, ability to run in parallel processing environments, independency against the specific knowledge and complexity of the problem [8].

Based on the abovementioned advantages, one of the well-recognized multi-objective evolutionary methods, non-dominated sorting genetic algorithm II (NSGA-II), is selected for the multi-objective optimisation problem in this study. The NSGA-II has high convergence rate, less complexity in computational aspect, and diversity preservation mechanism in comparison with other MOEMs.

The optimisation algorithm for optimal sizing of components is demonstrated in Fig. 6-3. The load profile, weather data and electricity rates in 10 years as well as the PV, WT and BS data are used as the input data. NSGA-II is used for optimal sizing of PV, WT and BS with the discussed triple objective functions. The core of NSGA-II is genetic algorithm by adding two new concepts: (1) non-dominated sorting and (2) crowding distance, in order to achieve desirable multi-objective solution [9]. The NSGA-II initializes the optimisation by setting initial population for the capacity of components. Then, the energy management of the GCH is evaluated over a long-period operation. By the long-period operation, the length of the operation period in the project lifetime is clarified, not the time resolution. In this study, the input data has been hourly arranged which results in 87,600-time intervals for the operation for 10 years. Once the 10-year operation is ended and the constraints are satisfied, the selection, crossover and mutation are implemented. Children and parent populations are then combined, and the Preto-optimal solutions are identified and stored.

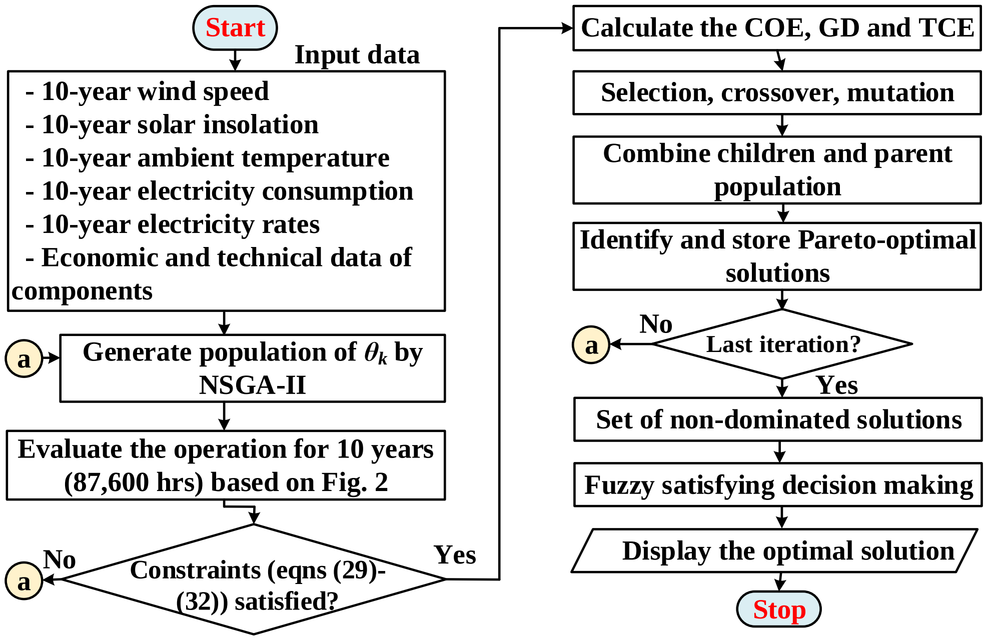

Figure 6-3. Optimisation algorithm for multi-objective optimal sizing of PV, WT, and BS in the grid-connected household.

The main parameters of NSGA-II are the initial population, iteration, crossover rate and mutation rate. Table 6-1 lists the NSGA-II parameters used in the optimisation model of this study. These parameters are taken from [10].

Table 6-1. Parameters of the non-dominated sorting genetic algorithm II.

Population	Iteration	Crossover rate	Mutation rate
200	200	0.9	0.01

When the set of non-dominated solutions is obtained, the fuzzy satisfying decision making is used to achieve a final solution based on the user-defined conditions. In the fuzzy decision-making strategy, each objective function (f_i) in solution x of Pareto-optimal front is assigned to a membership function ($\mathcal{U}_{f_i}$)

indicating the satisfaction level as follows:

$$\mathcal{U}_{f_i}(x) = \begin{cases} 0 & f_i(x) > f_i^{max} \\ \dfrac{f_i^{max} - f_i(x)}{f_i^{max} - f_i^{min}} & f_i^{min} \le f_i(x) \le f_i^{max} \\ 1 & f_i(x) < f_i^{min} \end{cases} \tag{6-33}$$

Based on equation (6-33), the decision maker is fully satisfied when $\mathcal{U}_{f_i}(x) = 1$ and not satisfied when $\mathcal{U}_{f_i}(x) = 0$. Once the membership functions are defined, the decision maker is asked to assign weighting factors $\mathcal{w}_{f_i}$ to each objective function. The following decision-making function (DCM) is then used to achieve the final solutions:

$$DCM = \min_{x \in X} \sum_{i=1}^{3} \mathcal{w}_{f_i} . \mathcal{U}_{f_i}(x) \tag{6-34}$$

In this study, DCM function is minimised using GA optimisation toolbox in MATLAB [11].

6.4 Case Study

The developed optimisation framework is applied to a typical GCH in South Australia (SA). In Australia, the householders possess the houses for a period of about 10-11 years [12] - [13]. Hence, a 10-year project lifetime has been chosen for the planning horizon in this study.

6.4.1 Load Consumption and Electricity Rates

The annual load consumption (P_h) of a typical household in SA is used. To generate the load demand for different years ($P_{h,y}$) during the project lifespan, a random number is added to the annual load as follows:

$$P_{h,y}(t) = P_h(t) + P_h(t).\mathfrak{I}.\mathcal{r}(t) \tag{6-35}$$

where $\mathfrak{I}$ and $\mathcal{r}(t)$ represent a deviation factor and a random number generator function, respectively. It is considered that the value of $\mathfrak{I}$ changes between 10% and 50% for different years, and the $\mathcal{r}(t)$ function generates random numbers between -1 and +1. Fig. 6-4a demonstrates the hourly-arranged 10-year electricity consumption of the household.

It is assumed that the GCH uses a time-of-use (ToU) pricing program for the retail price (RP) (import electricity rate) and feed-in-tariff (FiT) price (export electricity rate). Table III lists the ToU prices with different electricity rates in the off-peak, shoulder and peak times of the weekdays, as well as off-peak and shoulder prices of the weekends. The RP and FiT in Table 6-2 are assumed as the base rates for the first year of project. These values are then updated based on interest and escalation rates for 10 consecutive years.

The interest/discount and escalation/de-escalation rates are considered as 8% and 2%, respectively. It is notable that all the prices are in Australian dollar. Based on the South Australian power network policy, a maximum of 5 kW export power from REs to the grid is allowed for single-phase GCHs, and the same constraint is used in this study.

Table 6-2. Weekly 24–hour ToU electricity rates of South Australia.

		Time (24–hour)	**RP (¢/kWh)**	**FiT (¢/kWh)**
Weekdays	**Off-peak**	22 – 7	25.41	5.00
	Shoulder	7 – 15	39.93	10.00
	Peak	15 – 22	49.00	18.00
Weekends	**Off-peak**	22 – 7	25.41	5.00
	Shoulder	7 – 22	39.93	10.00

6.4.2 Weather Data

The actual hourly data of ambient temperature, solar insolation, and wind speed in an urban area of SA over a period of 10 years are used. Figs. 6-4b-4d illustrate the hourly-arranged stochastic behavior of wind speed, solar insolation, and ambient temperature of realistic data for the location of the case study for 10 years.

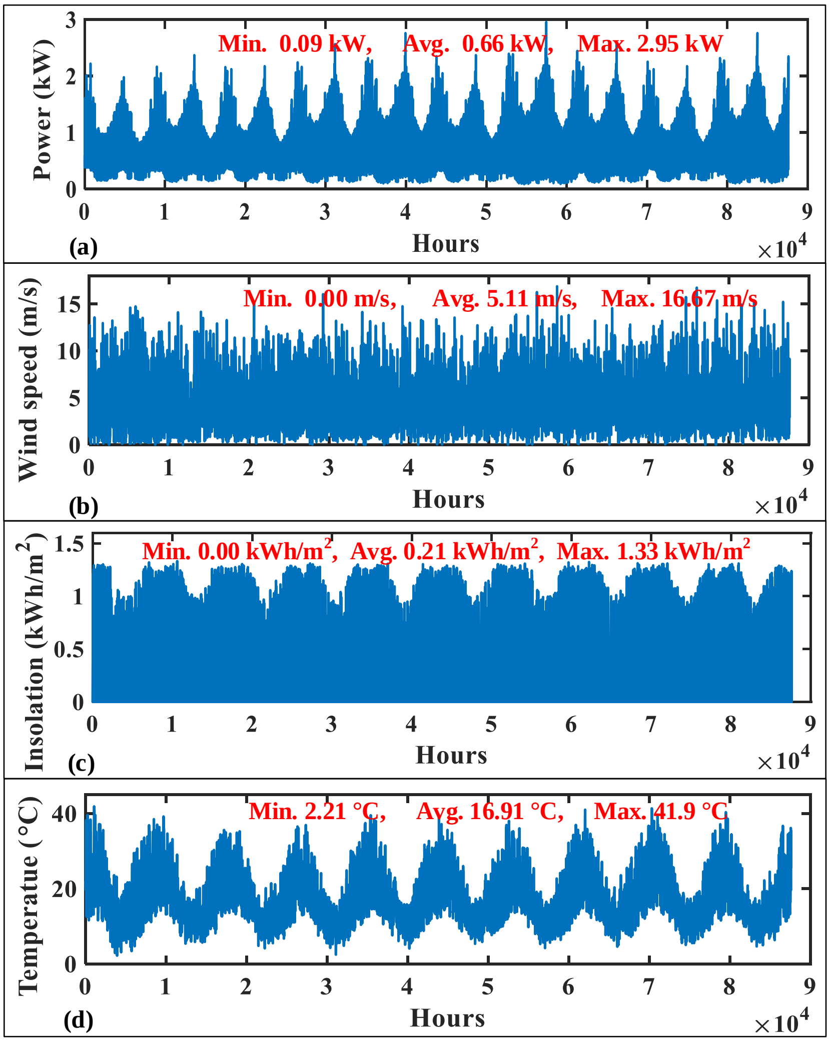

Figure 6-4. Hourly-arranged 10-year real input data: (a) Electricity consumption, (b) Wind speed, (c) Solar insolation, and (d) Ambient temperature.

6.4.3 Components Data

Table 6-3 lists the costs and lifetimes associated with each component in the system. The minimum and maximum values of battery's SOC are considered as 20% and 95%. The BS charging/discharging efficiency is 95%. The maximum capacity of PV, WT and BS are considered as 10-kW, 10-kW, and 50-kWh, respectively. The annual degradation of solar PV is considered as 0.95%.

Table 6-3. Costs and Lifetimes of Wind Turbine, Solar PV and Battery.

PV	Unit size= 0.1 kW PV lifetime = 25 years Inverter lifetime = 10 years	Capital cost = $150 Inverter replacement cost = $30 Maintenance cost= $3/year
WT	Unit size= 1 kW WT lifetime = 20 years Inverter lifetime = 10 years	Capital cost = $3,000 Inverter replacement cost = $300 Maintenance cost= $50/year
BS	Unit size= 0.4 kW/ 1 kWh Maintenance cost= $50/year	Capital cost = $600 Replacement cost = $400

6.5 Results and Discussions

This section presents the set of non-dominated solutions in Pareto-optimal front, effects of salvation value, NSGA-II parameters and adding electric vehicle on the optimal results, decision making for the system, and the comparison of long- and short-period data for optimal sizing.

6.5.1 Multi-objective Optimisation Results

Fig. 6-5 shows the set of non-dominated solutions in Pareto-optimal front for the trade-offs between objective functions in MO optimisation framework. It is evident that the GD of the GCH decreases with the increase in COE. This is reasonable as for lower GD percentages, capacity of battery is increased to compensate the role of the grid in load supply. There exists a high COE difference between the GCHs with low GD percentages (lower than 0.5%). For example, the COE difference between GCHs with a GD of 0.5% (Point A) and a GD of 0.01% (Point B) is more than 50 ¢/kWh. When the COE varies between 20 ¢/kWh and 40 ¢/kWh, DE is less than 20 MWh. However, for the COEs higher than 40 ¢/kWh, as the COE increases, the TCE grows significantly.

The highest TCE (around 100 MWh) is achieved for the most expensive system with the minimum GD (Point C). There is almost no TCE for a GCH with the highest GD percentage and low COE value (Point D).

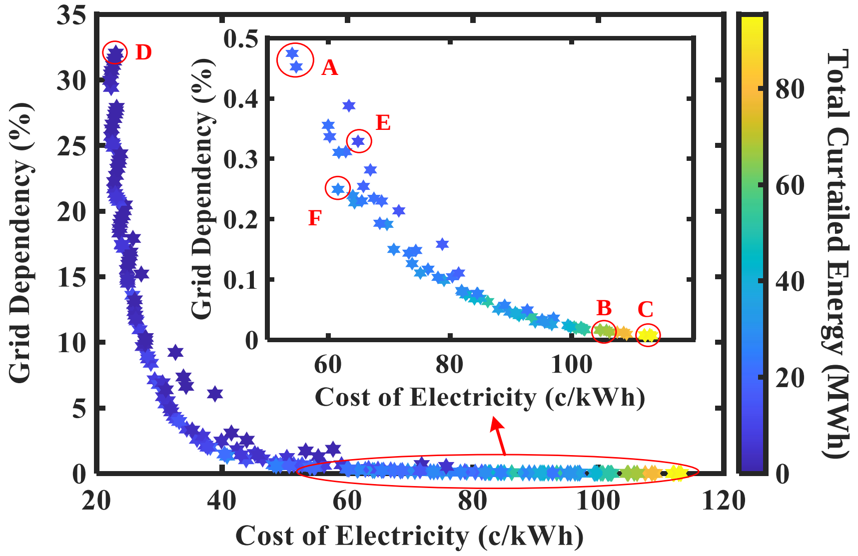

Figure 6-5. Set of non-dominated solutions in Pareto-front for optimal sizing.

The proposed optimisation model in this study solves the problem with three conflicting objective functions (COE, GD and TCE). Therefore, all objective functions are effective in optimal solutions, and it is common to obtain a non-monotonous Pareto-optimal front for such a problem. Please note that the solutions which appear dominated in the GD-COE graph, are indeed nondominated when the third objective (TCE), in the color bar, is considered. This can be explained by points E and F in Fig. 6-5. Since Point E has higher COE compared to Point F, it is expected to obtain lower GD for Point E. However, the GD of Point E is about 0.1% greater than Point F. This can be described by comparing the associated TCE of Points E and F. As illustrated in Fig. 6-5, the curtailed energy of Point F is higher than Point E. Hence, although Point E has greater GD, it has lower curtailed energy compared to Point F.

Fig. 6-6 indicates the impacts of the objective functions on the optimal battery capacity (colour bars) and total CD (dashed lines) in 10 years. Fig. 6-6a shows that the optimal battery capacity increases with the increase in COE. For the COEs between 20 ¢/kWh and 40 ¢/kWh (Interval A), BS capacity is smaller than 15 kWh. On the other hand, Interval B shows that the highest BS capacity (50 kWh) occurs at the highest COEs (higher than 90 ¢/kWh) and lowest GDs (lower than 5%). It is evident that as the GD decreases from 30% to 10%, the capacity degradation of battery increases. Fig. 6-6b shows the optimal BS capacity and its total CD versus the COE and TCE. It is evident that the total CD increases with the decrease in TCE from 100 MWh to 20 MWh. For example, the total battery CD in Point A (where the DE is 80 MWh and COE is 100 ¢/kWh) is 3% lower than the total CD in Point B (where the TCE is 20 MWh and COE is 45 ¢/kWh). Fig. 6-6c exhibits the impacts of GD and TCE on the optimal battery capacity and total CD. It is evident that the highest battery capacities are obtained when the GD has a low value and TCE has a high value. For example, the BS capacity is about 40 kWh in Point C where the GD is 2% and TCE is 80 MWh. However, lower BS capacities are obtained for the low percentages of GD and low values of TCE. Point D shows a 15 kWh of BS for the GD of 2% and TCE of 20 MWh.

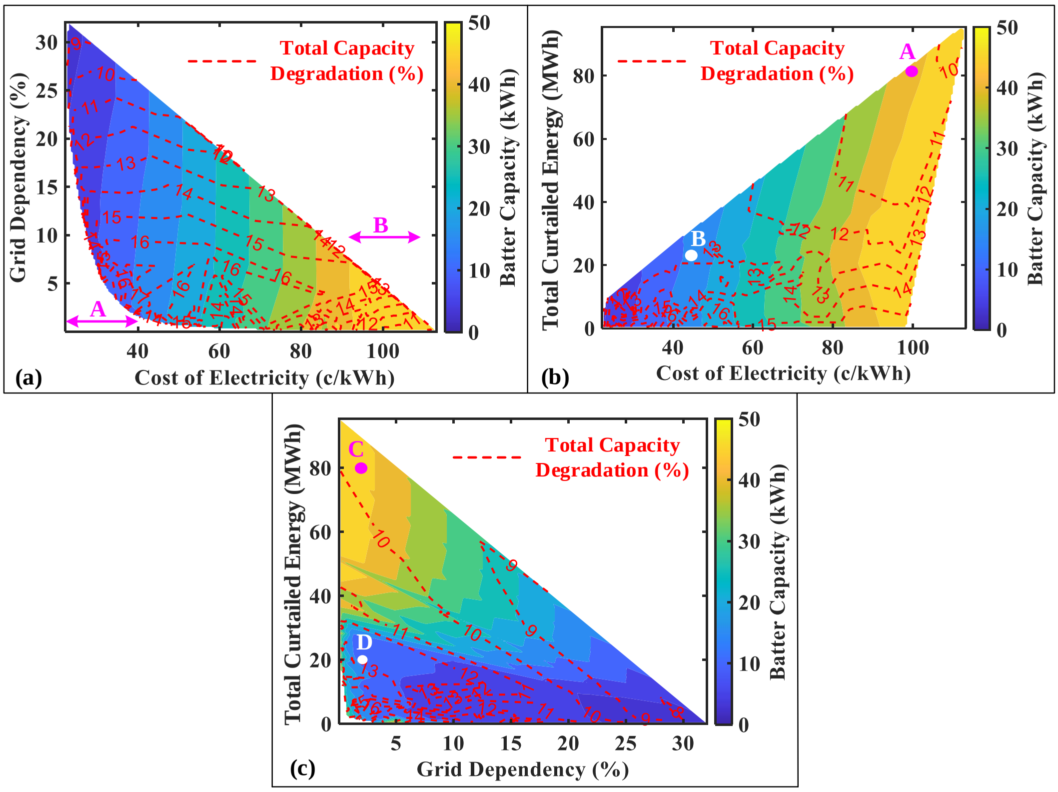

Figure 6-6. Optimal results of battery capacity and total CD versus the objective functions. (a) COE-GD-Battery, (b) COE-TCE -Battery, and (c) GD-TCE -Battery.

Fig. 6-7 indicates the optimal WT capacity (colour bars) and PV capacity against the objective functions. It is evident that larger capacities of REs (PV and WT) are obtained for higher values of TCE and COE, and lower percentages of GD in the GCH. Fig. 6-7a shows that the variation range of PV's optimal capacity is in between 6 kW and 2 kW when the COE decreases from 60 ¢/kWh to 28 ¢/kWh (Interval A). However, in this interval, the optimal capacity of WT does not exceed 2 kW. This means that a higher capacity of PV is preferable than higher capacity of WT in cost reduction. Fig. 6-7b illustrates that when the optimal capacities of PV and WT exceed 8 kW (Interval B), 10-year TCE value is about 100 MWh. Fig. 6-7c demonstrates that 10 kW PV and 10 kW WT are needed to achieve the minimum GD (Point C).

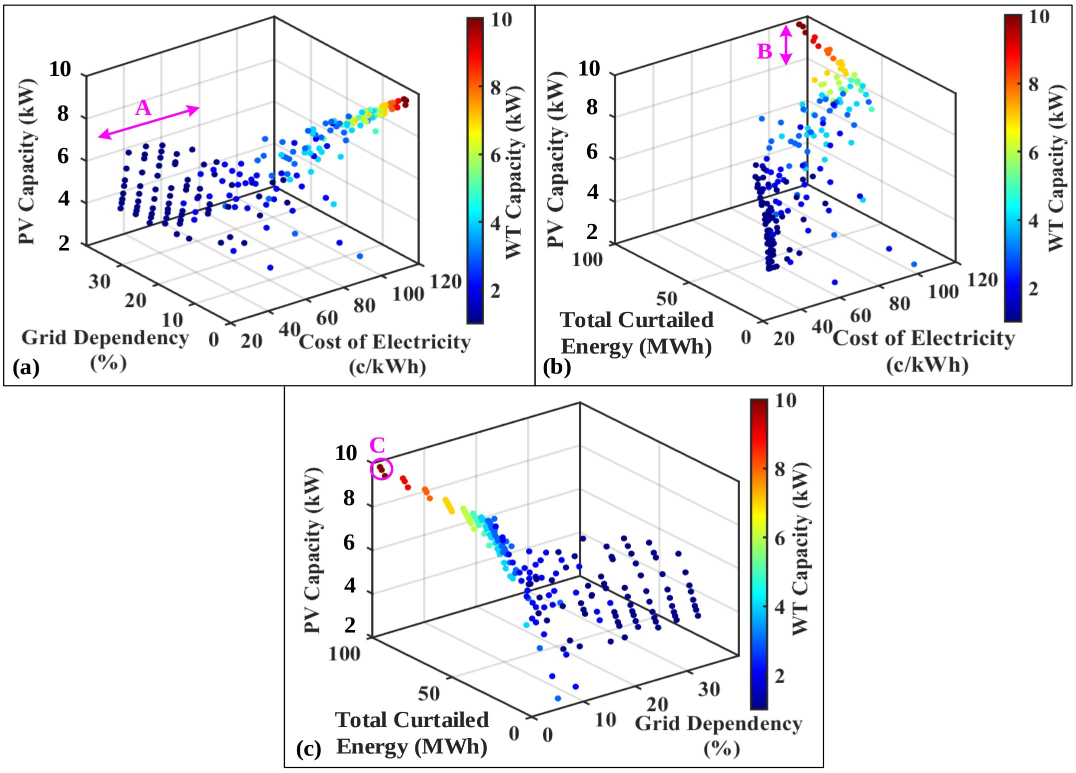

Figure 6-7. Optimal results of PV and WT capacities versus objective functions. (a) COE-GD-RE, (b) GD-TCE-RE, and (c) COE-TCE-RE.

6.5.2 Analysis of GD Variations Between 10% and 30%

Fig. 6-5 shows that the lowest COE (22 ¢/kWh) is achieved when the GD is about 30%. However, when the GD reduces from 30% to 10%, the COE increment rate is less than 6 ¢/kWh. A detailed analysis is provided for this critical GD interval (30% to 10%). Fig. 6-8 shows the capital expenditure (Capex), operation expenditure (Opex), COE, and average of optimal capacities of BS, PV and WT for the critical GD interval. Lowering GD in the critical interval increases the capacity of the components which increases the Capex; however, Opex value (with a negative sign) decreases significantly. This means that higher investments (Capex) for components make reasonable profits in this critical GD interval. For example, the customer pays a high Capex of k$19.8 (for 8 kWh BS, 6 kW PV and 2 kW WT) to achieve a GD of 10% and a COE of 28 ¢/kWh. However, a total Opex of k$ -9.7 (this is the profit of the system) returns about half of Capex during the project lifespan. Hence, it is rational for the customers to pay more for the components to achieve lower GDs in the studied critical interval.

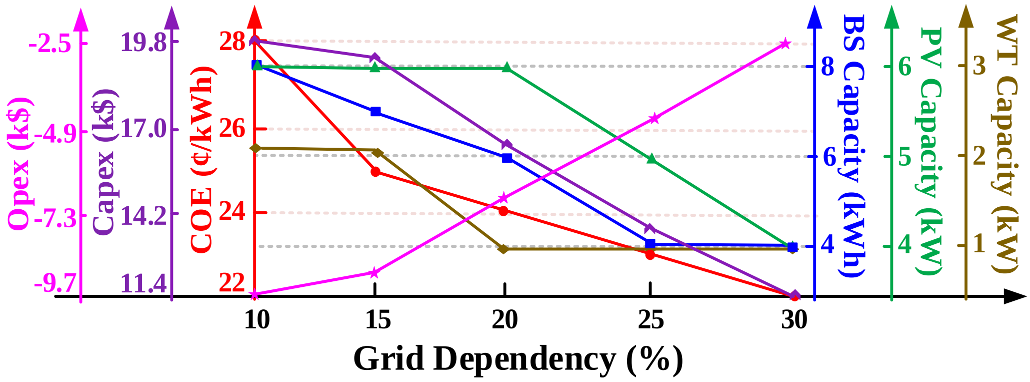

Figure 6-8. Effects of GD variations between 10% and 30% on optimal capacities, Capex, Opex and COE.

6.5.3 *Effect of Salvation Value*

To investigate the effect of salvation cost on the results of the optimisation model, the non-dominated solutions in Pareto-front of the systems with/without considering salvation cost are demonstrated in Fig. 6-9. As it can be inferred from the figure, neglecting the salvation cost efficiently increases the cost of electricity and grid dependency in the Pareto-optimal front. It is observed in Zone 1, when the salvation cost is neglected, the minimum COE is 9 ¢/kWh greater than the minimum COE of the optimal system with salvation cost. In Zone 2, by ignoring the salvation cost, the maximum COE increases to around 200 ¢/kWh, while the maximum value of COE is just 115 ¢/kWh when the salvation cost is considered. Therefore, it is inferred that neglecting the salvation cost result in incorrect Pareto-optimal front.

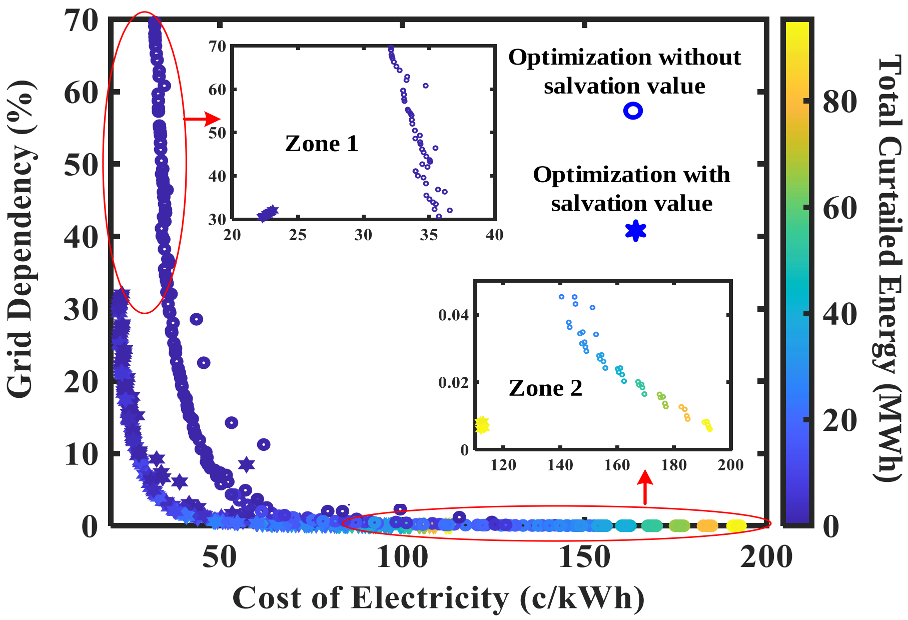

Figure 6-9. Set of non-dominated solutions in Pareto-front for the systems with/without considering

salvation cost.

6.5.4 Adding Electric Vehicle to Load Profile

The effect of adding electric vehicle (EV) to the load profile after certain number of years is investigated. For this purpose, Renault Zoe is considered as the studied EV which has a 22-kWh battery with a 3-kW charging/discharging power limit (single-phase). Uncertainties of departure time, arrival time and initial state of charge (at arrival) of the EV are produced using a stochastic model for 10 years. Table 6-4 lists the parameters of the uncertainties produced by truncated Gaussian distribution.

Table 6-4. Probability Parameters to Produce EV's Uncertainties.

	Mean	**S.D.**	**Min.**	**Max.**
Initial SOC at arrival (%)	50	30	20	85
Arrival time (hr)	18	3	15	21
Departure time (hr)	8	3	5	10

It is assumed that the EV can be added to the load profile in different years of the operation. For example, a householder may purchase an EV from the beginning of the project and another householder may purchase in the ninth year of the project. Hence, a proper analysis and guideline is necessary to obtain the Pareto-optimal fronts in the presence of EV. For each year of adding EV, the optimisation model is run separately. Fig. 6-10 demonstrates the effect of adding EV (in different years of the operation) to the load profile on the Pareto-optimal front. If the EV is added to the load profile in the final year of the operation (Year 10), the GD cannot be lower than 8% in the Pareto-optimal front. This means that by adding the EV to the load profile, the electricity demand of the household will increase, and the renewable-storage system thereupon cannot support a high level of load. It can be seen that by decreasing the year of adding EV to the load profile, the level of GD of the household increases. For example, when the EV is added in the first year (Year 1), GD cannot reach less than 40%. For the Year 9, however, the minimum GD reaches to around 11%. Adding of EV also affects the maximum GD of the Pareto-optimal front. When the household is without EV, the maximum GD is around 33%. Adding of EV in the Year 10, however, increases the maximum GD to 40%. In addition, adding of EV in the Year 1 increases the maximum GD to around 65%.

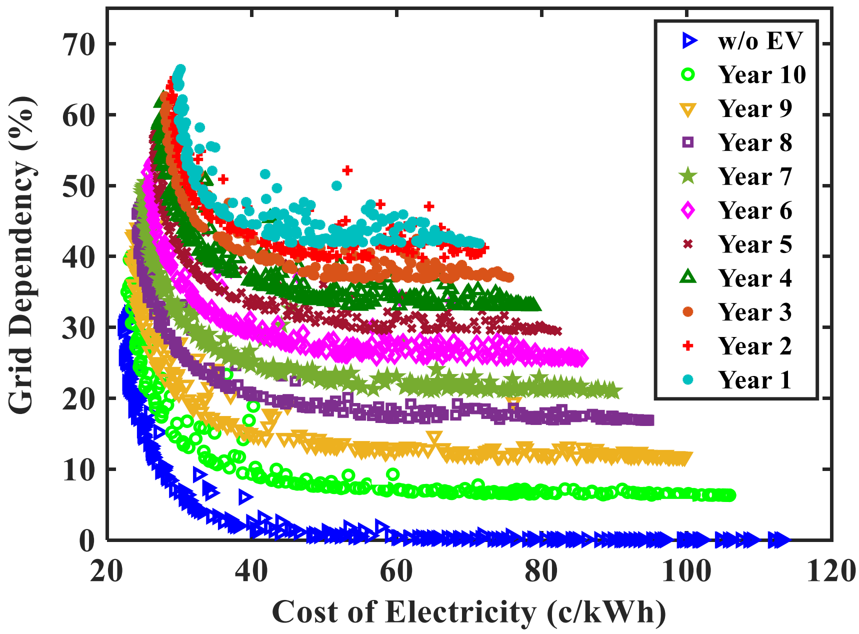

Figure 6-10. Effect of adding EV (in different years of the operation) to the load profile on the Pareto-optimal front.

6.5.5 Sensitivity Analysis of NSGA-II Parameters

A sensitivity analysis is provided to assess the effects of NSGA-II parameters on the optimal results. Fig. 6-11 illustrates the effects of iteration, population as well as crossover and mutation rates on the range of the objective functions in the Pareto-optimal fronts. The boxplots indicate that almost the same results are obtained for 150 and 200 iterations. For lower number of iterations (less than 150), the range of the variations and the average of the objective functions are higher. Since all objective functions should be minimised by the NSGA-II, less than 150 iterations will not achieve optimal results for the capacity optimisation problem in this study. The number of populations shows the number of the solutions in each iteration. It is indicated that by decreasing the number of the population lower ranges of the solutions for the objective functions are obtained. Hence, the boxplots are smaller, and an accurate analysis cannot be achieved. The sensitivity of crossover and mutation rates shows that the results will slightly change when the crossover rate is the lowest (0.5) and mutation rate is the highest (0.1). For the other rates, almost the same results are obtained.

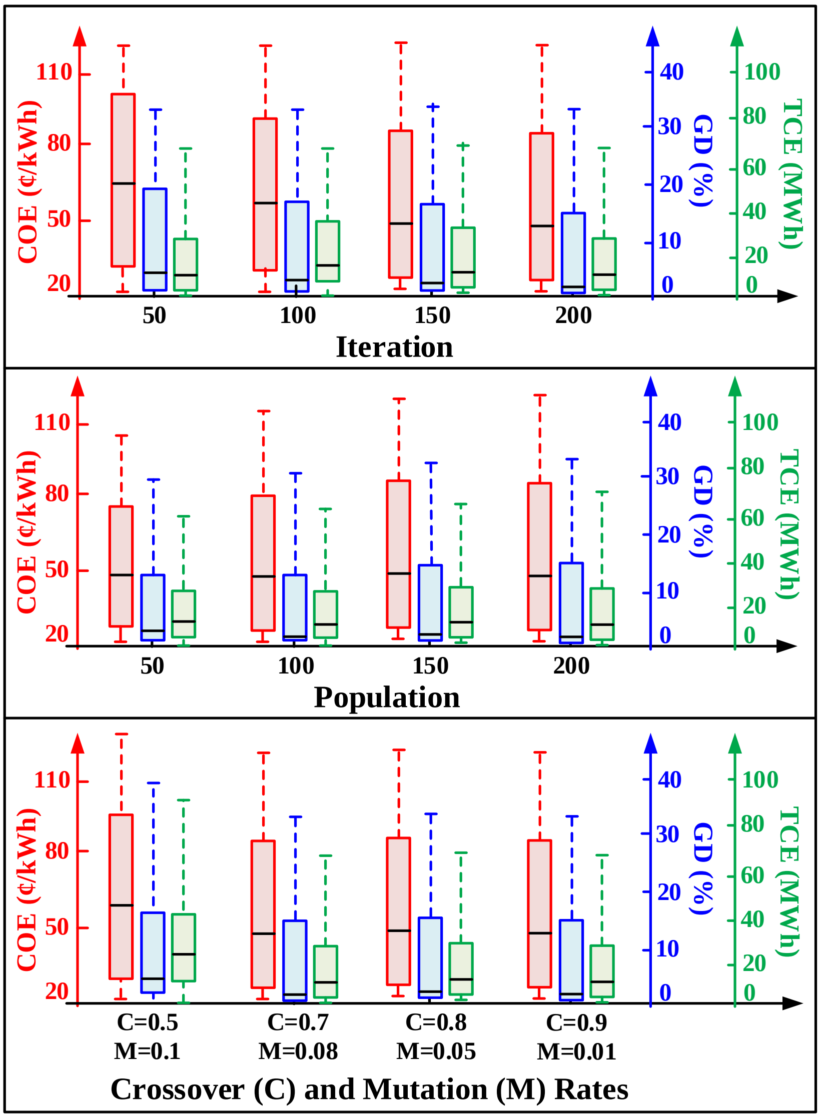

Figure 6-11. Sensitivity of the optimal results against the NSGA-II parameters: Iteration, Population, and Rates of Crossover and Mutation.

6.5.6 Decision Making

Four design scenarios based on the user-defined conditions are selected:

- Scenario-1: similar satisfaction level for all objective functions.
- Scenario-2: higher satisfaction level for COE.
- Scenario-3: higher satisfaction level for GD.
- Scenario-4: higher satisfaction level for DE.

Table 6-5 shows the weighting factors for each objective function in the design scenarios to achieve the final solutions. Table 6-6 lists the values of the objective functions and the capacity of components in each design scenario. For Scenario-1, capacities of PV, WT and BS are 6.6 kW, 2 kW and 11 kWh, respectively. For Scenario-2, as a higher weighting factor is assigned to the cost, the

COE value is the minimum compared to the other scenarios, however, the GD percentage is high. The capacity of BS decreases which shows that higher capacity of battery is not economic. For Scenario-3, the GD has the lowest value among the scenarios while the COE and BS capacity of GCH increase significantly. Indeed, 19 kWh BS alongside 3kW WT and 6.5 kW solar PV result in a GD of 1.6% with a COE of 46.73 ¢/kWh. The minimum TCE (0.31 MWh) is obtained for Scenario-4 where the WT capacity is only 1 kW.

Table 6-5. Four Design Scenarios based on Weighting Factors.

Design Scenarios		**1**	**2**	**3**	**4**
Weighting factors	w_{f_1}	0.8	0.8	0.3	0.3
	w_{f_2}	0.8	0.3	0.8	0.3
	w_{f_3}	0.8	0.3	0.3	0.8

Table 6-6. Optimal Results of GCH for the Studied Four Design Scenarios.

Design Scenarios	**Objective values**			**Component's capacity**		
	COE (¢/kWh)	**GD (%)**	**TCE (MWh)**	**PV (kW)**	**WT (kW)**	**BS (kWh)**
1	31.76	5.01	2.66	6.6	2	11
2	27.29	10.69	0.62	5.6	2	8
3	46.73	1.60	4.28	6.5	3	19
4	31.16	9.36	0.31	6.1	1	12

Fig. 6-12 demonstrates the annual battery CDs and number of charge/discharge cycles over the project lifespan for each design scenario. The battery CD varies for the design scenarios in each year of operation based on the collected SOC of that year. Scenario-2 has the lowest number of cycles (less than 1.33×10^4 in each year) and hence the lowest annual CDs compared to other scenarios. On the other hand, Scenario-4 has the highest number of cycles in each year ($>1.65\times10^4$) and hence the highest annual CDs. Thus, the higher number of cycles results in higher battery CD of design scenarios.

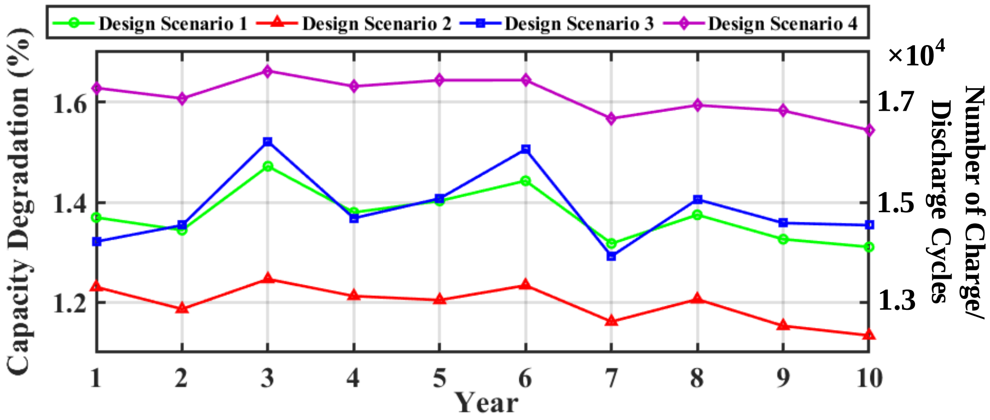

Figure 6-12. Battery CD and number of charge/discharge cycles in each year of operation for the studied four design scenarios.

The curtailed power of design scenario 3 (with the highest battery capacity) in Table 6-6 is investigated. Fig. 6-13 shows the curtailed power in 10 years for design scenario 3. The curtailed power is obtained for 626 hours in 10 years. The average value of curtailed power is 0.05 kW with a maximum value of 3.45 kW. As illustrated in the figure, the amount of curtailed power is different for each year of operation during the 10 years of the project lifespan.

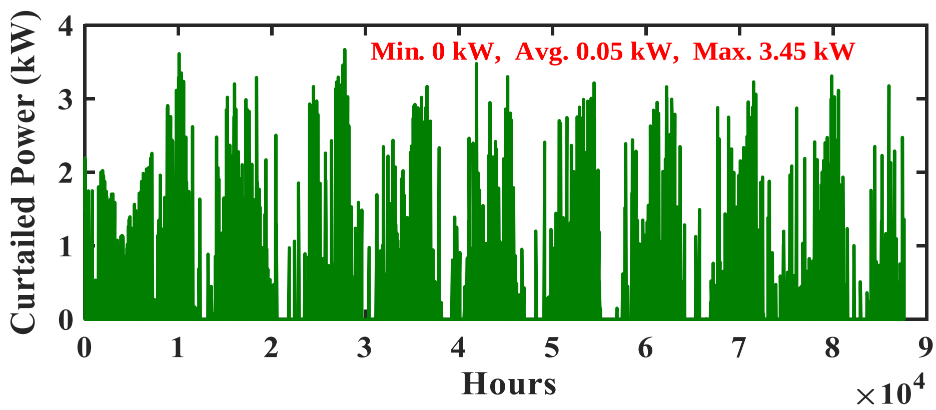

Figure 6-13. Curtailed power for 10 years operation in design scenario 3.

6.5.7 *Comparison of Long- and Short- Period Operations*

The described optimisation model is applied to the same GCH by considering one-year operation against the 10 years operation. It is notable that the weather data and load consumption of year 1 in Fig. 6-4 are used for the short-period operation optimisation. In the short-period operation, the operation period of the system is only one tenth of the project lifespan. The short-period operation has only considered the stochastic behavior of weather and load data for one year of the available ten years. In addition, the battery degradation cannot be considered since the system is only operated for one year. Furthermore, the same system operation, as year one, is considered for project lifespan. Moreover, the initial SOC of battery at the beginning of the operation is constant for all years during project lifespan. The deficiencies in short-period operation are fully addressed when the system is operated for a long-period. In long-period operation, the project lifespan and operation period are the same. So that the 10-year stochastic behavior of weather and load is fully conducted for the system operation. The battery and solar PV degradations are applied, and their capacities are updated after each year of operation. The initial SOC of battery is updated at the beginning of each year based on the operation of the last year. It can be seen that the long-period operation is robust against the variations of load consumption and renewable generation of the past 10 years.

The optimisation results of long- and short- period operations are compared. Three cases are investigated:

- Case-1: short-period operation (one year) without CD
- Case-2: long-period operation (10 years) without CD
- Case-3: long-period operation (10 years) with CD

It is notable that in the short-period operation, CD of battery, which should be calculated after annual operation, is not applicable. The non-dominated solutions of the trade-off between COE and GD in all three cases are shown in Fig. 6-14. As illustrated in Zone 1, a fully grid independent ($\mathrm{GD} = 0$) GCH is not achievable in Case-3, and the minimum GD in this case is around 0.05% (Point A). However, a fully grid independent GCH is achieved in Case-1 (Point B) and Case-2 (Point C). Zone 2 demonstrates that Case-1 and Case-2 result in lower values for the minimum COE (Points D and E) compared to Case-3 (Point F). The main reason for lower COEs and GDs in Case-1 and Case-2 is the neglecting of battery’s CD in the operation of the GCH. The BS operates within its full capacity during the project lifespan; thus, the BS has higher capacity to supply the load in Case-1 and Case-2.

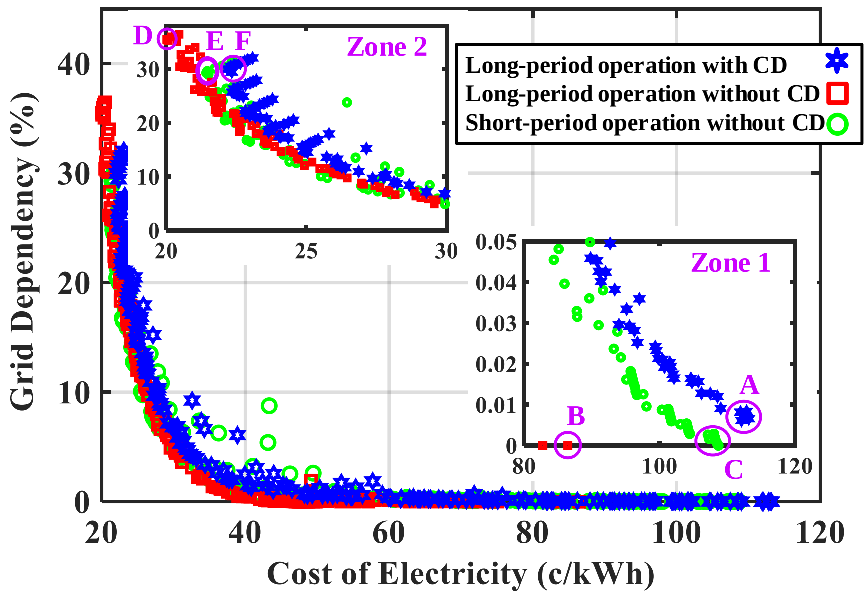

Figure 6-14. Non-dominated solutions for the trade-off between COE and GD based on long- and short- period operations.

For the sake of robustness analysis, operation of the obtained fully grid independent GCH in Case-1 (Point B in Fig. 6-10) is investigated for the other 9 years separately to check the robustness of the designed GCH against the variations of renewable generation and load consumption. The results show that the system is only reliable for an uninterruptible supply in 3 years of the provided data. For the other 6 years, the system is not reliable since it cannot supply the loads uninterruptedly. Hence, the optimal sizing of components based on short-period operation is not robust. This is while the long-period operation considers all 10 years and achieves robust capacities of components against the variations in load and renewable generation. It is notable that considering one scenario (one-year variations of load and renewable) with the extreme condition (low generation of RE resources and high electricity consumption) may result in a robust operation sometime. However, selecting the extreme scenario is not an easy procedure since there are wind speed, solar insolation, ambient temperature, and load consumption uncertainties in the system. For example, the extreme data of wind speed may not satisfy the extreme data of solar PV and load.

6.6 Conclusion

This chapter developed a multi-objective optimisation framework for sizing of solar photovoltaic (PV), wind turbine (WT) and battery storage (BS) in a grid-connected household (GCH). A long-period operation was examined by updating the PV and BS capacities at the end of each year based on the degradation in the last year. The electricity rates were updated in each year based on interest and escalation rates. Three objective functions were selected: (1) cost of electricity (COE), (2) grid dependency (GD), and (3) total curtailed energy (TCE). A fuzzy satisfying decision making was adopted to achieve the final solutions (capacity of PV, WT and BS) based on the user-defined conditions. The optimisation scheme was examined for a GCH in South Australia based on 10 years actual weather data and load profiles, as well as the technical/ economic data of components and grid in Australian concept.

Lower percentages of GD increase the values of COE and TCE in the GCH. A residential GCH with the minimum GD (0.008%) resulted in a COE of 116 ¢/kWh and a TCE of 100 MWh in 10 years. Based on the decision-making procedure, the most recommended system to decrease all objective functions for the customers, resulted in 6.6 kW, 2 kW and 11 kWh as the optimal capacities for PV, WT and BS, respectively. It was found that the optimal sizing based on short-period (one year) operation is neither accurate (due to neglecting the capacity degradation of BS) nor robust (due to variations of renewable generation and load consumption in each year).

Nomenclature

A. Sets	
k	Type of component: $k \in \{\mathrm{PV}, \mathrm{WT}, \mathrm{BS}\}$
X	Set of non-dominated solutions
B. Superscripts	
ch	Charging
di	Discharging
in	Input
max	Maximum
min	Minimum
ou	Output
C. Parameters	
$\mathbb{C}_k^a$	Capital cost of components ($)
$\mathbb{C}_k^e$	Replacement present value of components ($)
$\mathbb{C}_k^m$	Maintenance present value of components ($)
$\mathbb{C}_k^s$	Salvation value of components ($)
L_k	Component’s lifetime (year)
$\mathcal{M}_k$	Component’s maintenance cost ($)
$\mathcal{R}_k$	Component’s replacement cost ($)
T	Total hours of a year (hr)
y	Year
Y	Project lifespan (year)
ξ	Electricity interest/discount rate (%)
ψ_k	Capital recovery factor of components
ψ_g	Capital recovery factor of electricity

ε	Escalation/ de-escalation rate (%)
Δt	Time interval (hr)
η_{β}	Efficiency of battery (%)
σ	Solar PV degradation (%)
γ	Interest/discount rate (%)
D. Variables	
$E_{\beta,y}$	Battery's capacity at year *y* (kWh)
$\mathbb{E}_{\beta}^{ch}, \mathbb{E}_{\beta}^{di}$	Total charge/ discharge energy of BS (MWh)
$\mathbb{E}_{h}$	Total electricity demand of household (MWh)
$\mathbb{E}_{i}, \mathbb{E}_{j}$	Total imported/ exported energy from/to grid (MWh)
$\mathbb{E}_{re}$	Total electricity generation by REs (MWh)
$I_{y}, \mathcal{J}_{y}$	Import/export electricity rates at year *y* (¢/kWh)
L_{β}	Battery lifetime (year)
$\mathbb{N}_{k}$	Net present value of components ($)
$\mathbb{N}_{g}$	Net present value of electricity trade with grid ($)
P_{β}	Battery's power (kW)
P_{d}	Curtailed power (kW)
P_{h}	Household's power consumption (kW)
P_{i}, P_{j}	Import/export power from/ to main grid (kW)
P_{re}	Output power of renewable energy resources (kW)
$P_{\rho,y}$	Solar PV's output power at year *y* (kW)
P_{ω}	Wind turbine's output power (kW)
S	State-of-charge of battery (%)
Z_{k}	Components remaining lifetime (year)
π_{y}	Battery CD at the end of each year (%)
π_{Y}	Battery CD at the end of project lifespan (%)
θ_{k}	Number of decision variables (components)

References

[1] M. Aghamohamadi, A. Mahmoudi and M. Haque, "Two-stage Robust Sizing and Operation Co-optimization for Residential PV-battery Systems Considering the Uncertainty of PV Generation and Load," *IEEE Trans. Indust. Infor.*, vol. 17, no. 2, pp. 1005-1017, Feb. 2021.

[2] S. Agnew, and P. Dargusch, "Consumer preferences for household-level battery energy storage," *Renewable and Sustainable Energy Reviews*, vol. 75, pp. 609-617, 2017.

[3] M. Musallam and C. M. Johnson, "An Efficient Implementation of the Rainflow Counting Algorithm for Life Consumption Estimation," *IEEE Trans. Reliability*, vol. 61, no. 4, pp. 978-986, Dec. 2012.

[4] T. Dragicevic, H. Pandzic, D. Skrlec, I. Kuzle, J. M. Guerrero, and D. S. Kirschen, "Capacity optimization of renewable energy sources and battery storage in an autonomous telecommunication facility," *IEEE Trans. Sustain. Ener.*, vol. 5, iss. 4, pp. 1367 - 1378, Oct. 2014.

[5] B. Mohandes, S. Acharya, M. S. E. Moursi, A. S. Al-Sumaiti, H. Doukas and S. Sgouridis, "Optimal Design of an Islanded Microgrid with Load Shifting Mechanism Between Electrical and Thermal Energy Storage Systems," *IEEE Trans. Power Syst.*, vol. 35, no. 4, pp. 2642-2657, Jul. 2020.

[6] C. A. Correa, A. Gerossier, A. Michiorri and G. Kariniotakis, “Optimal scheduling of storage devices in smart buildings including battery cycling” *2017 IEEE Manchester PowerTech*, Manchester, 2017, pp. 1-6.

[7] P. Manganiello, M. Balato, and M. Vitelli, “A survey on mismatching and aging of PV modules: The closed loop,” *IEEE Trans. Industrial Electronics*, vol. 62, pp. 7276 – 7286, Nov 2015.

[8] A. Abraham and L. Jain, *Evolutionary multiobjective optimization*, Springer, 2005.

[9] K. Deb, A. Pratap, S. Agarwal, and T. Meyarivan, “A fast and elitist multi-objective genetic algorithm: NSGA-II,” *IEEE Trans. Evol. Comput.*, vol. 6, pp. 182–197, Apr. 2002.

[10] M. A. Abido, “Multiobjective evolutionary algorithms for electric power dispatch problem,” *IEEE Trans. Evol. Comput.*, vol. 10, no. 3, pp. 315-329, June 2006.

[11] MATLAB. “Global Optimization Toolbox” [Online]. Available: https://au.mathworks.com/products/global-optimization.html

[12] https://www.savings.com.au/home-loans/australians-are-holding-onto-their-homes-for-twice-as-long-as-they-were-10-years-ago

[13] https://www.corelogic.com.au/news/the-typical-home-in-australia-is-now-owned-for-10-5-years

Chapter 7

Conclusion and Future Work

A summary of the main contributions, components, achievements, and key findings of this thesis is described in this chapter. The directions for possible future works are also presented.

7.1 Summary

Optimal sizing of renewable energy sources and battery energy storage system for residential sector was conducted in this thesis. All capacity optimisation problems were conducted for practical and real case studies in Australia. For this purpose, all real data were collected for the case study.

A practical optimal sizing of solar PV and battery energy storage was presented for a grid-connected household. Two system configurations, PV only and PV-BES, were considered for the capacity optimisation. Rule-based home energy management systems were developed for each system configuration. A case study in South Australia was conducted by incorporation of real annual data of solar insolation, ambient temperature, and electricity consumption, as well as real technical and economic data like electricity prices, interest/inflation rate, and components data. The grid constraint to not accept more than a maximum power from grid-connected households was considered to achieve a more practical optimisation. The operation of each system configuration was investigated for two sample days in summer and winter. A cashflow analysis was provided to indicate the payment by the customer in each year of the project lifetime. An uncertainty analysis was presented based on 10-year real data of solar insolation and ambient temperature. Sensitivity analyses were provided based on the cost and capacity of components, average electricity demand of the household, as well as the retail price and feed-in-tariff. A practical guideline was provided for the customers in South Australia to purchase the correct capacity of components to achieve the minimum cost. Capacity optimisation of the two system configurations were also investigated for various states of Australia.

A practical capacity optimisation was conducted for small wind turbine and battery energy storage in grid-connected households with/without electric vehicle. Novel rule-based home energy management systems were developed, with grid constraint, for two different configurations of the grid-connected household: (i) with only wind turbine, and (ii) with wind turbine and battery. For each configuration, the energy management systems were developed for two cases: with and without an electric vehicle in the premises of the grid-connected household. Uncertainties were also included in the arrival time, departure time, and initial state of charge (at arrival) of the electric vehicle. This technique was then applied to a typical household in South Australia using the yearly load profile of the household and actual yearly wind speed data at an interval of one hour. To investigate the effects of stochastic nature of household load and wind power generation on various results, the optimisation process was repeated using 10-year of actual wind speed data and probabilistic load uncertainty. The results of several sensitivity analyses of various system parameters were also presented.

A novel and practical demand side management approach was developed to incorporate in optimal sizing of solar PV, wind turbine, and battery energy storage for a standalone household. The DSM strategy was based on the state-of-charge level of battery and day-ahead forecasts of solar insolation and wind speed. The core of the DSM was a fuzzy logic method which decided for efficient load shifting and/or load curtailment in the household. The day-ahead forecasting errors, obtained by an artificial neural network technique, were considered not only in the DSM strategy but also in maintaining an operating reserve. All essential parameters like operating reserve, salvation cost and battery capacity degradation were considered in the optimisation model. The battery capacity degradation was calculated using the Rainflow cycle counting algorithm to obtain a realistic battery model and estimate its lifetime. A typical household in South Australia was considered as the case study by incorporating rea annual data of wind speed, solar insolation, temperature, and load profile. Three different configurations (PV-BES, WT-BES, and PV-WT-BES) of the electricity supply system were optimised using the proposed method. The main feature of the developed DSM was its easy implementation in standalone households.

A comprehensive and practical design framework was proposed for optimal sizing of renewable and battery systems in a grid-connected household. An optimisation model based on a long-period (10-year) operation was developed by incorporating detailed models of electricity purchase and sell back prices, as well as components capacity degradations. The electricity prices were updated based on interest and escalation rates for each year of operation. The components capacity degradations were estimated to not only obtain the lifetime of battery but also to consider their effect on entire project lifetime. Salvation value of components, which was rarely considered by the existing studies, was applied to achieve a practical model for electricity cost. The capacities of PV, WT and BES were optimised in a residential grid-connected household based on three objective functions: (1) cost of electricity, (2) grid dependency, and (3) total curtailed energy. A novel rule-based operation strategy based on home energy management system and degradations of components was developed. The non-dominated sorting genetic algorithm II (NSGA-II) was used to cope with the multi-objective problem. A fuzzy decision-making strategy was developed to attain the final solutions. The proposed optimisation technique was applied to a grid-connected household in South Australia by incorporating long-period (10 years) real data of wind speed, solar insolation, ambient temperature, and load consumption. The PV-WT-BES electricity system optimised by the long-period data was compared to the same system optimised by short-period data (one year).

7.2 Concluding Remarks

After optimisation of the capacity of the renewable and battery components for grid-connected and standalone residential sector, the following are some of the derived concluding remarks.

It was realized that a 9-kW solar PV is the optimal capacity to achieve the minimum electricity cost in a typical grid-connected household (within 15.6 kWh daily electricity demand) in South Australia. With 9-kW solar PV, the COE of the household decreased by about 40% compared to the household without PV. The current battery cost was not attractive in an economic view to be integrated in the household. The battery price should decrease to $350/kWh for an economic integration in which the optimal battery capacity is 11 kWh for that price. The total benefit of PV only and PV-battery (with a battery cost of $350/kWh) systems for the grid-connected household was about $42,000 and $50,000 respectively, during the project lifetime. The uncertainty analysis based on ten-year real data confirmed that the optimised PV (9 kW) and battery (11 kWh) capacities remain almost the same over a period of ten years. Evaluation of the system configurations optimisation for different states in Australia showed that the PV only system (without battery subsidy) is the most beneficial for households in South Australia because of the highest RP. South Australia has the highest potential for BES integration among the other states. In Chapter 3, the practical guideline indicated that the optimal PV capacity should be determined based on not only the available rooftop space but also on the daily energy consumption.

It was found that the optimal capacity of wind turbine for a grid-connected household is 6 kW which decreases the COE of the household by 35% (without an EV) and 27% (with an EV). The current BES price is unable to reduce the COE further. To obtain any further financial benefit, the net battery price, after the government subsidy, should reduce to 250 $/kWh. Using load uncertainty and actual wind speed data for 10 years in South Australia, it was found that the optimal capacity of both wind turbine and battery remains almost the same over the above period. It was found that when the grid-connected household has an optimal capacity of wind turbine, the operating cost of an electric vehicle is about 50% lower than that of an internal combustion engine vehicle.

It was realized that without DSM strategy, the WT-BES system configuration required the highest battery capacity and that caused the highest LCOE for the standalone household. However, the battery capacity degradation was found to be the lowest because of its less utilization. The PV-WT-BES system configuration was found to be the most optimal having the lowest value of BES capacity and the LCOE. The LCOE of the PV-BES system is found to be in between that of the WT-BES and PV-WT-BES configurations. When the developed DSM strategy was applied, the battery capacity of all configurations was reduced while the capacity of renewable sources remained the same. Because of the reduction of battery capacity, the NPV and hence the LCOE of all configurations were decreased compared to that found without applying the DSM. For the optimal configuration (PV-WT-BES), the battery capacity was found as 24 kWh (a reduction of 11 kWh) and LCOE of 57 ¢/kWh (a reduction of 8 ¢/kWh). In previous studies, the LCOE with hybrid generating system was found as 61 ¢/kWh (without demand response) and 59 ¢/kWh (with demand response). The actual or existing system, based on diesel generator, had a LCOE of 74 ¢/kWh. Note that both hybrid and existing systems emit CO_2 because of the use of diesel generators. However, the optimal configuration found by the proposed DSM strategy not only had the lowest LCOE but also had no CO_2 emission as it was completely based on renewable and storage systems. The lowest LCOE was achieved at an expense of annual load shifting of 66.5 kWh for six days and an annual load curtailment of 22.7 kWh.

It was found that lower percentages of grid dependency increase the values of COE and curtailed energy in the grid-connected household. A residential grid-connected household with the minimum grid dependency (0.008%) resulted in a COE of 116 ¢/kWh and a total curtailed energy of 100 MWh in 10 years. Based on the decision-making procedure, the most recommended system to decrease all objective functions for the customers, resulted in 6.6 kW, 2 kW and 11 kWh as the optimal capacities for PV, WT and BES, respectively. It was found that the optimal sizing based on short-period (one year) operation was neither accurate (due to neglecting the capacity degradation of BS) nor practical (due to variations of renewable generation and load consumption in each year).

7.3 Future Work

The following research directions are recommended to be considered as future work for the researchers:

- Even though a flat retail price and feed-in-tariff of electricity was used in the optimal sizing of components in this thesis, the technique presented in this article can be extended for time-of-use and real-time pricing tariffs. For this case, new rule-based home energy management systems should be developed based on the electricity rate programs. As a result, better guideline can be provided for the electricity consumers based on the most economical option of flat, time-of-use, or real-time pricing tariffs.
- Selling electricity from discharging the battery energy storage system in peak hours can be investigated as a potential research direction. This can affect the optimal sizing of components and may achieve lower cost of electricity for customers if appropriate home energy management system is developed.

- Considering vehicle-to-home and vehicle-to-grid modes of electric vehicle operation in the home energy management system for optimal sizing model is another aspect which can be further investigated. To do so, the degradation of electric vehicle’s battery should be added to the cost of the system in the optimal sizing. As a result, a comprehensive guideline can be provided for the customers with an electric vehicle.
- A resiliency-oriented optimal sizing is an interesting topic for a future study. For this purpose, the designed renewable-battery system should supply the electricity demand of the residential household during grid outages. In order to achieve a practical optimal sizing framework for a resilient optimal sizing, a long-period operation can be considered by applying grid outages in different times through the project lifetime.
- Considering feed-in-tariff for customers in remote areas can be a potential aspect of research for the future. The customers with PV and WT should be able to export their excess energy to the main grid to achieve more cost reduction. In this regard, a peer-to-peer electricity sharing is an option in which the customer with the PV and WT can sell the extra power to neighbours.
- A peer-to-peer electricity trading between residential customers in a relatively large test system, while optimising the size of WT and BES, may represent an excellent direction of future studies. In this case, the customer can share its energy from the installed WT and BES with other consumers to achieve more benefits.

Publications

The majority of the works presented in this thesis are published or submitted for publication.

Book Chapters

[Pub.1] **R. Khezri**, A. Mahmoudi, and H. Aki, “Intelligent Demand Response in Microgrid Planning,” Chapter 9, **Wiley/IEEE Publisher**, 2021.

[Pub.2] **R. Khezri** and A. Mahmoudi, “Optimal Energy Management Strategies for Integrating Renewable Sources and EVs into Micro-Grids,” Chapter 10, **IET Publisher**, UK, 2021.

[Pub.3] **R. Khezri**, A. Mahmoudi, and M.H. Khooban, “Microgrids Planning for Electrification of Residentials in Rural Areas,” Chapter 1, **Elsevier**, 2021.

[Pub.4] K. Jalilpoor, **R. Khezri**, A. Mahmoudi, and A. Oshnoei, “Optimal Sizing of Energy Storage System,” Chapter 8, in Variability, Scalability, and Stability of Microgrids by S. M Muyeen, Syed Islam, and Frede Blaabjerg, **IET Publisher**, UK, June 2019, pp. 263–289.

Published Journal Papers

[Pub.5] **R. Khezri**, A. Mahmoudi, and M. Haque, “A Demand Side Management Approach for Optimal Sizing of Standalone Renewable-Battery Systems,” ***IEEE Transactions on Sustainable Energy***, Early Access, 2021.

[Pub.6] **R. Khezri**, A. Mahmoudi and M. H. Haque, "Optimal Capacity of Solar PV and Battery Storage for Australian Grid-Connected Households," ***IEEE Transactions on Industry Applications***, vol. 56, no. 5, pp. 5319-5329, Sept.-Oct. 2020.

[Pub.7] **R. Khezri**, A. Mahmoudi, and H. Aki, “Optimal Sizing of Solar Photovoltaic and Battery Storage Systems for Grid-connected Residential Sector: Review, Challenges and New Perspectives,” ***Renewable and Sustainable Energy Review***, 2020.

[Pub.8] **R. Khezri**, and A. Mahmoudi, "Review on the state-of-the-art multi-objective optimisation of hybrid standalone/grid-connected energy systems," ***IET Generation, Transmission & Distribution***, vol. 14, iss. 20, pp. 4285–4300, Oct. 2020.

[Pub.9] **R. Khezri**, A. Mahmoudi, H. Aki, and SM Muyeen, “Optimal Planning of Remote Area Electricity Supply System: Comprehensive Review, Recent Developments and Future Scopes,” ***Energies***, 2021.

[Pub.10] S. Merrington, **R. Khezri**, and A. Mahmoudi, “Capacity Optimization of Solar Photovoltaic and Battery Storage for Electric Vehicle Owner Households with Time-of-Use Tariff,” ***IET Generation, Transmission & Distribution***, pp. 1-13, 2021.

[Pub.11] M. Fathi, **R. Khezri**, A. M. Yazdani, and A. Mahmoudi, “Comparative Study of Metaheuristic Algorithms for Optimal Sizing of Standalone Microgrids in a Remote Area Community,” ***Neural Computing and Applications***, 2021.

[Pub.12] I. Javeed, **R. Khezri**, A. Mahmoudi, A. Yazdani, GM Shafiullah, “Optimal Sizing of Rooftop PV and Battery Storage for Grid-Connected Houses Considering Flat and Time-of-Use Electricity Rates,” ***Energies***, 2021.

[Pub.13] X. Pan, **R. Khezri**, A. Mahmoudi, A. Yazdani, GM Shafiullah, “Energy Management Systems for Grid-Connected Houses with Solar PV and Battery by Considering Flat and Time-of-Use Electricity Rates,” ***Energies***, 2021.

[Pub.14] M. Combe, A. Mahmoudi, M. H. Haque, and **R. Khezri,** “Cost effective sizing of an AC mini-grid hybrid power system for a remote area in South Australia,” ***IET Generation, Transmission & Distribution***, vol. 13, iss. 2, pp. 277–287, Jan. 2019.

[Pub.15] M. Combe, A. Mahmoudi, M. H. Haque, and **R. Khezri,** “Optimal sizing of an AC-coupled hybrid power system considering incentive-based demand response,” ***IET Generation, Transmission & Distribution***, vol. 13, iss. 15, pp. 3354 – 3361, Jun. 2019.

[Pub.16] M. Combe, A. Mahmoudi, M. H. Haque, and **R. Khezri,** “AC-Coupled

Hybrid Power System Optimisation for an Australian Remote Community,” ***International Transactions on Electrical Energy Systems***, vol. 30, iss. 9, Jun. 2020.

Submitted Journal Papers (Under Review)

[Pub.17] **R. Khezri**, A. Mahmoudi, and M. Haque, “Impact of Optimal Sizing of Wind Turbine and Battery Energy Storage for a Grid-Connected Household With/Without an Electric Vehicle,” ***IEEE Transactions on Industrial Informatics***, Under Revision, 2020.

[Pub.18] **R. Khezri**, A. Mahmoudi, and H. Aki, “Resiliency-Oriented Capacity Optimization of Renewable Resources and Battery Storage,” ***IEEE Transactions on Industry Applications***, Under Revision, 2021.

[Pub.19] **R. Khezri**, A. Mahmoudi, and H. Aki, “Optimal Design Framework for a Residential Grid-connected Renewable-Battery System,” ***IEEE Transactions on Industry Applications***, 2021.

[Pub.20] **R. Khezri**, A. Mahmoudi, and D. Whaley, “Comparative Study of Rooftop PV and Battery for Grid-Connected Households with All-Electricity and Gas-Electricity Utility in Australia,” ***Energy***, 2021.

[Pub.21] S. Merrington, **R. Khezri**, and A. Mahmoudi, “Optimal Sizing of Rooftop Solar PV and Battery Energy Storage for Grid-Connected Households with Electric Vehicle,” ***IEEE Systems Journal***, 2021.

[Pub.22] X. Pan, R. Khezri, and A. Mahmoudi, “Solar PV and Battery Storage Capacity Optimization with Energy Management Systems for Time-of-Use and Flat Electricity Tariffs,” ***IET Renewable Power Generation***, 2021.

Conference Papers

[Pub.23] **R. Khezri**, A. Mahmoudi and M. H. Haque, "Optimal Capacity of PV and BES for Grid-connected Households in South Australia," 2019 IEEE Energy Conversion Congress and Exposition (ECCE), Baltimore, MD, USA, 2019, pp. 3483-3490.

[Pub.24] **R. Khezri**, A. Mahmoudi and M. H. Haque, "SWT and BES Optimisation for Grid-connected Households in South Australia," 2019 IEEE Energy Conversion Congress and Exposition (ECCE), Baltimore, MD, USA, 2019, pp. 418-425.

[Pub.25] **R. Khezri**, A. Mahmoudi and M. H. Haque, "Optimal WT, PV and BES based Energy Systems for Standalone Households in South Australia," 2019 IEEE Energy Conversion Congress and Exposition (ECCE), Baltimore, MD, USA, 2019, pp. 3475-3482.

[Pub.26] **R. Khezri**, A. Mahmoudi and H. Aki, "Optimal Planning of Renewable Energy Resources and Battery Storage System for an Educational Campus in South Australia," 2020 IEEE Energy Conversion Congress and Exposition (ECCE), Detroit, MI, USA, 2020, pp. 3677-3683.

[Pub.27] **R. Khezri**, A. Mahmoudi and M. H. Haque, "Two-Stage Optimal Sizing of Standalone Hybrid Electricity Systems with Time-of-Use Incentive Demand Response," 2020 IEEE Energy Conversion Congress and Exposition (ECCE), Detroit, MI, USA, 2020, pp. 2759-2765.

[Pub.28] **R. Khezri**, A. Mahmoudi and M. H. Khooban, and N. Ertugrul, " Optimal Sizing of Grid-tied Residential Microgrids Under Real-Time Pricing," 2021 IEEE Energy Conversion Congress and Exposition (ECCE), Vancouver, BC, Canada, 2021.

[Pub.29] **R. Khezri**, A. Mahmoudi and M. H. Haque, and K. Khalilpour, " Energy Management and Optimal Planning of a Residential Microgrid with Time-of-Use Electricity Tariffs," 2021 IEEE Energy Conversion Congress and Exposition (ECCE), Vancouver, BC, Canada, 2021.

[Pub.30] **R. Khezri**, A. Mahmoudi and M. H. Haque, "A Comparative Study of Optimal Battery Storage and Fuel Cell for a Clean Power System in Remote Area," 2020 IEEE International Conference on Power Electronics, Drives and Energy Systems (PEDES), 2020, pp. 1-5.

[Pub.31] **R. Khezri**, A. Mahmoudi and H. Aki, "Multi-Objective Optimization of Solar PV and Battery Storage System for A Grid-Connected Household," 2020 IEEE International Conference on Power Electronics, Drives and Energy Systems (PEDES), 2020, pp. 1-6.

[Pub.32] **R. Khezri**, A. Mahmoudi N. Ertugrul, M. Shaaban, and A. Bidram, "Battery Lifetime Modelling in Planning Studies of Microgrids: A Review," 2021 31st Australasian Universities Power Engineering Conference (AUPEC), 2021, pp. 1-6.